



HAL
open science

Synthesis of new amino-containing π -conjugated polymers via dimerization of acyclic aminoarylcabenenes

Quentin Sobczak

► **To cite this version:**

Quentin Sobczak. Synthesis of new amino-containing π -conjugated polymers via dimerization of acyclic aminoarylcabenenes. Polymers. Université de Bordeaux, 2019. English. NNT: 2019BORD0208 . tel-02505796

HAL Id: tel-02505796

<https://theses.hal.science/tel-02505796>

Submitted on 11 Mar 2020

HAL is a multi-disciplinary open access archive for the deposit and dissemination of scientific research documents, whether they are published or not. The documents may come from teaching and research institutions in France or abroad, or from public or private research centers.

L'archive ouverte pluridisciplinaire **HAL**, est destinée au dépôt et à la diffusion de documents scientifiques de niveau recherche, publiés ou non, émanant des établissements d'enseignement et de recherche français ou étrangers, des laboratoires publics ou privés.

THÈSE PRÉSENTÉE
POUR OBTENIR LE GRADE DE
**DOCTEUR DE
L'UNIVERSITÉ DE BORDEAUX**

École Doctorale des Sciences Chimiques

Spécialité : Polymères

Par **Quentin SOBCZAK**

**Synthesis of new amino-containing π -conjugated polymers
via dimerization of acyclic aminoarylcarbenes**

Synthèse de nouveaux polymères aminés π -conjugués obtenus par dimérisation
d'aminoarylcabènes acycliques

Sous la direction de : Pr. Daniel TATON, Pr. Yannick LANDAIS et Dr. Cyril
BROCHON

Soutenue le 07 novembre 2019

Membres du jury :

Mme. REYNAUD, Stéphanie,	Chargée de recherche, Université de Pau	Rapporteur
M. MARTIN, David,	Directeur de recherche, Université Grenoble Alpes	Rapporteur
M. GIGMES, Didier,	Directeur de recherche, Aix-Marseille université	Président
M. TATON, Daniel,	Professeur, Université de Bordeaux	Directeur de thèse
M. LANDAIS, Yannick,	Professeur, Université de Bordeaux	Directeur de thèse
M. BROCHON, Cyril,	Maître de conférences, Université de Bordeaux	Directeur de thèse
M. VIGNOLLE, Joan,	Chargé de recherche, CNRS	Invité
M. CLOUTET, Éric,	Directeur de recherche, CNRS	Invité

« Il n'y a que celui qui persévère jusqu'à la fin qui obtient le prix »
Recueil d'apophtegmes et axiomes (1855)

« Le succès, c'est se promener d'échecs en échecs tout en restant motivé »
Winston Churchill

Remerciements

Ah ce moment des remerciements, cette fameuse partie qui vient clore ces 4 « longues ? » années de thèse. En lisant ces lignes, tu es certainement entrain d'avoir le souffle court, tu as l'appréhension mêlée à l'excitation de lire ce que je vais dire sur toi en espérant que je sois gentil avec toi ! et bien je te laisse donc découvrir cela sur ces quelques pages qui doivent « tout ? » résumer de ce périple qu'a été ma thèse.

Je souhaite avant tout à remercier respectueusement les membres du jury qui m'ont fait l'honneur d'accepter de juger ces travaux de thèse, Mr. David Martin, professeur à l'Université de Grenoble-Alpes, Mme. Stéphanie Reynaud, chargée de recherche à l'Université de Pau et des Pays de l'Adour et Mr. Didier Gignes, directeur de recherche à l'Université d'Aix-Marseille. Je les remercie pour leurs commentaires constructifs et positifs à mon égard ainsi que pour la discussion très intéressante que nous avons pu avoir lors de la soutenance qui a permis d'améliorer et d'enrichir ce manuscrit.

Je remercie les Pr. Henry Cramail et Sébastien Lecommandoux pour m'avoir accueilli au sein du Laboratoire de Chimie des polymères Organiques, le Pr. Yannick Landais à l'Institut des Sciences Moléculaires et m'avoir permis de travailler dans de bonnes conditions. Je remercie également grandement tout le personnel du laboratoire (administratif, ingénieurs et techniciens) pour m'avoir aidé tout au long de ces années et d'avoir été aussi gentil et adorable avec moi qu'efficace (et c'est pas rien !).

Viens maintenant le moment de remercier mes nombreux chefs, même si je n'ai pas passé autant de temps avec chacun de vous, vous m'avez tous apporté votre savoir et votre vision de la chimie (même si parfois différentes de la mienne), et malgré des débuts compliqués vous avez toujours su me faire confiance et m'encourager à aller le plus loin possible. Plus personnellement, merci Yannick, pour toujours avoir gardé votre sérieux lors de nos discussions et m'avoir donné des idées brillantes qui ne me seraient jamais venu à l'esprit. Merci Cyril, pour ta bonne humeur, nos discussions sur le sport et la course et ton expertise sur ces polymères conjugués. Expertise partagée avec Éric, qui m'a évité de dire pas mal de bêtises lors de mes présentations. Merci Éric d'avoir été disponible quand j'avais des questions et pour tes corrections avisées. Daniel, que de sentiments mitigés, je te remercie de m'avoir boosté pour

commencer à écrire cette publication et m'avoir fait confiance sur mes capacités, je regrette cependant que l'on ne se soit pas plus entendu au quotidien, j'aurais pu en apprendre beaucoup plus sur cette chimie que tu maîtrises. Joan, quel courage, me côtoyer pendant 4 ans au quotidien c'est pas rien ! Je sais que je t'en ai fait voir de toute les couleurs avec nos incompréhensions (RIP analyseur de la GB), cette rédaction qui a duré pour notre plus grand plaisir (j'en suis sûr !) et mes nombreuses questions. Merci en tout cas d'avoir pris tout ce temps pour moi, d'avoir toujours su garder ta porte ouverte peu importe l'heure de la journée (enfin quand tu courrais pas pour attraper ton train, si train il y avait !), d'avoir su me remotiver et m'aider à aller de l'avant quand rien ne marchait (comme ce satané bis-iminium par exemple !) et pour tout ça je te remercie encore une fois. Je tiens également à remercier les membres permanents du LCPO et de l'ISM pour leurs bonnes humeurs et les discussions occasionnelles que j'ai eu avec eux.

Je remercie le LabEx AMADEus pour avoir financé mon projet de thèse et pour m'avoir permis de présenter mes travaux sous forme de communication orale chaque année.

Je tiens également à remercier nos partenaires pour ce projet qui ont apporté une grande richesse scientifique et une ouverture d'esprit : le Dr. Jean-Marc Sotiropoulos, Dr. Karinne Miqueue et Dr. Daiann Sosa Carrizo de l'Institut des sciences analytiques et de physico-chimie pour l'environnement et les matériaux pour tous les calculs effectués et pour leur rapidité de réponse quand je leur demandais une information supplémentaire au dernier moment. Merci à Brice Kauffmann et Stéphane Massip de l'Institut Européen de Chimie et biologie pour toutes ces diffractions aux rayons X de mes cristaux qui sont sensibles à toutes les conditions possibles et imaginables et d'avoir pris le temps de m'expliquer comment analyser ces cristaux et de répondre à la moindre de mes questions. Merci à Thierry Buffeteau et Joseph Grondin de l'Institut des Sciences Moléculaires pour les analyses infrarouges en inertes et la préparation des échantillons en boîte à gants. Merci à Eric Leroy de l'Institut de chimie de Toulouse pour ses analyses de spectrométrie de masses en inerte. Enfin, je tiens à remercier le Dr. Laurent Bouffier et sa doctorante Alice Dauphin pour les mesures de voltampérométrie cyclique (domaine méconnu et détesté de ma part) vous avez réussi à me faire aimer cette technique d'analyse et à apprécier d'obtenir des pingouins à une ou deux bosses. Alice courage pour la suite avec tes cinquante projets en parallèles tu vas réussir cette thèse avec brio !

Ah voilà le moment qui sera peut-être le seul à être lu de cette partie ou du moins le sera avec envie. Tout d'abord je tiens à remercier mon stagiaire Alexandre Holmes, merci d'avoir été de bonne humeur et plein d'envie chaque matin en arrivant au labo, d'avoir un esprit vif et d'être toujours avide d'en apprendre plus sur cette chimie. J'espère que la découverte de ce laboratoire de chimie t'a plu et que malgré cette chimie compliquée j'ai réussi à te donner envie de continuer dans ce domaine et d'aller encore plus loin ! Un grand merci à mon post-doc Aravindu le magicien, qui avec des techniques dont seul toi as le secret arrive à faire des miracles ! Je me rappellerai de nos fou rire dans le labo. Un immense merci à Dam qui a partagé mon quotidien à la paillasse pendant deux ans, ta bonne humeur et nos discussions m'ont permis de progresser en anglais comme dans la vie ! Et n'oublions pas la question que l'on s'est posé le plus, as-tu vu le boss aujourd'hui ? Suivi d'un : tu sais si il sera là? J'en garde que de bon souvenirs.

C'est au tour des collègues, d'abord ceux de mon bureau le N1-15 (le meilleur ?) Julie (la pro du caoutchouc), Dounia (au martèlement de clavier de l'enfer), Julien (et ton franc parlé), Amaury, Léa (j'ai toujours pas goûté ton gâteau allemand au nom imprononçable), Sethun (on se fera une soirée jeux un jour t'inquiètes), Marianna (et ton vin du Beijo qui nous a fait tourner la tête), Guillaume (et tes goûts musicaux éclectiques j'aime bien le style rétro mais la porte qui grince toute la journée ahhhhh !) merci pour votre bonne humeur au quotidien, de m'avoir permis de garder le moral pendant ma rédaction et nos discussions scientifiques comme privées, courage pour la suite. Je vais regrouper tous les autres membres du LCPO et de l'ISM qui ont contribué à cette ambiance chaleureuse de tous les jours de 7h du mat à 20h sinon je vais doubler le volume de cette thèse (petit aparté, merci au N2 de m'avoir accueilli avec gentillesse et bienveillance dans ce bureau pour ma fin de rédaction) donc merci à Thomas et Audrey les deux permanents « jeun's » du labo, les petites pauses chocolat à 16h vont me manquer courage avec les vieux ! Antoine qui m'a accompagné dans cette aventure de la boîte à gants, Qiley, Medhi, Loïc, Hanaé et Valentin, Bobo (qui a subi mes choix de musiques et mes chants « cris ? » par dessus jusqu'à tard le soir, courage tu es à la fin !), Martin C (miaoooouu), Jessie (Miaou²²²), Christopher et tes chansons (faut m'apprendre je suis mauvais a s'kip), Fiona, Quentin P, Jamie, Victor, Anderson, Peroline, Poline, Nicolas, Florian, Jeremy (le pro des gâteaux basques), Cédric (my movie guy), Tim (on se fait un tour de vélo ?), Coco Theblue (je te retiens pour la photo du book ahah), Manon (Cerberé addict), Florian, Marie, Tintin, Martin F (tu m'acceptes quand sur Fb ? ahah), Laura, Gauvin, Arianne, Lélé, Rakot, Geoffrey, Michelle, Kindy, Lauriane (Makélé masséré je te jure j'ai entendu ça !), Alizée (yoga master), Vava, Solène, Geoffrey (merci pour toute ces heures passées en salle blanche à faire des « film »

ahah), Moby (euh Flo pardon !), Daniele (et les soirées à la cidrerie), Camille, Ségolène, Anna, Jo l'poireau (je viendrai te botter les fesses aux jeux de ton choix t'inquiètes), Vincent, Claire (courage plus qu'un an !!), Nitin, Gülbin, Imane, Lisa, Nico, Julien, Charlène, Laura et tous ceux que j'aurais pu oublier dans cette marée de personnes qui m'ont tant apporté. Je vous souhaite ainsi qu'aux nouveaux arrivant de réussir dans votre vie professionnelle autant que personnelle !

Quoi j'en ai oublié ? Ah oui ceux qui m'ont supporté aussi bien dans la vie au labo qu'en dehors, les pauvres je les ai épuisés (et c'est peu dire) ! On m'a toujours dit choisi bien tes amis et je crois que j'ai fait un sans-fautes ! (Ne te comptes pas dedans Werner tu es l'erreur qui confirme la règle) Merci à toi Hélène pour ton soutien au quotidien, d'avoir « accepter » mes choix musicaux au labo, ta bonne humeur, nos fou rire et n'oublions pas la découverte des fléchettes dans ta coloc et l'existence d'allumettes comestible ! Loulou, ton positivisme est contagieux j'ai jamais vu ça ! et je ne soupçonnais pas que cela me ferait autant de bien, merci pour ça et pour nos nombreuses discussions quand ça allait ou pas. Et surtout prend garde, la guerre n'est pas finis le jeu du rond reprendra et je redeviendrai roi ! Babouli, c'est simple, toujours le sourire, partant pour tout, même quand je t'appelle à l'autre bout du monde deux jours avant ma soutenance pour me donner tes conseils et répondre à mes questions de chimie des polymères tu réponds présent. Un grand merci ! Sofiem, merci pour cette année et demi très intense à galérer avec nos chefs dont je ne prononcerai pas le nom, à me faire visiter des nouveaux endroits et restau (toujours des bons plans c'est fou !), à se faire des petits déj aux capu le dimanche matin au top ! Faudra vite remettre ça quand tu repasses en France sinon je viendrai à San Seb ! Arthur Werner, que dire... non ça ne se raconte pas à l'écrit ça serait trop long, demande plutôt à Annick elle sait déjà tout ! Et le p'tit dernier Dayvid (dit Dadou), alors toi du courage c'est un euphémisme, encore avant ils pouvaient m'avoir à petite dose en me partageant, autant toi tu m'as pris de plein fouet à 100% ! Tu m'as permis de passer une très belle année malgré les difficultés de la vie, on a vécu des hauts et des bas mais on s'est serré les coudes et on a réussi à surpassé tout ça et pour ça je n'arriverai jamais assez à te remercier. Merci également de m'avoir fait découvrir le vélo et de m'aider à m'améliorer malgré mon niveau de néophyte, j'adore ça ! Il est évident que ceci n'est qu'un ersatz de ce que je pense de vous et j'ai toute la vie pour vous raconter le reste car maintenant que vous êtes rentré dans le mienne je vous lâche plus ! Je vous souhaite le meilleure dans vos vies et à la revoyure !

Enfin le dernier paragraphe, celui-ci je vous laisse deviner c'est celui des amis et de la famille.

Comment ne pas remercier mes parents, grands-parents, tantes, oncles et cousins qui m'ont permis d'être la personne que je suis aujourd'hui en me soutenant sans faille à la moindre de mes décisions, c'est grâce à vous que j'en suis là et je vous remercie pour ça. Je tiens ensuite à remercier les amis que j'ai rencontrés tout au long de ma vie, Charley, Antoine (et nos longues discussions autour d'un subway à parler sans fin de notre thèse), Gaïa, Gonzague (je ne sais pas quoi dire, notre relation va au-delà des mots), Emilie (la chimie > la physique), Alexandra (la touriste et nos révisions de dernières minutes), Thibaut, Maxence, Mégane (poutou, amataxia, pickle rick et j'en passe !), Thibault (et notre rencontre atypique et nos révisions dans toutes les BU de Paris), Pauline, les potes de paris avec Frifri (qui m'as appris la rigueur au labo alors que je n'étais qu'un simple stagiaire, et qui m'as encouragé jusqu'au jour j !), Laura, Brendan, The original, Anthony et Magle ou Dr TATA (ça va être difficile de te battre dans ces remerciements tellement tu en as dit et tu sais que je pense la même chose mais je peux quand même te dire que je suis chanceux de t'avoir rencontré même si tu écoutes papillons de lumière et que tenir l'alcool n'est pas ton fort, il y a eu la période en tant que stagiaire mais aussi après en tant que thésard avec nos sorties à Bordeaux et Lyon, les campings à deux ou plusieurs, sans mentionner l'UCPA que d'aventures et de rigolades que je n'oublierais pas, j'ai hâte d'en avoir d'autres dans un futur proche mais cette fois en tant que confrère !! Prépare toi j'arrive !), et il y aussi les potes rencontrés à bordeaux, Marmotte, Aimery, Armand, Tibalt et le groupe entier de basket sur ces 4 ans ça fait pas mal de monde et de soirées au long island. Je remercie également ceux que je n'ai pas cités et qui m'ont aidé tout au long de ces quatres années. Courage à tous et bonne continuation !

List of abbreviations

- ADAC: Acyclic diaminocarbenes
- ATRP: Atom transfer Radical Polymerization
- BAMH-PPV: Poly(2,5-bis[N-methyl-N-hexyl amino] phenylene vinylene)
- BDE: Bond dissociation energy
- n*-BuLi: *n*-Butyl lithium
- n*-Bu₄NBF₄: Tetrabutylammonium tetrafluoroborate
- CAAC: Cyclic Alkyl AminoCarbene
- CGMT: Carter-Goddard-Malrieu-Trinquier
- CCl₄: Carbon tetrachloride
- CHCl₃: Chloroform
- CH₂Cl₂: Dichloromethane
- CH₃CN/ACN: Acetonitrile
- CO₂: carbon dioxide
- CS₂: carbon disulfide
- CV: Cyclic voltammetry
- DAA: Diaminoalkene
- DAC: Diaminocarbene
- DBU: 1,8-Diazabicyclo[5.4.0]undec-7-ene
- DCA: Dicyanoarene
- DDQ: 2,3-Dichloro-5,6-dicyano-1,4-benzoquinone
- DFT: Density Functional theory
- DMAc: N,N-dimethylacetamide
- DMSO: Dimethylsulfoxide
- DP_n: Degree of polymerization
- D*: Dispersity
- E⁰_{ox}: Oxidation potential
- E^{0*}: Excited state reduction potential
- EBP: ethyl α -bromoisobutyrate
- EBPA: α -bromophenylacetate
- ET₂O: Diethyl ether
- ΔE_{S-T} : Singlet-triplet energy gap

ΔH : Enthalpy of dimerization
 ΔG : Gibbs free energy
HCl: Hydrochloric acid
 $\text{Hg}(\text{SiMe}_3)_2$: Bis-(trimethylsilyl)-mercury
HOMO: Highest Occupied Molecular Orbital
 $\pm I$: Inductive effect
ITO: Indium Tin Oxide
KH: Potassium hydroxide
KHMDS: Potassium hexamethyldisilazane
 K_2S : Potassium sulfide
LDA: lithium diisopropylformamide
LiHMDS: Lithium Hexamethyldisilazane
LiOTf: Lithium triflate
LUMO: Lowest Unoccupied Molecular Orbital
 $\pm M$: Mesomer effect
 \overline{M}_n : Number average molar mass
 \overline{M}_w : Mass average molar mass
MAC: Monoaminocarbene
m-CPBA: *meta*-Chloroperoxybenzoic acid
MMA: Methyl methacrylate
MeOH: Methanol
MeONa: Sodium methoxide
MeOTf: Methyl trifluoromethanesulfonate
NHC: *N*-heterocyclic carbene
NMR: Nuclear Magnetic Resonance
N-PPV: Amino-containing poly(phenylene vinylene)
OATRP: Organocatalyzed Atom Transfer Radical polymerization
OR-PPV: Alkoxy-containing poly(phenylene vinylene)
 P_4 -*t*Bu: Phosphazene
PMMA: Poly(methyl methacrylate)
PPV: Poly(phenylene vinylene)
PS: Polystyrene
PTZ: 10-Phenylphenothiazine

RAFT: Reversible Addition Fragmentation Chain Transfer

S₈: Octasulfur

SEC: Size-exclusion chromatography

SCE: Saturated calomel electrode

SO₂: Sulfur dioxide

TAA: Tetraaminoalkene

TBD: 1,5,7-Triazabicyclo[4.4.0]dec-5-ene

t-BuOH: *tert*-Butanol

t-BuOK: Potassium *tert*-Butoxide

TDAE: Tetrakis(dimethylamino)ethylene

TEBAC: Triethylbenzylammonium chloride

Tf₂O: Trifluoromethanesulfonic anhydride

TfOH: Trifluoromethanesulfonic acid

Tf₂NH: Bis(trifluoromethane)sulfonimide

THF: Tetrahydrofuran

TMPLi: Lithium tetramethylpiperidide

V_{oc}: Open-circuit voltage

WE: Working-electrode

ε: Molar extinction coefficient,

Résumé en français

De nos jours, les polymères sont utilisés dans de nombreux domaines de la vie quotidienne. Parmi ces polymères, certains ont la particularité de conduire l'électricité et sont utilisés dans le domaine de l'électronique organique. Bien que de tels semi-conducteurs organiques aient déjà été décrits dès le début du XX^e siècle,¹ ces polymères originaux ont véritablement été développés grâce aux travaux réalisés par Hideki Shirakawa, Alan G. MacDiarmid et Alan J. Heeger sur les propriétés de conduction électrique du polyacétylène (Figure 1). Ces travaux leur ont d'ailleurs valu le prix Nobel de Chimie pour la « découverte et le développement des polymères semi-conducteurs » en 2000.²

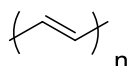
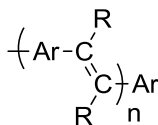


Figure 1. Structure du polyacétylène.

Cependant, la plupart des voies de synthèse de polymères semi-conducteurs implique l'utilisation de protocoles complexes comportant des catalyseurs métalliques coûteux et non renouvelables. Or, la présence de traces métalliques résiduelles après l'emploi de ces processus organométalliques affecte fortement les performances optoélectroniques des polymères π -conjugués et nécessite des étapes de purification longues et fastidieuses ce qui constitue un problème majeur pour l'obtention de polymères à haute performance dans l'optoélectronique.^{3,4} Afin d'outrepasser ces problèmes, nous nous sommes dirigés vers des stratégies de synthèses sans métaux. De plus, la structure aryl-vinyl et plus précisément celle des poly(phénylène-vinylène) (PPV) a été sélectionnée car, non seulement ces polymères π -conjugués montrent des caractéristiques optoélectroniques remarquables notamment pour des applications dans des diodes organiques électroluminescentes flexibles (OLED), mais aussi différentes options existent quant à la construction de doubles liaisons C=C (Figure 2).



R = diisopropylamino, piperidino

Ar = Ph, fluorenyl

Figure 2. Structure générale des polymères ciblés comportant le motif aryl-vinyle.

C'est dans ce contexte qu'une nouvelle stratégie se basant sur l'idée originale d'utiliser les carbènes en tant que briques de base de polymères π -conjugués a été abordée dans cette thèse. Dans notre cas, les bis-aminoarylcabènes acycliques ciblés permettront l'obtention de polymères PPV originaux,

comportant deux groupes amino sur chaque double liaison, par dimérisation/polymérisation. De plus, la présence d'atomes d'azote permet de moduler les propriétés physicochimiques des polymères obtenus. Enfin, il est important de préciser que ce nouveau type de polymères n'est accessible que par cette méthodologie (Schéma 1). Aussi, nous proposons d'étudier une nouvelle facette de la chimie des carbènes. En effet, jusqu'à aujourd'hui, les carbènes étaient uniquement considérés comme ligands des métaux de transition, organocatalyseurs ou réactifs stœchiométriques pour diverses réactions (C-H insertion, la cyclopropanation, la 1,2-migration et la dimérisation).⁵⁻⁸ Ici, c'est bien leur utilisation en tant que brique élémentaire pour la construction de polymère qui est visée.

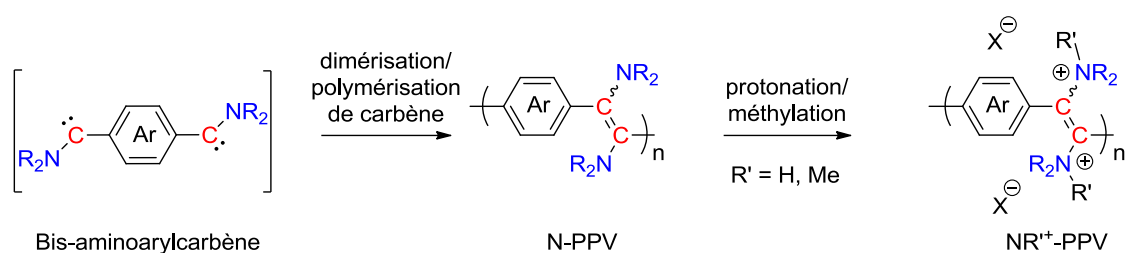


Schéma 1. Synthèse de PPV contenant des groupes amino (N-PPV) par dimérisation successive de bis-aminoarylcarbènes. Modification des N-PPV par protonation/méthylation des groupes amino.

Le chapitre bibliographique présente les carbènes, d'un point de vue synthèse, caractérisation et propriétés, avec une attention particulière portée aux monoaminocarbènes et à leur dimérisation. Dans la littérature, seuls quelques aminoarylcarbènes ont été isolés et leur dimérisation a généralement été observée dans le cas où le centre carbénique n'est pas suffisamment protégé (pas de substituants en ortho sur le groupement aryl). Bien qu'il existe différentes voies de synthèse pour l'obtention d'aminoarylcarbènes, elles impliquent généralement des précurseurs assez sophistiqués et/ou des réactifs toxiques.^{12,13} Par conséquent, nous nous sommes tournés vers une méthode plus simple et plus robuste impliquant la déprotonation de sels d'iminium par une base forte (Schéma 2).

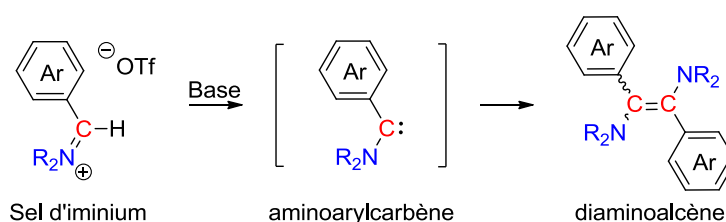


Schéma 2. Dimérisation d'aminoarylcarbène formés *in situ* par déprotonation de sel d'iminium.

L'étude de la déprotonation de sels d'iminiums a été réalisée par addition lente d'une base forte à basse température. De manière remarquable, cette réaction conduit sélectivement aux diaminoalcènes correspondants, sous forme d'un mélange E/Z en faveur de l'isomère E. Cette réaction de dimérisation

a été étendue à différents substrats, comportant notamment des groupes phényles et fluorényles pour la partie aryle du carbène, des groupes diisopropyle et pipéridinyyle pour la partie amino (Figure 3).

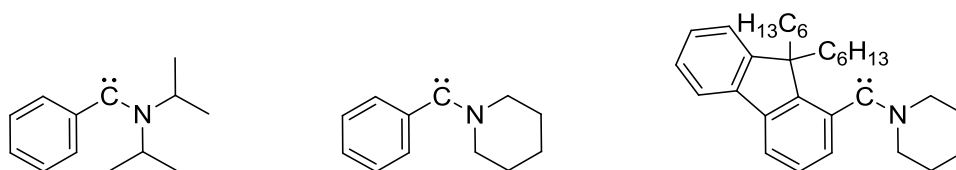


Figure 3. Carbènes employés lors de la réaction de dimérisation.

Cette réaction a ensuite été étudiée avec différentes bases fortes, afin d'observer leur influence sur le mélange d'isomères E/Z. Dans le cas des alcoolates (*t*BuOK, MeONa), la dimérisation n'est pas observée mais la formation d'un aminal est obtenue. Ce composé est en réalité un carbène masqué, qui par chauffage et perte de ROH conduit à la formation *in-situ* d'aminoarylcarbènes qui se dimérisent instantanément. Ce procédé nécessite néanmoins d'être optimisé car la génération des carbènes n'est pas totale dans les conditions utilisées. Pour l'utilisation des autres bases (LiHMDS, DBU, TBD, P₄-*t*Bu), une tendance se dégage. Plus la base est forte, plus l'isomère E est prédominant dans le mélange. Dans le cas de la base métallique LiHMDS, le rapport est exclusivement en faveur de l'isomère E. Cependant, après purification, des rapports E/Z de 80/20 en faveur de l'isomère E sont obtenus avec les différentes bases, ce qui pour le moment demeure assez énigmatique.

Afin d'étudier le mécanisme de dimérisation, la déprotonation a été suivie par RMN à basse température. Aucun carbène n'a pu être observé dans ces conditions. Cependant, l'isolation et l'identification (RX) d'un dimère protoné ont été réalisées. Il semble donc qu'un mécanisme indirect, impliquant l'addition d'un carbène sur son acide conjugué, opère dans ces conditions bien qu'on ne puisse pas totalement exclure un mécanisme direct (Schéma 3).

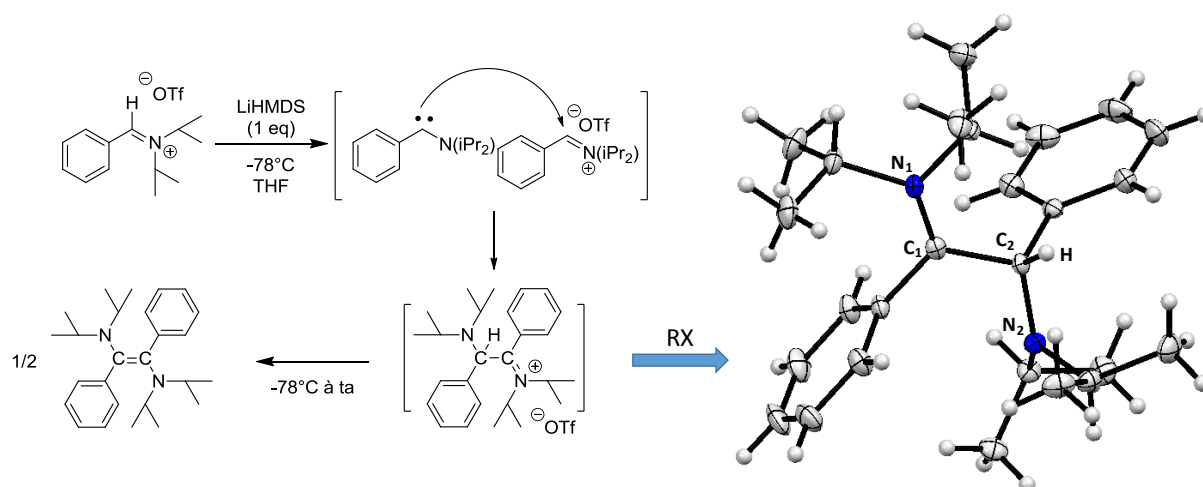


Schéma 3. Dimérisation des aminoarylcarbènes par la voie indirecte et RX du dimère protoné.

Afin de confirmer ce mécanisme indirect, des calculs DFT ont été réalisés par les Dr Miqueu et Sotiropoulos (IPREM, Pau), lesquels ont montré que l'énergie requise par cette voie, comparée à la voie directe, est nettement inférieure ($1-2 \text{ kcal.mol}^{-1}$ vs 18 kcal.mol^{-1} respectivement). Par ailleurs, l'isomère E obtenu est le produit thermodynamique, expliquant sa présence majoritaire dans le mélange d'isomères. Bien que l'existence de carbènes générés lors de la déprotonation de leurs précurseurs, n'a pu être observée expérimentalement, plusieurs tentatives de piégeage du carbène ont donc été tentées afin de prouver l'existence de cette espèce transitoire. Ainsi, les aminoarylcarbènes générés par déprotonation réagissent avec le CS_2 et S_8 pour former la bétaine et le thioamide correspondants. Il est intéressant de noter que la réaction avec CS_2 est en compétition avec leur dimérisation car un mélange de dimères et de bétaines est observé par spectroscopie RMN ^1H (Schéma 4).

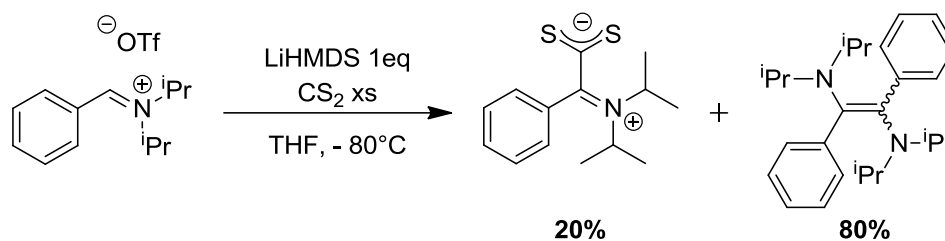


Schéma 4. Addition d'aminocarbène sur CS_2 .

Enfin, une étude sur l'isomérisation du mélange d'isomères sous irradiation et en présence d'électrophiles en quantité catalytique a été menée. En présence de composés de plus en plus électrophiles, le rapport évolue vers une majorité d'isomère Z avec un rapport E/Z maximal de 36/64.

La stratégie de dimérisation au niveau moléculaire présentée au chapitre 2, a ensuite été adaptée au niveau macromoléculaire dans le chapitre 3. Des aminoarylcarbènes difonctionnels ont ainsi été développés afin de réaliser une polymérisation par étape conduisant à de nouveaux polymères poly(*para*-phénylène vinylène) (N-PPV) contenant des groupes amino sur le système vinylique (Schéma 5).

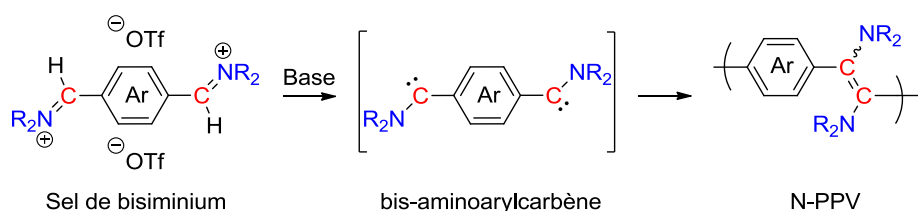


Schéma 5. Synthèse de PPV contenant des groupes amino sur la double liaison par dimérisation/polymérisation.

La synthèse et la caractérisation de trois précurseurs de bisaminoarylcarbènes présentant des fonctions amino et aryle variées a été réalisée *via* les voies non métalliques présentées au chapitre II (Figure 4). Il est important de préciser que ces dications sont extrêmement sensibles aux traces d'eau et doivent donc être manipulés avec grande précaution sous atmosphère inerte et dans des solvants très secs.

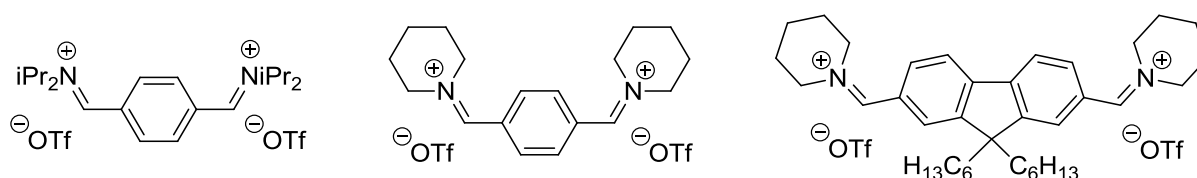


Figure 4. Précurseurs des bisaminoarylcarbènes étudiés.

La génération de nouveaux NPPV par dimérisations répétées de bis-aminoarylcarbènes, obtenus par déprotonation de leurs dications correspondant, a été étudiée. Lors de la réaction, la solution rouge obtenue atteste d'une extension de la conjugaison, laquelle est confirmée par analyse spectrophotométrique (voir Figure 5). Ces polymères, caractérisés par spectroscopie RMN ^1H , ont révélés un rapport E/Z similaire à leurs diaminoalcènes respectifs et la présence de fonction aldéhyde (provenant de l'hydrolyse des carbènes) en bouts de chaînes. L'intégration de ces bouts de chaînes par rapport au CH_3iPr donne un degré de polymérisation de 48.

Le DPn obtenu par chromatographie d'exclusion stérique (SEC) dans le THF est d'environ 10, ce qui est éloigné de celui trouvé par RMN ^1H . La valeur réelle devrait se situer entre ces deux valeurs extrêmes. Un $\overline{M}_n = 3000\text{-}5200 \text{ g.mol}^{-1}$ ($\text{Đ} = 2.05\text{-}2.08$) a également été obtenu. Les polymères étant π -conjugués, des analyses spectrophotométriques ont été effectuées. La comparaison entre les polymères et leurs modèles moléculaires respectifs par analyse UV/Vis montre un décalage global de leur maximum d'absorption vers le rouge pour la transition $n\text{-}\pi^*$ ($\lambda_{\text{max}} = 465 \text{ vs } 388 \text{ nm}$ respectivement), témoignant de l'allongement du système π -conjugué. La même tendance est observée avec leur spectres d'émission ($\lambda_{\text{max}} = 592 \text{ vs } 540 \text{ nm}$ respectivement) (Figure 5).

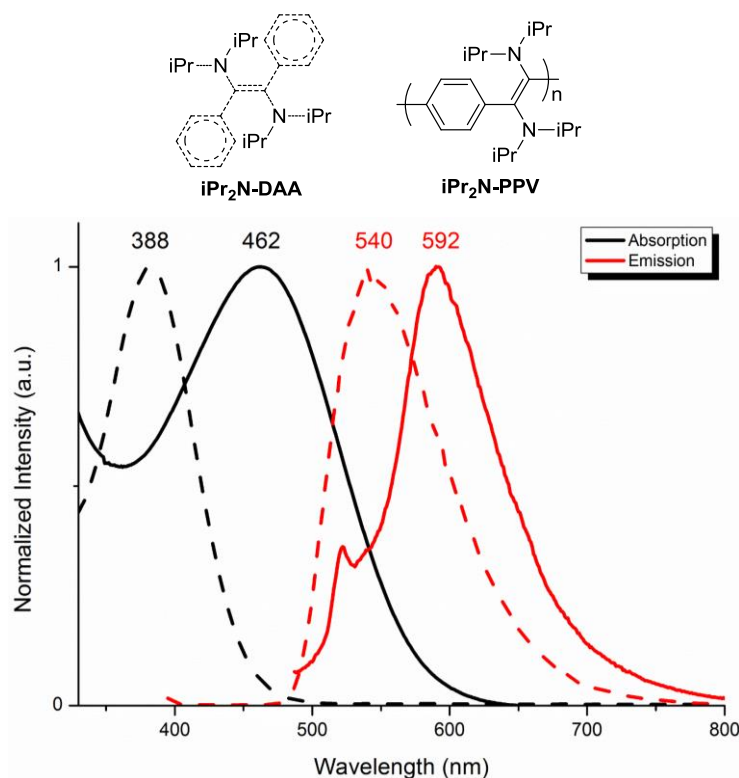


Figure 5. Spectres d'absorption et d'émission dans CHCl_3 de **$\text{iPr}_2\text{N-DAA}$** et **pipN-DAA** .

Il est également important de noter que grâce à un faible recouvrement entre les maxima d'émission et d'absorption, et une émission allant du domaine du visible jusqu'à l'infrarouge, ces polymères pourraient être de bons candidats pour des applications dans des dispositifs OLED.

Les N-PPV synthétisés ont la particularité de comporter deux fonctions amine sur chaque double liaison. Cette spécificité nous a conduit à envisager de modifier les propriétés des polymères par simple protonation ou méthylation de ces fonctions (Schéma 6).

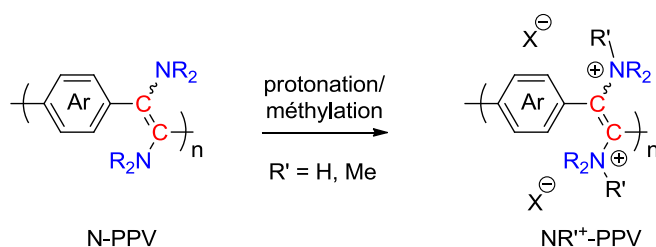


Schéma 6. Modifications des propriétés du polymère par protonation/méthylation des groupes amino.

La protonation par TfOH du polymère et dimère comportant un substituant diisopropyle (**$\text{iPr}_2\text{N-PPV}$** , **$\text{iPr}_2\text{N-DAA}$**) conduit à un effet hypsochrome sur la transition $n-\pi^*$ de leur absorption maximales. Ce résultat peut être attribué à la perte d'interaction entre la paire libre des atomes d'azote et les orbitales $\pi_{\text{C}=\text{C}}$, comme observé dans le cas du dimère où deux protons sont additionnés sur les atomes d'azote.

Malgré les similitudes entre **iPr₂N-PPV** et **pipN-PPV**, un comportement totalement différent a été observé lors de leur protonation. En effet pour le polymère **pipN-PPV** aucune transition n-π* n'a été observée, seule la transition π-π* correspondant au système carboné π étant conservée (Figure 6). Pour comprendre l'origine de ces différences, la protonation des deux diaminoalcènes modèles **pipN-DAA** et **iPr₂N-DAA** a été étudié. Tandis que la protonation des deux atomes d'azote est observée par diffraction des rayons-X pour le composé **iPr₂N-DAA**, pour le dimère **pipN-DAA** la protonation a lieu sur un atome d'azote et un atome de carbone de la double liaison C=C, interrompant la conjugaison au sein de la molécule et donc dans le polymère **pipN-PPV** par analogie. Dans les conditions utilisées, seul le polymère pipéridine peut être protoné et déprotoné de façon réversible (Figure 6).

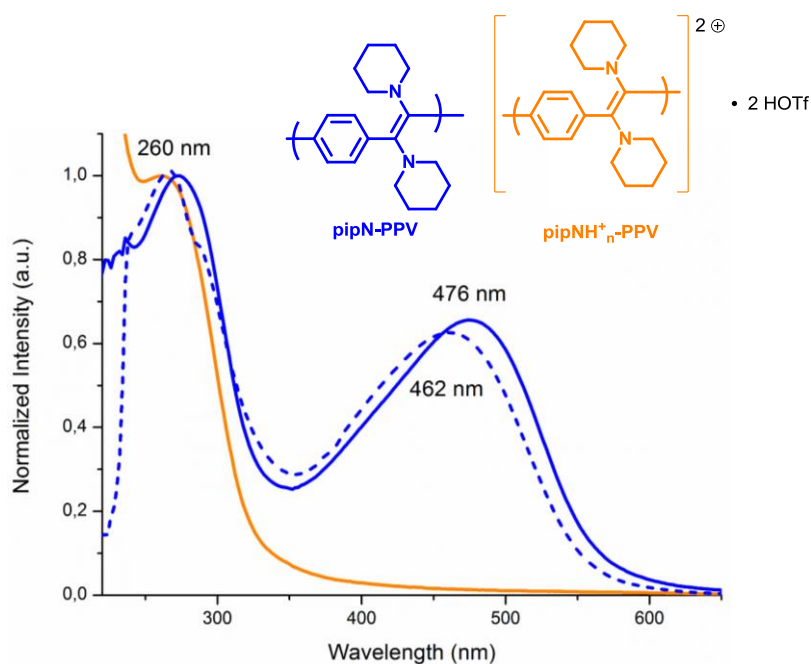


Figure 6. Analyse UV/Vis du polymère **pipN-PPV** avant (ligne bleu pleine) et après protonation (ligne orange) ainsi qu'après déprotonation (ligne bleu en pointillé).

La méthylation a aussi été tentée sur les composés modèles et n'a fonctionné qu'avec le substituant pipéridine, sans doute à cause de l'encombrement trop important du groupement iPr₂N.

Afin de compléter ce chapitre, des couches minces des polymères neutres ont été réalisées par dépôt à la tournette. Des problèmes de mouillabilité ont cependant été rencontrés dans le cas des polymères protonés. Dans le cas des polymères neutres, aucune conductivité n'a pu être observée. Pour le polymère protoné **iPr₂NH⁺-PPV** le même résultat a été obtenu, lequel pourrait être attribué à la mauvaise qualité des films. Malgré cela, la mesure de la conductivité électrique du polymère protoné **pipNH⁺PPV** tend à montrer que ce dernier est un polymère de type n, un type peu courant dans la chimie des polymères π-conjugués.

Dans le dernier chapitre, nous nous sommes intéressés à deux applications potentielles des diaminoalcènes (DAA). En effet, la présence de groupements amino sur la double liaison des dimères synthétisés rend ces molécules organiques très riches en électrons. On sait que les composés analogues portant 4 atomes d'azote sur la double liaison (c'est-à-dire les tétraaminoéthylène, TAA) sont de puissants agents réducteurs. Cependant, nos DAA ne possédant que deux atomes d'azotes, leur pouvoir réducteur devrait être plus faible. Ce défaut apparent s'avère être un avantage si ces composés sont utilisés en tant que catalyseurs organiques dans la polymérisation radicalaire par transfert d'atomes photo-induite (OATRP). Dans ce chapitre, nous avons ainsi décrit la caractérisation électrochimique du dimère **iPr₂N-DAA** et son utilisation comme agent réducteur stœchiométrique et photo-organocatalytique (Figure 7). Comme attendu, le dimère **iPr₂N-DAA** à l'état fondamental ($E_{1/2} = -0.137$ V vs SCE) ne peut pas concurrencer le TAA ($E_{1/2} = -0.61$ to -1.71 V vs SCE) pour la réduction des liaisons C-X (X = Br, I), ce qui a été confirmé expérimentalement. Nous avons ensuite testé la capacité du dimère à amorcer l'OATRP.

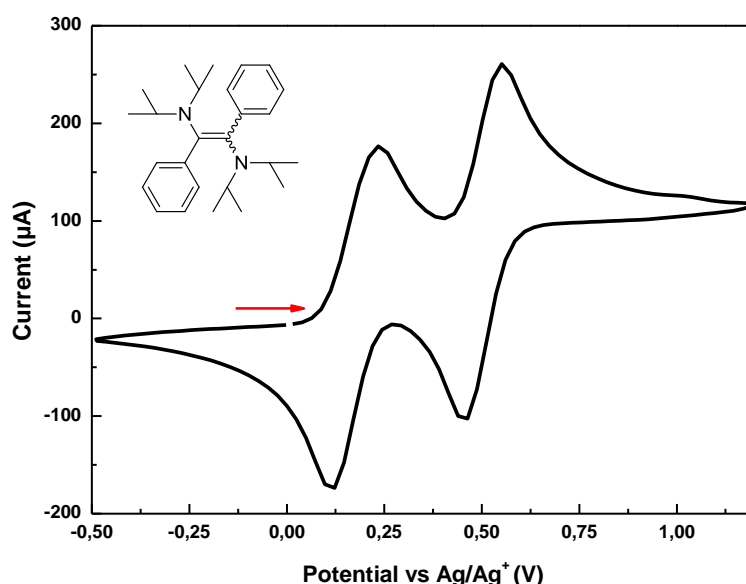


Figure 7. Voltammétrie cyclique du dimère **iPr₂N-DAA**. (0.1 M TBAPF₆/ACN, WE: Pt, CE: Pt, Ref: Ag, scan rate: 100mV.s⁻¹)

Historiquement, l'élimination complète des entités métalliques dans l'ATRP n'a été rendu possible que récemment (2012). L'utilisation d'un organocatalyseur spécifique a permis de synthétiser des polymères avec des fonctions en bout de chaînes, des masses molaires et des dispersités contrôlées. Dans ce domaine de recherche émergent, l'ATRP photoinduite sans métaux présente un large éventail d'avantages économiques et écologiques. La polymérisation radicalaire par des processus photochimiques dans des conditions douces permet ainsi un contrôle spatial et temporel à température ambiante et donne accès à des architectures macromoléculaires complexes. Plusieurs critères ont été

définis afin de disposer de photocatalyseurs (PC) de plus en plus efficace. Parmi eux, un PC doit absorber dans le spectre visible afin d'éviter de générer de réactions parasites pendant l'irradiation, présenter un faible potentiel d'oxydation à l'état fondamental et un potentiel de réduction élevé à l'état excité. En effet, un fort potentiel de réduction permet de réduire la liaison C-Br de l'amorceur, permettant d'initier la polymérisation. Le faible potentiel d'oxydation est nécessaire pour l'étape de désactivation où le complexe oxydé $PC^+\bullet Br^-$ désactive la chaîne en croissance et retourne à son état initial. Le dimère **iPr₂N-DAA**, qui remplit ces critères, a donc été testé dans la polymérisation du MMA par OATRP (Schéma 7).

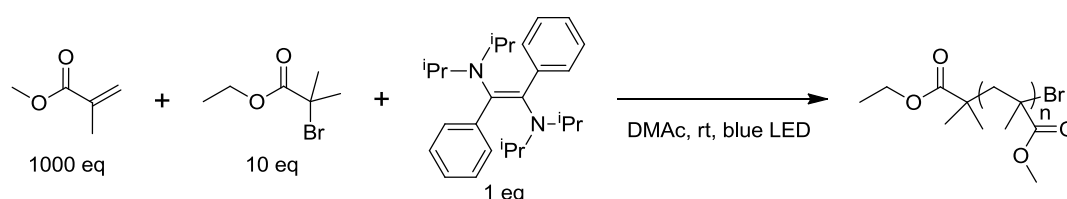


Schéma 7. Synthèse de PMMA par OATRP avec le dimère **iPr₂N-DAA**.

Ces expériences préliminaires ont révélé que **iPr₂N-DAA** joue le rôle de catalyseur puisque sans sa présence, aucune polymérisation n'est observée. Cependant, les polymères obtenus présentent une dispersité et une masse molaire supérieures à celles visées. Ceci peut être expliqué par l'incapacité du dimère oxydé **iPr₂N-DAA** à désactiver les chaînes en croissance et à retourner à son état fondamental, empêchant ainsi le cycle catalytique. Afin de contourner ce problème, il conviendrait donc d'optimiser la conception des catalyseurs (un meilleur potentiel d'oxydation à l'état fondamental par exemple) et les rendre plus efficaces pour permettre la synthèse de polymères bien définis.

La synthèse de nouveaux polymères PPV comportant des atomes d'azotes sur la double liaison n'est accessible que par la méthodologie originale développée dans notre laboratoire, basée sur la dimérisation de bis-aminoarylcabènes. La présence de ces groupements amino a permis par ailleurs de moduler les propriétés physicochimiques de ces polymères par simple protonation/méthylation. Dans le but de les intégrer dans des dispositifs électroniques, une optimisation de leur dépôt en couches minces doit cependant encore être effectuée. Sous forme protonée, ces polymères possèdent les propriétés des Poly(liquides ioniques) (PILs) en terme de conductivité ionique et la combinaison avec la conduction électronique est un aspect à aborder dans le futur.

1. N. S. Hush, *Ann. N. Y. Acad. Sci.*, 2003, **1006**, 1–20.
2. C. K. Chiang, C. R. Fincher, Y. W. Park, A. J. Heeger, H. Shirakawa, E. J. Louis, S. C. Gau and A. G. MacDiarmid, *Phys. Rev. Lett.*, 1977, **39**, 1098–1101.
3. R. S. Ashraf, B. C. Schroeder, H. A. Bronstein, Z. Huang, S. Thomas, R. J. Kline, C. J. Brabec, P. Rannou, T. D. Anthopoulos, J. R. Durrant and I. McCulloch, *Adv. Mater.*, 2013, **25**, 2029–2034.

4. Ö. Usluer, M. Abbas, G. Wantz, L. Vignau, L. Hirsch, E. Grana, C. Brochon, E. Cloutet and G. Hadziioannou, *ACS Macro Lett.*, 2014, **3**, 1134–1138.
5. D. Bourissou, O. Guerret, F. P. Gabbaï and G. Bertrand, *Chem. Rev.*, 2000, **100**, 39–92.
6. A. P. Dove, R. C. Pratt, B. G. G. Lohmeijer, H. Li, E. C. Hagberg, R. M. Waymouth and J. L. Hedrick, in *N-Heterocyclic Carbenes in Synthesis*, ed. S. P. Nolan, Wiley-VCH Verlag GmbH & Co. KGaA, Weinheim, Germany, 2006, pp. 275–296.
7. J. Vignolle, X. Cattoën and D. Bourissou, *Chem. Rev.*, 2009, **109**, 3333–3384.
8. M. N. Hopkinson, C. Richter, M. Schedler and F. Glorius, *Nature*, 2014, **510**, 485–496.
9. M. Otto, S. Conejero, Y. Canac, V. D. Romanenko, V. Rudzevitch and G. Bertrand, *J. Am. Chem. Soc.*, 2004, **126**, 1016–1017.
10. S. Conejero, Y. Canac, F. S. Tham and G. Bertrand, *Angew. Chem. Int. Ed.*, 2004, **43**, 4089–4093.

General Table of Contents

List of Abbreviations	III
French resume	VI
General Table of Content	XVI
General introduction	1
Chapter I: Similarities and differences between diaminocarbenes (DACs) and monoaminocarbenes (MACs) with special emphasis on the dimerization reaction	5
I.1 History.....	8
I.2 Ground state spin multiplicity of carbenes	9
I.2.1 Factors determining the spin multiplicity	9
I.2.2 Stabilization of carbenes	11
I.3 Stables carbenes	15
I.3.1 Push-push stabilized diamino and related amino-X carbenes (X =O,S)	17
I.3.2 Push-spectator Monoaminocarbenes	24
I.4 Common reactivity to mono and diaminocarbenes	37
I.4.1 Ligands for transition metals	38
I.4.2 Addition to cumulene (CCC, CS ₂ , CO ₂) and activated olefins.....	38
I.4.3 Insertion into activated C-H bonds and strongly polarized N-H, O-H bonds	38
I.5 The dimerization reaction	40
I.5.1 The wanzlick equilibrium	42
I.5.2 The dimerization reaction: mechanisms	45
I.5.3 Theoretical investigations of the carbene dimerization reaction.	55
I.5.4 Dimerization reaction: from molecular to polymer chemistry	66

II.4.3.3 Indirect dimerization	118
II.4.3.4 Investigation of side reactions	121
II.5 Isomerization of diaminoalkenes	124
II.6 Conclusion	126
II.7 Experimental Part.....	128
II.8 References	142
Chapter III: Synthesis of amino-PPV by metal free dimerization/polymerization of novel bis-aminoarylcarbenes....	145
III.1. Introduction.....	147
III.1.1 PPV synthesized from metal-based strategies	148
III.1.2 Synthetic access to PPV from transition metal-free routes.....	150
III.1.2.1 Synthesis of PPV from non-conjugated pre-polymers (<i>via</i> precursor routes) ..	150
III.1.2.2 Formation of PPV-like derivatives <i>via</i> direct routes.....	153
III.1.2.3 Electrochemistry	156
III.2 Synthesis of bis-iminium precursors	158
III.2.1 Alder's route.....	159
III.2.2 The Schroth's route	162
III.3 Synthesis of new amino-containing PPV derivatives through dimerization/polymerization of <i>in-situ</i> generated bis-aminoarylcarbenes	163
III.3.1 Synthesis of N-PPV's.....	163
III.3.2 N-PPV characterizations	164

III.3.3 Optoelectronic properties	167
III.4 Physicochemical properties of polymers and their model compounds.	173
III.4.1 Chemical modifications on the iPr_2N -PPV and iPr_2N -DAA	173
III.4.1.1 Modification of Polymer iPr_2N -PPV	173
III.4.1.2 Modification of dimer iPr_2N -DAA	175
III.4.1.3 Optical properties	184
III.4.1.4 Methylation of dimer iPr_2N -DAA	188
III.4.2 Chemical modifications on the $pipN$ -PPV and $pipN$ -DAA.....	190
III.4.2.1 Modification of Polymer $pipN$ -PPV	190
III.4.2.2 Modification of dimer with piperidine groups	193
III.4.3 Conductivity measurements	200
III.5 Conclusions.....	203
III.6 Experimental part.....	206
III.7 References.....	223
Chapter IV: Electron-rich diaminoalkenes as potential stoichiometric electron-transfer reagents or as organophotocatalysts	227
IV.1 Introduction	229
IV.1.1 Stoichiometric electron-transfer reagent.....	229
IV.1.1.1 Synthesis and stabilization.....	232
IV.1.1.2 Reactivity	235

IV.1.2 Photo-induced Organocatalyzed Atom Transfer Radical Polymerization (OATRP)	236
IV.1.2.1 Photoredox catalysis in molecular chemistry	236
IV.1.2.2 Photoredox catalysis in polymer chemistry	241
IV.2 Electrochemical and photo-physical characterizations of diaminoalkenes 19 with diisopropyl substituents.....	245
IV.2.2 Potential of oxidation.....	245
IV.2.1 UV absorption.....	249
IV.2.3 Excited state oxidation potential.....	249
IV.3 Photo-induced metal-free atom transfer radical polymerization	251
IV.4 Conclusion.....	258
IV.5 Experimental part	260
IV.6 References	263
General conclusion.....	267
Experimental part (general)	273
Materials.....	273
Characterization apparatus	273

General introduction

Although the preparation of π -conjugated polymers was described in the early 20th,¹ in depth investigation of their properties was performed following the work of Hideki Shirakawa, Alan G. MacDiarmid and Alan J. Heeger in 1977, on the semi-conducting property of polyacetylene (Figure 1).²

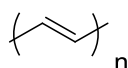
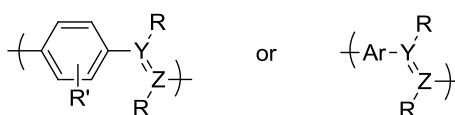


Figure 1. Polyacetylene structure.

Synthetic routes to semiconducting polymers usually rely on complex protocols using costly and non-renewable metal catalysts. Although the presence of metallic catalysts during the chain or step-by-step polymerization allows high selectivity and fast kinetic to be reached, their removal from the final material is a non-trivial process. Furthermore, the presence of residual metal traces into the final polymer may strongly affect their optoelectronic performances.^{3,4} Therefore, increasing interest has been devoted to develop alternative metal-free strategies to overcome such limitation. In this context, PPV, which represents one of the most studied π -conjugated polymer and are among the most efficient semi-conducting polymers for application in optoelectronics, has been targeted as model polymer (Figure 2).



Y, Z = C, N, O, S ...

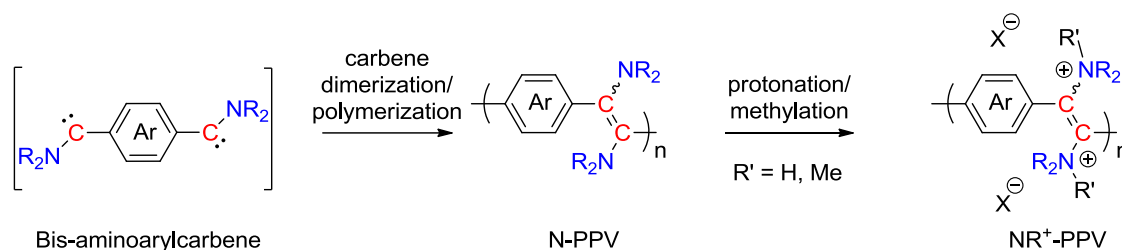
R', R = alkyl, electron-withdrawing or electron-donating substituent

Ar = conjugated cyclic structures

Figure 2. General structure of targeted PPV-like polymers.

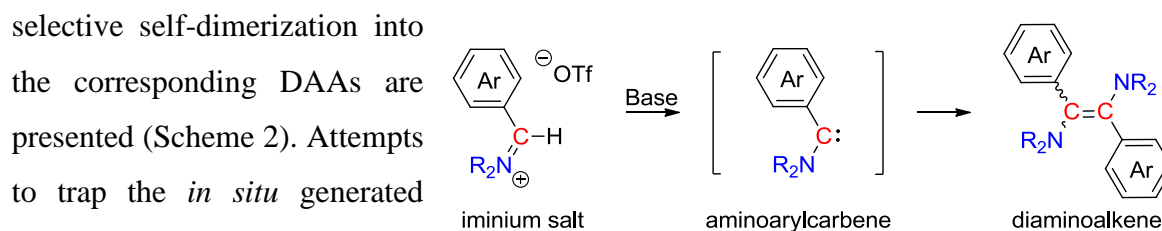
Although different C-C bond coupling strategies may lead to PPV, we resonate that the formation of the C=C bond could result from the dimerization of the corresponding aminoarylcarbene. Moreover, in contrast to the few metal-free routes reported, this strategy allows the facile introduction of amino groups in α position of the C=C double bond, ultimately

leading to amino-containing PPV polymers whose optoelectronic properties may be easily tuned upon derivatization of the amino moieties (Scheme 1).



Scheme 1. Synthesis of N-PPV *via* the dimerization of bis-aminoarylcarbene and modification of N-PPV through protonation/methylation.

In comparison to cyclic diaminocarbenes (DACs), monoaminocarbenes (MACs) have only been scarcely studied. Thus, **chapter I** is dedicated to present the similarities and differences between DACs and MACs, in terms of reactivities and properties. Obviously, a special focus on their dimerization reaction is presented. The dimerization reaction of aminoarylcarbene into the corresponding diaminoalkene (DAA) was first investigated on monofunctional compound in **chapter II**. First, the generation of MAC by deprotonation of its conjugated acid and its



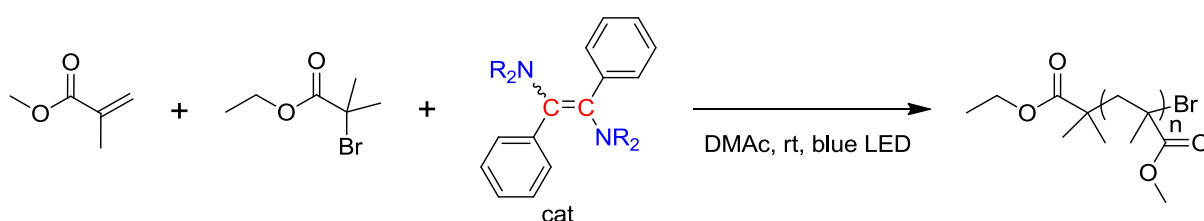
Scheme 2. Formation and dimerization of monoaminoarylcarbene

selective self-dimerization into

the corresponding DAAs are presented (Scheme 2). Attempts to trap the *in situ* generated aminoarylcarbenes with electrophilic species are also discussed. Finally, the mechanism of dimerization is then studied both experimentally and by DFT calculations.

The selective dimerization of monofunctional carbenes was transposed at the macromolecular level in **chapter III**, by designing hitherto unknown bis-carbenes monomers. Thus, deprotonation of bis-iminium salts afforded, upon dimerization/polymerization of *in situ* generated bis-carbenes, original N-PPV polymers, which were characterized by multiple techniques (Scheme 1). Chemical modifications of the amino groups on the double bond by protonation was performed to investigate their influence on the optoelectronic properties. Similar experiments were performed on the model compounds to rationalize the behavior of N-PPVs. Finally, electrical characterization of the polymers as thin films was performed in order to determine the type (n or p) of the N-PPVs semi-conducting polymers.

In the **last chapter**, preliminary experiments related to the potential applications of DAAs are presented. Because, diaminoalkenes are electron-rich molecules thanks to the interaction of two amino groups with the central C=C bond. They were first tested as organic reducing reagent. Moreover, several properties of diaminoalkenes fit with those required for efficient organophotocatalyst in Organocatalyzed Atom Transfer Radical Polymerization. Thus, preliminary investigation of their use as photocatalyst in the polymerization of methyl methacrylate (MMA) under irradiation is presented (Scheme 3).



Scheme 3. Synthesis of PMMA via Organocatalyzed Atom Transfer Radical polymerization of MMA in presence of diaminoalkenes under blue irradiation.

Chapter I: Similarities and differences between diaminocarbenes (DACs) and monoaminocarbenes (MACs) with special emphasis on the dimerization reaction

**Chapter I: Similarities and differences
between diaminocarbenes (DACs) and
monoaminocarbenes (MACs) with special
emphasis on the dimerization reaction**

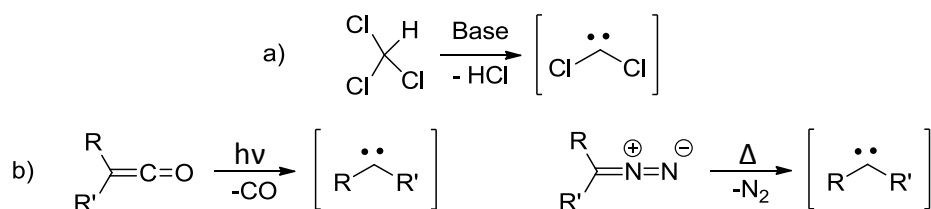
Chapter I: Similarities and differences between diaminocarbenes (DACs) and monoaminocarbenes (MACs) with special emphasis on the dimerization reaction

Chapter I: Similarities and differences between diaminocarbenes (DACs) and monoaminocarbenes (MACs) with special emphasis on the dimerization reaction

The goal of this chapter is to introduce carbenes as reaction partners that can dimerize to generate C=C double bond and access new electron-rich molecules. Indeed, the center of interest of this PhD work is the study of the dimerization reaction of tailored aminoarylcarbenes leading to new diaminoalkenes (DAA) (see chapter II). This dimerization reaction can be adapted to access new π -conjugated amino-poly(phenylene vinylene) (N-PPV) polymers *via* the use of bis-aminoarylcarbenes (see chapter III). This bibliographic chapter will introduce: first, the discovery and stabilization modes of carbenes. Then, the specific and common reactivity of stable carbenes, namely monoaminocarbenes and diaminocarbenes will be discussed. Finally, a focus on the dimerization reaction of such carbenes will be presented.

Introduction

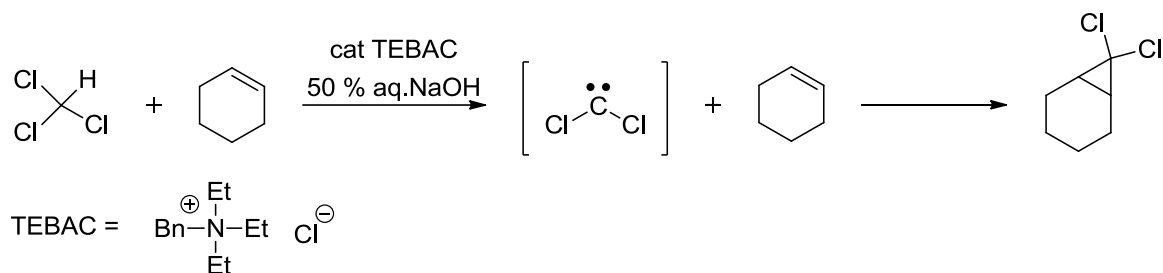
Carbenes are a particular form of low valent carbon species. In nature, carbon is usually tetravalent and abundant in this form. Nevertheless, carbon atom can exist with a valence of only two in carbenes or three in carbocations, carbanions and free radicals.^{1,2} The divalent carbene species we are focusing on are highly reactive with lifetime of less than 1s. They can be trapped in matrices at low temperatures (<77K),³ giving access to their spectroscopic characterization. Historically, transient carbenes have been generated following two main routes: (a) *via* dehydrohalogenation, *i.e.* an α -elimination promoted by a base as, for instance, in the generation of dichlorocarbene,⁴ (b) *via* thermal or photochemical decomposition of cumulenic-type compounds such as ketenes or diazocompounds (Scheme I.1).⁵⁻⁹



Scheme I.1. Generation of carbenes by a) dehydrohalogenation b) thermolysis of diazocompounds (right) and photolysis of ketenes (left).⁴⁻⁹

Due to their fugacity, carbenes have generally been trapped as exemplified with the cyclopropanation of cyclohexene by the *in-situ* generated dichlorocarbene (Scheme I.2).^{10,11}

Chapter I: Similarities and differences between diaminocarbenes (DACs) and monoaminocarbenes (MACs) with special emphasis on the dimerization reaction



Scheme I.2. Trapping of transient dihalogenocarbene with cyclohexane to yield the corresponding dihalogenocyclopropane; TEBAC: Benzyltriethylammonium chloride.¹¹

I.1 History

Pioneering studies on carbenes date back to 1835 with the first attempt by to prepare the parent carbene ($:\text{CH}_2$) by dehydration of methanol. It is noteworthy that, at that time, the tetravalency of carbon was not yet established. In the early 20s, studies by Curtius¹² and Staudinger¹³, on the decomposition of diazo compounds, recognized carbenes as highly reactive species. Undoubtedly, the non-respect of the octet rule with their six electrons in their valence shell, was at the origin of their fugacity. In parallel, the first carbene transition-metal complexes were synthesized by Tschugajeff,¹⁴ but also by Fischer¹⁵, Ofele¹⁶ and Lappert¹⁷, paving the way for the use of carbenes as ligands in organometallic chemistry. Besides, carbenes on their own became more popular in the 1940s, thanks to the cyclopropanation reaction discovered by Doering¹⁰. A few years later, Breslow¹⁸ and Wanzlick¹⁹ observed that carbenes containing amino substituents, such as bis-[1,3-diphenyl-2-imidazolidinylidene], exhibited higher thermodynamic stability. Although, only “carbene dimer” could be isolated because of the insufficient kinetic stabilization provided by the phenyl substituents on the nitrogen atoms.

The first stable singlet carbene was isolated by Bertrand *et al.*²⁰ in 1988 as an acyclic phosphinosilyl carbene, followed by the isolation of cyclic diaminocarbenes namely *N*-heterocyclic carbene (NHC) by Arduengo in 1991.²¹ However, suitable single crystals for XRay diffraction analyses of phosphinosilyl carbene were only obtained 12 years later,²² allowing a better insight into their stabilization mode to be gained. These two pioneering studies definitely paved the way toward the development of carbene chemistry with stable species.

Another breakthrough in carbene chemistry concerns the synthesis of persistent carbenes with a triplet ground state by Tomioka *et al.*²³⁻²⁵ In particular, amino-containing carbenes, such as

Chapter I: Similarities and differences between diaminocarbenes (DACs) and monoaminocarbenes (MACs) with special emphasis on the dimerization reaction

DACs or MACs have been raised from laboratory curiosities to molecules of enormous practical significance, as these compounds could be involved in numerous industry applications. Indeed, they proved to be excellent ligands for transition metals,^{17,26–34} leading to highly active, yet stable, catalysts for a variety of transformation, such as the metathesis of olefins.³⁵ They also exhibit unique properties, which allow the stabilization of a great variety of low valent main group compounds but also a spectacular reactivity in carbene-mediated organocatalyzed transformations.^{36–43}

I.2 Ground state spin multiplicity of carbenes

I.2.1 Factors determining the spin multiplicity

Carbenes possess only six electrons in their valence shell. Four of these electrons participate in σ -bonds with two adjacent substituents and the two remaining non-bonding electrons can be placed in different manners, depending on the energy difference between the sp^2 (σ) and p (p_π) frontier orbitals. The ground state multiplicity is dictated by the geometry around the carbene center, which is related to its degree of hybridization. The linear geometry involves an sp -hybridized carbene center with two degenerated orbitals (p_x and p_y). By bending the molecule, this degeneracy is broken leading to a sp^2 -type hybridization of the carbon atom. Thus, while the p_x orbital gains in stability by acquiring some s character (called σ), the p_y orbitals remains relatively unchanged (called p_π) (Figure I.1). The linear geometry defines the limit of the widening angle at the carbene center, but most of synthesized carbenes contain an sp^2 -hybridized carbon atom, making their geometry bent and not linear.^{44–47,36,48}

Chapter I: Similarities and differences between diaminocarbenes (DACs) and monoaminocarbenes (MACs) with special emphasis on the dimerization reaction

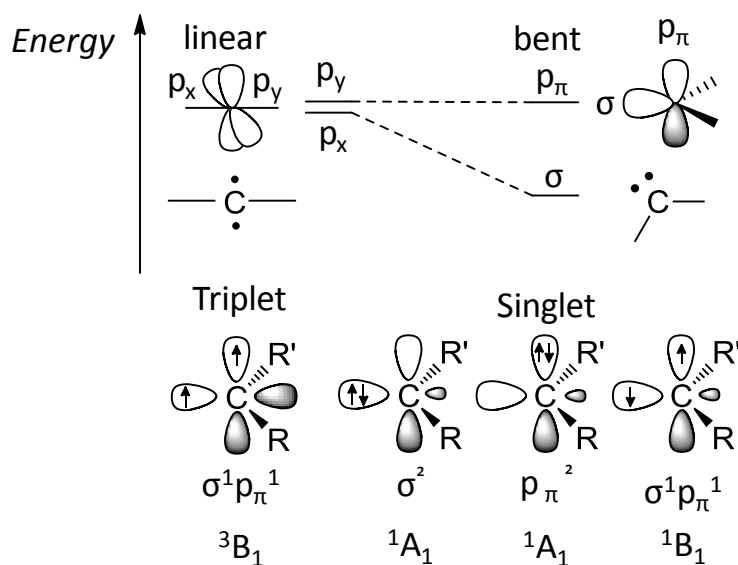


Figure I.1. Electronic configurations of carbenes and relative energy of frontiers orbitals.⁴⁹

Four electronic configurations can be envisaged (Figure I.1). The two non-bonding electrons can be located in two different orbitals (p_x and p_y) with parallel spins (triplet state); and the molecule is linear and is described by the $\sigma^1 p_\pi^1$ configuration (3B_1 state). On the other hand, for singlet carbenes, the two non-bonding electrons can be paired with an antiparallel spin orientation in the σ or p_π orbital (1A_1 states). The σ^2 ground state is usually more stable than the p_π^2 . In addition, an excited singlet state, where the two electrons are located in the p_π and σ orbitals with antiparallel spins can be envisaged too (1B_1 state).

The ground-state multiplicity eventually determines the properties and the reactivity of a carbene.^{49,50} **Singlet carbenes** feature a filled sp^2 (σ) and a vacant p (π) orbitals and therefore display an ambiphilic behavior; they are both nucleophilic and electrophilic. In contrast, **triplet carbenes** have two singly occupied orbitals and can be considered as diradicals; they are thus highly reactive. The energy difference between σ and p_π orbitals determines the multiplicity of the ground state. A large σ - p_π separation will favor the singlet ground state 1A_1 if $\Delta E_{ST} > 2$ eV, as calculated by Hoffmann.⁵¹ If the energy difference (ΔE_{ST}) is below 1.5 eV, a triplet 1B_1 ground state will be favored. The ground state spin multiplicity strongly depends on the substituents attached to the carbene center.

Chapter I: Similarities and differences between diaminocarbenes (DACs) and monoaminocarbenes (MACs) with special emphasis on the dimerization reaction

I.2.2 Stabilization of carbenes

Mainly two factors can affect the ground state multiplicity of a carbene. While in triplet carbenes, only a kinetic stabilization may result from the introduction of bulky substituents, singlet carbenes may benefit from both kinetic and thermodynamic stabilizations. In particular, unlike triplet carbenes, the use of suitable substituents allows the ΔE_{ST} gap to be increased by lowering the energy of the σ orbital and destabilizing the p_{π} orbital (thermodynamic stabilization).

I.2.2.1 Thermodynamic stabilization

I.2.2.1.1 Inductive effects

Singlet carbenes can mainly be thermodynamically stabilized *via* electronic effects (inductive and mesomeric) of both substituents. In absence of mesomeric effect, inductive effect may dictate the ground state spin multiplicity of carbenes.⁵²⁻⁵⁶ In the case of σ -electron withdrawing substituents (-I), the electron density at the carbene center is withdrawn (“pull”), leading to a stabilization of the σ non-bonding orbital, the p_{π} orbital remaining unchanged. As a result, the electronic gap σ - p_{π} is increased and thus, the singlet state is favored (Figure I.2). In contrast, for σ -electron-donating substituents (+I), the σ - p_{π} gap is reduced and the triplet state is favored, as in the case of the dilithiocarbene.^{57,58}

Chapter I: Similarities and differences between diaminocarbenes (DACs) and monoaminocarbenes (MACs) with special emphasis on the dimerization reaction

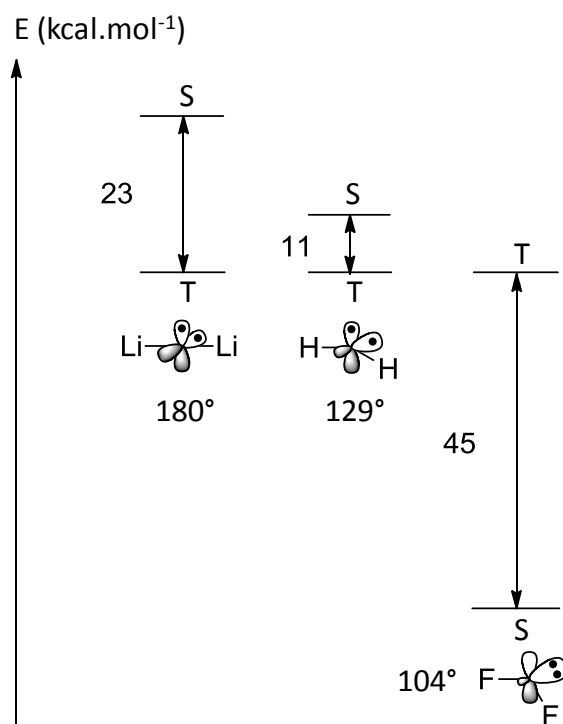


Figure I.2. Influence of the substituents electronegativity on the carbene ground state multiplicity.⁴⁹

1.2.2.1.2 Mesomeric effects

The second electronic effect consists in the interaction of the carbene carbon orbitals (σ , p_π or p_x , p_y) with the adequate p or π orbitals of the two substituents. The mesomeric effect (+M) involves the interaction of a p -type orbital of the substituent with the vacant p orbital of the carbene center. Groups such as $-F$, $Cl-$, $-Br$, $-I$, $-NR_2$, $-PR_2$, $-OR$, $-SR$, $-SR_3$, ... can be classified as π -electron donating groups. On the other hand, π -electron withdrawing groups ($-COR$, $-CN$, $-CF_3$, $-BR_2$, $-SIR_3$, $-PR_3^+$) interact with the filled sp^2 orbital of the carbene. Hence, singlet carbenes can be classified according to the stabilization brought by the mesomeric effect of their substituents: “**push**” for donating group (+M) and “**pull**” for withdrawing group (-M) (Figure I.3). Moreover, to maximize the stability of singlet carbenes, the electroneutrality of the carbene center should be maintained, as postulated by Pauling in 1960.⁵⁹ From the combination of the mesomeric effect of the two substituents, singlet carbenes can thus be stabilized in three different ways:

Chapter I: Similarities and differences between diaminocarbenes (DACs) and monoaminocarbenes (MACs) with special emphasis on the dimerization reaction

- The push-push stabilization (+M/+M) involves two π -electron donating (and σ -withdrawing) substituents. The most famous examples are the diaminocarbenes, with the archetypal NHCs, that are predicted to be bent singlet carbenes (σ^2).^{54,59,55} The lone pairs of electrons of each nitrogen atom strongly interact with the formally vacant p_π -orbital of the carbene center and thus enhance its electron density. Consequently, this increases the relative energy of the p_π orbital. In combination with their inductive effect (-I), the energy gap between the two frontier orbitals increases and therefore the singlet ground state is further stabilized (Figure I.3).
- The pull-pull stabilization is obtained from two π -withdrawing (and often σ -donating) substituents. Diborylcarbenes are good “putative” representatives, which are predicted to be linear despite their singlet ground state (π^2). In this case, the vacant p orbital of both substituents interacts with the filled p_y orbital of the carbene. This interaction does not change the p_x orbital and thus, the (p_x, p_y) degeneracy is broken which explains that they are linear with a singlet ground state (Figure I.3).^{54,59}
- The push-pull stabilization results from the combination of a π -donating and a π -withdrawing substituents. Phosphinosilyl and phosphinophosponiocarbenes are good representative examples of this category (Figure I.3).
- The push-spectator stabilization. Although most stable singlet carbenes are stabilized *via* two mesomerically active substituents, the work of Bertrand⁶⁰ on MACs has allowed to evidence a fourth stabilization mode, namely, the push-spectator. In this case, a single π -donating amino group is sufficient to stabilize such species. The other group remains spectator, at least from a mesomeric point of view. This type of stabilization can typically be found in amino-alkyl, -aryl, -phosphino, -phosphonio and -silyl-substituted carbenes (Figure I.3).

Chapter I: Similarities and differences between diaminocarbenes (DACs) and monoaminocarbenes (MACs) with special emphasis on the dimerization reaction

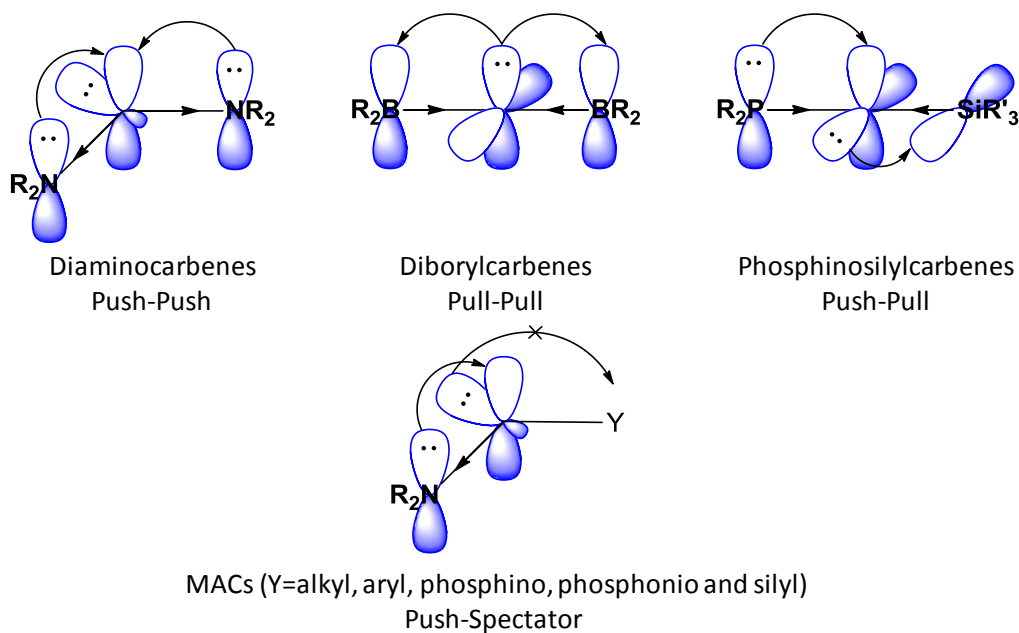


Figure I.3. Different stabilization modes of singlet carbenes.⁴⁹

1.2.2.2 Kinetic stabilization

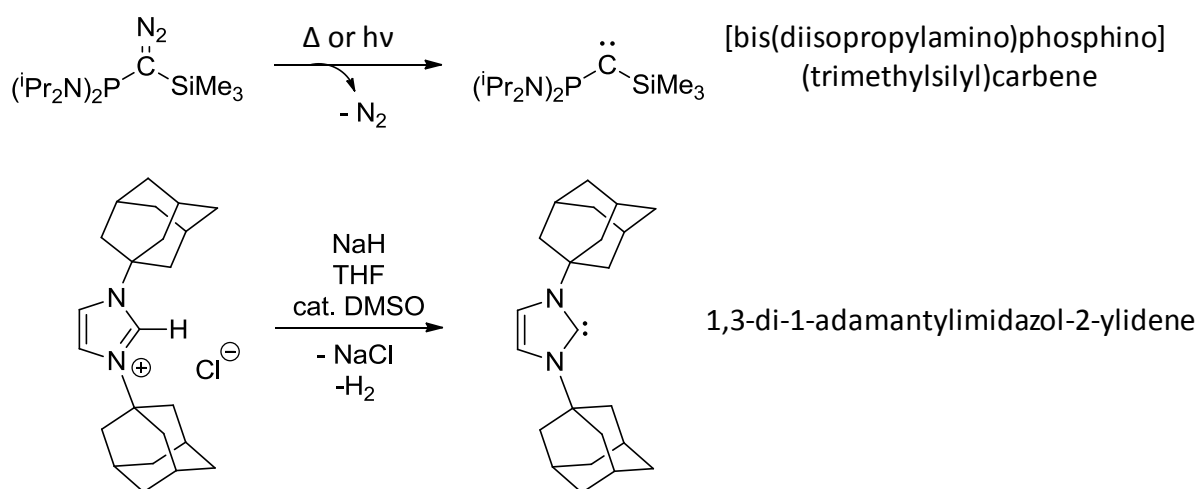
The kinetic stabilization involves bulky substituents to protect the electron-deficient carbene center of both singlet and triplet carbenes; such a stabilization may also dictate the ground-state multiplicity in the case where electronic effects are negligible. Bulky substituents will broaden the carbene bond angle and favor a linear geometry, and thus a triplet state. For instance, the dimethyl carbene has a bent geometry and a singlet ground state, while, the di-*tert*-butyl carbene has a triplet ground state and a linear geometry. In absence of sufficient steric bulk, dimerization of carbenes generally occurs. This particular reactivity will be detailed in section I.5. Only singlet carbenes will be considered in this chapter because they can be tamed to be characterized and handled as classical molecules. In particular, with suitable substituents, carbenes can be designed to be stable, while displaying the typical reactivity of their transient congeners, including H-migration, carbenoid coupling, cyclopropanation, C-H insertion and dimerization.

In the next part, the synthesis of the first stable carbenes is first presented. It is followed by the description of the properties and specific reactivities of the most important family of amino-containing carbenes, namely DACs and MACs.

Chapter I: Similarities and differences between diaminocarbenes (DACs) and monoaminocarbenes (MACs) with special emphasis on the dimerization reaction

1.3 Stables carbenes

The synthesis of two types of stable singlet carbene, namely, phosphinosilylcarbene and diaminocarbene (NHC), by Bertrand and Arduengo, respectively (Scheme I.3), in the 1990s allowed for a better understanding of their mode of stabilization, but also for studying the properties and reactivities of those novel compounds.^{20,21}



Scheme I.3. First stable carbenes synthesized by respectively Bertrand (up) and Arduengo (down).^{20,21}

The synthesis of phosphinosilylcarbene was performed through extrusion of N_2 from its diazo precursor, following a thermal or photochemical activation (Scheme I.3).²⁰ The phosphorus atom stabilizes the carbene center by π -donation of its lone pair of electrons into the vacant p_π orbital of the Csp^2 carbon atom (push effect), as represented by the mesomeric form II. The silicon atom induces a π -back donation of the carbene σ orbital into its σ^* orbital (pull effect), so that a cumulenlic structure (III) can be written. Alternatively, a phosphalkyne (IV) can be derived from the interaction between the negatively charged carbon atom and the phosphonium center. Overall, phosphinosilylcarbene benefit from a push-pull mode of stabilization and is best represented by the mesomeric form IV (Figure I.4). Moreover, because of the rather modest $\Delta E_{\text{S-T}}$ (11.1 kcal.mol⁻¹), this carbene has a reactivity close to its transient congeners, with the

Chapter I: Similarities and differences between diaminocarbenes (DACs) and monoaminocarbenes (MACs) with special emphasis on the dimerization reaction

ability to perform cyclopropanation, C-H insertion, coupling with carbenoids and the dimerization reaction as well.^{48,49}

In sharp contrast with the generation of the phosphinosilyl carbene, the synthesis of DACs involves the deprotonation of its corresponding imidazolium precursor with a strong base (Scheme I.3).²¹ Those carbenes have a push-push stabilization mode, where both amino groups stabilize the carbene by π -donation of their lone pairs of electrons into the vacant p_π orbital (Figure I.4). Such strong interaction result in a high lying LUMO and a very large ΔE_{S-T} (83.4 kcal.mol⁻¹). As a consequence, DACs do not display the typical reactivity of their transient congeners, but are excellent ligands for transition metals, and powerful organocatalysts because of their high Lewis basicity.^{27,34,36,61,62}

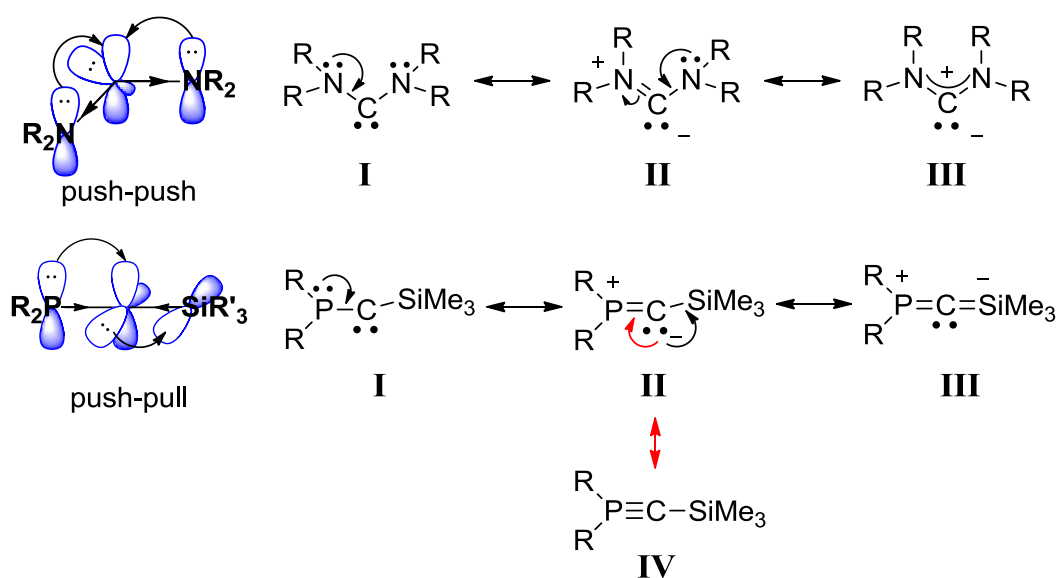


Figure I.4. Resonance structures of singlet carbenes according to their stabilization mode.

While the first stable carbenes involved two strongly interacting heteroatoms, a variety of stable singlet carbenes stabilized by the presence of a single amino or phosphino group, has also been described. Only diamino and monoamino-stabilized carbenes will be described in the following part, given that notable differences exist with phosphino-type carbenes, in particular regarding their synthesis and reactivity. In the next sections, push-push diamino and related amino-X carbenes (X = O,S...) will be first described. MACs, stabilized by a push-spectator mode, will then be presented and the reactivity of those carbenes will be compared.

Chapter I: Similarities and differences between diaminocarbenes (DACs) and monoaminocarbenes (MACs) with special emphasis on the dimerization reaction

1.3.1 Push-push stabilized diamino and related amino-X carbenes (X=O,S)

Push-push aminocarbenes are thermodynamically stabilized by +M effect *via* two strongly interacting heteroatoms with the carbene p-orbital (mesomeric effect); the σ orbital may also be stabilized by -I effect (inductive effect). They may also be additionally stabilized by aromaticity.

1.3.1.1 Structural diversity and synthesis

Since the first isolation in 1991 by Arduengo *et al.*²¹ of the 1,3-di-1-adamantylimidazol-2-ylidene (NHC) with adamantyl groups, NHCs of type **1** represent the archetypal cyclic diaminocarbenes that have been the most studied. The first diaminocarbene discovered was the cyclic unsaturated imidazole-2-ylidene **1**.²¹ The formal replacement of a carbon atom by a nitrogen atom in **1** leads to triazol-2-ylidenes **2**.⁶³ It was also possible to fuse a phenyl ring with the imidazole-2-ylidene **1** to give rise to benzimidazol-2-ylidene **3**.⁶⁴ Finally, the formal replacement of one amino group by a sulfur atom, affords the thiazol-2-ylidenes **4**.⁶⁵ The cyclic saturated diaminocarbene **5** could be synthesized with various ring size (from 5 to 7), the five-membered ring being the most popular.^{66,49} The phosphorus containing four-membered ring carbene **6** was also reported by Grubbs *et al.*⁶⁷

Apart from cyclic carbenes, a variety of stable acyclic diamino, aminoxy and aminothio carbenes have been described.^{68,69} Although, carbenes **10**, **11** and **12** are cyclic and contain 2 amino groups, their properties and reactivities contrast with those of aforementioned cyclic DACs. Indeed, the diaminocarbene **10** is much more electrophilic than NHCs because of the weaker +M effect of amido compared to amino substituents.⁷⁰ Similarly, the bicyclic structure of **11**⁷¹ with a bridgeheaded nitrogen atom prevents its planarization; as a consequence **11** can be considered as a push-spectator DACs since only one single nitrogen atom interacts with the carbene center. Accordingly, this carbene features a smaller ΔE_{S-T} than NHCs and thus some typical reactivity of their transient congeners. Cyclopropenylidene **12** represents a particular example of DACs, with both nitrogen atoms in β -position of the carbene center.⁷² The

Chapter I: Similarities and differences between diaminocarbenes (DACs) and monoaminocarbenes (MACs) with special emphasis on the dimerization reaction

3-membered ring system leads to a very acute carbene angle, which explains its stability and high nucleophilicity (Figure I.5).⁷⁰⁻⁷²

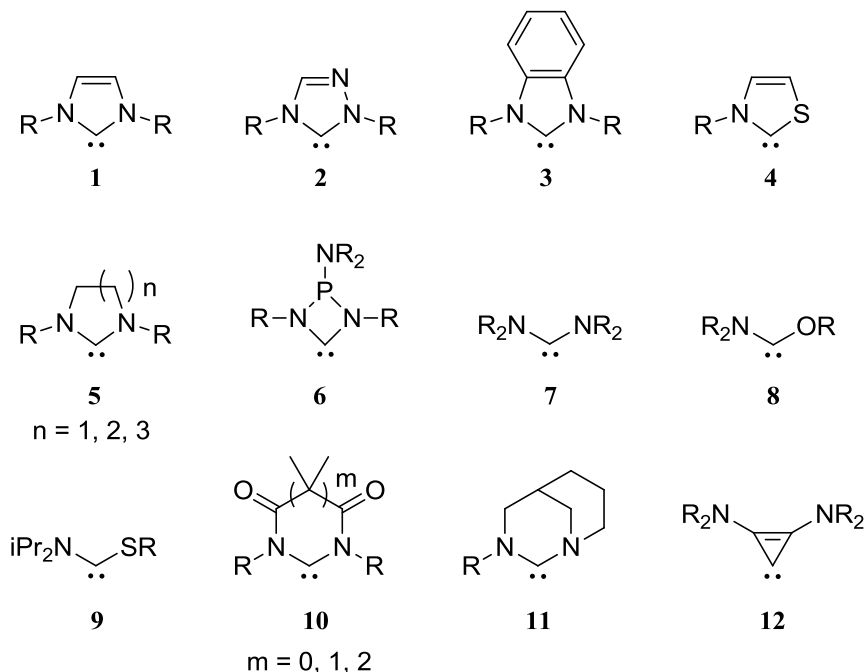
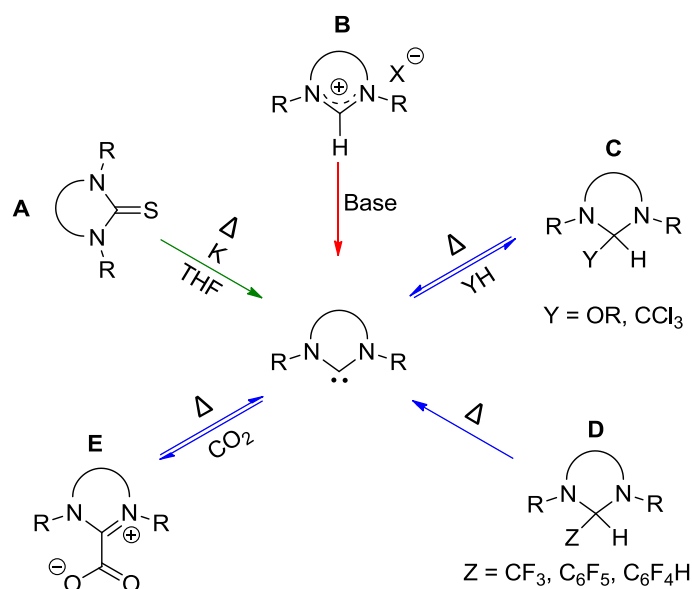


Figure I.5. Most representative push-push stabilized diamino and related amino-X carbenes (X = O, S).^{31,49,63,67,69-74}

The main route to access such carbenes relies on the deprotonation of the corresponding conjugated acid **B** with a strong base (Scheme I.4, in red). However, alternative routes have been developed.^{49,75} For instance, Kuhn *et al.* reported the reduction of cyclic unsaturated thiourea **A** with potassium in boiling THF (Scheme I.4, in green).⁷⁶ Alternatively, a variety of 1,1'-adducts, such as **C** or **D**, have been reported to generate the corresponding carbene, by α -elimination of a volatile small molecule, upon thermal activation.^{63,75} It is worthy to note that only saturated DACs, can be accessed in this way. While this reaction is reversible with **C**, the irreversibility of the α -elimination from adducts **D** originates from the weakly polarized CH bond involved. Lastly, because of the reversible reaction between DACs and CO₂, imidazoliumcarboxylate **E** are useful precursor for the *in situ* generation of DACs. This strategy also represents a powerfull way to make and unmake carbenes, thanks to this reversible carboxylation reaction.⁷⁷

However, with CS₂ the adducts obtained are thermally too stable (<200°C) and are not used to generate the free carbene (Scheme I.4, in blue).

Chapter I: Similarities and differences between diaminocarbenes (DACs) and monoaminocarbenes (MACs) with special emphasis on the dimerization reaction



Scheme I.4. Main routes to access diaminocarbenes by “the masked carbene strategy” (in blue), by deprotonation of iminium precursor (in red) and by thione reduction (in green).^{19,21,75,76,78}

1.3.1.2 Structural and electronic features of push-push amino containing carbenes

NMR Characterization

Carbenes can be unambiguously characterized by ^{13}C NMR spectroscopy because of their characteristic signature. Indeed, very downfield signals ($\delta = 189\text{-}296$ ppm) are observed for the carbene center, as compared to that of their iminium precursor ($\delta = 135\text{-}180$ ppm) (Figure I.6).

Chapter I: Similarities and differences between diaminocarbenes (DACs) and monoaminocarbenes (MACs) with special emphasis on the dimerization reaction

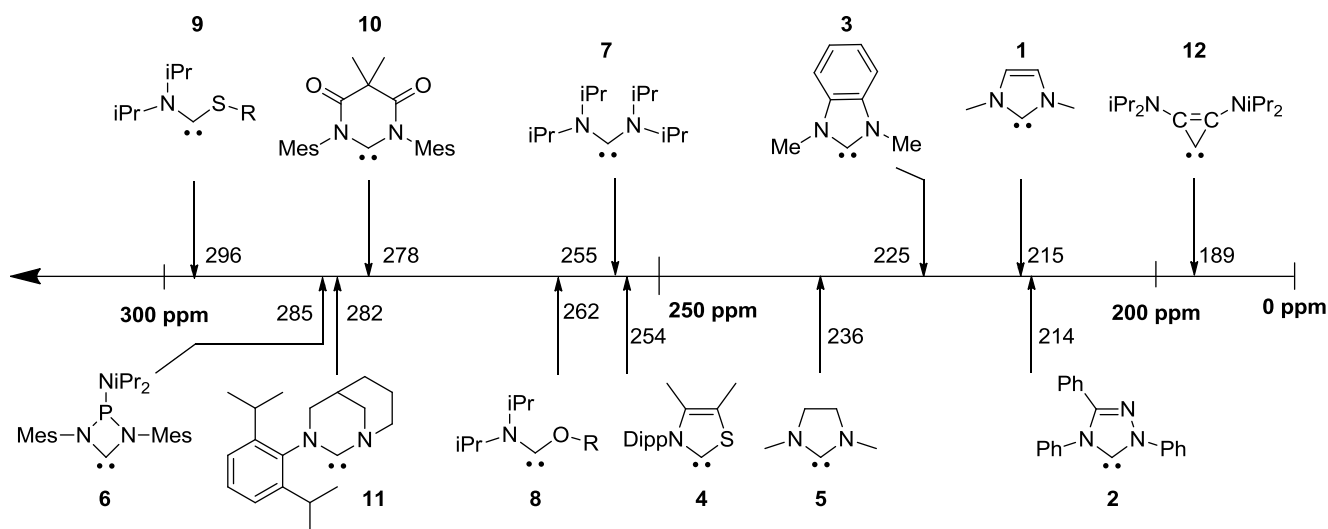


Figure I.6. ^{13}C NMR shifts of the carbenic carbon atom of push-push stabilized carbenes **1-12**.^{28,68-}

72,78-80

Structural characterization

The solid-state structure of the stable derivatives **1-12** has been elucidated by single-crystal X-ray diffraction. The first parameter obtained from the solid-structure is the N-C_{carbene} bond length. For each carbene, the CN bond distance lies between 1.34 and 1.36 Å, which is much shorter than a regular C-N bond (1.47 Å; Figure I.7). This bond distance results from the strong interaction between the amino groups and the carbene center. However, compared to a C-N_{azolium} bond (~1.30 Å), the N-C_{carbene} bond distance is longer because of the stronger amino/carbocation interaction in the azolium form. In the case of **8**, both heteroatoms are involved in the stabilization of the carbene center, as judged by the short N-C_{carbene} (1.32 Å) and O-C_{carbene} (1.38 Å) bonds. Yet, the N-C_{carbene} bond is shorter than in diaminocarbenes (1.35 Å) because the single amino group compensates the weaker ability of oxygen to donate its lone pair of electron into the p_π orbital of the carbene center (effect +M). Remarkably, despite the presence of two nitrogen atoms, **12** is stabilized by a push-spectator mode because of the bridgehead position of one amino group. Accordingly, significant differences are observed between the N-C_{carbene} bond lengths (1.35 Å and 1.40 Å for N-C_{carbene} and N_{pyramidal}-C_{carbene} respectively). This longer N_{pyramidal}-C_{carbene} length attests the weak or non-existent π -donation of the pyramidal nitrogen with the carbene center.

Chapter I: Similarities and differences between diaminocarbenes (DACs) and monoaminocarbenes (MACs) with special emphasis on the dimerization reaction

The second characteristic parameter is the carbene bond angle (N-C-X, X = N,O,S) that is found between 97 and 104° for 4- and 5-membered ring diaminocarbenes **1-6**.^{28,81} In particular cases the angle increases for 6-membered rings **5** (in red, 116°), **10** (114°) and **11** (113°), and 7-membered ring **10** (in green, 123°) respectively.^{71,74,82,83} This angle is wider for acyclic carbenes **7** (~121°), as they do not have any constraint due to acyclic structure. However, the presence of an oxygen instead of an amino reduces this angle to 109° for **8** (Figure I.7).⁶⁹ As expected, because of its 3-membered ring structure, **12** displays a narrower angle (57°)⁷².

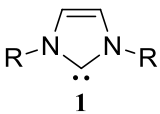
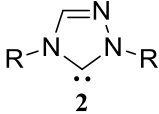
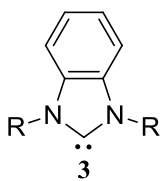
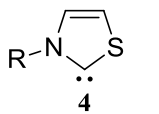
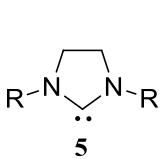
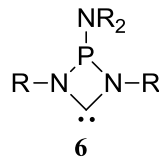
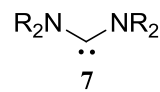
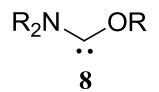
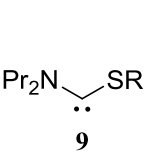
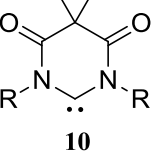
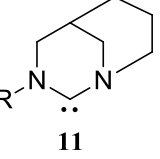
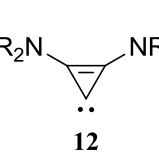
				
N-C-N [°]	102	100	104	104
NC _{carbene} [Å]	1.34	1.35	1.36	1.34
				
N-C-N [°]	106/116	97	121	109
NC _{carbene} [Å]	1.34/1.34	1.33	1.36/1.38	1.32
				
N-C-N [°]	not crystallized	114/123	113	57
NC _{carbene} [Å]		1.37/1.35	1.35	1.40

Figure I.7. X-ray analysis of most representative diaminocarbene types with their NC_{carbene}N angle and NC_{carbene} bond length. 6-membered carbene **5** is in red and 7-membered **10** is in green.^{49,63–65,67,69–72,81}

[Frontier orbitals](#)

Chapter I: Similarities and differences between diaminocarbenes (DACs) and monoaminocarbenes (MACs) with special emphasis on the dimerization reaction

The push-push stabilized diamino and amino-X carbenes are characterized by their singlet-triplet gap that is the gap between the HOMO and LUMO levels. The singlet ground state is favored when $\Delta E_{S-T} > 2\text{eV}$ according to the work Hoffmann *et al.*⁸⁴

Looking at their HOMO level, only a slight difference is observed between carbenes **1-5**, **7**, **10** and **12** (Figure I.8) with a value around $\sim -5\text{ eV}$ which makes them good nucleophile. Among them, acyclic diaminocarbenes, **7**, are the most nucleophilic with the highest HOMO level (-4 eV). For all carbenes, the LUMO is very high in energy due to the strong π -interaction of the two amino groups, which destabilizes the carbene $p\pi$ orbital. Therefore, diaminocarbenes are not electrophilic except in the case of the cyclic diamidocarbene **10**, which has a low-lying LUMO (Figure I.8). Cyclic DACs also possess a very large ΔE_{S-T} ($72.9\text{-}91.6\text{ kcal.mol}^{-1}$), so that they are only nucleophilic species. In sharp contrast, the weaker ability of amido groups to stabilize the carbene center results in very small ΔE_{S-T} of $27.5\text{ kcal.mol}^{-1}$ in **10**. As a result, an ambiphilic reactivity may be expected from **10**.^{73,85,86} Finally, the value of ΔE_{S-T} can somehow be translated into a measure of the thermodynamic stability of carbenes.

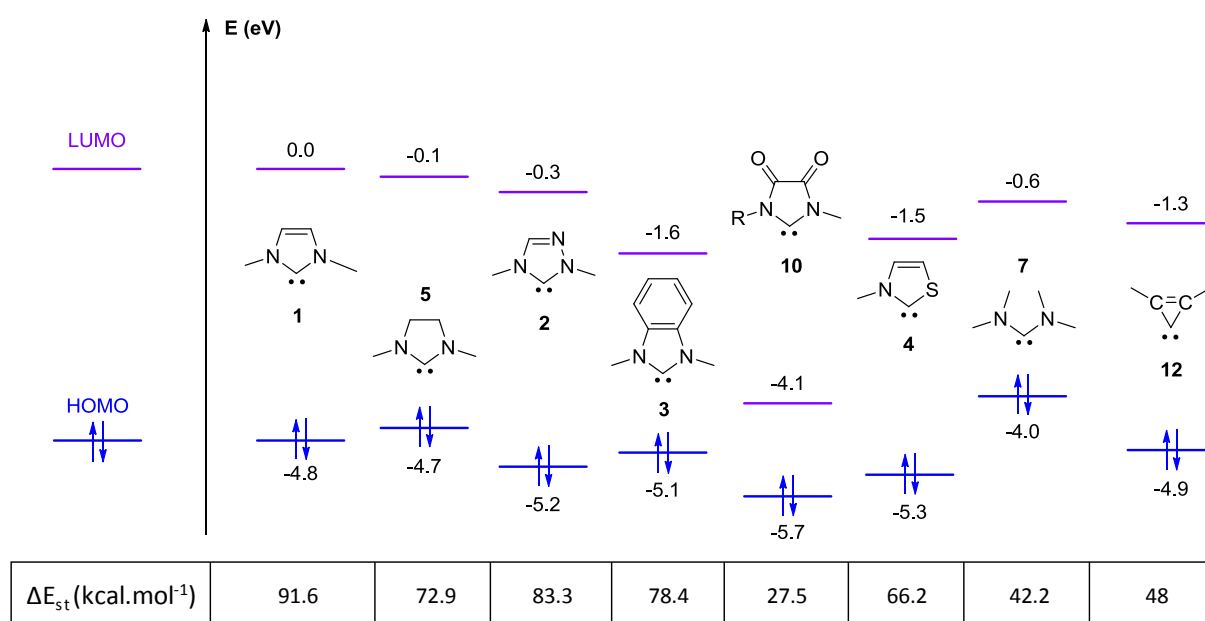


Figure I.8. Energy level of frontier orbitals (BP86/def2-TZVPP) of push-push amino-containing carbenes and their corresponding singlet-triplet gap.^{85,86}

1.3.1.3 Main reactivities

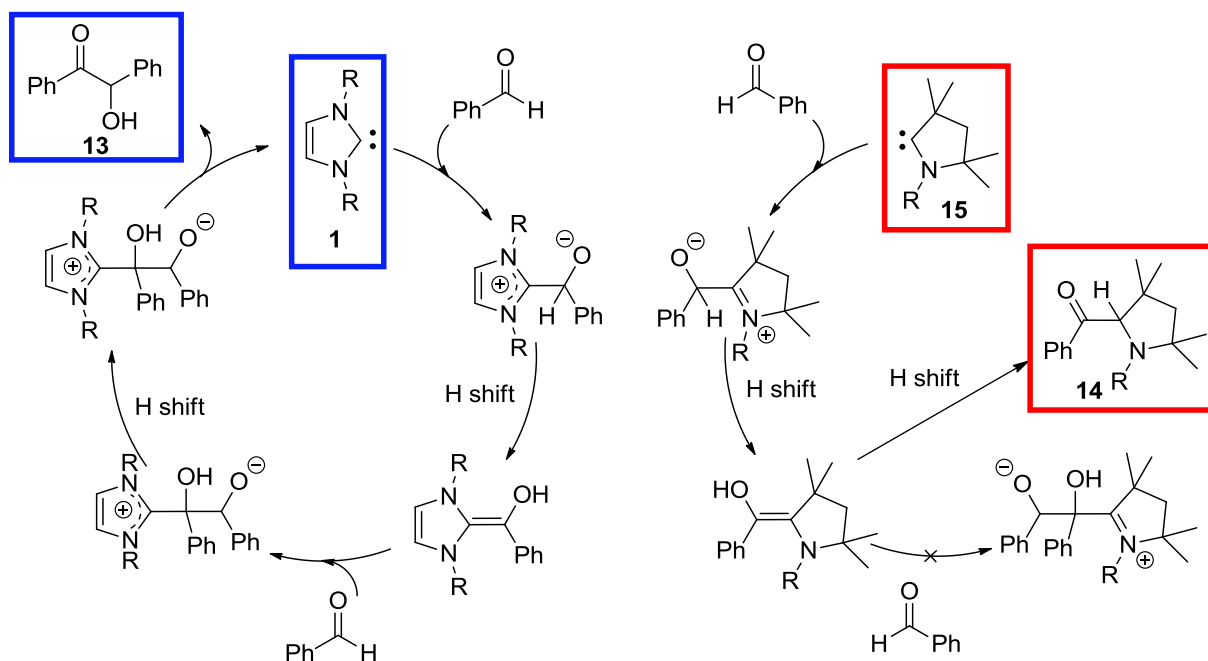
Chapter I: Similarities and differences between diaminocarbenes (DACs) and monoaminocarbenes (MACs) with special emphasis on the dimerization reaction

Because of the strong interaction of two heteroatoms with the carbene center, cyclic diaminocarbenes are not ambiphilic. In fact, they are mainly strongly nucleophilic and Lewis basic. They are thus excellent ligands for transition metals. Interestingly, cyclic DACs display a specific reactivity toward organic molecules; indeed, they are powerful nucleophilic and basic catalysts for various organic transformations (*i.e.*: benzoin condensation, Mukaiyama-aldol reaction...). They also react stoichiometrically with a variety of electrophiles, affording the corresponding adducts. Finally, such carbenes have also been shown to insert into polarized X-H bond (X = C, N, O) *via* a stepwise mechanism involving a deprotonation/addition sequence. Such reactivities, which are common to push-push cyclic DACs and push-spectator MACs, will be discussed in section I.4.

I.3.1.3.1 Specific reactivity: catalysis.

The specific properties of push-push stabilized diamino and amino-X carbenes (X = O, S) explain their ability to catalyze various reactions. This specificity results from the proper balance between their nucleophilicity and their leaving group ability. In fact, these properties are related to the position of their HOMO level. For example, in the benzoin condensation, the addition of push-push stabilized diaminocarbenes or push-spectator monoaminocarbenes leads to different final products. In the first case, addition of benzaldehyde to the cyclic unsaturated carbene **1** leads, after H-shift, to the Breslow intermediate. Addition of a second equivalent of benzaldehyde released the benzoin **13** and the starting carbene **1** upon H-shift. In the second case, the addition of benzaldehyde to carbene **15** led to the similar Breslow intermediate, which evolves into compound **14** upon H-shift. Same results as **15** were observed for carbenes **7**, **11** and MACs (Scheme I.5).

Chapter I: Similarities and differences between diaminocarbenes (DACs) and monoaminocarbenes (MACs) with special emphasis on the dimerization reaction



Scheme I.5. Mechanism for the catalytic benzoin condensation (carbene **1**) and formation of compounds **14** from carbenes **15**.⁸⁷

I.3.2 Push-spectator Monoaminocarbenes

I.3.2.1 Structure and synthesis

The synthesis of the first stable monoaminocarbene (MAC) *i.e.* the aminoarylcabene **27** (Scheme I.6) by Bertrand *et al.*⁶⁰ is a milestone in carbene chemistry, because it demonstrates that a single amino group is sufficient to thermodynamically stabilize the carbene center. In that example, the aryl group is spectator at least from a mesomeric point of view, because of the rather acute carbene bond angle (121°), which prevents the interaction between the σ orbital of the carbene and the π^* of the aryl moiety. Furthermore, this work has opened the door to a great variety of stable carbenes, with virtually unlimited choice of substituents providing that one amino group is present to stabilize the carbene.

Here are presented the most representative monoaminocarbenes **15-25** incorporating, alkyl, aryl, phosphonio, phosphino and silyl groups (Figure I.9). It is worth noting that most of stable MACs are acyclic.

Chapter I: Similarities and differences between diaminocarbenes (DACs) and monoaminocarbenes (MACs) with special emphasis on the dimerization reaction

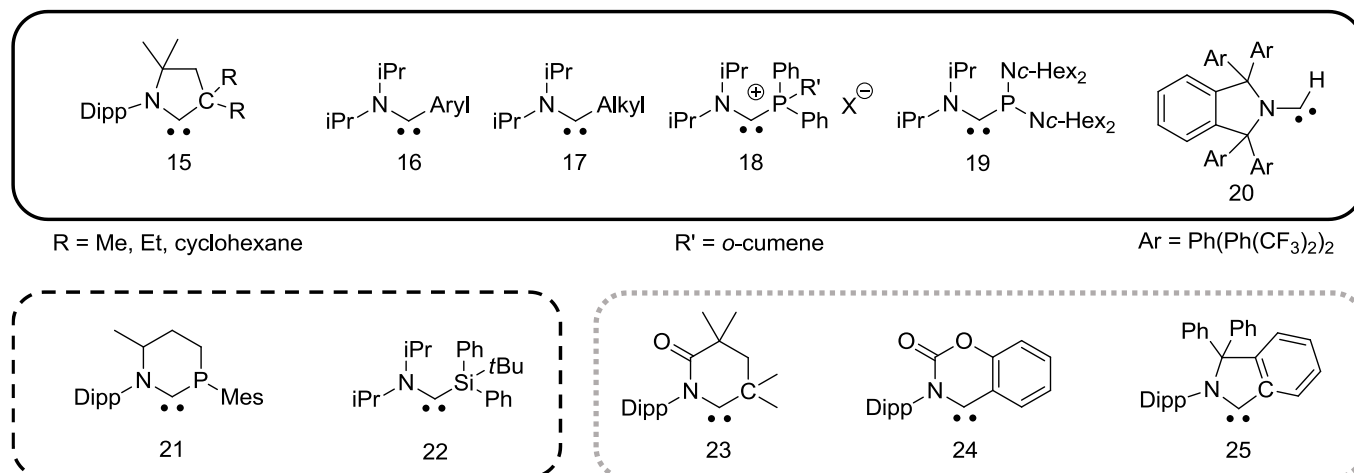
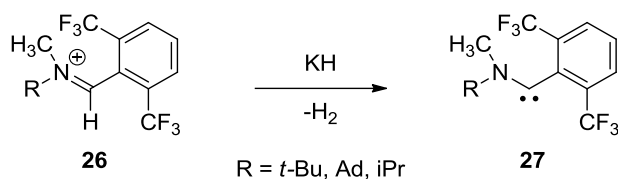


Figure I.9. Most representative example of stable (black), persistent (dotted black) and transient (grey) monoaminocarbenes.^{88–97}

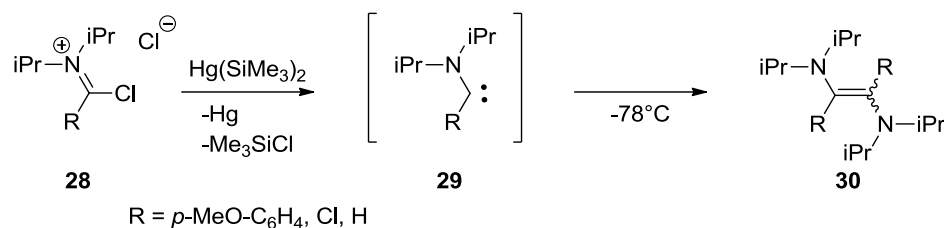
In general, these carbenes are generated similarly as their cyclic diamino counterparts, that is, by deprotonation of their corresponding iminium salt (Scheme I.6).⁶⁰



Scheme I.6. First stable monoaminoarylcarbene **27** obtained by deprotonation of its iminium precursor **26**.⁶⁰

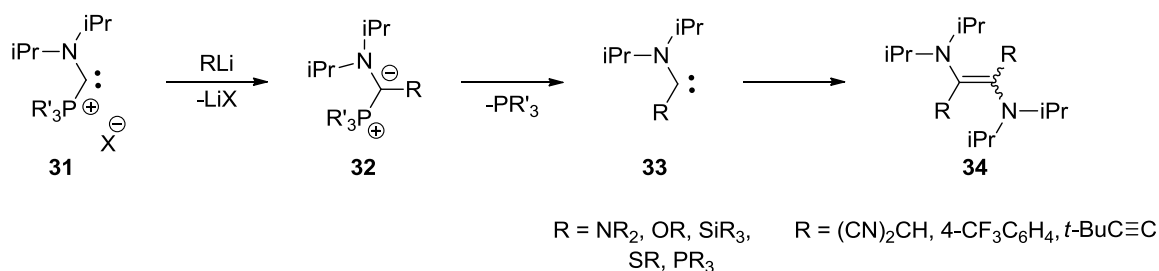
Alternatively, three other routes have been developed by Bertrand *et al.*^{90,98} The first one involves bis(trimethylsilyl)mercury and C-chloroiminium **28**. When R = *p*-MeO-C₆H₄, Cl or H, only the corresponding diaminoalkene **30**, likely resulting from the direct carbene dimerization, could be observed. Indeed, in this particular case, no proton can be involved to promote the indirect route. Moreover, compared to other methodologies, this synthetic route allows the generation of free carbene **29**, which is not complexed by any cation, as it is usually the case when strong anionic bases are used. (Scheme I.7).⁹⁸

Chapter I: Similarities and differences between diaminocarbenes (DACs) and monoaminocarbenes (MACs) with special emphasis on the dimerization reaction



Scheme I.7. Generation of free acyclic monoaminocarbene by reduction of a chloroiminium precursor with a mercury agent and further dimerization.⁹⁸

Another route relies on the nucleophilic substitution at the carbene center of a stable aminophosphino ylide intermediate, which fragments into the corresponding carbene, and one equivalent of phosphine. The ylide stability depends on the basicity of the phosphine, which is dictated by its substituents. For example, with phenyl substituents, only a complex mixture is observed by NMR. Replacing the phenyl on the phosphine by a cyclohexyl group leads to the corresponding ylide **32**, which can be characterized by ^{31}P NMR spectroscopy ($\delta = 14.9$ ppm). ^{31}P NMR spectroscopy allows following the ylide dissociation within a few minutes at -20°C to give a phosphane and the corresponding carbenes **33**. The latter further dimerizes instantly into **34**. Depending on the nature of the nucleophilic species, stable carbenes or transient carbenes (which dimerize instantaneously)⁹⁰ can be obtained (Scheme I.8). This powerful reaction also allows for the preparation of novel type of carbenes, such as aminosilylcarbene and aminophosphinocarbene, which could not be achieved by other routes.^{91,99}

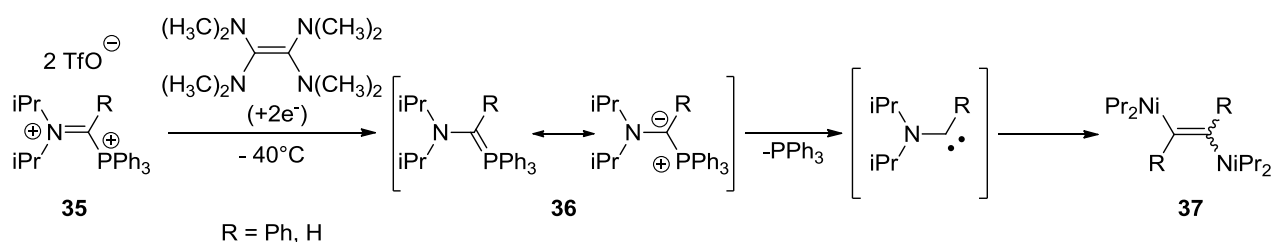


Scheme I.8. Nucleophilic substitution on aminophosphinocarbene to access the corresponding carbenes^{90,91}

The last route to access MACs involves the reduction of phosphonioiminium salts **35** by tetrakis(dimethylamino)ethylene (TDAE) at -40°C in acetonitrile. Here again, the resulting

Chapter I: Similarities and differences between diaminocarbenes (DACs) and monoaminocarbenes (MACs) with special emphasis on the dimerization reaction

aminophosphino ylide intermediate, **36**, fragments into the corresponding carbene and one equivalent of phosphine. As before the ylide can be isolated and characterized in the case of strongly basic phosphines, such as tris(dimethylamino)-phosphane. However, no fragmentation occurs. In contrast, with triphenylphosphane, ylide **36** dissociate into the phosphine and the corresponding carbene (Scheme I.9).¹⁰⁰ With small R groups such as H or Ph, the corresponding carbene is not stable and instantaneously dimerizes.



Scheme I.9. Reduction of phosphonioiminium dications with organic reducing agent.¹⁰⁰

Overall, these results demonstrate that, in contrast to cyclic diaminocarbenes, MACs may readily dimerize. Of particular interest, this dimerization appears to be selective when the carbene is suitably substituted, that is without methyl on the nitrogen atom, and no alkyl group in ortho position of the aromatic moiety.

In summary, among all of these monoaminocarbenes, only a few are stable enough to be characterized, and often, the second substituent group is not bulky enough to prevent its dimerization. In the next part, are discussed the main characteristics of isolable monoaminocarbenes.

1.3.2.2 Characteristics of monoaminocarbenes

Stable and persistent aminocarbenes have been successfully characterized *via* NMR analysis. The formal replacement of one nitrogen from diaminocarbene by a carbon atom gives a strongly downfield-shifted signals in ¹³C NMR spectroscopy for the carbene center. Indeed, as compared to diaminocarbenes showing signals between 189 and 296 ppm, monoaminocarbene signals resonate at even lower fields, *i.e.* between 300-380 ppm (Figure I.10).

Chapter I: Similarities and differences between diaminocarbenes (DACs) and monoaminocarbenes (MACs) with special emphasis on the dimerization reaction

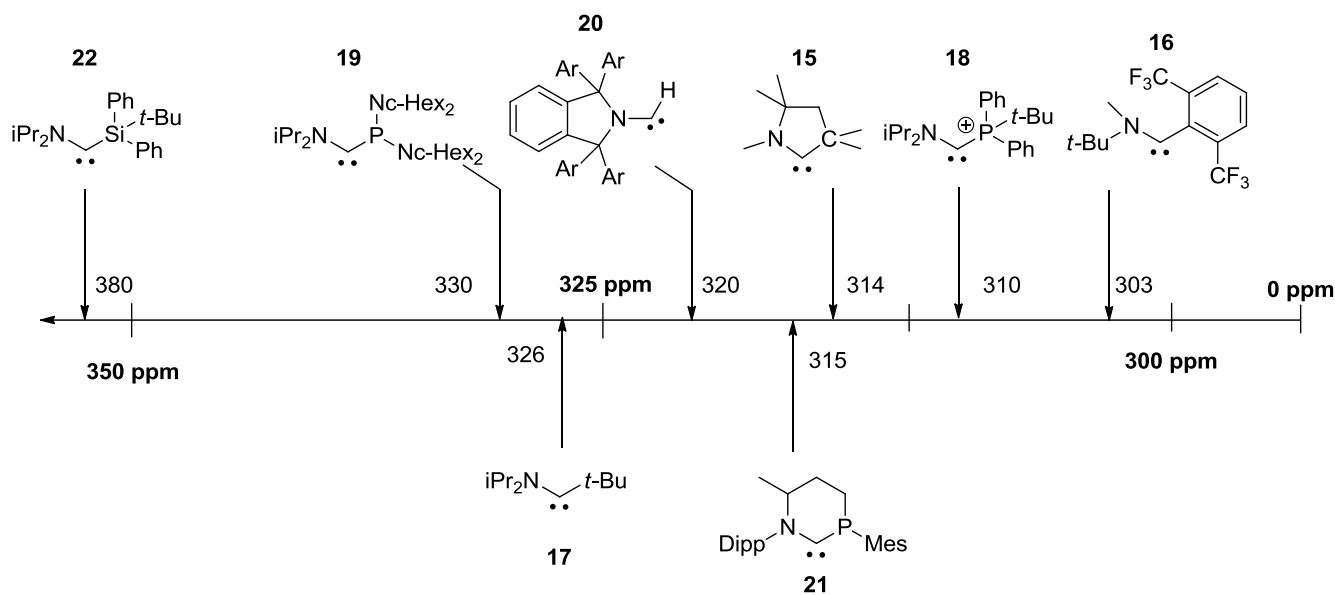


Figure I.10. Overview of the ^{13}C NMR chemical shift of monoaminocarbenes.^{48,73,88}

X-ray analysis on monocrystals of MACs has provided some insight into the stabilization mode of such species. In particular, they possess a very short N-C_{carbene} bond distance (1.28-1.32 Å), shorter than those observed for diaminocarbenes (1.35 Å). This reflects the stronger interaction of the single amino group with the carbene center in MAC, in comparison with diaminocarbenes. The carbene bond angle is very acute, which prevents any stabilization of the σ orbital by the second substituent X. Thus, each C_{carbene}-X bond distance (X = P, P⁺, Aryl) are simple bonds. This confirms the absence of interaction between the substituents, which are mesomeric spectators, and the carbene. For example, in the aminophosphinocarbene, the C-P bond length is characteristic of a single bond (1.85 Å) and the phosphorus atom remains pyramidal, confirming that the phosphine group is a mesomeric spectator (Figure I.11).

Chapter I: Similarities and differences between diaminocarbenes (DACs) and monoaminocarbenes (MACs) with special emphasis on the dimerization reaction

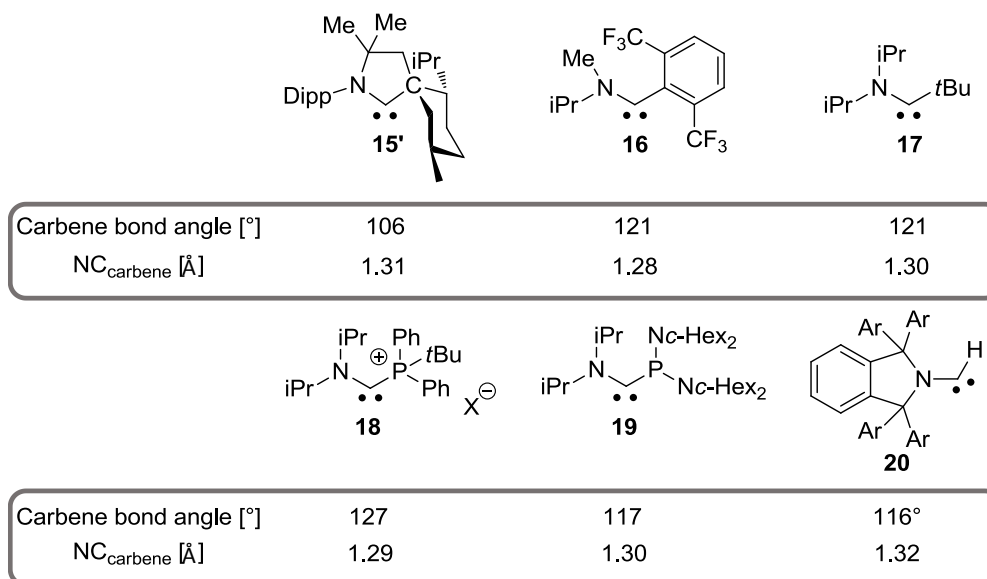


Figure I.11. NC_{carbene}C angles and NC_{Carbene} bond lengths obtained by X-ray measurements.^{48,60,97,101}

Finally, DFT calculations have been performed on MACs (**15**, **17**) to assess and compare their electronic properties. The singlet-triplet gap calculated (ΔE_{ST}) for MACs has been found smaller than the ones of diaminocarbenes (NHCs). For **15**, the gap of $\Delta E_{ST} = 45 \text{ kcal.mol}^{-1}$ is smaller than the $\Delta E_{ST} = 68 \text{ kcal.mol}^{-1}$ of its corresponding saturated diaminocarbene NHC **5**. The same trend is observed for the acyclic MACs **17** ($\Delta E_{ST} = 27 \text{ kcal.mol}^{-1}$), as compared to acyclic diaminocarbenes **7** ($\Delta E_{ST} = 58 \text{ kcal.mol}^{-1}$). Moreover, a small gap indicates that MACs have a more accessible LUMO, as compared to NHCs, which results from the presence of only one nitrogen atom next to the carbene center. As a result, MACs are much more electrophilic than DACs. The MACs have a higher HOMO, as compared to NHCs, which makes them better nucleophiles (**15**: -4.9 eV vs **5**: -5.2 eV ; **17**: -4.3 eV vs **7**: -5.2 eV).^{102,103,95} Moreover, acyclic carbenes are more nucleophilic than cyclic ones because of a larger carbene bond angle.

1.3.2.3 Specific reactivity of MACs

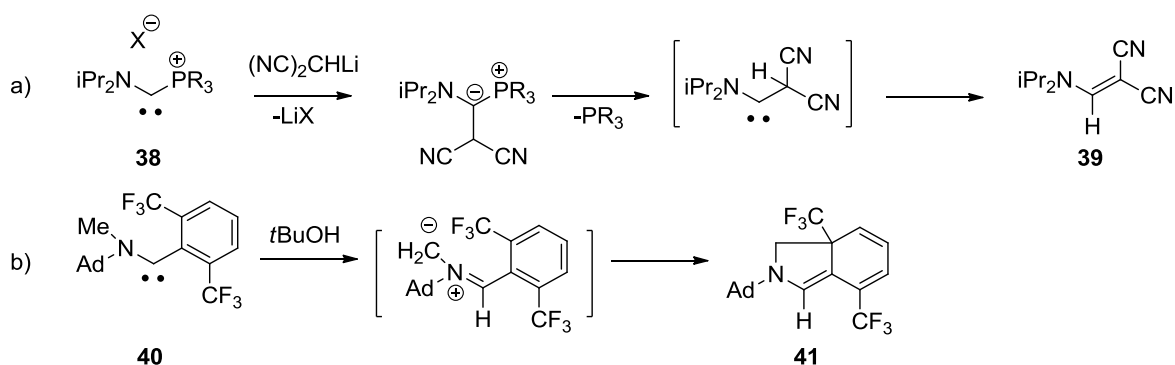
In comparison with push-push stabilized carbenes, where two heteroatoms strongly interact with the carbene center, the push-spectator stabilization of MACs affords a least perturbed character at the carbene center. In particular, their p orbital remains accessible enough so that MACs display an ambiphilic behavior, similar to that of their transient congeners (not stabilized by heteroatoms). They thus exhibit some specific and typical reactivity, including: insertion

Chapter I: Similarities and differences between diaminocarbenes (DACs) and monoaminocarbenes (MACs) with special emphasis on the dimerization reaction

into non activated C-H bond, cyclopropanation of olefins, intramolecular migration reactions and coupling with carbenoids. They can also activate enthalpically strong bonds such as H₂ and NH₃, which will be detailed hereafter. However, in contrast to diamino type carbenes, they are poor catalysts due to their low leaving group ability. In general, they have been shown to form different adducts in the presence of a variety of substrates (see Scheme I.5).⁸⁷

1.3.2.3.1 Migration reactions

Migrations are fundamental reactions, in particular 1,2-migration for transient singlet carbenes,^{104–108} which go through an unimolecular process. A 1,2-hydrogen shift was observed in the case of transient aminoalkylcarbenes **38** and **40** (Scheme I.10 a).^{90,92} A 1,3-hydrogen shift was also reported with an acyclic aminoarylcabene. In this reaction the carbene, which was generated by deprotonation with *t*-BuOK, was proposed to be protonated by the formed *t*-BuOH. Deprotonation of the N-methyl group by *t*-BuOK yielded the transient azomethine ylide, which gave the final compound, **41**, by ring closing nucleophilic addition on the *ipso* carbon of the CF₃ group (Scheme I.10 b).¹⁰⁹ In comparison, no intramolecular migration was observed for diaminocarbenes **1** and the only case reported of migration was an intermolecular 1,2-silyl shift.¹¹⁰ This was due to the rigid cyclic planar structure of NHC, preventing the intramolecular migration.



Scheme I.10. 1,2-migration reactions for acyclic MACs **38** and **40**.⁴⁸

1.3.2.3.2 Insertion reactions

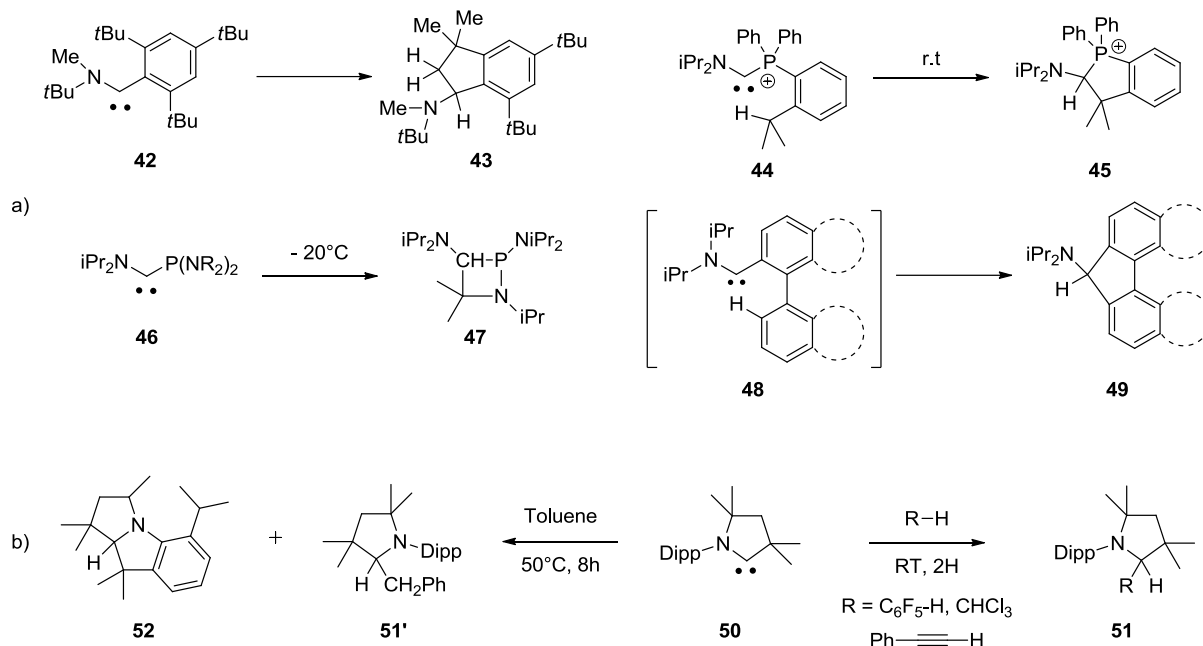
Chapter I: Similarities and differences between diaminocarbenes (DACs) and monoaminocarbenes (MACs) with special emphasis on the dimerization reaction

While insertion of carbenes into polarized X-H (X= O, N) and activated C-H (sp) bonds is common to both cyclic diamino type carbenes and MAC (see section I.5.2), insertion into non activated C-H bond (sp² and sp³) has only been observed with MACs.^{60,111} Such insertions generally occurred in an intramolecular fashion, especially for acyclic MACs. Remarkably, the specific properties of MACs have also allowed for the activation of enthalpically strong bonds, such as H₂, PH, BH, resulting in the formal insertion of the carbene into these bonds.

I.3.2.3.2.1 Insertion into non-activated C-H bonds

The insertion into non-activated C-H bond (sp² and sp³) has been first reported by Solé in 2001 with the aminoarylcarbene **42**, which undergoes a C-H insertion into the CH₃ of the *t*-Bu substituent.^{60,111} As mentioned before, MACs generally perform intramolecular C-H insertion, especially for acyclic ones. Indeed, aminophosphino **46**, aminophosphonio **44** and aminoaryl **48** have been reported to insert into the C-H bond of their substituents (Scheme I.11 a).^{48,95,112} This insertion into C-H bond (sp, sp² and sp³) has also been observed intramolecularly with the cyclic (alkyl)(amino)carbene (CAAC) leading to products **51**. In the case where toluene is used with CAAC, a mixture of products **51'** and **52** is obtained, which results from the intra and intermolecular C-H bond insertion of the carbene center (Scheme I.11 b). It is worth mentioning that thanks to their amide functions, diamidocarbenes **10** provide a reactivity similar to that of transient carbenes, hence intramolecular C-H bond insertion has also been reported.¹¹²

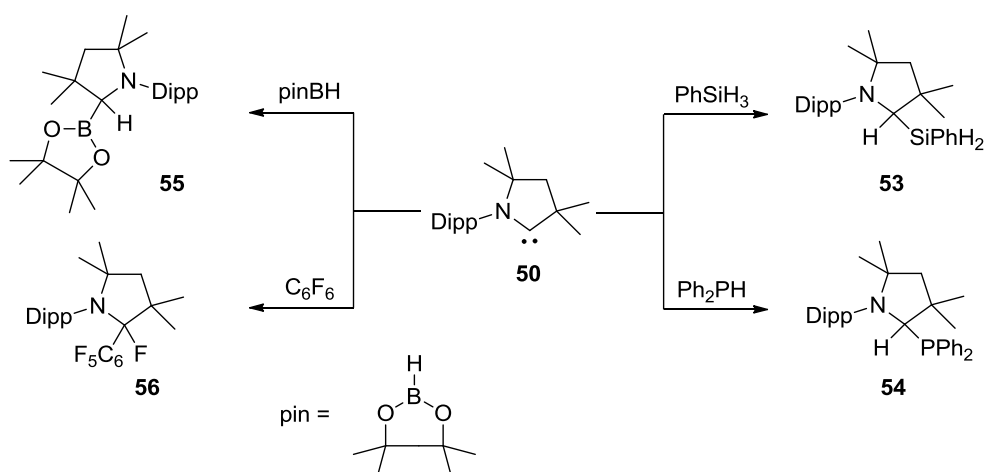
Chapter I: Similarities and differences between diaminocarbenes (DACs) and monoaminocarbenes (MACs) with special emphasis on the dimerization reaction



Scheme I.11. Insertion into non-activated C-H bond.^{60,48,95}

I.3.2.3.2.2 Intermolecular insertion into enthalpically strong P-H, B-H, Si-H and C-F bonds

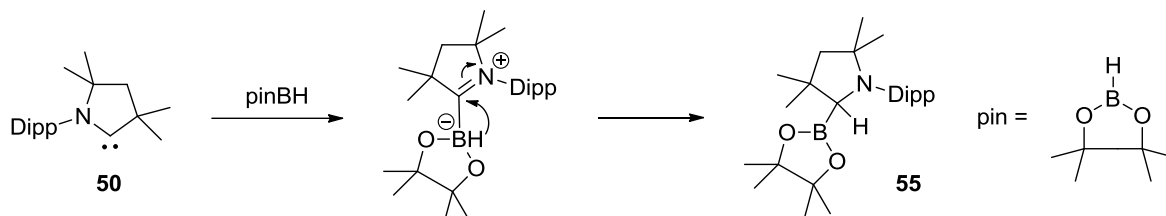
CAACs **50** is the first non-metal compound, which has been reported to activate enthalpically strong bonds such as P-H (322 kJ.mol⁻¹), B-H (389 kJ.mol⁻¹), Si-H (318 kJ.mol⁻¹) and C-F bonds (488 kJ.mol⁻¹).¹¹³ Indeed, such activation was only known for transition-metal centers (Scheme I.12).¹¹⁴⁻¹¹⁶



Scheme I.12. Activation of enthalpically strong bonds (Si-H, P-H and B-H).⁹⁵

Chapter I: Similarities and differences between diaminocarbenes (DACs) and monoaminocarbenes (MACs) with special emphasis on the dimerization reaction

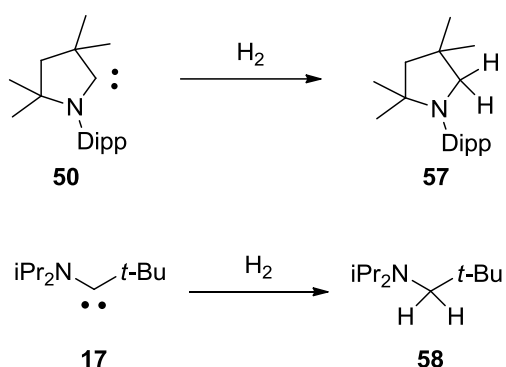
The activation of the X-H bond (X = Si, B) involves the Lewis acid character of the substrate and the nucleophilicity of the carbene, which adds on the heteroatom forming a Lewis acid-base adduct. Then, a hydride migrates from the heteroatom center to the carbenic center (Scheme I.13).¹¹⁷



Scheme I.13. Mechanism of the activation of X-H bond when X = Si or B (here with HBpin as example).

I.3.2.3.2.3 Activation of enthalpically strong H-H bond

The splitting of H₂ (432 kJ.mol⁻¹) has been almost exclusively the domain of metals for a long time. However, considerable progress has been achieved recently. Although no insertion has been reported with diaminocarbenes, which remains inert when in contact with bubbling dihydrogen, the use of the more nucleophilic and electrophilic CAAC **50** and monoaminoalkylcarbene **17** has been shown to result in the activation of such strong bond (Scheme I.14).



Scheme I.14. H-H insertion of CAAC **57** and amino-*t*-butylcarbene **58**.¹¹⁸

For transition metals (TM), the splitting of H₂ proceeds through the σ -donation of the H₂ bonding orbital onto the empty d orbital of the metal. Then, the back-donation of the filled d

Chapter I: Similarities and differences between diaminocarbenes (DACs) and monoaminocarbenes (MACs) with special emphasis on the dimerization reaction

orbital of the metal onto the H_2 σ^* orbital leads to the homolytic cleavage of the bond. For singlet carbenes, the splitting goes through a formal oxidative addition of the carbene onto H_2 . The HOMO of the carbene interacts with the H_2 σ^* orbital and the σ orbital of H_2 interacts with the p_π of the carbene. These interactions lead to an hydride-like hydrogen that adds onto the positively polarized carbon center.

Overall, both transition metals and carbenes share similar orbitals with appropriate symmetry, which allow the splitting of H_2 . Therefore, an analogy can be made between them (Figure I.11).¹¹⁹

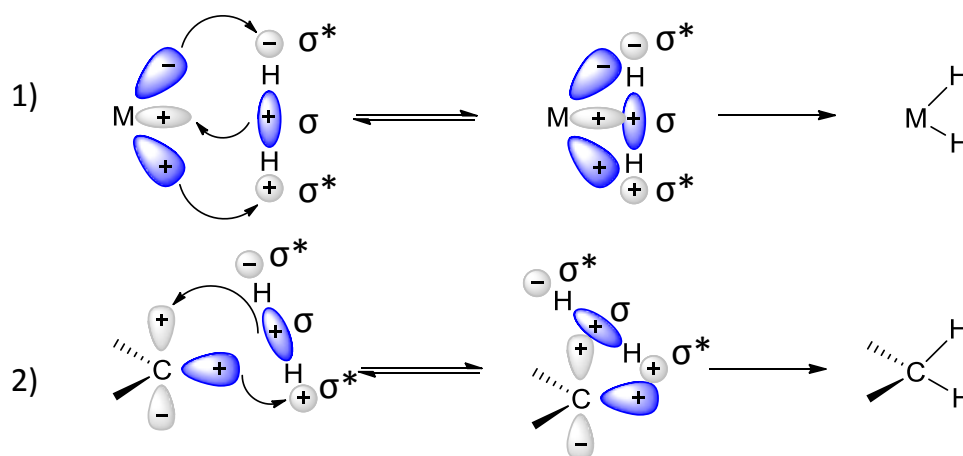


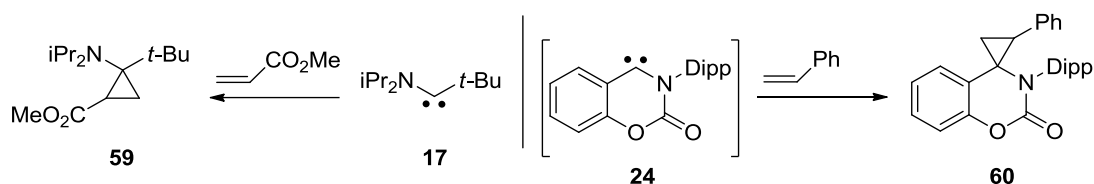
Figure I.11. Representations of the two modes of activation of H_2 1) by TM 2) by stable singlet carbene. In blue are the filled orbitals and in grey the vacant orbitals.¹¹⁹

I.3.2.3.3 Cyclopropanation of alkenes

The addition of transient carbenes to alkenes provides an efficient access to cyclopropanes. This reaction has been historically used to determine the carbene nucleophilicity, electrophilicity and ambiphilicity, which is referred to as the Moss classification,^{120,121} as well as their ground-state multiplicity. Indeed, by looking at the stereochemistry of the resulting cyclopropanes, one can trace back to the ground-state multiplicity because of the different mechanisms involved for triplet (stepwise) and singlet carbenes (concerted). So far, cyclopropanation has only been reported for MACs **17**,¹⁰² in the presence of acrylate as electron poor olefin. More recently, the transient monocarbamoyl carbene **24** has been reported to undergo the cyclopropanation of styrene (Scheme I.15).⁹⁶

Chapter I: Similarities and differences between diaminocarbenes (DACs) and monoaminocarbenes (MACs) with special emphasis on the dimerization reaction

Similarly, thanks to its small ΔE_{ST} gap, the diamidocarbene **10** is able to add on electron-poor and electron-rich olefins to yield the respective cyclopropanes.¹¹² In the case of diamino type carbene, the large ΔE_{ST} gap prevents the cyclopropanation to occur. Nevertheless, depending on the nature of the carbene involved, different reaction outcomes have been observed with acrylates as substrates.^{122,123,87}



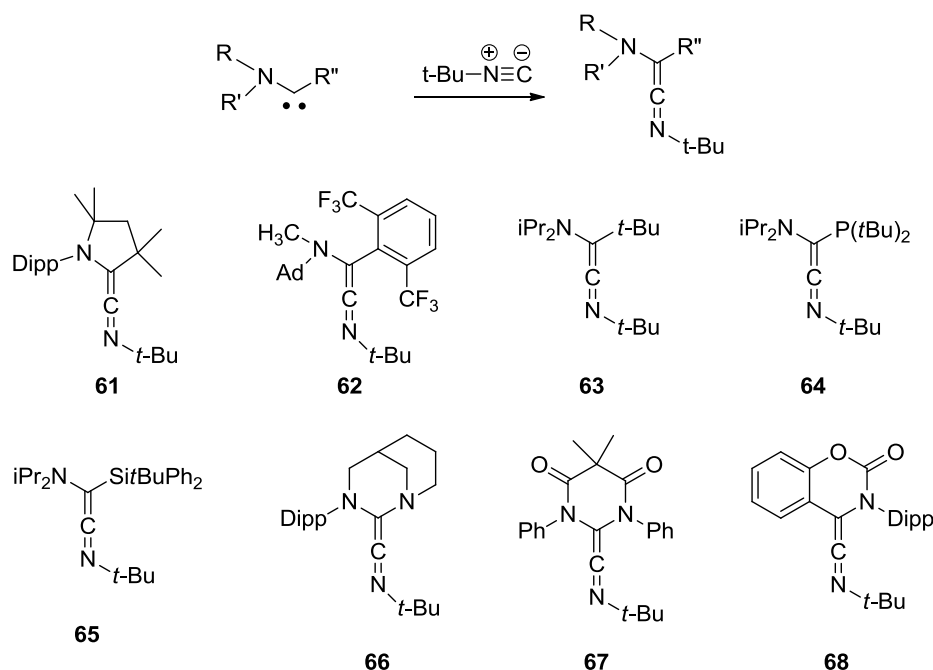
Scheme I.15. Cyclopropanation of olefins involving MACs.^{112,102}

1.3.2.3.4 Coupling reactions

1.3.2.3.4.1 Carbene-Isonitrile coupling

Coupling to isonitrile and carbon monoxide also requires ambiphilic carbenes. In particular, such carbenes should display a rather low-lying LUMO to interact with the HOMO of the isocyanide. This explains why no reaction has been reported for diaminocarbenes due to the highly destabilized p_{π} orbital. Thus, this reaction with isocyanide is particularly well suited to show the electrophilicity of carbenes, and both MACs **15**, **16**, **17**, **19** and **22** have proven to react with *tert*-butyl isocyanide, leading to the corresponding ketenimines **61-65**, respectively (Scheme I.16).^{60,87,91,129} Interestingly, beside MACs, only a few other carbenes including the saturated bicyclic NHC with a pyramidalized nitrogen **11**,⁷¹ the diamidocarbene **10**¹¹² and carbamoylcarbene **24**⁹⁶ have been reported to successfully couple with isocyanide, yielding compounds **66**, **67** and **68**, respectively, thanks to their low lying LUMO.

Chapter I: Similarities and differences between diaminocarbenes (DACs) and monoaminocarbenes (MACs) with special emphasis on the dimerization reaction

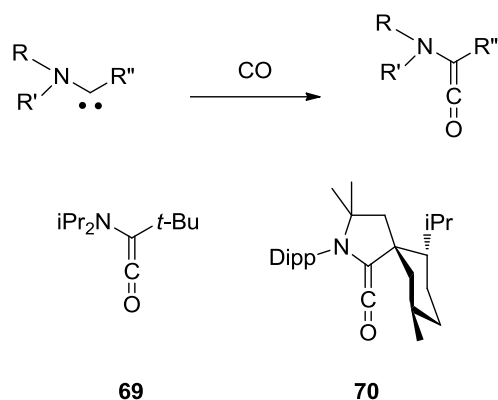


Scheme I.16. Isonitrile coupling with monoaminocarbenes and electrophilic diamino-like carbenes.^{60,71,87,91,96,112,129}

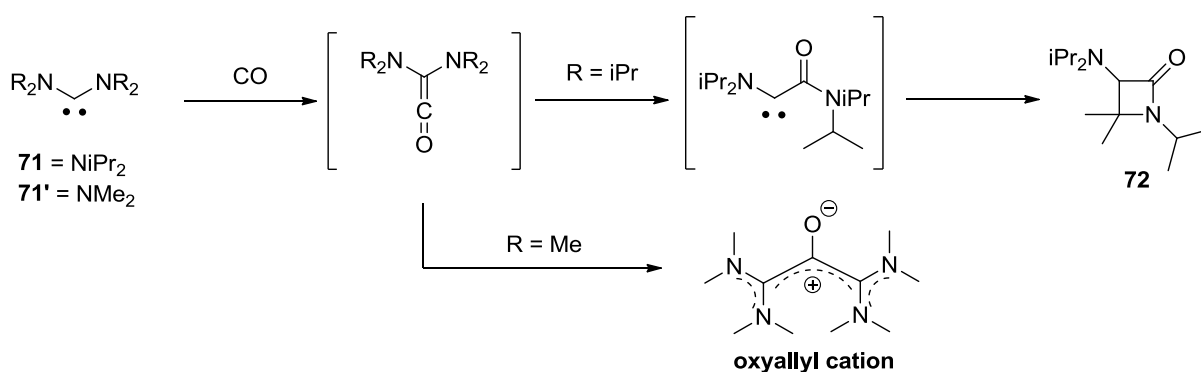
I.3.2.3.4.2 Carbene-Monoxide coupling

The first unambiguous example of carbon monoxide coupling with carbenes has been reported in 2006 by Bertrand and coworkers with acyclic monoaminoalkylcarbenes **17**.¹⁰³ Besides **17**, only CAAC **15**^{130,131} has been shown to react with carbon monoxide (CO), affording the corresponding aminoketenes **69** and **70** (Scheme I.17). As expected from the reaction with isocyanide, diamidocarbene family (**10**) has also enough electrophilic character to trap CO, here reversibly.^{112,132} It is worth noting that one example of a ferrocene-based NHC has been reported to couple with CO.¹³² In 2010, Frenking *et al.* have reported the rearrangement of the transient diaminoketene, obtained from the reaction of diaminocarbene **71** with CO, into the corresponding β -lactam **72**. In the case where methyl groups are on the amino functions, no β -lactam was observed but the oxyallyl cation betain instead (Scheme I.18).^{132,133}

Chapter I: Similarities and differences between diaminocarbenes (DACs) and monoaminocarbenes (MACs) with special emphasis on the dimerization reaction



Scheme I.17. Monoxide coupling with aminocarbenes **15** and **17**.¹⁰³



Scheme I.18. Trapping of diaminocarbenes **71**, **71'** with CO and its rearrangement in β -lactam **72** or oxyallyl cation respectively.¹³³

In this part has been presented the properties and specific reactivities of the push-push stabilized diaminocarbenes with its most representative carbene, namely *N*-Heterocyclic carbene (NHC). Then, the push-spectator monoaminocarbenes has been presented in order to show the difference in their synthesis, properties and reactivities compared to the first family. However, both families share also similar reactivities that are presented hereafter.

I.4 Common reactivity to mono and diaminocarbenes

Despite their differences, diamino and monoamino type carbenes share some similarities. In particular, they are both excellent Lewis bases due to their rather high lying HOMO orbital. Thus, they behave as good ligands in organometallic chemistry;^{34,61} they are also able to add onto heterocumulenes such as CO₂ and CS₂ and onto activated olefins as well.^{71,112,134} Moreover, because of the presence of a formally empty p π orbital, they can also insert into

Chapter I: Similarities and differences between diaminocarbenes (DACs) and monoaminocarbenes (MACs) with special emphasis on the dimerization reaction

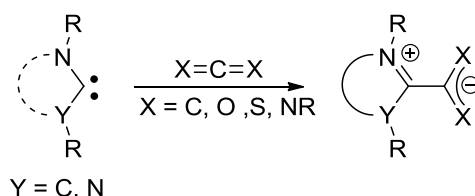
polarized X-H bonds (X = N, O)^{49,78,130} and activated C-H bonds (acetonitrile, acetylene).^{135,136} Finally, in the absence of any reagent, and providing that the carbene center is not too protected, both type of carbene can dimerize.

I.4.1 Ligands for transition metals

Diaminocarbenes type and MACs can coordinate to a wide variety of metals. Moreover, cyclic carbenes generate much more robust complexes than their acyclic counterparts. Therefore, NHCs and CAACs are the most powerful ancillary ligands and they have been used in a variety of transformations involving transition metal-carbene complexes (Suzuki,^{137,138} Heck,^{139,140} Sonogashira coupling (Pd),^{141,142} Kumada coupling (Rh)¹⁴³, cyclopropanation¹⁴⁴ and hydrogenation¹⁴⁵ of olefins (Ru)).

I.4.2 Addition to cumulene (CCC, CS₂, CO₂) and activated olefins

Mainly diamino-type carbenes have been reported to react with heterocumulenes, such as carbon dioxide, carbon disulfide, phenyl iso(thio)cyanate and carbodiimide, to yield the corresponding betaines (Scheme I.19).¹⁴⁶⁻¹⁵⁰ The reaction with CO₂ is particularly useful because it is a simple and efficient way to protect the carbene. Upon heating, CO₂ is released, thus delivering the NHC in solution without the need for a strong base. Because of their higher nucleophilicity, MACs likely react in the same way with these electrophiles; however, only a few examples, involving CAAC **15** (with CO₂ and CS₂) and the very specific bicyclic diaminocarbene **11** (CO₂), have been reported so far.^{71,151}

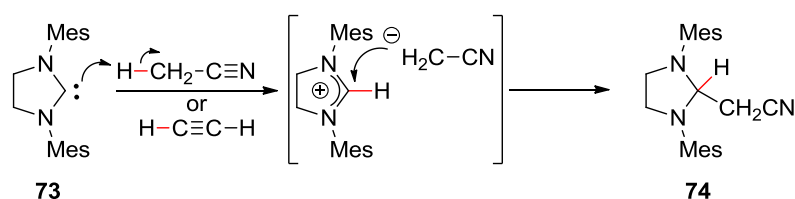


Scheme I.19. Addition of carbenes to heterocumulenes leading to the corresponding betaines.^{147,146,148-}

Chapter I: Similarities and differences between diaminocarbenes (DACs) and monoaminocarbenes (MACs) with special emphasis on the dimerization reaction

I.4.3 Insertion into activated C-H bonds and strongly polarized N-H, O-H bonds

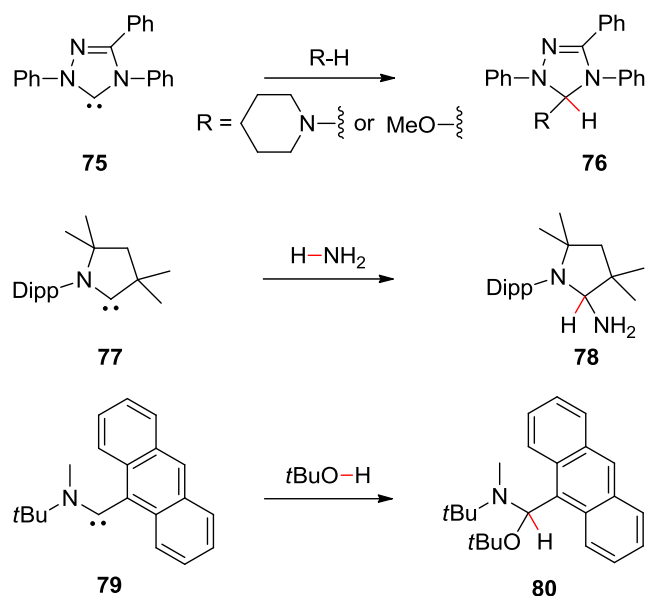
The C-H bond is weakly polarized and is generally inert toward insertion with most carbenes. Only ambiphilic carbenes with low ΔE_{S-T} (i.e. MACs) have thus been reported to insert into C-H bonds *via* a concerted process, albeit in an intramolecular fashion. As previously described, insertion into non-activated C-H bonds (sp^2 and sp^3) was only performed by some MACs. In contrast, insertion into activated sp and sp^3 CH bonds have been observed for both diamino and MACs.¹⁵²⁻¹⁵⁴ In this case, the reaction generally proceeds *via* a stepwise mechanism involving the deprotonation of the acidic CH bond, followed by the collapse of the imidazolium/anion pair. For instance, imidazolin-2-ylidenes **73** reacts through a formal insertion into acetylene and acetonitrile C-H bonds (Scheme I.20).^{135,136} Up to now, no unsaturated NHCs **1** have been reported to insert in CH bonds.



Scheme I.20. Insertion in C-H activated bond of saturated NHC **73**.^{135,136}

Another type of bonds, in which both diamino carbene-type and MACs insert in, are the polarized N-H and O-H bonds.^{49,78,130} Those insertions have been reported for the diaminocarbenes with triazol-2-ylidene (N-H,O-H), DAC (N-H), and bicyclic diaminocarbene (N-H).^{63,83,155} For MACs, the insertion of CAAC (N-H), aminoalkylcarbene (N-H) and aminoarylcarbene (O-H) have been reported (Scheme I.21).^{119,130,156}

Chapter I: Similarities and differences between diaminocarbenes (DACs) and monoaminocarbenes (MACs) with special emphasis on the dimerization reaction



Scheme I.21. Insertion into polarized N-H and O-H bond of triazolylidene **75** and MAC **77** and **79**.^{63,156,130}

In this part has been shown the similar reactivities of both families *i.e.* coordination to metals, addition to heterocumulenes and insertion into N-H, O-H and C-H activated bond. In the next part, the last common reactivity that was used in this PhD, namely the dimerization reaction, is presented in detail.

1.5 The dimerization reaction

Another common reactivity of both diaminocarbenes and MACs is the dimerization reaction, which is often considered as deleterious, as it usually prevents carbenes from being isolated. This peculiar reaction has been central in this PhD work and thus it will be discussed in detail hereafter.

Dimerization is one of the classical reactions of carbenes, which has been observed with both DACs and MACs, despite their different properties.^{48,49} This reaction generally occurs when the carbene center is not sufficiently protected and represents the main obstacle towards isolation of the free carbene. It is often exergonic and leads to the thermodynamically more stable alkene. The ability to dimerize is closely linked to the thermodynamic and kinetic stability of the “monomeric carbene” and its corresponding dimer. The thermodynamic aspect

Chapter I: Similarities and differences between diaminocarbenes (DACs) and monoaminocarbenes (MACs) with special emphasis on the dimerization reaction

is mainly correlated with the presence of heteroatoms (N, O, S) next to the carbene center that will stabilize the carbene by both inductive and mesomeric effects, as discussed in section I.2.2, but will also destabilize the corresponding dimer. The kinetic aspect is determined by the steric hindrance of the substituents that will disfavor or even prevent this reaction from happening.

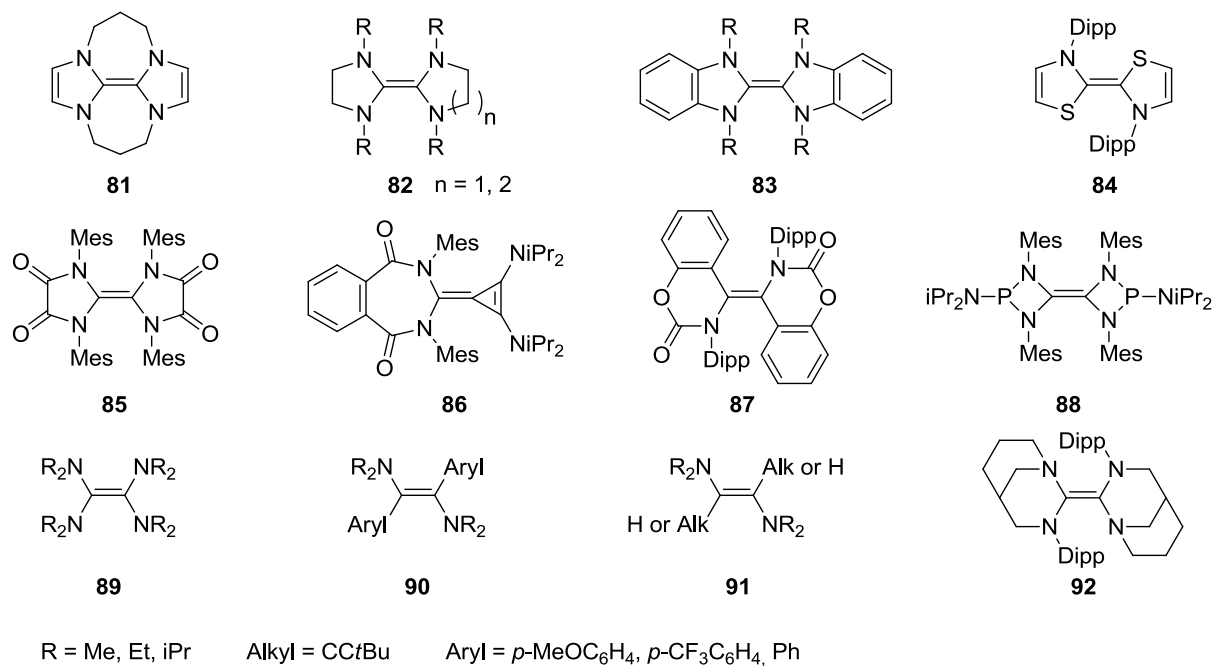


Figure I.12. Main stable dimers obtained through carbene homo or hetero dimerization.^{48,71,67,81,112,157–}

160

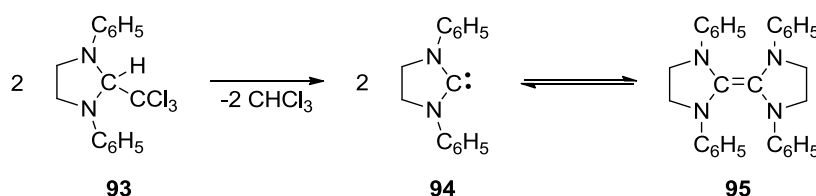
A variety of homo-dimers, resulting from the dimerization of stable, persistent and transient carbenes have been isolated. Most homodimers obtained from the dimerization of cyclic diamino and diamidocarbenes involve a 5-membered ring (**81-85**).^{19,161,162,112} In the case of the unsaturated diaminocarbenes, nitrogen atoms have to be tethered to isolate dimer **81**.⁸⁰ In absence of such constraints, the carbene is more stable in its “monomeric form”. In the case of aminothiocarbene, dimer **84** can be obtained without tethering because of the small ΔE_{S-T} .¹⁵⁷ For saturated diaminocarbenes of 4-, 5- and 6-membered ring, dimers **82**, **88** and **92** have been reported.^{161,163,71,67} Apart from stable carbene, the dimerization of the transient carbamoyl carbene successfully led to dimer **87**.⁹⁶ Homodimers **89**, **90** and **91** can also be obtained from acyclic DACs and MACs.^{81,98,100} Most of these dimers are highly symmetric olefins with at least one mirror plane, a C₂ axis and/or an inversion center. When carbenes involve two different substituents (like in MACs), homodimers are characterized by two different

Chapter I: Similarities and differences between diaminocarbenes (DACs) and monoaminocarbenes (MACs) with special emphasis on the dimerization reaction

configurations namely, *Z* and *E*. Remarkably, one heterodimer (**86**)¹⁵⁹ has been successfully synthesized by Bertrand *et al.*, using carbenes with complementary electronic properties. This particular example of selective cross dimerization will be described in detail in this part (Figure I.12).

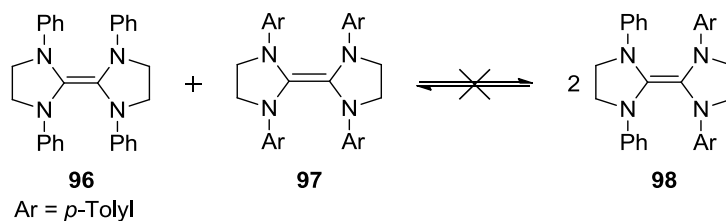
I.5.1 The wanzlick equilibrium

The first case of dimerization was reported as early as 1960 with the seminal work of Wanzlick *et al.*^{19,164–167} In an attempt to prepare free imidazolin-2-ylidene, **94**, from the chloroform adduct **93**, the authors were only able to isolate the corresponding tetraaminoethylene **95** (Scheme I.22). Wanzlick thus postulated that carbene **94** was an intermediate in the formation of dimer **95**. Moreover, based on the determination of molecular weight of **95** at high temperature (170 °C) in absence of oxygen, results indicated 50% dissociation and Wanzlick thus assumed the existence of an equilibrium between **94** and **95**.¹⁹



Scheme I.22. Proposed Wanzlick equilibrium¹⁹

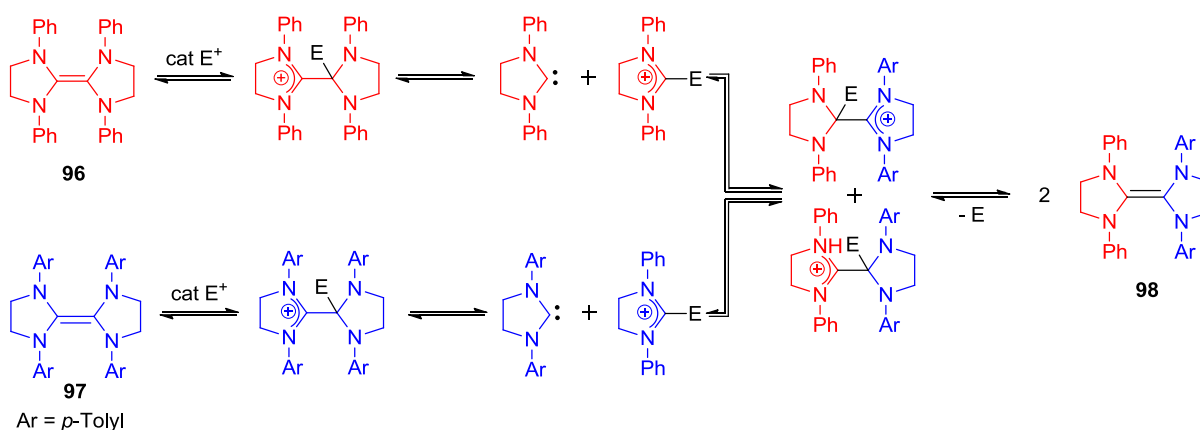
Few years after Lemal *et al.* performed a cross-over experiment between two similar tetraaminoethylenes differing by the nature of the substituents (*C*₆H₅ versus *p*-tolyl) on the nitrogen atoms. If dimers **96** and **97** dissociated in solution into their corresponding NHC, apparition of a novel unsymmetrical tetraaminoalkene **98** should be observed. However, only signals corresponding to the starting dimers were noted by NMR (Scheme I.23).¹⁶¹



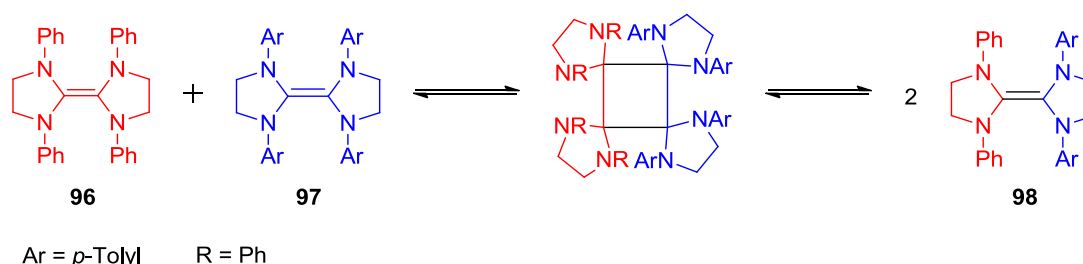
Scheme I.23. Negative cross-over experiment between tetraaminoethylenes.¹⁶¹

Chapter I: Similarities and differences between diaminocarbenes (DACs) and monoaminocarbenes (MACs) with special emphasis on the dimerization reaction

While this reaction suggests the irreversibility of the dimerization, it has been the starting point of the controversy of the Wanzlick equilibrium. Its existence, indeed, has been questioned over the years.^{158,161,168,169} Based on the same cross-over experiment, two independent papers by Lemal and Denk reported the appearance of the new dissymmetrical dimer **98**. In one paper however, **98** likely originated from the presence of electrophilic impurities that would catalyze the cleavage of dimers **96** and **97** (Scheme I.24).¹⁶¹ In the other paper, even in absence of electrophiles, the existence of **98** did not necessarily involved carbene intermediates and could be explained by the [2+2]-cycloaddition, followed by the [2+2]-cycloreversion of the resulting cyclobutane between the enetetramines **96** and **97** (Scheme I.25).¹⁶⁸ Therefore, both results were not in favor of the original equilibrium between the free carbene and its dimer proposed by Wanzlick.



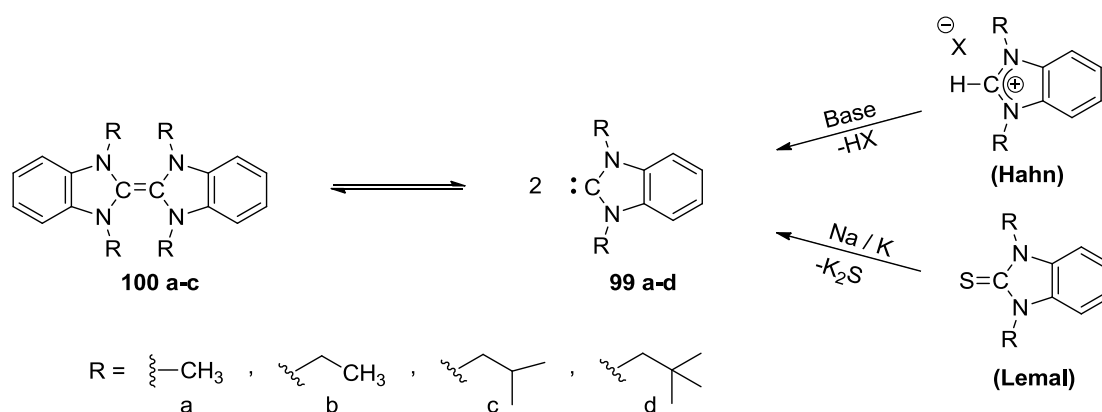
Scheme I.24. Wanzlick equilibrium catalyzed by electrophilic impurities (E⁺).¹⁶¹



Scheme I.25. Wanzlick equilibrium explained by [2+2]-cycloaddition/[2+2]-cycloreversion mechanism.¹⁶⁸

Chapter I: Similarities and differences between diaminocarbenes (DACs) and monoaminocarbenes (MACs) with special emphasis on the dimerization reaction

One piece of evidence for the existence of the Wanzlick equilibrium would be the observation of a mixture of the free carbene and the corresponding alkene, under electrophilic-free conditions. Hahn *et al.*⁷⁹ and Lemal *et al.*¹⁷⁰ have independently reported such observations with the benzimidazol-2-ylidene **99**, which was found in equilibrium with its corresponding dimer **100**, when suitable substituents, such as methyl, ethyl, isobutyl and neopentyl, are present on the nitrogen atom of **99**. Indeed, with R = isobutyl (c), both **99c** and **100c** could simultaneously be identified by ¹H and ¹³C NMR spectroscopy at ambient temperature. With bulkier groups (isobutyl, neopentyl) the equilibrium is shifted towards the free carbene. The same Wanzlick equilibrium has been found for N-methyl and N-ethyl substituted benzimidazolylidene, albeit at much higher temperature (140°C). Although it could be argued that the two synthetic routes to **100** involve electrophiles, such as K₂S (thione reduction) or H⁺ (deprotonation of benzimidazolium salts), the careful purification of **100** by multiple recrystallization has allowed the authors to evidence the Wanzlick equilibrium under electrophilic-free conditions.



Scheme I.26. Synthesis of **100 a**) by reduction of the corresponding thione b) by deprotonation of benzimidazolium salt; c) Wanzlick equilibrium between **100** and **99** under electrophilic-free conditions.¹⁵⁸

The equilibrium proposed by Wanzlick has only been observed in particular cases. For instance, the carefully purified benzimidazol-2-ylidene carrying specific substituents (Me, Et, isobutyl), equilibrate with its corresponding dimer.¹⁵⁸ In another case, a successful cross-over experiment on two different enetetramines has eventually demonstrated the existence of the equilibrium, but the reaction is strongly expected to be catalyzed by electrophilic impurities.^{161,163}

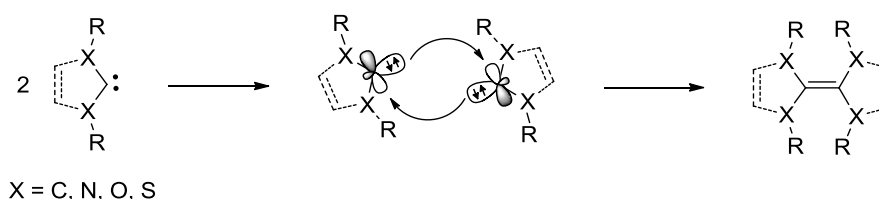
Chapter I: Similarities and differences between diaminocarbenes (DACs) and monoaminocarbenes (MACs) with special emphasis on the dimerization reaction

1.5.2 The dimerization reaction: mechanisms

The question of the carbene dimerization mechanism has thus been raised from the study of the controversial “Wanzlick equilibrium”. Two mechanisms have been envisaged for the formation of the double bond, namely a direct non-catalyzed pathway and an indirect proton-catalyzed pathway.

1.5.2.1 Non-catalyzed dimerization of singlet carbenes

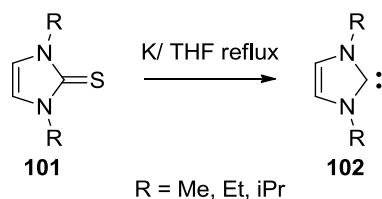
The former mechanism, which is also the most intuitive, is the direct dimerization of free singlet carbenes in absence of any catalyst. This non-least motion pathway involves a nucleophilic attack of the filled in plane σ -orbital of one carbene onto the out-of-plane formally vacant p_π -orbital of a second carbene (Scheme I.27).^{171–173} Although this mechanism generally leads to a thermodynamically more stable dimer, it is hampered by a significant energy barrier, which results from the destabilization of the p_π orbital by the strong interaction with adjacent nitrogen atoms. To test this mechanism experimentally, it appears necessary to generate carbenes without any protic impurities.



Scheme I.27. Direct non-catalyzed carbene dimerization mechanism.¹⁷⁴

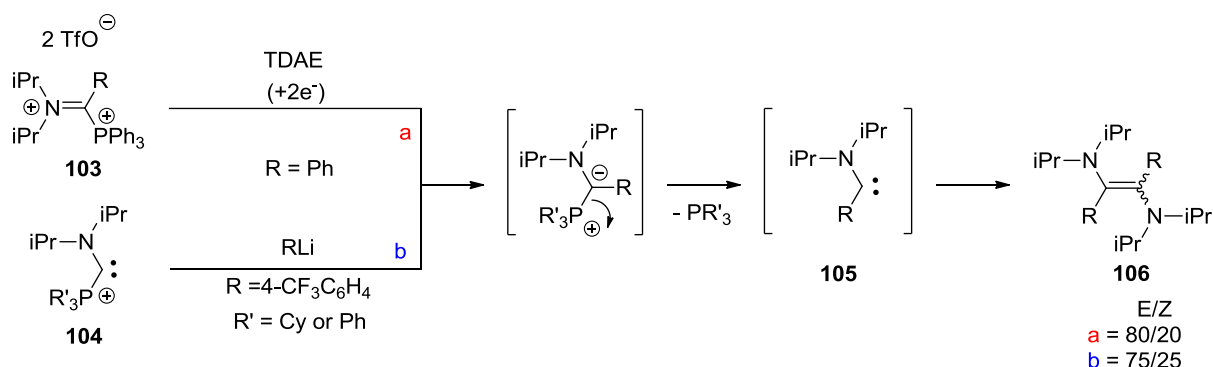
For this purpose, novel carbene precursors and original routes have been developed. The first reaction reported is the reduction of thione by Kuhn *et al.*,⁷⁶ where a mixture of potassium metal and thione precursor **101**, in boiling THF, gives the stable carbene **102** (Scheme I.28).

Chapter I: Similarities and differences between diaminocarbenes (DACs) and monoaminocarbenes (MACs) with special emphasis on the dimerization reaction



Scheme I.28. Reduction of imidazol-2(3H)thiones **101** by potassium metal.⁷⁶

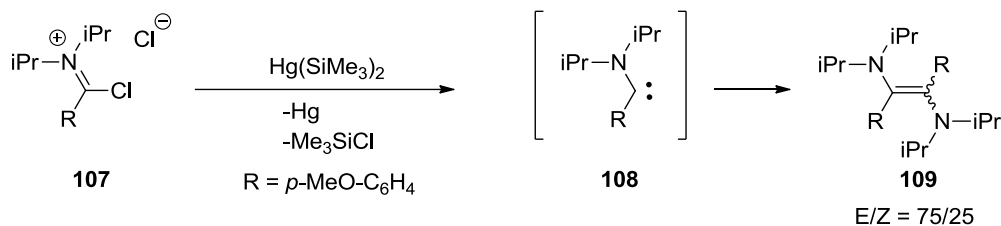
In the case of acyclic MACs, Bertrand *et al.* have reported three methodologies,^{90,98,100} which do not involve any protic reagents. Thus, the reduction of phosphonio-iminium salts **103** with an organic reducing agent, such as tetrakis(dimethylamino)ethylene (TDAE), affords the *E/Z* diaminoalkene by direct dimerization of the *in situ* generated MAC.¹⁰⁰ The second route is the nucleophilic substitution at the carbene center of a stable aminophosphoniocarbene **104** by an anionic nucleophile.⁹⁰ The resulting transient ylide intermediate fragments into the corresponding carbene and phosphine. The resulting carbene then dimerizes to afford a mixture of *E/Z* diaminoalkene (Scheme I.29).



Scheme I.29. Dimerization of *in-situ* generated carbene **105** via protic-free routes a) reduction of phosphoiminium salt by an organic reducing agent b) nucleophilic substitution at the carbene center of aminophosphoniocarbene.^{90,100}

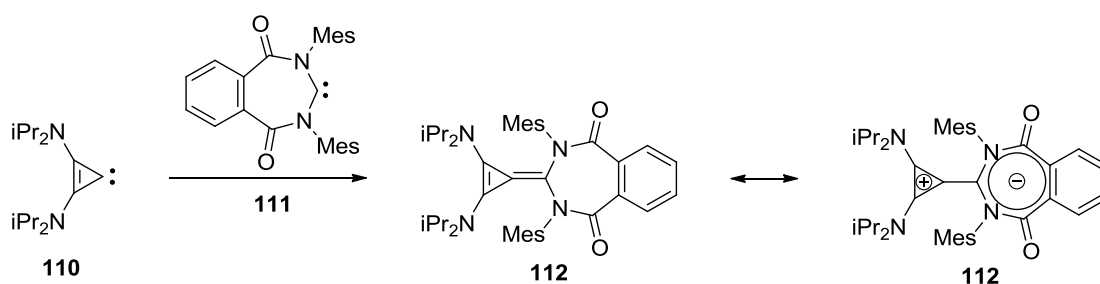
The last route is the reductive dechlorination of a chloroiminium salt **107** with bis(trimethylsilyl)mercury, which leads to the formation of mercury (0), trimethylsilylchloride and the transient MAC that instantly dimerizes into the corresponding *E/Z* diaminoalkene (Scheme I.30).⁹⁸

Chapter I: Similarities and differences between diaminocarbenes (DACs) and monoaminocarbenes (MACs) with special emphasis on the dimerization reaction



Scheme I.30. Dimerization of *in-situ* generated carbene **108** via the last protic-free route: reductive dechlorination of chloroiminium **107**.⁹⁸

Interestingly, the first direct dimerization of two different stable carbenes has been reported in 2014 by the same group.¹⁵⁹ As already mentioned, the non-catalyzed dimerization has a high energetic barrier. In order to decrease it, specific carbenes with distinct electronic properties, such as **110** and **111** have been selected. More precisely, the combination of the poorly hindered bis-aminocyclopropenylidene **110**, which displays a high-energy HOMO with the 7-membered ring electrophilic diamidocarbene **111**, results in the selective formation of the expected heterodimer **112** (Scheme I.31).^{74,175} A single X-ray diffraction of **112** has confirmed the structure with a C-C bond in the range of typical alkenes (1.35 Å). This strategy could be extended to other electrophilic carbenes, providing the corresponding heterodimer; the latter then rearranges by ring expansion of the cyclopropenylidene moiety into allenic compounds.



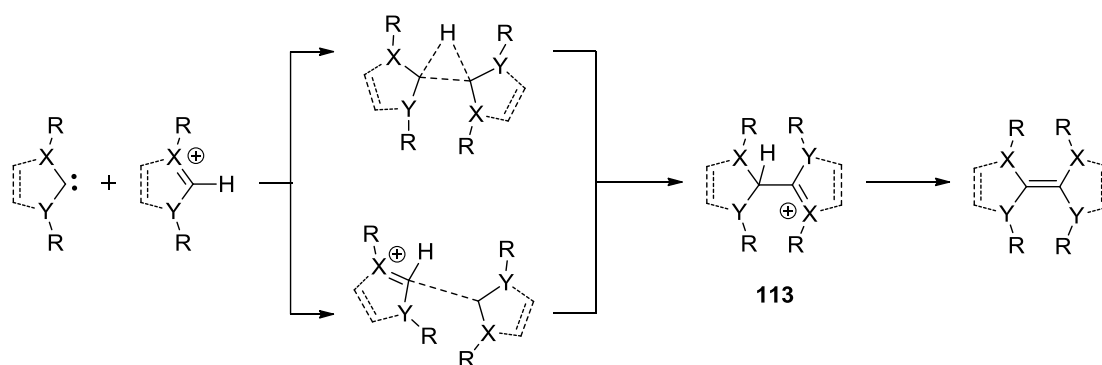
Scheme I.31. First evidence of the direct dimerization mechanism by cross-coupling of two different stable carbenes.¹⁵⁹

Overall, the direct dimerization may be observed when: 1) the carbene precursor is free from protic impurities, 2) a suitable methodology generates carbenes without electrophilic side products, 3) the energy barrier of dimerization is lowered by using carbenes of complementary electronic properties, *i.e* possessing a HOMO high enough and a LUMO low enough.

Chapter I: Similarities and differences between diaminocarbenes (DACs) and monoaminocarbenes (MACs) with special emphasis on the dimerization reaction

1.5.2.2 Proton-catalyzed dimerization of singlet carbenes

The non-catalyzed direct dimerization is thermodynamically favorable, but possesses a significant energy barrier. A way to reduce this energy is to lower the LUMO of the carbene. In this context, protonation of the carbene center appears as an efficient way to make its LUMO energetically accessible. The latter mechanism involves both the basicity and nucleophilicity of the carbene. In particular, the carbene generated by deprotonation of its corresponding azolium salt is nucleophilic enough to add onto its amidinium salt precursor, leading to a protonated dimer intermediate **113**. Finally, deprotonation of **113** in the presence of a base (carbene or external base) generates the final dimer (Scheme I.32). The proton-catalyzed dimerization was proposed to involve either an insertion of the carbene into the CH bond of its conjugated acid or a nucleophilic addition onto the electro deficient carbene center. However, the strongly basic nature of the carbene and the weakly polarized CH bond make the insertion unlikely.¹⁷⁶

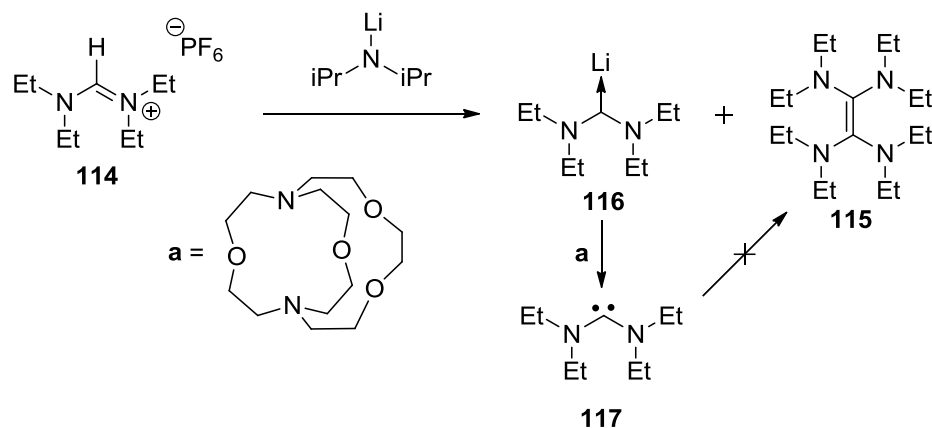


Scheme I.32. Indirect carbene dimerization *via* proton-catalyzed mechanism.¹⁷⁴

This type of mechanism has been evidenced first by Alder *et al.*⁸¹, while working on the preparation of acyclic bis(diethylamino)carbene by deprotonation of amidinium salts **114**. Addition of one equivalent of lithium diisopropylamide (LDA) to the iminium salt **114**, has led to a mixture of dimer **115** and the lithium-carbene complex **116** in a 70/30 ratio, respectively. This complexation of lithium has been proposed to account for the upfield shift observed for the carbene signal in the ¹³C NMR spectrum (244 ppm) relative to the free carbene ($\Delta = 12$ ppm). To rule out the direct dimerization mechanism, an excess of cryptand **a** (specific for lithium) has been added to the carbene-lithium complex to remove any lithium and generate the free carbene **117**. Interestingly, the same 70/30 ratio has been observed after several weeks,

Chapter I: Similarities and differences between diaminocarbenes (DACs) and monoaminocarbenes (MACs) with special emphasis on the dimerization reaction

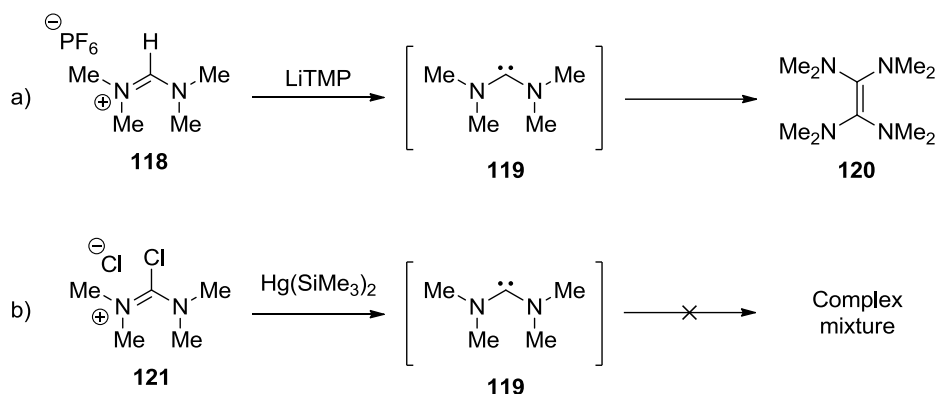
evidencing that no further dimerization can take place *via* a non-catalyzed pathway (Scheme I.33).



Scheme I.33. Dimerization of bis(diethylamino)carbene through proton catalyzed mechanism and addition of [2.1.1]cryptand to remove the Li-carbene complex.⁸¹

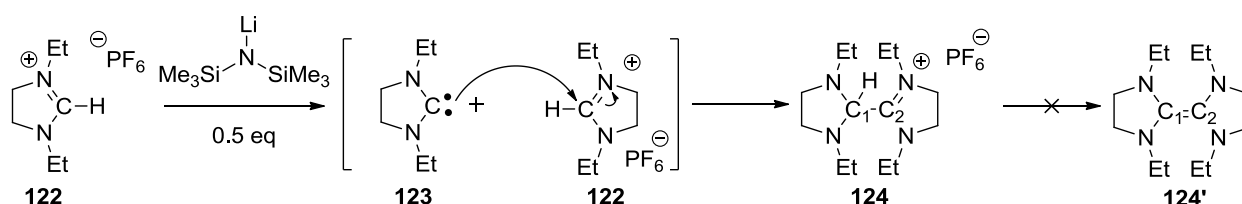
The other and indirect evidence of the proton-catalyzed dimerization mechanism has been reported by the same group, while studying the deprotonation of aldiminium **118** with the bulky and strong TMPLi base. Because of the very weak steric protection of the carbene center, complete dimerization has been observed. The direct mechanism could be ruled out by using the proton-free methodology developed by Bertrand *et al.*,⁹⁸ where the C-chloroiminium undergoes a reductive dechlorination with Hg(SiMe3)2. In this case, no trace of the dimer **120** could be detected, and only a complex mixture resulting from the decomposition of carbene **119** was observed (Scheme I.34).

Chapter I: Similarities and differences between diaminocarbenes (DACs) and monoaminocarbenes (MACs) with special emphasis on the dimerization reaction



Scheme I.34. Indirect evidence of the proton-catalyzed mechanism by generating bis(dimethylamino)carbene **119** via a) deprotonation of amidinium **118** and b) reductive dechlorination of **121**.⁸¹

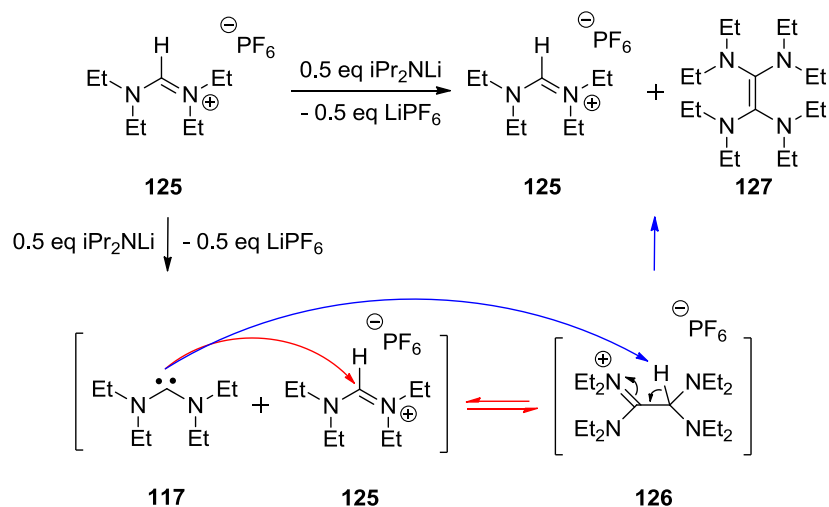
Investigations of the proton-catalyzed mechanism has been performed by deprotonation of iminium **122** with 0.5 equivalent of a strong base. In this way, the protonated dimer **124** was quantitatively formed. The latter compound proves stable and does not evolve to its corresponding dimer **124'**. The structure of **124** could be confirmed both in the solid and in solution by X-ray diffraction analysis and ¹³C NMR spectroscopy, where characteristic signals for C₁ and C₂ were observed at 78.7 and 165.0 ppm (Scheme I.35).



Scheme I.35. Evidence of proton-catalyzed dimerization through the isolation of the protonated intermediate **124** via addition of *in-situ* generated carbene **123** onto its corresponding amidinium **122**.^{81,157}

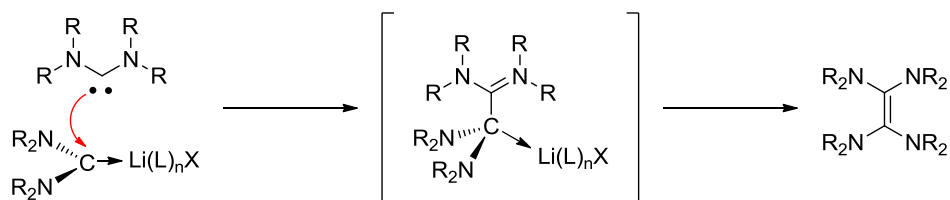
The same experiment has been carried out with acyclic aldiminium salt **125**. However, the protonated dimer **126** could not be observed. Instead, the reaction led to a 1/1 mixture of dimer **127** and the starting aldiminium **125**. It has been suggested that the transient protonated dimer could be deprotonated by a free acyclic diaminocarbene **117**, which is more basic than the previous cyclic diaminocarbene **123** (Scheme I.36).

Chapter I: Similarities and differences between diaminocarbenes (DACs) and monoaminocarbenes (MACs) with special emphasis on the dimerization reaction



Scheme I.36. Deprotonation of acyclic aldiminium salt **125** with 0.5 equivalent of base which leads to final dimer **127** and starting compound **125** in a 1:1 mixture, highlighting the high basicity of acyclic diaminocarbene.

From these results, it appears that dimerization of diaminocarbenes generally follows a proton-catalyzed mechanism, when carbenes are generated by deprotonation of amidinium salts with a strong base. Thus, this mechanism is likely involved in the formation of dimers **124'** and **127**, although the direct mechanism cannot be ruled out. In addition, proton and lithium species have also been proposed to catalyze carbene dimerization reaction, as suggested by Alder *et al.*⁸¹ A free carbene may indeed react more rapidly with a lithium complexed carbene, as the coordination should lower its LUMO, similarly to protonation. Up to now, however, no evidence of such lithium-catalyzed dimerization has been demonstrated (Scheme I.37).

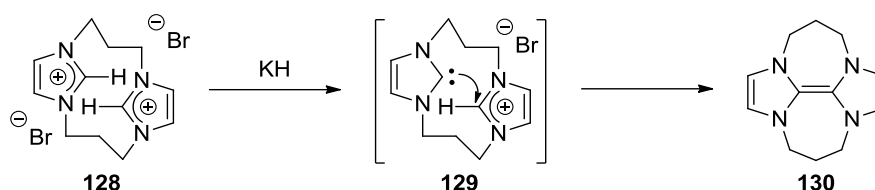


Scheme I.37. Suggested mechanism of the lithium-promoted dimerization by Alder *et al.*⁸¹

Based on this hypothesis, the other dimers shown in Figure 12, are proposed to be synthesized *via* the proton-catalyzed mechanism when deprotonation route is used.^{67,112,160}

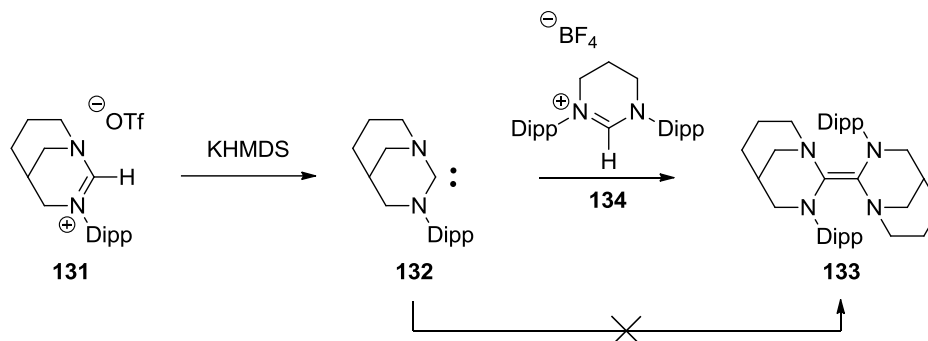
Chapter I: Similarities and differences between diaminocarbenes (DACs) and monoaminocarbenes (MACs) with special emphasis on the dimerization reaction

NHCs such as imidazol-2-ylidenes, are generally not prone to dimerize, even if they are generated by deprotonation by a strong base. Dimerization may yet be observed in doubly-tethered imidazolium salts, such as **128**. In this case, deprotonation with potassium hydroxide (KH) affords dimer **130**, likely *via* the intermediate **129**, although experimental evidences are lacking (Scheme I.38).⁸⁰



Scheme I.38. Dimerization of NHC **128** *via* proposed proton-catalyzed mechanism.⁸⁰

Dimer **133** shown in scheme 39 has been obtained by dimerization of N-bridgehead carbene **132**. Starting from the corresponding amidinium salt **131**, deprotonation with KHMDS at low temperature leads to the stable carbene **132**. The latter has been successfully characterized in solution and in the solid state. In the absence of any other reagents, no dimerization is noted though. In contrast, addition of a catalytic quantity of amidinium salt **134** triggers the spontaneous dimerization of **132** into the corresponding dimer **133**. Indeed, compound **134**, featuring bulky substituents to prevent the addition of **132**, is used as a proton donor. Thus, protonation of **132** into **131** is possible and leads to the dimerization following the proton-catalyzed pathway (Scheme I.39).⁷¹



Scheme I.39. Dimerization of carbene **131** through a unique proton-catalyzed mechanism.⁷¹

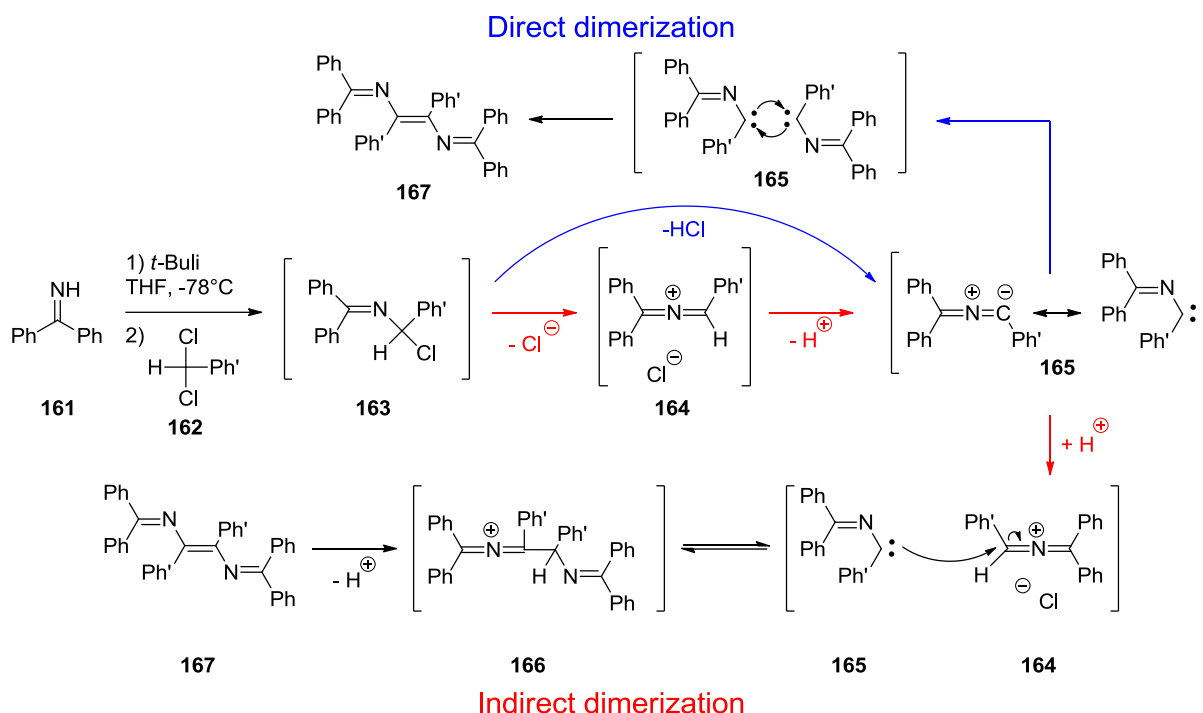
Chapter I: Similarities and differences between diaminocarbenes (DACs) and monoaminocarbenes (MACs) with special emphasis on the dimerization reaction

In this part, two possible mechanisms of carbene dimerization have been presented. The first mechanism involves the direct dimerization between two carbenes following a route that prevents the presence of protic impurities. This dimerization has been reported for the first time by Bertrand *et al.* in 2014 with two stable carbenes of complementary electronic properties. The second mechanism presented is the indirect, and proton-catalyzed dimerization, *i.e.* a protic starting iminium salt precursor is employed in presence of a strong base. This mechanism has been evidenced through the fact that in absence of protic impurities, carbenes remain stable or decompose. Moreover, the existence of a protonated dimer intermediate obtained through the addition of a carbene onto its corresponding iminium has been demonstrated. Therefore, most of the carbenes generated through this route are believed to dimerize following the latter mechanism.

1.5.2.3 Miscellaneous dimerization reaction

Somewhat related with MACs, Hegarty *et al.*^{177,178} have reported that nitrile ylides can dimerize. The reaction involves the condensation of diaryl ketimines **135** first with different α,α -dichlorotoluenes, in the presence of *tert*-butyl lithium at -78°C in THF. The resulting ketimines **136** can subsequently ionize into **137**. After proton release, the transient nitrile ylide **138**, which is a mesomeric form of the iminoarylcarbene, subsequently dimerizes *via* the proton-catalyzed mechanism, yielding the final dimer **139**. Another possibility for generating **138** would be the concerted 1,1-elimination of HCl. Its rapid direct dimerization would then afford compound **139** (Scheme I.40).

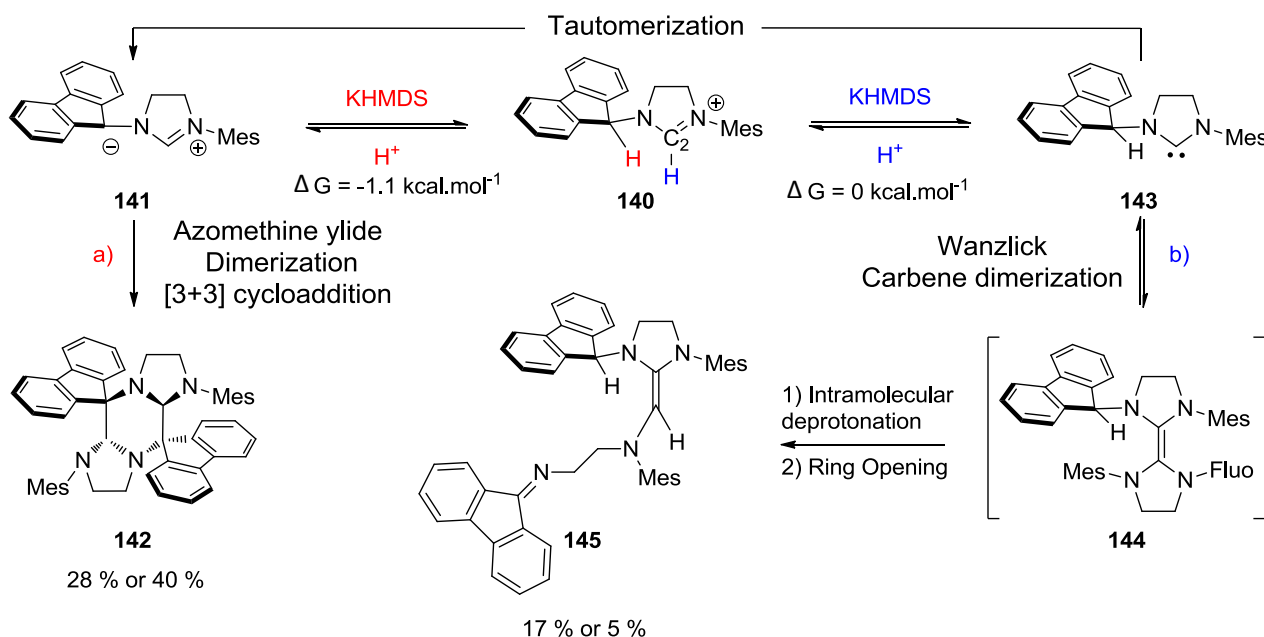
Chapter I: Similarities and differences between diaminocarbenes (DACs) and monoaminocarbenes (MACs) with special emphasis on the dimerization reaction



Scheme I.40. Nitrile-ylide dimerization through either direct and/or indirect pathway.¹⁷⁸

Recently, Grela *et al.*¹⁷⁹ have observed a competition during the dimerization of imidazoliminium salt **140**, possessing a fluorene substituent on one amino group. As expected, deprotonation with KHMDS is not selective for the C₂ proton as it can also occur at the acidic proton of the fluorenyl group. The two products obtained are isoenergetic, the azomethine ylide **141** ($\Delta G = -1.1 \text{ kcal.mol}^{-1}$) originally dimerizing into **142** via a [3+3] cycloaddition and a carbene **143** ($\Delta G = 0 \text{ kcal.mol}^{-1}$), and dimerizing into **144** following the aforementioned proton-catalyzed mechanism. Due to the acidic proton on the fluorenyl moiety, **143** can undergo an intramolecular deprotonation, followed by a ring-opening to yield the stable compound **145** (Scheme I.41).

Chapter I: Similarities and differences between diaminocarbenes (DACs) and monoaminocarbenes (MACs) with special emphasis on the dimerization reaction



Scheme I.41. Competition between a) azomethine ylide dimerization and b) carbene dimerization.¹⁷⁹

I.5.3 Theoretical investigations of the carbene dimerization reaction.

I.5.3.1 Singlet-triplet gap (ΔE_{S-T})

A key parameter to understand the relative carbene stability towards dimerization is the singlet-triplet energy gap (ΔE_{S-T}). The larger the gap is, the more stable the carbene is, hence the lesser its tendency to dimerize. Heinemann *et al.*¹⁸⁰ has been the first to perform such theoretical calculations regarding the stability of the prototype imidazol(in)-2-ylidenes (**II**, **III**) and acyclic diaminocarbenes (**I**). Using a more accurate level of theory (B3LYP/AUG-cc-pVTZ//B3LYP/6-31+G*) the group of Kassae¹⁸¹ has found a ΔE_{S-T} of 54.3 kcal.mol⁻¹ for the acyclic carbene **I**. As for the cyclic carbene **II**, the calculated gap is increased by 15.6 kcal.mol⁻¹, which is due to the small carbene bond angle. Furthermore, adding an unsaturation into the ring, *e.g.* with carbene **III**, gives the largest gap ($\Delta E_{S-T} = 83.4 \text{ kcal.mol}^{-1}$) compared to **I** and **II** because of the aromatic stabilization of the singlet state brought by $6e^- \pi$ (Figure I.13).

Chapter I: Similarities and differences between diaminocarbenes (DACs) and monoaminocarbenes (MACs) with special emphasis on the dimerization reaction

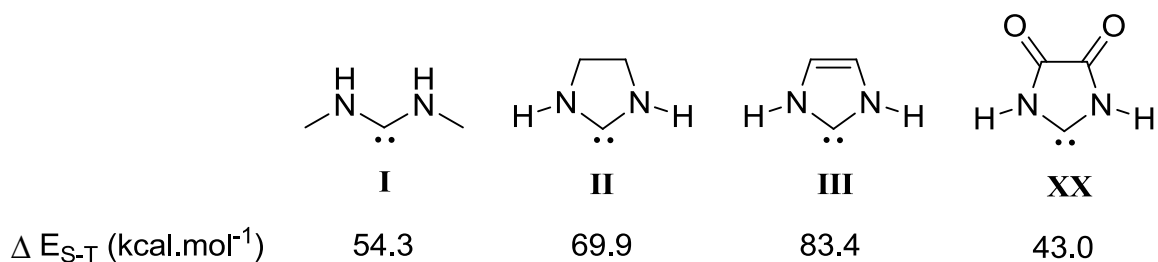


Figure I.13 Calculated ΔE_{S-T} of carbenes **I**, **II**, **III** and **XX** using MP2 theory.¹⁸⁰

Calculations with B3LYP level, as reported by Lai¹⁸² estimate the ΔE_{S-T} of the diamidocarbene **XX** at about 43 kcal.mol⁻¹, which is lower than the saturated **II**, unsaturated **III** and acyclic diamino carbene **I**. Therefore, the dimerization should be favored with diamidocarbenes as observed by Ganter *et al.*¹⁸³

The group of Alder has investigated the influence of the ring size in the cyclic saturated carbene type **II**. It has been found that by increasing the ring size (from five to seven) the ΔE_{S-T} decreases. For 5-membered ring **IV**, $\Delta E_{S-T} = 71.9$ kcal.mol⁻¹, as compared to 61.7 kcal.mol⁻¹ for the six-membered ring **V** ($\Delta E_{S-T} = 61.7$ kcal.mol⁻¹) and $\Delta E_{S-T} = 50.2$ kcal.mol⁻¹ for the seven-membered ring **VI**. As discussed before, with acyclic carbene **VII**, the value decreases with $\Delta E_{S-T} = 41.3$ kcal.mol⁻¹. These results are explained by the higher flexibility of the ring as they get larger. Indeed, the wider carbene bond angle (115° for **V**, 117° for **VI** and 120° for **VII**) allows one amino group to rotate around the CN bond, leading to a weaker stabilization of the carbene center due to the weaker interaction of the amino groups with the carbene center (Figure I.14).^{81,180,184}

Chapter I: Similarities and differences between diaminocarbenes (DACs) and monoaminocarbenes (MACs) with special emphasis on the dimerization reaction

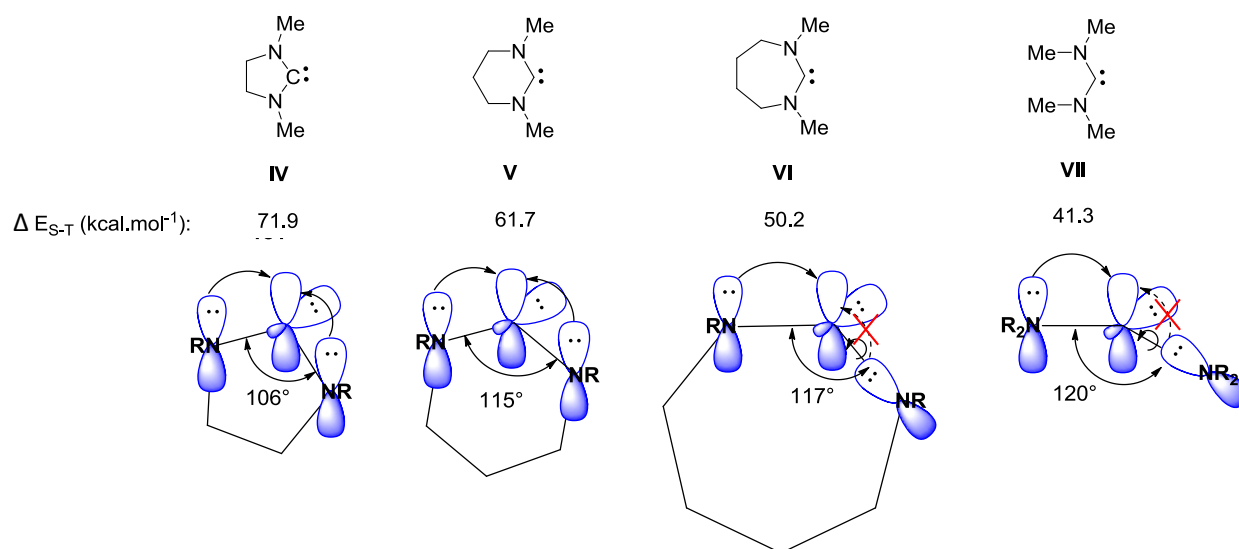

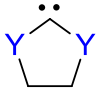



Figure I.14. ΔE_{S-T} of saturated diaminocarbenes **IV-VI** and **VII** (calculated at a B3LYP/6-31G* level of theory) with their NCN angle.^{81,180,184}

The influence of heteroatoms in the carbene stability has then been investigated by Kassae *et al.*,^{181,185} focusing on carbenes type **VIII**, **IX** and **X** with different heteroatoms, such as N, O, S, P, Si, for which the ΔE_{S-T} have been calculated (Figure I.26). In the case of diheteroatomic carbenes ΔE_{S-T} increases from acyclic carbenes **VIII** to saturated acyclic carbene **IX** and to unsaturated cyclic carbene **X**, in agreement with previous studies. For the carbene type **X**, the authors have found the largest ΔE_{S-T} when nitrogen ($\Delta E_{S-T} = 83.4$ kcal.mol⁻¹) and oxygen atoms ($\Delta E_{S-T} = 75.2$ kcal.mol⁻¹) are used.¹⁸¹ This large gap is due to their +M and -I properties, which stabilize the singlet state. The use of a sulfur atom gives a smaller gap ($\Delta E_{S-T} = 52.4$ kcal.mol⁻¹)¹⁸¹ because of its lower electronegativity, compared to N and O atoms. Despite its +M effect, phosphino-based carbenes display a very small gap of $\Delta E_{S-T} = 21.5$ kcal.mol⁻¹, which is related to its high inversion barrier.¹⁸¹ When a carbon atom is used, almost no stabilization is noted with a gap of $\Delta E_{S-T} = 7.4$ kcal.mol⁻¹ because of the absence of noticeable mesomeric and inductive effects.¹⁸¹ Finally, replacing the heteroatoms with the electropositive silicon (σ -donor) induces, in the case of dihetero and monohetero-atomic carbenes, a triplet ground state carbene ($\Delta E_{S-T} < 0$ kcal.mol⁻¹).¹⁸¹ Stabilization of carbenes, through the evaluation of their ΔE_{S-T} is therefore as follows: N \approx O > S > P > C > Si. This trend is the same for carbenes of the type **VIII** and **IX**. The same order of stabilization has been found with monoheteroatomic

Chapter I: Similarities and differences between diaminocarbenes (DACs) and monoaminocarbenes (MACs) with special emphasis on the dimerization reaction

carbenes, although the presence of a single heteroatom leads to smaller ΔE_{S-T} compared to the diheteroatomic carbenes, as discussed in section I.3.1.2 (Figure I.15).¹⁸⁵

Diheteroatomic carbene						
	VIII	IX	X			
$X =$	O	NH	S	PH	CH ₂	SiH ₂
ΔE_{S-T} (kcal.mol ⁻¹):	55.4	54.3	28.1	11.9	2.3	-21.8
$Y =$	O	NH	S	PH	CH ₂	SiH ₂
ΔE_{S-T} (kcal.mol ⁻¹):	71.0	69.9	44.3	19.0	8.1	-14.7
$Z =$	NH	O	S	PH	CH ₂	SiH ₂
ΔE_{S-T} (kcal.mol ⁻¹):	83.4	75.2	52.4	21.5	7.4	-16.3

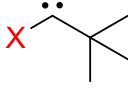
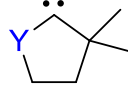
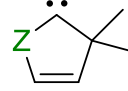
Monoheteroatomic carbene						
	XI	XII	XIII			
$X =$	OCH ₃	N(CH ₃) ₂	SCH ₃	P(CH ₃) ₂	C(CH ₃) ₃	Si(CH ₃) ₃
ΔE_{S-T} (kcal.mol ⁻¹):	29	27.8	18.7	8.6	-4.2	-15.9
$Y =$	NCH ₃	O	S	PCH ₃	C(CH ₃) ₂	Si(CH ₃) ₂
ΔE_{S-T} (kcal.mol ⁻¹):	56.4	37.3	29.6	12.1	5.5	-7.0
$Z =$	NCH ₃	O	S	PCH ₃	C(CH ₃) ₂	Si(CH ₃) ₂
ΔE_{S-T} (kcal.mol ⁻¹):	47.1	35.1	29.9	12.2	5.7	-9.1

Figure I.15. Stabilities of the carbenes expressed by their ΔE_{S-T} (calculated at a B3LYP/AUG-cc-pVTZ//B3LYP/6-31pG* level of theory) regarding the heteroatom employed.^{181,185}

The group of Huynh¹⁸⁶ has calculated the singlet-triplet gap of NHCs having three or four nitrogen atoms, within the structure. No correlation has been found between the ΔE_{S-T} gap and the number of N (84.84 kcal.mol⁻¹ calculated at the B3LYP/aug-cc-pVTZ level) (Figure I.16). Therefore **XV** and **XVI** are also stable and do not have a tendency to dimerize.

Chapter I: Similarities and differences between diaminocarbenes (DACs) and monoaminocarbenes (MACs) with special emphasis on the dimerization reaction

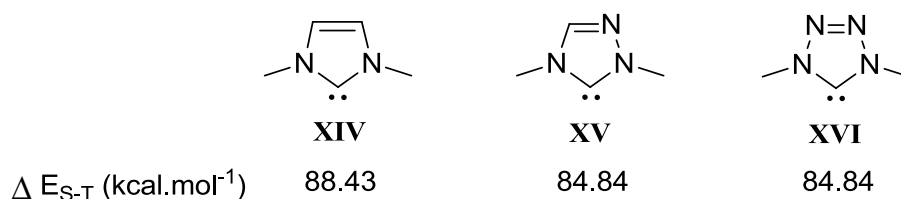


Figure I.16. ΔE_{S-T} of unsaturated diaminocarbenes **XIV**, **XV** and **XVI** calculated at the B3LYP/aug-cc-pVTZ level.¹⁸⁶

Finally, Cheng and Hue¹⁸⁷ have calculated the ΔE_{S-T} of substituted imidazol-2-ylidenes. By adding chlorine atom at the C₄ and C₅ positions, the authors have reported a decrease of the gap energy by 4.5 kcal.mol⁻¹, as compared to the unsubstituted imidazol-2-ylidenes **III**. Furthermore, the replacement of the hydrogen atom on the nitrogen atoms by methyl groups have shown a limited influence on the gap, with a difference less than 1 kcal.mol⁻¹ (Figure I.17). However, despite their small electronic effect on the ΔE_{S-T} , alkyl substituents do introduce some steric hindrance that can prevent carbenes from dimerizing (ΔG).

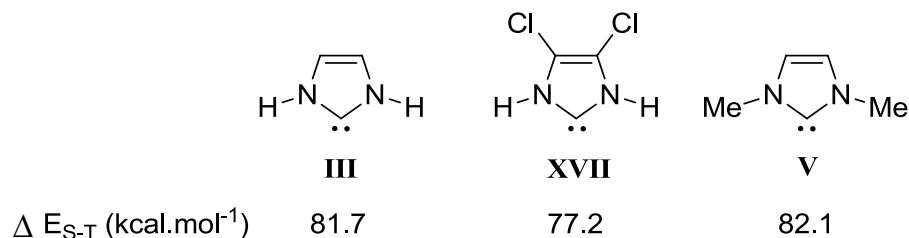


Figure I.17. ΔE_{S-T} of cyclic diaminocarbenes **III**, **XVII**, **V** calculated using the BLYP/6-31G* level.

1.5.3.2 Gibbs free energy (ΔG) / Dimerization energy ($E_{dim} = \Delta H$)

Two parameters can be calculated to anticipate whether a carbene is susceptible to dimerize, namely ΔE_{S-T} , which gives information about the carbene stability, and the Gibbs free energy (ΔG), which is indicative of the relative stability of the carbene and respective dimer.

a) Gibbs free energy (ΔG)

The group of Nyulászi has investigated the Gibbs free energy of the direct dimerization between two diaminocarbenes (Equation 1) using the B3LYP/6-311+G(2D) level of theory.¹⁸⁸

Chapter I: Similarities and differences between diaminocarbenes (DACs) and monoaminocarbenes (MACs) with special emphasis on the dimerization reaction



For instance, a negative ΔG for **I** ($\Delta G = -28.1 \text{ kcal.mol}^{-1}$) and **II** ($\Delta G = -21.2 \text{ kcal.mol}^{-1}$) have been observed along with a positive ΔG for **III** ($\Delta G = 0.9 \text{ kcal.mol}^{-1}$). In the two former cases, the reaction is highly exergonic ($\Delta G < 0 \text{ kcal.mol}^{-1}$) evidencing that dimers are more stable than the carbene precursor. For the unsaturated carbene **III** however, the $\Delta G > 0 \text{ kcal.mol}^{-1}$, demonstrating that the dimer is no more stable. Those results have been confirmed experimentally by Alder *et al.*⁸¹ and Taton *et al.*⁸⁰ (Figure I.18).

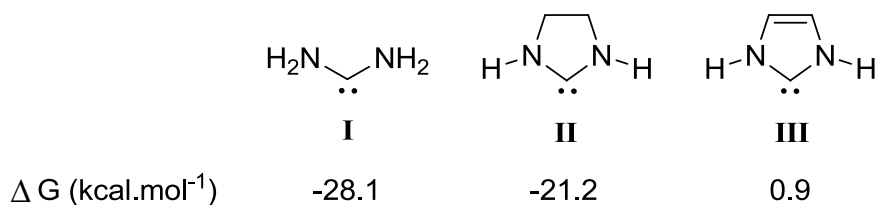


Figure I.18. Gibbs free energies of **I**, **II**, **III** calculated with the B3LYP/6-311+G(2D) level of theory.

Alder *et al.* have further investigated the influence of the ring size of saturated carbene of type **II** by evaluating the Gibbs free energy of the dimerization reaction. For carbenes **IV-VII** the dimerization reaction is exergonic ($\Delta G < 0 \text{ kcal.mol}^{-1}$). Interestingly, both seven-membered ring **VI** and ADAC **VII** display a comparable ability to dimerize with $\Delta G = -31.5 \text{ kcal.mol}^{-1}$ and $-32.9 \text{ kcal.mol}^{-1}$ respectively (Figure I.19). Their high energy of dimerization is directly related to the higher flexibility of their backbone and their large carbene bond angle, which lead to a weaker stabilization of the carbene center.

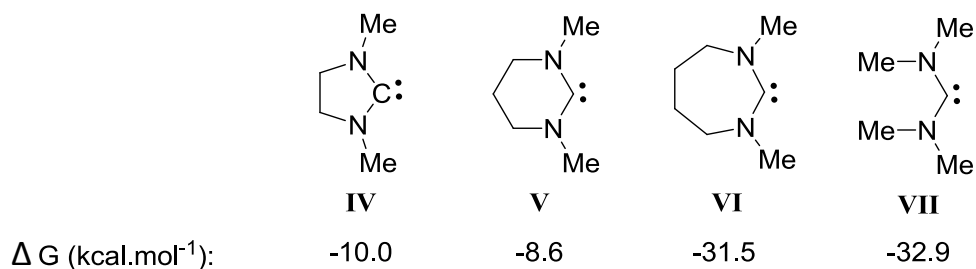


Figure I.19. Calculated ΔG of saturated NHC **IV-VI** and acyclic carbene **VII** via B3LYP/6-31G* level of theory.⁸¹

Chapter I: Similarities and differences between diaminocarbenes (DACs) and monoaminocarbenes (MACs) with special emphasis on the dimerization reaction

Moreover, Alder *et al.* have calculated the ΔG energies of carbenes **IV-VII** with different alkyl groups. By increasing the bulkiness of the alkyl group, ΔG increases, indicating less probability for dimerization.⁸¹

Denk *et al.*¹⁸⁹ have further studied the electronic influence of alkyl groups on the stabilization of carbene **II**. They have thus compared the ΔG value of the direct homodimerization of unsubstituted carbene **II**, with the direct cross dimerization of carbene **II** with a saturated carbene with only one alkyl group on the nitrogen atom. The steric effect of alkyl group is thus prevented and only its electronic effect is observed. As a result, the N-alkyl substituents has proven to electronically stabilize the carbene following the order Me<Et<iPr<*t*-Bu (Figure I.20). However, this electronic stabilization is too weak to prevent the dimerization when Me, Et and iPr groups are introduced. Indeed, the steric effect has to be taken into account and, after calculations, gives the same results with a $\Delta G < 0$ kcal.mol⁻¹ for Me, Et and iPr. Overall, only the *t*-Bu group prevents the dimerization from occurring, owing to its significant steric hindrance (ΔG_{steric}).

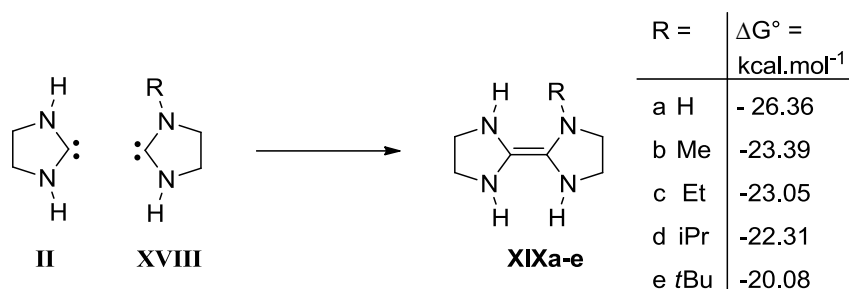


Figure I.20. Dimerization of unsymmetrical diaminocarbenes to analyze the contribution of each alkyl group on the carbene stability ΔG (the destabilization of the final dimer) at the B98/6-31G(d) level.¹⁸⁹

A drawback encountered for the determination of the Gibbs free energy, with reasonably accurate level is that such computation is prohibitively expensive. Based on a paper from Nyulászi *et al.*¹⁸⁸ which has reported an excellent correlation between the enthalpy of reaction (ΔH) with the Gibbs free energy (ΔG), alternative methodologies, evaluating energies of dimerization in correlation with the ΔH values, have been developed.

Chapter I: Similarities and differences between diaminocarbenes (DACs) and monoaminocarbenes (MACs) with special emphasis on the dimerization reaction

b) Enthalpy of dimerization ($E_{\text{dim}} = \Delta H$)

One methodology is the bond dissociation energy (BDE) developed in 1986, by Carter and Goddard using the CGMT model to correlate the carbene ΔE_{S-T} gap with the C=C energy bond of the corresponding dimer.^{171,190-192} This model is based on a computational experiment where a dimer's double bond is cleaved homolytically into two carbenic fragments which can be either in a singlet or triplet state. It was shown that the C=C energy bond can be obtained from the intrinsic C=C bond energy of the ethylene ($172 \pm 2 \text{ kcal.mol}^{-1}$) minus the sum of the ΔE_{S-T} of each carbenes (Equation 2).

$$E_{C=C} = E_{C=C} (\text{ethylene}) - 2\Delta E_{S-T} \quad (2)$$

Therefore, the higher the ΔE_{S-T} is, the higher the carbene stability (towards dimerization) will be, and the lower the C=C bond strength will be. The BDE method showed excellent correlation with the enthalpy of dimerization. As described earlier, the ΔE_{S-T} of imidazole-2-ylidenes **I**, imidazolin-2-ylidenes **II** and acyclic diaminocarbenes **III** with hydrogen as substituents on the nitrogen atoms, were found at $\Delta E_{S-T} = 84.5 \text{ kcal.mol}^{-1}$, $69.4 \text{ kcal.mol}^{-1}$ and $58.5 \text{ kcal.mol}^{-1}$ respectively. As a consequence, dimer **146** obtained from **I** features the weakest C=C bond energy ($E_{C=C} = 0.9 \text{ kcal.mol}^{-1}$). However, because of the unsaturated carbene **I** that are stable towards dimerization, dimer **146** is not isolable experimentally. Taton and Chen have found a way to isolate dimers, such as **147**, by tethering the two nitrogen atoms by a C₃ linker. Remarkably, using a C₄ linker, no dimer was observed; but instead, bis-(NHC) **148** was found formed, highlighting the dramatic influence of the number of carbon atoms in the linker (Figure I.21).¹⁹³ Despite the weakness of the C=C bond energy of **147**, the length observed by X-ray diffraction studies (1.337 \AA) was found in the range of regular C=C bonds (1.330 \AA).

Chapter I: Similarities and differences between diaminocarbenes (DACs) and monoaminocarbenes (MACs) with special emphasis on the dimerization reaction

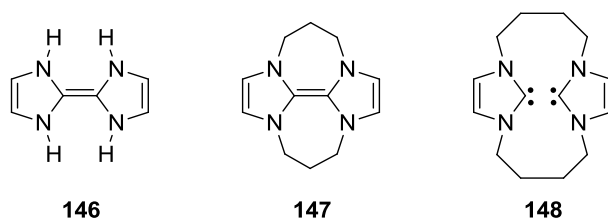
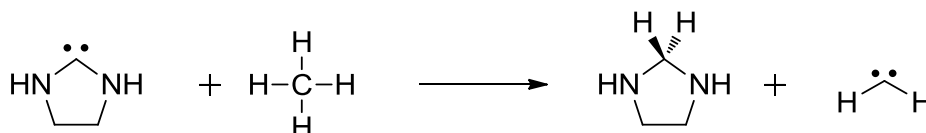


Figure I.21. Theoretical dimer **146** used for the calculation of the double bond strength, dimerization of imidazolylidene depending on the length of the bridges.¹⁹³

Another methodology proposed by Nyulászi *et al.*¹⁸⁸ is based on the isodesmic reaction which is a reaction where the type of chemical bonds broken in the reactant are the same as the type of bonds formed in the reaction product. Using this methodology the stabilization energies of carbenes can be calculated. The authors have plotted the energy of isodesmic reaction against the dimerization energy (ΔH) and the Gibbs free energy (ΔG) and have found an excellent linear correlation (Scheme I.42). This has been rationalized by the fact that the substituent effects stabilizing the carbene monomer are the same destabilizing the dimer. It is worth noting that the difference between the dimerization energy and the Gibbs free energy is due in majority to the entropy factor, which is expected to disfavor the dimerization step by $\sim 10 \text{ kcal.mol}^{-1}$.^{187,188}



$$\Delta E_{\text{isodesmic}} = 92.5 \text{ kcal.mol}^{-1} \quad \Delta H = -33.3 \text{ kcal.mol}^{-1} \quad \Delta G = -21.5 \text{ kcal.mol}^{-1}$$

Scheme I.42. Isodesmic reaction of imidazolin-2-ylidenes with its corresponding energies calculated at the B3LYP/6-311+G(2D) level of theory.¹⁸⁸

Finally, Cavallo and coworkers¹⁹⁴ have described an empirical method to rationalize the dimerization behavior of NHC, based on the electronic and steric effects (eq. 3).

$$E_{\text{dim}} = A \times \text{NHC}_{\text{steric}} + B \times \text{NHC}_{\text{electronic}} + C \quad (3)$$

$$A = 3.28 \text{ kcal.mol}^{-1} \quad B = 2.08 \text{ kcal.mol}^{-1} \quad C = -233.25 \text{ kcal.mol}^{-1}$$

Chapter I: Similarities and differences between diaminocarbenes (DACs) and monoaminocarbenes (MACs) with special emphasis on the dimerization reaction

In this equation, the electronic component is represented by $\text{NHC}_{\text{electronic}} = \Delta E_{\text{S-T}}$, while $\text{NHC}_{\text{steric}} = \%V_{\text{Bur}}$ represents the steric term, where $\%V_{\text{Bur}}$ is defined by the volume of a sphere centered on a metal which is buried by overlapping of a NHC. This structural parameter can be considered as analogous to Tolman's cone angle, which allows to classify tertiary phosphines according to their steric bulk (Figure I.22).^{195,196} The empirical parameters A, B and C are fitted to reproduce a set of E_{dim} values (Equation 3).

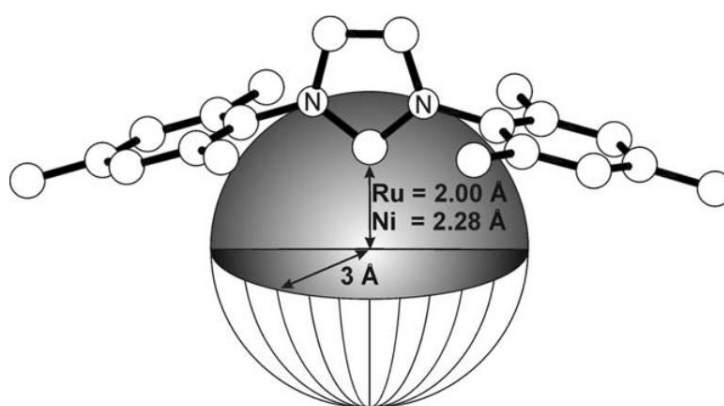


Figure I.22. Schematic representation of the sphere dimensions used for determination of the steric parameter $\%V_{\text{Bur}}$ (Reproduced from Cavallo *et al.*)¹⁹⁷

Thus, the ΔE_{dim} values obtained from this equation can predict the behavior of NHC. If $\Delta E_{\text{dim}} \leq -20 \text{ kcal.mol}^{-1}$, the NHC exist as a dimer, while if $\Delta E_{\text{dim}} \geq 0 \text{ kcal.mol}^{-1}$, the NHC is stable as a “monomer”. If values are found in between $-20 \leq \Delta E_{\text{dim}} \leq 0 \text{ kcal.mol}^{-1}$, hence there is an existing equilibrium between the free NHC and its dimer (Figure I.23).

Chapter I: Similarities and differences between diaminocarbenes (DACs) and monoaminocarbenes (MACs) with special emphasis on the dimerization reaction

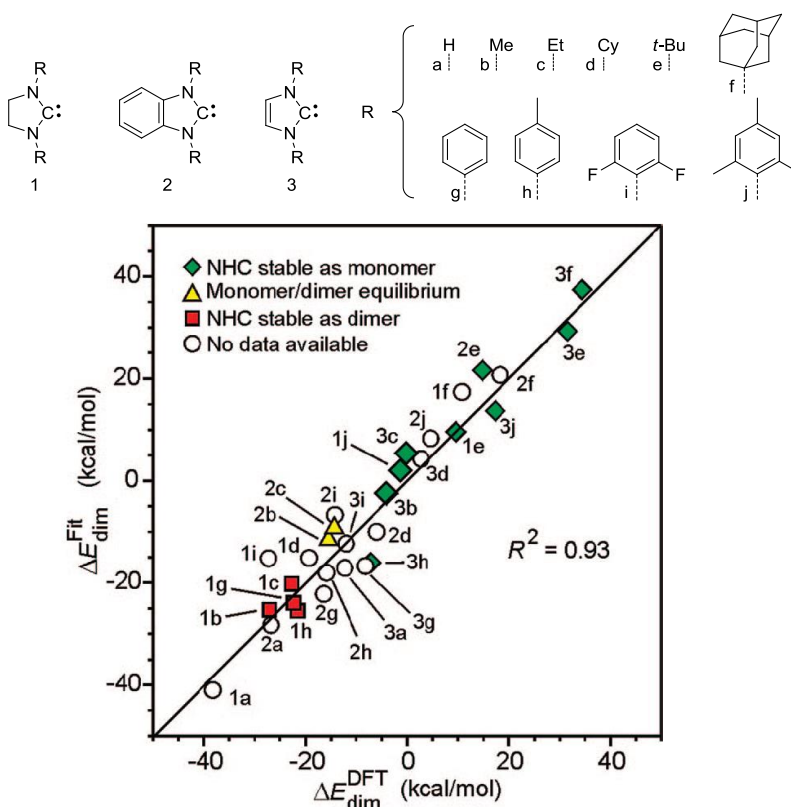


Figure I.23. Plot of E_{Dim}^{Fit} versus E_{Dim}^{DFT} for the NHCs in the inset. The diagonal line is plotted to guide the eye. The color scheme indicates the experimental behavior (Reproduced from Poater *et al.*).¹⁹⁴

Figure 23 highlights the three distinct behaviors described above, with the examples of NHC **1**, **2** and **3**. Imidazole-2-ylidene **3** (green rhombus) behaves as a stable “monomer”. These results are in agreement with the experimental experiences.^{21,198–201} In contrast, imidazolin-2-ylidenes **1** (red square) behave as stable dimers,^{169,200} except when bulky substituents (t-Bu or Mes) are introduced onto the amino group. In the latter case **1e** and **1j** exist as “monomers”.^{66,200,201} Finally, the structural properties of benzimidazol-2-ylidene **2** (yellow triangle), are close to those of imidazol-2-ylidene **3**, with similar Csp^2 carbon in the back of the N-heterocyclic ring. However, it shares the electronic properties of imidazolin-2-ylidenes **1**. Thus, these carbenes can be viewed as “monomers” or dimers.^{170,202}

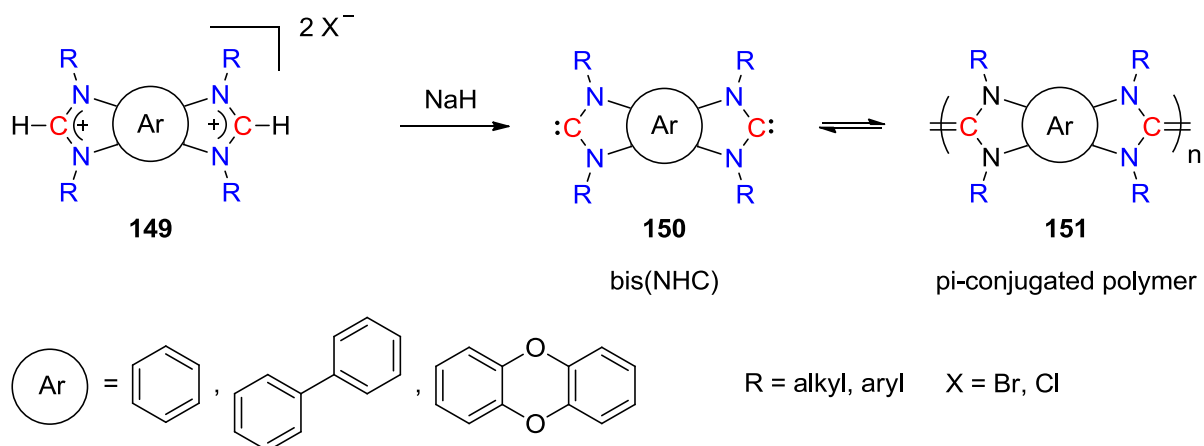
In this part the controversy of the Wanzlick equilibrium has been presented along with the study of the two mechanisms available for the dimerization of carbenes. Then, calculation methods to anticipate if a carbene is likely to dimerize or to stay stable in its free form have been discussed. The goal of this PhD work is to use the carbenes as true monomer substrates in

Chapter I: Similarities and differences between diaminocarbenes (DACs) and monoaminocarbenes (MACs) with special emphasis on the dimerization reaction

polymer synthesis by taking advantage of their dimerization reaction to generate substituted double bond in an original way and thus, synthesize new π -conjugated polymers. This area of research has received very little attention, thus, in the last part, the work reported by Bielawski using the dimerization/polymerization reaction of bis-benzimidazol-2-ylidene-type NHCs to synthesize thermally reversible (dynamic) covalent π -conjugated polymers is presented.

I.5.4 Dimerization reaction: from molecular to polymer chemistry

In 2006, Bielawski *et al.* took advantage of the propensity of carbenes to dimerize to construct original dynamic materials for electronic, sensing and catalytic applications (*i.e.* ROP of lactides).^{203–206} More precisely, by using the reversible dimerization of bis-benzimidazolylienes **150**, they reported the first dynamic conjugated polymer. **150** were prepared by deprotonation of bis-benzimidazolium salt **149** with NaH. After 12 hours at room temperature, the polymerization of bis-carbenes **150** was observed by ¹H NMR spectroscopy. The analysis of the crude mixture revealed the presence of broad signals attributed to polymer **151** and sharp ones corresponding to the monomeric carbenes **150**. As expected, the polymer/monomer ratio was found to be highly dependent of the substituents on the nitrogen atoms. When methyl groups are used, polymerization is favored and leads to insoluble high molecular weight polymers. However, with bulkier substituents, the equilibrium is shifted towards monomeric bis-carbenes **150** (Scheme I.43).

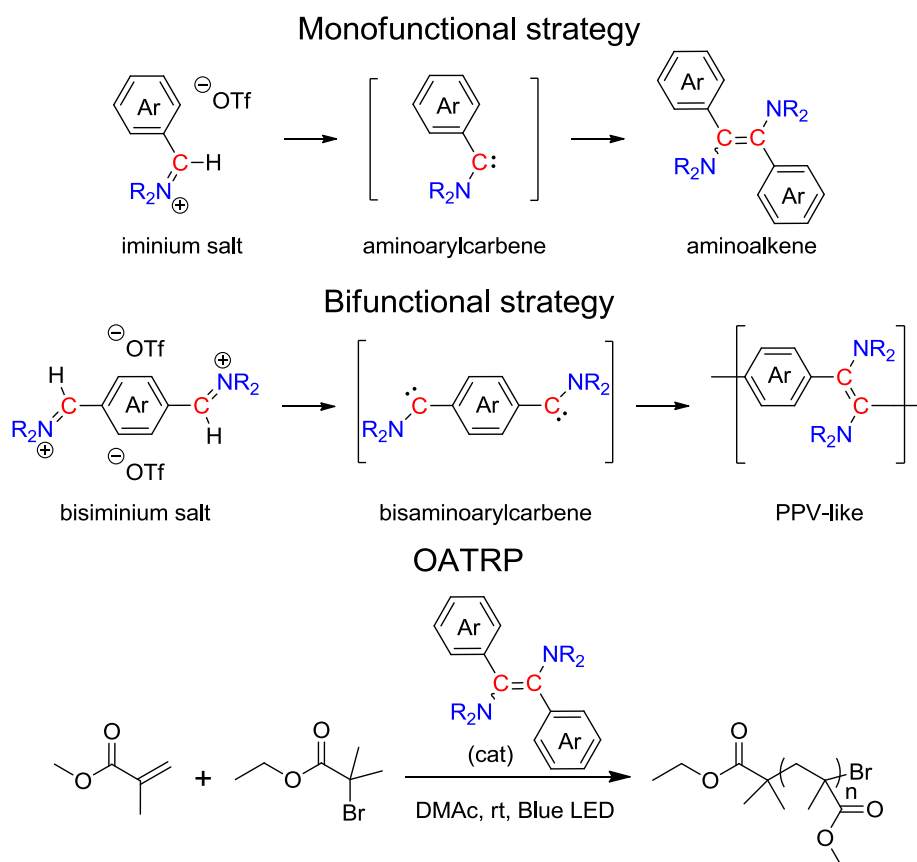


Scheme I.43. Difunctional carbene dimerization into original dynamic conjugated polymers.^{203–205}

Chapter I: Similarities and differences between diaminocarbenes (DACs) and monoaminocarbenes (MACs) with special emphasis on the dimerization reaction

This PhD work focus on the use of carbenes as monomer substrates in polymer synthesis, in particular, the attention is directed on the aminoarylcarbene, a class of carbenes very poorly studied. Compared to the bis-benzimidazol-2-ylidene-type NHCs used by Bielawski, leading to thermally reversible covalent conjugated polymers with limited electron delocalization along the polymer chain, the dimerization of bis-aminoarylcarbene should be thermally irreversible and lead to new poly(phenylene vinylene)(PPV)-like polymers which are known to be useful for electronic applications. Furthermore, thanks to this route, amino groups can easily be incorporated onto the double bond in sharp contrast with conventional synthetic strategies. Moreover, modifications of the aryl or amino moieties should allow a fine-tuning of the amino-containing PPV polymers properties. Therefore, this work is divided in three part. First, the study of the dimerization reaction of monoaminoarylcarbene generated *in-situ* by deprotonation of the corresponding iminium is presented in chapter II. Then, the dimerization/polymerization performed with the use of bis-aminoarylcarbene was performed to access original N-PPV polymers, followed by their characterizations and studies of their properties after modifications (quaternization, protonation of the amino groups) is discussed (chapter III). Finally, the dimers obtained in chapter II are structurally related to the tetraaminoethylenes, which are known to be strong reducing agent. Hence, a study of their potential reduction ability as stoichiometric reagent and as catalyst in photoinduced atom transfer radical polymerization (ATRP) is described (chapter IV; Scheme I.44).

Chapter I: Similarities and differences between diaminocarbenes (DACs) and monoaminocarbenes (MACs) with special emphasis on the dimerization reaction



Scheme I.44. Synthesis of diaminoalkenes *via* dimerization of monoaminoarylcarbenes. Synthesis of new N-PPV polymers obtained through dimerization/polymerization of bis-aminoarylcarbenes. Synthesis of PMMA polymers through OATRP using the synthesized diaminoalkenes.

I.6 Conclusion

Since their first isolation and characterization, carbenes which started as academic curiosities, became one of the most powerful tools in organic chemistry. The most popular carbenes are the push-push stabilized diaminocarbenes, including *N*-Heterocyclic carbene. This type of carbenes revealed to be excellent catalyst in various reactions such as, the benzoin condensation, the ring opening polymerization, atom transfer radical polymerization and step-growth polymerization, which is due to their good balance between the nucleophilicity and the ability to act as good leaving group. The other family presented is the push-spectator monoaminocarbenes (MAC). The latter have the peculiar reactivity of their transient species which is used in various organic reactions such as, the migrations, the insertion in X-H bond (X = H, C, B, Si, P, O, N), the cyclopropanation and the coupling reactions. Both families, however, share common

Chapter I: Similarities and differences between diaminocarbenes (DACs) and monoaminocarbenes (MACs) with special emphasis on the dimerization reaction

reactivities by being both excellent ancillary ligands in organometallic field, adding onto heterocumulenes (CCC, CS₂, CO₂) and being able to insert into activated C-H bonds. Last common reactivity is their ability to dimerize. The latter reaction is the center of interest of this PhD work thus, it was deeply investigated. The Wanzlick equilibrium was first investigated and evidence was found by working with the benzimidazol-2-ylidene moiety where both the free carbene form and its dimeric form were observed simultaneously. However, the equilibrium was strongly expected to be catalyzed by electrophilic impurities. Then, the dimerization was proposed to go through two mechanisms (a direct and an indirect pathway). The direct and non-least motion pathway involves a nucleophilic attack of the filled in plane σ -orbital of one carbene onto the out-of-plane formally vacant p_{π} -orbital of a second carbene. For the proton-catalyzed pathway the carbene generated by deprotonation of its corresponding amidinium salt is nucleophilic enough to add onto its amidinium salt precursor, leading to a protonated dimer intermediate. The latter is deprotonated by a base leading to the final dimer. The dimerization of diaminocarbenes and most MACs has been reported to proceed through a proton-catalyzed mechanism despite the fact that a direct approach have yet been ruled out experimentally. Calculations to anticipate the ability of a carbene to dimerize has been shown by measuring their singlet-triplet energy gap (ΔE_{S-T}) and Gibbs free energy (ΔG). Finally, the use of carbenes as building block to synthesize original π -conjugated polymers has been described with the work of Bielawski *et al.* and the dimerization/polymerization of bis-benzimidazol-2-ylidene-type NHCs leading to thermally reversible covalent conjugated polymers.

In the next chapter, the study of the reactivity, including the dimerization reaction, of aminoarylcarbenes will be presented. It will be followed in chapter 3 by the study of the dimerization/polymerization of bis-aminoarylcarbenes leading to new amino-containing PPV (N-PPV) and the study of their properties after modifications of their amino groups. In the last chapter, the dimers obtained *via* dimerization of monoaminoarylcarbenes showed interesting reducing properties, thus a study on their reduction potential as stoichiometric reagents and as catalysts in organic atom transfer radical polymerization will be presented.

Chapter I: Similarities and differences between diaminocarbenes (DACs) and monoaminocarbenes (MACs) with special emphasis on the dimerization reaction

I.7 References

- 1 M. Alcarazo, C. W. Lehmann, A. Anoop, W. Thiel and A. Fürstner, *Nat. Chem.*, 2009, **1**, 295–301.
- 2 C. A. Dyker and G. Bertrand, 2009, 2.
- 3 M. B. Smith and J. March, *March's Advanced Organic Chemistry*, John Wiley & Sons, Inc., Hoboken, NJ, USA, 2006.
- 4 E. C. Ashby, A. K. Deshpande and F. Doctorovich, *J. Org. Chem.*, 1993, **58**, 4205–4206.
- 5 M. T. H. Liu, *Chem Soc Rev*, 1982, **11**, 127–140.
- 6 R. W. Saalfrank, *Angew. Chem.*, 1987, **99**, 1335–1335.
- 7 J.-M. Fedé, S. Jockusch, N. Lin, R. A. Moss and N. J. Turro, *Org. Lett.*, 2003, **5**, 5027–5030.
- 8 R. A. Moss and X. Fu, *Org. Lett.*, 2004, **6**, 3353–3356.
- 9 W. Kirmse and M. Buschhoff, *Angew. Chem. Int. Ed. Engl.*, 1965, **4**, 692–692.
- 10 W. von E. Doering and A. K. Hoffmann, *J. Am. Chem. Soc.*, 1954, **76**, 6162–6165.
- 11 M. Mpkosza and Y. Waurzynienioz, *Tetrahedron Lett.*, 1969, 4659–4662.
- 12 E. Buchner and Th. Curtius, *Berichte Dtsch. Chem. Ges.*, 1885, **18**, 2377–2379.
- 13 H. Staudinger and O. Kupfer, *Berichte Dtsch. Chem. Ges.*, 1912, **45**, 501–509.
- 14 L. Tschugajeff, M. Skanawy-Grigorjewa, A. Posnjak and M. Skanawy-Grigorjewa, *Z. Für Anorg. Allg. Chem.*, 1925, **148**, 37–42.
- 15 E. O. Fischer and A. Maasböl, *Angew. Chem. Int. Ed. Engl.*, 1964, **3**, 580–581.
- 16 K. Öfele, *J Organomet Chem*, 1968, 42–43.
- 17 D. J. Cardin, B. Cetinkaya and M. F. Lappert, *Chem Rev*, 1972, **72**, 545–573.
- 18 R. Breslow, *J. Am. Chem. Soc.*, 1958, **80**, 3719–3726.
- 19 H. W. Wanzlick, *Angew. Chem. Int. Ed.*, 1962, **1**, 75–80.
- 20 A. Igau, H. Grutzmacher, A. Baceiredo and G. Bertrand, *J. Am. Chem. Soc.*, 1988, **110**, 6463–6466.
- 21 A. J. Arduengo III, R. L. Harlow and M. Kline, *J. Am. Chem. Soc.*, 1991, **113**, 361–363.
- 22 T. Kato, H. Gornitzka, A. Baceiredo, A. Savin and G. Bertrand, *J. Am. Chem. Soc.*, 2000, **122**, 998–999.
- 23 T. Takui, K. Furukawa, K. Itoh, I. Miyahara, K. Hirotsu, T. Watanabe, K. Hirai and H. Tomioka, *Mol. Cryst. Liq. Cryst. Sci. Technol. Sect. Mol. Cryst. Liq. Cryst.*, 1996, **278**, 247–252.
- 24 H. Tomioka, E. Iwamoto, H. Itakura and K. Hirai, *Nature*, 2001, **412**, 626–628.
- 25 K. Hirai, T. Itoh and H. Tomioka, *Chem. Rev.*, 2009, **109**, 3275–3332.
- 26 W. A. Herrmann and C. Köcher, *Angew. Chem. Int. Ed. Engl.*, 1997, **36**, 2162–2187.
- 27 W. A. Herrmann, *Angew. Chem. Int. Ed.*, 2002, **41**, 1290–1309.
- 28 F. E. Hahn and M. C. Jahnke, *Angew. Chem. Int. Ed.*, 2008, **47**, 3122–3172.
- 29 S. Díez-González, N. Marion and S. P. Nolan, *Chem. Rev.*, 2009, **109**, 3612–3676.
- 30 D. Tapu, D. A. Dixon and C. Roe, *Chem. Rev.*, 2009, **109**, 3385–3407.
- 31 P. de Frémont, N. Marion and S. P. Nolan, *Coord. Chem. Rev.*, 2009, **253**, 862–892.
- 32 O. Schuster, L. Yang, H. G. Raubenheimer and M. Albrecht, *Chem. Rev.*, 2009, **109**, 3445–3478.
- 33 M. N. Hopkinson, C. Richter, M. Schedler and F. Glorius, *Nature*, 2014, **510**, 485–496.
- 34 In *The Organometallic Chemistry of N-heterocyclic Carbenes*, John Wiley & Sons, Ltd, Chichester, UK, 2017, pp. 17–51.
- 35 US9676676B2, .
- 36 D. Enders, O. Niemeier and A. Henseler, *Chem. Rev.*, 2007, **107**, 5606–5655.

Chapter I: Similarities and differences between diaminocarbenes (DACs) and monoaminocarbenes (MACs) with special emphasis on the dimerization reaction

- 37 N. Marion, S. Díez-González and S. P. Nolan, *Angew. Chem. Int. Ed.*, 2007, **46**, 2988–3000.
- 38 J. Raynaud, W. N. Ottou, Y. Gnanou and D. Taton, *Chem. Commun.*, 2010, **46**, 3203.
- 39 X. Bugaut and F. Glorius, *Chem. Soc. Rev.*, 2012, **41**, 3511–3522.
- 40 D. M. Flanigan, F. Romanov-Michailidis, N. A. White and T. Rovis, *Chem. Rev.*, 2015, **115**, 9307–9387.
- 41 M. H. Wang and K. A. Scheidt, *Angew. Chem. Int. Ed.*, 2016, **55**, 14912–14922.
- 42 E. Reyes, U. Uria, L. Carrillo and J. Vicario, *Synthesis*, 2016, **49**, 451–471.
- 43 X.-Y. Chen, Q. Liu, P. Chauhan and D. Enders, *Angew. Chem. Int. Ed.*, 2018, **57**, 3862–3873.
- 44 A. P. Marchand and N. M. Brockway, *Chem. Rev.*, 1974, **74**, 431–469.
- 45 P. J. Stang, *Acc. Chem. Res.*, 1978, **11**, 107–114.
- 46 P. J. Stang, *Acc. Chem. Res.*, 1982, **15**, 348–354.
- 47 K. G. Taylor, *Tetrahedron*, 1982, **38**, 2751–2772.
- 48 J. Vignolle, X. Cattoën and D. Bourissou, *Chem. Rev.*, 2009, **109**, 3333–3384.
- 49 D. Bourissou, O. Guerret, F. P. Gabbaï and G. Bertrand, *Chem. Rev.*, 2000, **100**, 39–92.
- 50 G. B. Schuster, in *Advances in Physical Organic Chemistry*, Elsevier, 1986, vol. 22, pp. 311–361.
- 51 Rolf. Gleiter and Roald. Hoffmann, *J. Am. Chem. Soc.*, 1968, **90**, 5457–5460.
- 52 J. F. Harrison, *J. Am. Chem. Soc.*, 1971, **93**, 4112–4119.
- 53 C. W. Bauschlicher, H. F. Schaefer and P. S. Bagus, *J. Am. Chem. Soc.*, 1977, **99**, 7106–7110.
- 54 W. W. Schoeller, *J. Chem. Soc. Chem. Commun.*, 1980, 124–125.
- 55 K. K. Irikura, W. A. Goddard and J. L. Beauchamp, *J. Am. Chem. Soc.*, 1992, **114**, 48–51.
- 56 M.-G. Song and R. S. Sheridan, *J. Phys. Org. Chem.*, 2011, **24**, 889–893.
- 57 Roald. Hoffmann, G. D. Zeiss and G. W. Van Dine, *J. Am. Chem. Soc.*, 1968, **90**, 1485–1499.
- 58 N. C. Baird and K. F. Taylor, *J. Am. Chem. Soc.*, 1978, **100**, 1333–1338.
- 59 L. Pauling, *J. Chem. Soc. Chem. Commun.*, 1980, 688–689.
- 60 S. Sole, H. Gornitzka, W. Schoeller W., D. Bourissou and G. Bertrand, *Science*, 2001, **292**, 1901–1903.
- 61 In *The Organometallic Chemistry of N-heterocyclic Carbenes*, John Wiley & Sons, Ltd, Chichester, UK, 2017, pp. 52–98.
- 62 S. Naumann and A. P. Dove, *Polym. Chem.*, 2015, **6**, 3185–3200.
- 63 D. Enders, K. Breuer, G. Raabe, J. Runsink, J. H. Teles, J.-P. Melder, K. Ebel and S. Brode, *Angew. Chem. Int. Ed. Engl.*, 1995, **34**, 1021–1023.
- 64 F. E. Hahn, L. Wittenbecher, R. Boese and D. Bläser, *Chem. - Eur. J.*, 1999, **5**, 1931–1935.
- 65 A. J. Arduengo, J. R. Goerlich and W. J. Marshall, *Liebigs Ann.*, 1997, **1997**, 365–374.
- 66 A. J. Arduengo III, J. R. Goerlich and W. J. Marshall, *J. Am. Chem. Soc.*, 1995, **117**, 11027–11028.
- 67 E. Despagnet-Ayoub and R. H. Grubbs, *J. Am. Chem. Soc.*, 2004, **126**, 10198–10199.
- 68 R. W. Alder, P. R. Allen, M. Murray and A. G. Orpen, *Angew. Chem. Int. Ed. Engl.*, 1996, **35**, 1121–1123.
- 69 Roger. W. Alder, C. P. Butts and A. G. Orpen, *J. Am. Chem. Soc.*, 1998, **120**, 11526–11527.
- 70 T. W. Hudnall and C. W. Bielawski, *J. Am. Chem. Soc.*, 2009, **131**, 16039–16041.
- 71 D. Martin, N. Lassauque, B. Donnadieu and G. Bertrand, *Angew. Chem. Int. Ed.*, 2012, **51**, 6172–6175.

Chapter I: Similarities and differences between diaminocarbenes (DACs) and monoaminocarbenes (MACs) with special emphasis on the dimerization reaction

- 72 V. Lavallo, Y. Canac, B. Donnadiou, W. Schoeller W. and G. Bertrand, *Science*, 2006, 6652–6655.
- 73 M. Melaimi, M. Soleilhavoup and G. Bertrand, *Angew. Chem. Int. Ed.*, 2010, **49**, 8810–8849.
- 74 T. W. Hudnall, A. G. Tennyson and C. W. Bielawski, *Organometallics*, 2010, **29**, 4569–4578.
- 75 G. W. Nyce, S. Csihony, R. M. Waymouth and J. L. Hedrick, *Chem. - Eur. J.*, 2004, **10**, 4073–4079.
- 76 N. Kuhn and T. Kratz, *Synthesis*, 1993, 561–562.
- 77 H. Zhou, W.-Z. Zhang, Y.-M. Wang, J.-P. Qu and X.-B. Lu, *Macromolecules*, 2009, **42**, 5419–5421.
- 78 D. Enders, K. Breuer, G. Raabe, J. Runsink, J. H. Teles, J.-P. Melder, K. Ebel and S. Brode, *Angew. Chem. Int. Ed. Engl.*, 1995, **34**, 1021–1023.
- 79 F. E. Hahn, L. Wittenbecher, D. Le Van and R. Fröhlich, *Angew. Chem. Int. Ed.*, 2000, **39**, 541–544.
- 80 T. A. Taton and P. Chen, *Angew. Chem. Int. Ed. Engl.*, 1996, **35**, 1011–1013.
- 81 R. W. Alder, M. E. Blake, L. Chaker, J. N. Harvey, F. Paolini and J. Schütz, *Angew. Chem. Int. Ed.*, 2004, **43**, 5896–5911.
- 82 R. W. Alder, M. E. Blake, C. Bortolotti, S. Bufali, C. P. Butts, E. Linehan, J. M. Oliva, A. Guy Orpen and M. J. Quayle, *Chem. Commun.*, 1999, 241–242.
- 83 T. W. Hudnall, J. P. Moerdyk and C. W. Bielawski, *Chem. Commun.*, 2010, **46**, 4288–4290.
- 84 Roald. Hoffmann, *J. Am. Chem. Soc.*, 1968, **90**, 1475–1485.
- 85 D. M. Andrada, N. Holzmann, T. Hamadi and G. Frenking, *Beilstein J. Org. Chem.*, 2015, **11**, 2727–2736.
- 86 D. Munz, *Organometallics*, 2018, **37**, 275–289.
- 87 D. Martin, Y. Canac, V. Lavallo and G. Bertrand, *J. Am. Chem. Soc.*, 2014, **136**, 5023–5030.
- 88 G. D. Frey, M. Song, J.-B. Bourg, B. Donnadiou, M. Soleilhavoup and G. Bertrand, *Chem. Commun.*, 2008, 4711–4713.
- 89 S. Goumri, Y. Leriche, H. Gornitzka, A. Baceiredo and G. Bertrand, *Eur. J. Inorg. Chem.*, 1998, **10**, 1539–1542.
- 90 S. Conejero, Y. Canac, F. S. Tham and G. Bertrand, *Angew. Chem. Int. Ed.*, 2004, **43**, 4089–4093.
- 91 Y. Canac, S. Conejero, B. Donnadiou, W. W. Schoeller and G. Bertrand, *J. Am. Chem. Soc.*, 2005, **127**, 7312–7313.
- 92 Y. Canac, S. Conejero, M. Soleilhavoup, B. Donnadiou and G. Bertrand, *J. Am. Chem. Soc.*, 2006, **128**, 459–464.
- 93 B. Rao, H. Tang, X. Zeng, L. Liu, M. Melaimi and G. Bertrand, *Angew. Chem. Int. Ed.*, 2015, **54**, 14915–14919.
- 94 Z. R. McCarty, D. N. Lastovickova and C. W. Bielawski, *Chem. Commun.*, 2016, **52**, 5447–5450.
- 95 M. Melaimi, R. Jazzar, M. Soleilhavoup and G. Bertrand, *Angew. Chem. Int. Ed.*, 2017, **56**, 10046–10068.
- 96 H. Song, H. Kim and E. Lee, *Angew. Chem. Int. Ed.*, 2018, **57**, 8603–8607.
- 97 R. Nakano, R. Jazzar and G. Bertrand, *Nat. Chem.*, 2018, **10**, 1196–1200.
- 98 M. Otto, S. Conejero, Y. Canac, V. D. Romanenko, V. Rudzevitch and G. Bertrand, *J. Am. Chem. Soc.*, 2004, **126**, 1016–1017.

Chapter I: Similarities and differences between diaminocarbenes (DACs) and monoaminocarbenes (MACs) with special emphasis on the dimerization reaction

- 99 N. Merceron-Saffon, A. Baceiredo, H. Gornitzka and G. Bertrand, 2003, 1223–1225.
- 100 S. Conejero, M. Song, D. Martin, Y. Canac, M. Soleilhavoup and G. Bertrand, *Chem. – Asian J.*, 2006, **1**, 155–160.
- 101 V. Lavallo, Y. Canac, C. Präsang, B. Donnadiou and G. Bertrand, *Angew. Chem. Int. Ed.*, 2005, **44**, 5705–5709.
- 102 V. Lavallo, J. Mafhouz, Y. Canac, B. Donnadiou, W. W. Schoeller and G. Bertrand, *J. Am. Chem. Soc.*, 2004, **126**, 8670–8671.
- 103 V. Lavallo, Y. Canac, B. Donnadiou, W. W. Schoeller and G. Bertrand, *Angew. Chem. Int. Ed.*, 2006, **45**, 3488–3491.
- 104 A. Nickon, *Acc. Chem. Res.*, 1993, **26**, 84–89.
- 105 Wolfram. Sander, Goetz. Bucher and Stefan. Wierlacher, *Chem. Rev.*, 1993, **93**, 1583–1621.
- 106 H. M. Sulzbach, M. S. Platz, H. F. Schaefer and C. M. Hadad, *J. Am. Chem. Soc.*, 1997, **119**, 5682–5689.
- 107
- 108
- 109 X. Cattoën, S. Solé, C. Pradel, H. Gornitzka, K. Miqueu, D. Bourissou and G. Bertrand, *J. Org. Chem.*, 2003, **68**, 911–914.
- 110 D. A. Culkin, W. Jeong, S. Csihony, E. D. Gomez, N. P. Balsara, J. L. Hedrick and R. M. Waymouth, *Angew. Chem. Int. Ed.*, 2007, **46**, 2627–2630.
- 111 J. Vignolle, M. Asay, K. Miqueu, D. Bourissou and G. Bertrand, *Org. Lett.*, 2008, **10**, 4299–4302.
- 112 J. P. Moerdyk, D. Schilter and C. W. Bielawski, *Acc. Chem. Res.*, 2016, **49**, 1458–1468.
- 113 Z. R. Turner, *Chem. - Eur. J.*, 2016, **22**, 11461–11468.
- 114 C. Deutsch, N. Krause and B. H. Lipshutz, *Chem. Rev.*, 2008, **108**, 2916–2927.
- 115 R. H. Morris, *Chem. Soc. Rev.*, 2009, **38**, 2282–2291.
- 116 R. Malacea, R. Poli and E. Manoury, *Coord. Chem. Rev.*, 2010, **254**, 729–752.
- 117 G. D. Frey, J. D. Masuda, B. Donnadiou and G. Bertrand, *Angew. Chem. Int. Ed.*, 2010, **49**, 9444–9447.
- 118 D. Martin, M. Soleilhavoup and G. Bertrand, *Chem Sci*, 2011, **2**, 389–399.
- 119 G. D. Frey, V. Lavallo, B. Donnadiou, W. W. Schoeller and G. Bertrand, *Science*, 2007, **316**, 439–441.
- 120
- 121
- 122 S. Matsuoka, Y. Ota, A. Washio, A. Katada, K. Ichioka, K. Takagi and M. Suzuki, *Org. Lett.*, 2011, **13**, 3722–3725.
- 123 T. Kato, Y. Ota, S. Matsuoka, K. Takagi and M. Suzuki, *J. Org. Chem.*, 2013, **78**, 8739–8747.
- 124 J. H. Boyer and W. Beverung, *J. Chem. Soc. Chem. Commun.*, 1969, 1377b.
- 125 Engelbert. Ciganek, *J. Org. Chem.*, 1970, **35**, 3631–3636.
- 126 N. Obata and T. Takizawa, *Tetrahedron Lett.*, 1969, 3403–3406.
- 127 J. A. Green and L. A. Singer, *Tetrahedron Lett.*, 1969, **58**, 5093–5095.
- 128
- 129 N. Merceron, K. Miqueu, A. Baceiredo and G. Bertrand, *J. Am. Chem. Soc.*, 2002, **124**, 6806–6807.
- 130 M. Melaimi, R. Jazzar, M. Soleilhavoup and G. Bertrand, *Angew. Chem. Int. Ed.*, 2017, **56**, 10046–10068.

Chapter I: Similarities and differences between diaminocarbenes (DACs) and monoaminocarbenes (MACs) with special emphasis on the dimerization reaction

- 131 V. Lavallo, Y. Canac, B. Donnadiou, W. W. Schoeller and G. Bertrand, *Angew. Chem. Int. Ed.*, 2006, **45**, 3488–3491.
- 132 U. Siemeling, C. Färber, C. Bruhn, M. Leibold, D. Selent, W. Baumann, M. von Hopffgarten, C. Goedecke and G. Frenking, *Chem. Sci.*, 2010, **1**, 697.
- 133 T. Schulz, C. Färber, M. Leibold, C. Bruhn, W. Baumann, D. Selent, T. Porsch, M. C. Holthausen and U. Siemeling, *Chem. Commun.*, 2013, **49**, 6834.
- 134 L. Delaude, *Eur. J. Inorg. Chem.*, 2009, **2009**, 1681–1699.
- 135 O. Wagner, M. Ehle and M. Regitz, *Angew. Chem. Int. Ed. Engl.*, 1989, **28**, 225–226.
- 136 H. memmesheimer and M. Regitz, *Rev Heteroat. Chem*, 1994, 61.
- 137 W. A. Herrmann, C.-P. Reisinger and M. Spiegler, *J. Organomet. Chem.*, 1998, **557**, 93–96.
- 138 C. Zhang, J. Huang, M. L. Trudell and S. P. Nolan, *J. Org. Chem.*, 1999, **64**, 3804–3805.
- 139 E. Peris, J. Mata, J. A. Loch and R. H. Crabtree, *Chem. Commun.*, 2001, 201–202.
- 140 C. Yang, H. M. Lee and S. P. Nolan, *Org. Lett.*, 2001, **3**, 1511–1514.
- 141 S. Caddick, F. G. N. Cloke, G. K. B. Clentsmith, P. B. Hitchcock, D. McKerrecher, L. R. Titcomb and M. R. V. Williams, *J. Organomet. Chem.*, 2001, **617–618**, 635–639.
- 142 C. Yang and S. P. Nolan, *Organometallics*, 2002, **21**, 1020–1022.
- 143 V. P. W. Böhm, C. W. K. Gstöttmayr, T. Weskamp and W. A. Herrmann, *Angew. Chem. Int. Ed.*, 2001, **40**, 3387–3389.
- 144 B. Çetinkaya, I. Özdemir and P. H. Dixneuf, *J. Organomet. Chem.*, 1997, **534**, 153–158.
- 145 H. M. Lee, D. C. Smith, Z. He, E. D. Stevens, C. S. Yi and S. P. Nolan, *Organometallics*, 2001, **20**, 794–797.
- 146 W. Krasuski, D. Nikolaus and M. Regitz, *Eur. J. Org. Chem.*, 1982, **1982**, 1451–1465.
- 147 L. Delaude, A. Demonceau and J. Wouters, *Eur. J. Inorg. Chem.*, 2009, **2009**, 1882–1891.
- 148 L. Delaude, *Eur. J. Inorg. Chem.*, 2009, **2009**, 1681–1699.
- 149 U. Siemeling, H. Memczak, C. Bruhn, F. Vogel, F. Träger, J. E. Baio and T. Weidner, *Dalton Trans.*, 2012, **41**, 2986.
- 150 Ai.-C. Blanrue and R. Wilhelm, 3.
- 151 G. Kuchenbeiser, M. Soleilhavoup, B. Donnadiou and G. Bertrand, *Chem. - Asian J.*, 2009, **4**, 1745–1750.
- 152 A. J. Arduengo III, J. C. Calabrese, F. Davidson, H. V. Rasika Dias, J. R. Goerlich, R. Krafczyk, W. J. Marshall, M. Tamm and R. Schmutzler, *Helv. Chim. Acta*, 1999, **82**, 2348–2364.
- 153 N. I. Korotkikh, G. F. Rayenko, O. P. Shvaika, T. M. Pekhtereva, A. H. Cowley, J. N. Jones and C. L. B. Macdonald, *J. Org. Chem.*, 2003, **68**, 5762–5765.
- 154 G. C. Lloyd-Jones, R. W. Alder and G. J. J. Owen-Smith, *Chem. - Eur. J.*, 2006, **12**, 5361–5375.
- 155 J. P. Moerdyk and C. W. Bielawski, *Chem. Commun.*, 2014, **50**, 4551–4553.
- 156 X. Cattoën, H. Gornitzka, D. Bourissou and G. Bertrand, *J. Am. Chem. Soc.*, 2004, **126**, 1342–1343.
- 157 A. J. Arduengo, J. R. Goerlich and W. J. Marshall, *Liebigs Ann.*, 1997, **1997**, 365–374.
- 158 V. P. W. Böhm and W. A. Herrmann, *Angew. Chem.*, 2000, **39**, 4036–4038.
- 159 C. M. Weinstein, C. D. Martin, L. Liu and G. Bertrand, *Angew. Chem. Int. Ed.*, 2014, **53**, 6550–6553.
- 160 H. Song, H. Kim and E. Lee, *Angew. Chem. Int. Ed.*, 2018, **57**, 8603–8607.
- 161 D. M. Lemal, R. A. Lovald and K. I. Kawano, *J. Am. Chem. Soc.*, 1964, **86**, 2518–2519.
- 162 Z. Shi and R. P. Thummel, *J. Org. Chem.*, 1995, **60**, 5935–5945.

Chapter I: Similarities and differences between diaminocarbenes (DACs) and monoaminocarbenes (MACs) with special emphasis on the dimerization reaction

- 163 H. E. Winberg, J. E. Carnahan, D. D. Coffman and M. Brown, *J Am Chem Soc*, 1965, 2055–2056.
- 164 H.-W. Wanzlick and E. Schikora, *Angew. Chem.*, 1960, **72**, 494–494.
- 165 H.-W. Wanzlick and E. Schikora, *Chem. Ber.*, 1961, **94**, 2389–2393.
- 166 H.-W. Wanzlick, F. Esser and H.-J. Kleiner, *Eur. J. Inorg. Chem.*, 1963, **96**, 1208–1212.
- 167 H.-J. Sch önherr and H.-W. Wanzlick, *Chem. Ber.*, 1970, **103**, 1037–1046.
- 168 M. Denk K., K. Hatano and M. Ma, 1999, 2057–2060.
- 169 Y. Liu and D. M. Lemal, *Tetrahedron Lett.*, 2000, **41**, 599–602.
- 170 Y. Liu, P. E. Lindner and D. M. Lemal, *J. Am. Chem. Soc.*, 1999, **121**, 10626–10627.
- 171 E. A. Carter and W. A. Goddard, *J. Phys. Chem.*, 1986, **90**, 998–1001.
- 172 J. P. Malrieu and G. Trinquier, *J. Am. Chem. Soc.*, 1989, **111**, 5916–5921.
- 173 H. Jacobsen and T. Ziegler, *J. Am. Chem. Soc.*, 1994, **116**, 3667–3679.
- 174 D. C. Graham, K. J. Cavell and B. F. Yates, *J. Phys. Org. Chem.*, 2005, **18**, 298–309.
- 175 C. D. Martin, C. M. Weinstein, C. E. Moore, A. L. Rheingold and G. Bertrand, *Chem. Commun.*, 2013, **49**, 4486–4488.
- 176 Y. T. Chen and F. Jordan, *J. Org. Chem.*, 1991, **56**, 5029–5038.
- 177 A. Orahovats, H. Heimgartner, H. Schmid and W. Heinzelmann, *Helv. Chim. Acta*, 1975, **58**, 2662–2677.
- 178 S. Fergus, S. J. Eustace and A. F. Hegarty, *J. Org. Chem.*, 2004, **69**, 4663–4669.
- 179 P. I. Jolly, A. Marczyk, P. Małeck, O. Ablialimov, D. Trzybiński, K. Woźniak, S. Osella, B. Trzaskowski and K. Grela, *Chem. - Eur. J.*, 2018, **24**, 4785–4789.
- 180 C. Heinemann and W. Thiel, *Chem. Phys. Lett.*, 1994, **217**, 11–16.
- 181 M. Z. Kassae, M. Ghambarian, F. A. Shakib and M. R. Momeni, *J. Phys. Org. Chem.*, 2011, **24**, 351–359.
- 182 C.-H. Lai, *J. Mol. Model.*, 2013, **19**, 4387–4394.
- 183 M. Braun, W. Frank, G. J. Reiss and C. Ganter, *Organometallics*, 2010, **29**, 4418–4420.
- 184 R. W. Alder, M. E. Blake and J. M. Oliva, *J. Phys. Chem. A*, 1999, **103**, 11200–11211.
- 185 M. Z. Kassae, F. A. Shakib, M. R. Momeni, M. Ghambarian and S. M. Musavi, *J. Org. Chem.*, 2010, **75**, 2539–2545.
- 186 J. C. Bernhammer, G. Frison and H. V. Huynh, *Chem. - Eur. J.*, 2013, **19**, 12892–12905.
- 187 M.-J. Cheng and C.-H. Hu, *Chem. Phys. Lett.*, 2000, **322**, 83–90.
- 188 L. Nyulászi, T. Veszpre mi and A. Forró, *Phys. Chem. Chem. Phys.*, 2000, **2**, 3127–3129.
- 189 M. K. Denk, A. Hezarkhani and F.-L. Zheng, *Eur. J. Inorg. Chem.*, 2007, **2007**, 3527–3534.
- 190 M. Driess and H. Grützmacher, *Angew. Chem. Int. Ed. Engl.*, 1996, **35**, 828–856.
- 191 G. Trinquier and J. P. Malrieu, *J. Am. Chem. Soc.*, 1987, **109**, 5303–5315.
- 192 J. P. Malrieu and G. Trinquier, *J. Am. Chem. Soc.*, 1989, **111**, 5916–5921.
- 193 T. A. Taton and P. Chen, *Angew. Chem. Int. Ed. Engl.*, 1996, **35**, 1011–1013.
- 194 A. Poater, F. Ragone, S. Giudice, C. Costabile, R. Dorta, S. P. Nolan and L. Cavallo, *Organometallics*, 2008, **27**, 2679–2681.
- 195 C. A. Tolman, *Chem. Rev.*, 1977, **77**, 313–348.
- 196 R. Dorta, E. D. Stevens, N. M. Scott, C. Costabile, L. Cavallo, C. D. Hoff and S. P. Nolan, *J. Am. Chem. Soc.*, 2005, **127**, 2485–2495.
- 197 L. Cavallo, A. Correa, C. Costabile and H. Jacobsen, *J. Organomet. Chem.*, 2005, **690**, 5407–5413.
- 198 A. J. Arduengo, H. V. R. Dias, R. L. Harlow and M. Kline, *J. Am. Chem. Soc.*, 1992, **114**, 5530–5534.

Chapter I: Similarities and differences between diaminocarbenes (DACs) and monoaminocarbenes (MACs) with special emphasis on the dimerization reaction

- 199 A. J. Arduengo, H. V. R. Dias, D. A. Dixon, R. L. Harlow, W. T. Klooster and T. F. Koetzle, *J. Am. Chem. Soc.*, 1994, **116**, 6812–6822.
- 200 M. K. Denk, A. Thadani, K. Hatano and A. J. Lough, *Angew. Chem. Int. Ed. Engl.*, 1997, **36**, 2607–2609.
- 201 A. J. Arduengo, R. Krafczyk, R. Schmutzler, H. A. Craig, J. R. Goerlich, W. J. Marshall and M. Unverzagt, *Tetrahedron*, 1999, **55**, 14523–14534.
- 202 D. M. Khramov and C. W. Bielawski, *J. Org. Chem.*, 2007, **72**, 9407–9417.
- 203 J. W. Kamplain and C. W. Bielawski, *Chem. Commun.*, 2006, 1727–1729.
- 204 B. C. Norris and C. W. Bielawski, *Macromolecules*, 2010, **43**, 3591–3593.
- 205 B. M. Neilson, A. G. Tennyson and C. W. Bielawski, *J. Phys. Org. Chem.*, 2012, **25**, 531–543.
- 206 B. C. Norris, D. G. Sheppard, G. Henkelman and C. W. Bielawski, *J. Org. Chem.*, 2011, **76**, 301–304.

Chapter I: Similarities and differences between diaminocarbenes (DACs) and monoaminocarbenes (MACs) with special emphasis on the dimerization reaction

**Chapter II: Selective dimerization of
monoaminoarylcabenens by deprotonation of
aldiminium salts**

Chapter II: Selective dimerization of monoaminoarylcarbenes by deprotonation of aldiminium salts

Chapter II: Selective dimerization of monoaminoarylcarbenes by deprotonation of aldiminium salts

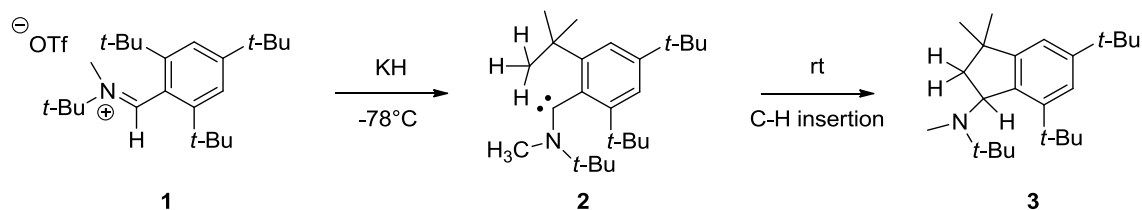
The use of carbenes and more particularly their capacity to dimerize is a key parameter in this PhD work. In the next part of this chapter, a quick reminder of the specific carbene selected, *i.e.* acyclic monoaminocarbenes (MACs), is presented. The discovery, synthesis and characterization of the first stable MACs is first presented. Then, their specific reactivities compared to diaminocarbenes is described. Finally, using alternative proton-free synthesis routes, a description of the transient monoaminocarbenes and their ability to dimerize is discussed.

II.1 State of the art

II.1.1 Synthesis of MACs

Since their first isolation and characterization in 1988 and in 1991,^{1,2} carbenes have been extensively studied and have become one of the most powerful tools in organic chemistry. As emphasized in the previous chapter, a large variety of stable diaminocarbenes (DACs) and monoaminocarbenes (MACs) have been synthesized.³⁻⁵ In comparison with their cyclic counterparts, acyclic MACs have been much less investigated. In particular, only a few aminoarylcarbenes have been described.^{3,6-10}

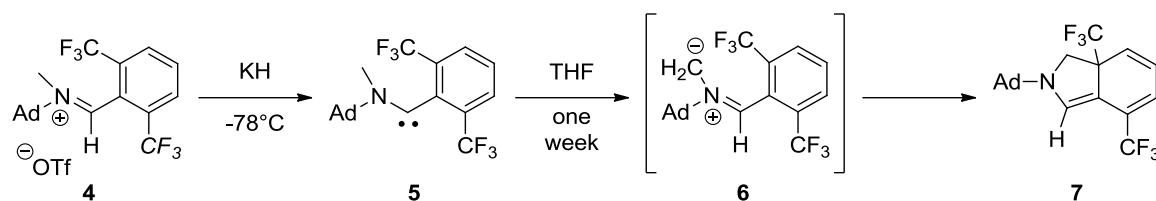
In 2001, Bertrand *et al.*³ reported the synthesis of an aminoarylcarbene (**2**) by deprotonation of the corresponding iminium salt (**1**) with KH (Scheme II.1). Compound **2** was characterized by ¹³C NMR spectroscopy showing the diagnostic carbene signal at 314.2 ppm. Although the introduction of bulky *t*-Bu group in ortho-position of the aryl group prevented the carbene from dimerizing, a C-H insertion reaction involving the carbene center onto the CH₃ group was evidenced upon heating at room temperature.



Scheme II.1. First synthesis and isolation of monoaminocarbene **2** which rearranges at rt to give **3**.³

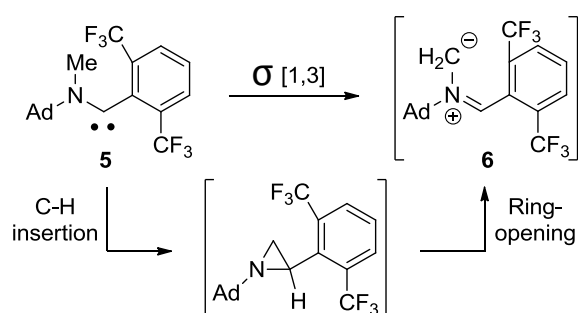
Chapter II: Selective dimerization of monoaminoarylcarbenes by deprotonation of aldiminium salts

Interestingly, replacing a *t*-Bu by a CF₃ group, as shown in **5**, greatly enhanced the carbene stability, as the C-F bond proved inert toward insertion reactions (Scheme II.2). Nevertheless, the presence of a methyl group on the nitrogen atom enabled **5** to isomerize into an azomethine ylide (**6**). The latter ylide was found to rearrange into the bicyclic compound, **7**, at room temperature, by dearomatizing cyclization (Scheme II.2).



Scheme II.2. Isolation and characterization of carbene **5** that isomerizes at RT into azomethine ylide **6** which further rearranges into the bicyclic compound **7**.⁶

Isomerization of carbene **5** to azomethine ylide **6** eventually proceeds either through a two-step process or *via* a concerted mechanism. In the former case, a C-H insertion of the carbene center onto the methyl group of the nitrogen atom, followed by a ring opening of the aziridine, yields the compound **6**. As for the concerted mechanism, a σ [1,3] rearrangement of **5** leads to the azomethine ylide **6** (Scheme II.3).

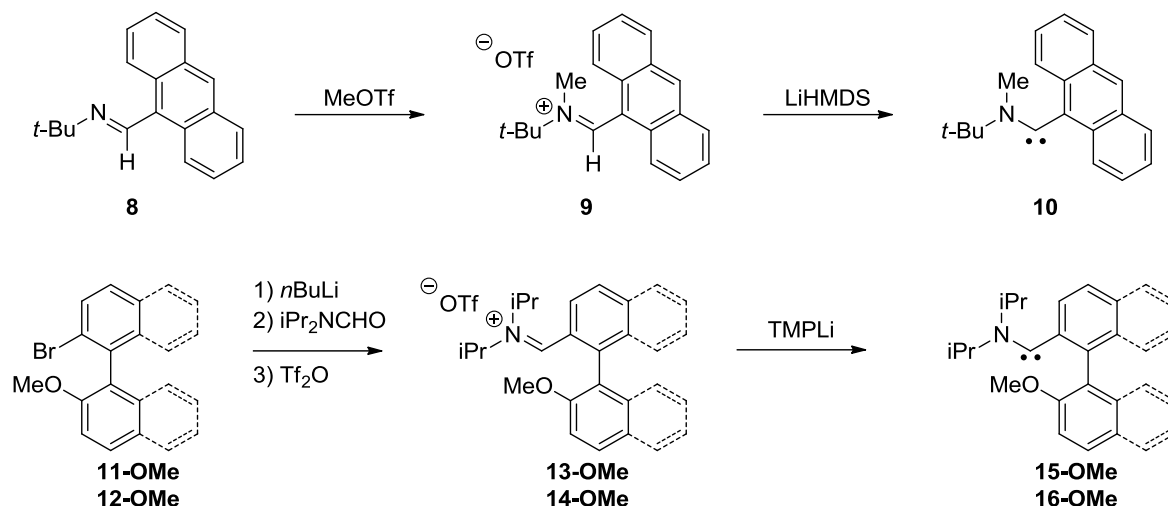


Scheme II.3. Transient azomethine ylide **6** obtained by stepwise or concerted mechanism from aminoarylcarbene **5**.⁶

These results highlight the importance of the substitution pattern, not only on the aromatic moiety, but also on the nitrogen atom for the reactivity/stability of aminoarylcarbenes. A few other stable/persistent aminoarylcarbenes have also been reported, namely, by deprotonation of their corresponding iminium-type conjugated acid.^{7,10} Again, dimerization has not been observed because of the presence of one or two bulky substituents in ortho-position of the aryl

Chapter II: Selective dimerization of monoaminoarylcarbenes by deprotonation of aldiminium salts

moiety (Scheme II.4).^{7,10} Table II.1 sums up the stability of these substituted aminoarylcarbenes by giving their respective half lifetime.



Scheme II.4. Synthesis of stable/persistent aminoarylcarbenes *via* “deprotonation route”.^{7,10}

The half lifetime of the reported persistent aminoarylcarbenes is reported in Table II.1.

Table II.1. Half lifetime of stable aminoarylcarbenes.¹¹

	$t_{1/2}$		$t_{1/2}$
<p>2</p>	days at -50°C	<p>15-OMe</p>	indefinitely at rt
<p>5</p>	days at rt	<p>16-OMe</p>	30 min at rt
<p>10</p>	days at -30°C	<p>32</p>	days at rt

Analysis of aminoarylcarbenes by X-ray diffraction has also been reported.^{12,7,10,11} The crystalline structure of compound **5** is characterized by a $\text{NC}_{\text{carbene}}\text{C}$ angle of 121° and a

Chapter II: Selective dimerization of monoaminoarylcarbene by deprotonation of aldiminium salts

$\text{NC}_{\text{carbene}}$ bond length around 1.28 Å. As these values are shorter than those of diaminocarbenes, this indicates a stronger π donation from the nitrogen atom to the carbene center. Despite its perpendicular arrangement respective to the NCC plane, the Csp^2 filled orbital of the carbene center does not interact with the π^* orbital of the phenyl because of the very acute NCC angle (Figure II.1). The $\text{C}_{\text{Ar}}\text{-C}_{\text{carbene}}$ is 1.45 Å, which is characteristic for a distance of a single bond. These data further supports that the aryl group is spectator, hence aminoarylcabene **5** is stabilized by a push-spectator mode.³

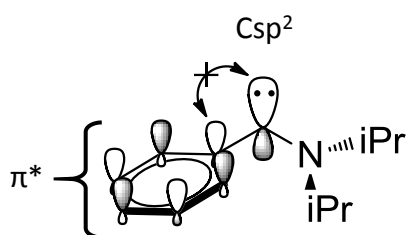
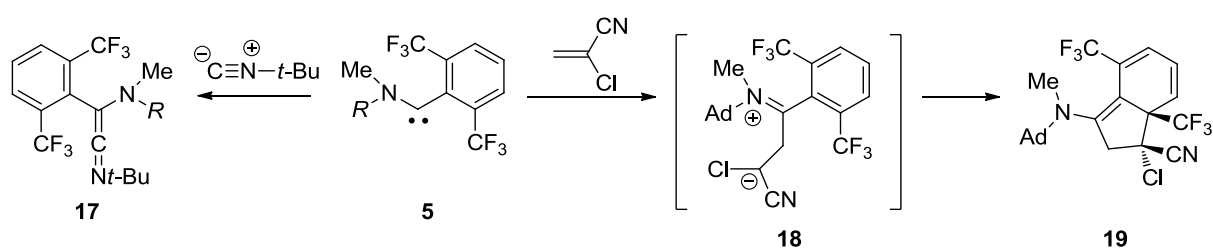


Figure II.1. Representation of the phenyl as a mesomeric spectator thanks to the acute $\text{C}_{\text{Ar}}\text{C}_{\text{carbene}}\text{N}$ angle that prevent the orbital interaction between the π^* and the Csp^2 orbitals.

II.1.2 Reactivity

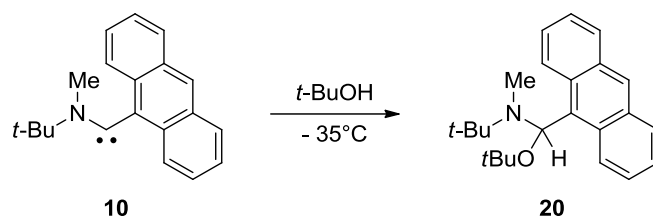
Compared to diaminocarbenes, the carbenic species **5** shown in Schemes II.2 and II.3 is both more electrophilic and more nucleophilic, as attested by its reactivity with *t*-Bu isocyanide and acrylonitrile.^{3,8} Such reactions indeed afford the corresponding ketenimine **17**, as established in Scheme II.5, a and the bicyclic compound **19**, respectively (Scheme II.5, b). Note that **19** results from the initial 1,4-addition of **5** onto acrylonitrile, followed by intramolecular cyclization of the zwitterionic **18**.^{3,8}



Scheme II.5. Coupling reaction of aminoarylcabene **5** with a nucleophilic and an electrophilic partner.^{3,8}

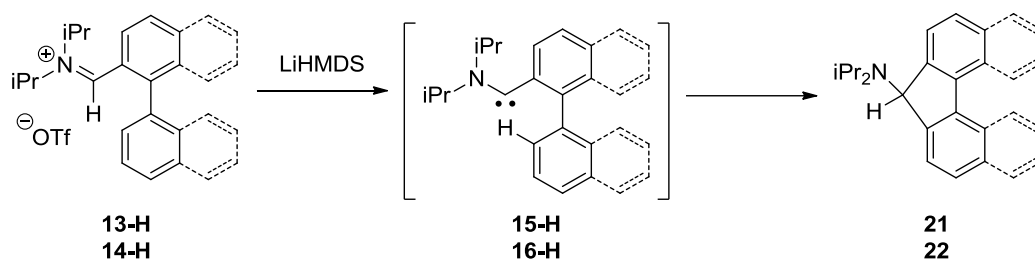
Chapter II: Selective dimerization of monoaminoarylcarbenes by deprotonation of aldiminium salts

Aminoarylcarbenes have been reported to undergo other reactions. For instance, compound **10** has been shown to selectively perform an O-H insertion in presence of *t*-BuOH at -35°C , as depicted in scheme II.6.⁷



Scheme II.6. O-H insertion of persistent carbene **10** at -35°C in presence of *t*-BuOH.⁷

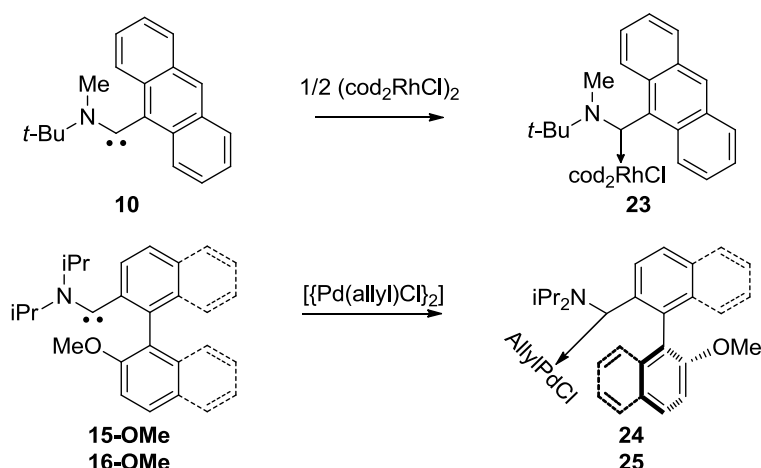
Transient carbenes **15-H** and **16-H** shown in scheme II.7 have been reported to spontaneously undergo intramolecular C-H insertion when generated by deprotonation.¹⁰



Scheme II.7. Intramolecular C-H insertion of in-situ generated aminoarylcarbenes **15-H** and **14-H**.¹⁰

Finally, carbenes **15-OMe** and **16-OMe** can act as ligands for various transition metals. Even though aminoarylcarbene ligands form less robust metal complexes than with using diaminocarbene ligands, they can catalyze various reactions and have provided promising results in asymmetric catalysis (Scheme II.8).^{7,9}

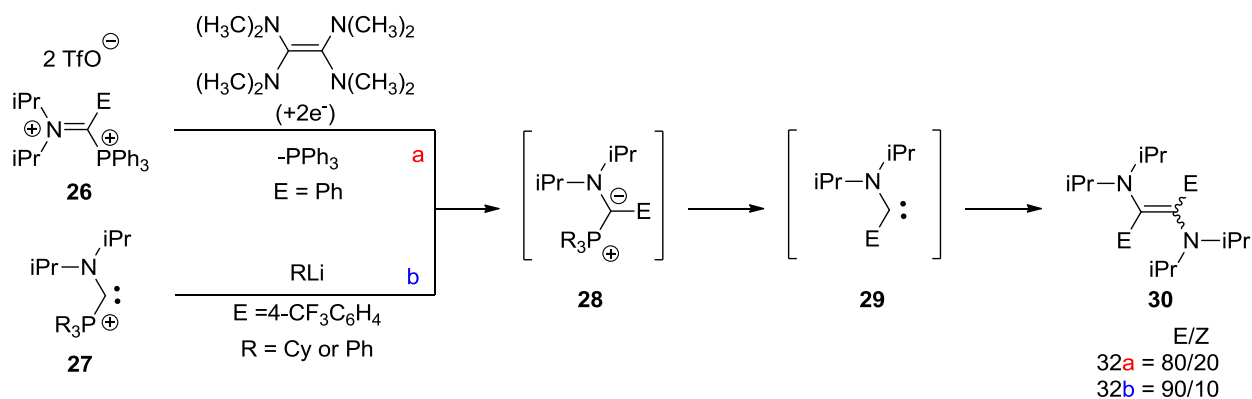
Chapter II: Selective dimerization of monoaminoarylcarbenes by deprotonation of aldiminium salts



Scheme II.8. Aminoarylcarbenes as ligand for transition metals Rh and Pd.^{7,9}

II.1.3 Transient monoaminoarylcarbenes: synthesis and characterization

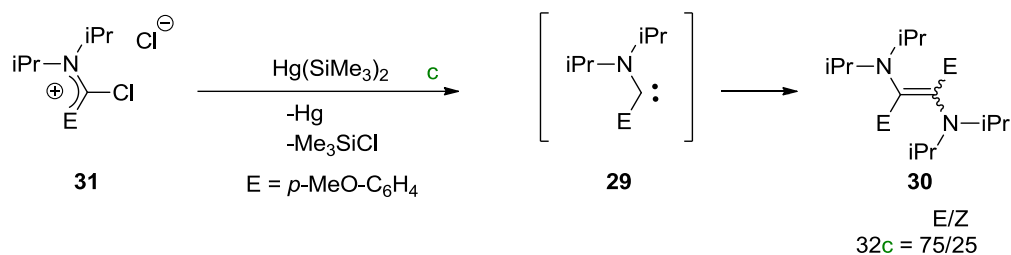
In order to isolate or characterize aminoarylcarbenes without any substituent in ortho position of the aryl group, different electrophile-free strategies have been developed by Bertrand *et al.*^{13–15} Indeed, deprotonation of iminium salts has proven unsuitable for isolating the corresponding carbene, simply because of the H^+ -catalyzed dimerization, which is favored when the carbene center is not sufficiently sterically protected. Two alternative strategies have thus been developed to access aminoarylcarbenes. One is achieved by reduction of dication or by nucleophilic substitution of the carbene center.^{13,15} Each reaction involves a mechanism leading to an ylide intermediate, which upon losing a phosphine (breaking of the C-P bond) gives the transient carbenes, as described in scheme II.9. Unfortunately, no characterization of these intermediates has been reported, likely owing to their high instability.



Scheme II.9. Synthesis of transient carbene **29** through two pathways. These pathways share the same mechanism which is the loss of a phosphine during the ylide intermediate step **28**.^{13,15}

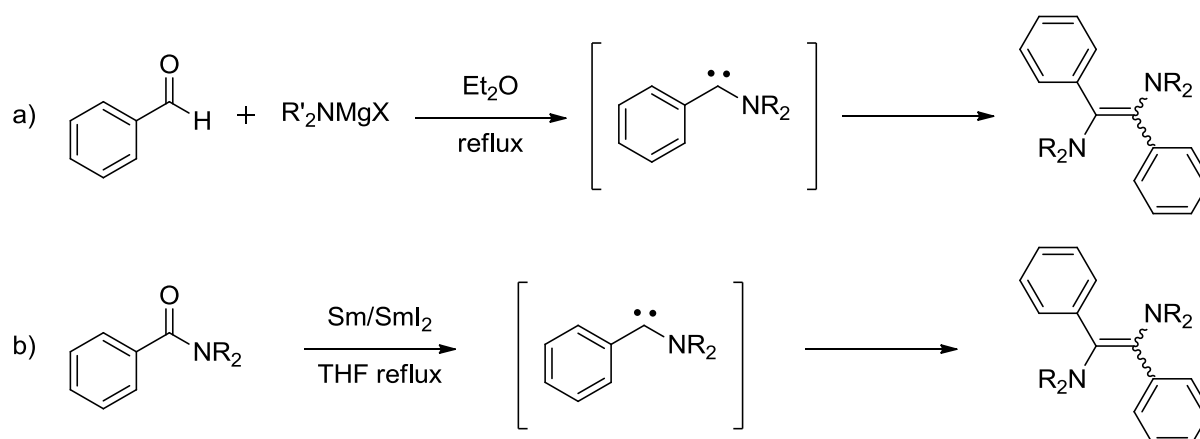
Chapter II: Selective dimerization of monoaminoarylcarbenes by deprotonation of aldiminium salts

The other strategy, as depicted in Scheme II.10, consists in the reductive dechlorination utilizing a mercury reagent of a chlorinated precursor, which leads to similar transient carbenes.¹⁴



Scheme II.10. Reductive dechlorination route to generate the *in-situ* transient carbene **29** which directly dimerize to give dimer **30**.¹⁴

A few other synthetic metallic routes to diaminoalkene compounds have been reported, which involves the prior formation of a transient carbene that further undergoes a dimerization reaction. One approach is by reaction of aromatic aldehydes with (dialkylamino)magnesium reagents, which leads to the diaminoalkene in moderate yields (Scheme II.11 a).¹⁶ The other route is by deoxygenative coupling of amides in presence of lanthanoid metals, *e.g.* based on samarium (Scheme II.11 b).¹⁷



Scheme II.11. Synthesis of diaminoalkene through transient carbene.^{17,16}

For all carbenes described, it can be noticed that their ability to dimerize is correlated to the absence of an ortho-substituents present on the aryl rings. If this is so, indeed, the carbene

Chapter II: Selective dimerization of monoaminoarylcarbenes by deprotonation of aldiminium salts

proves more stable, otherwise, the dimerization of the *in-situ* generated transient carbenes is operative.

From these results, it appears that aminoarylcarbenes can readily dimerize into the corresponding diaminoalkenes, providing that the aryl moiety is not substituted in ortho position. Moreover, for persistent/stable carbenes, other reactivities have been reported like the O-H insertion and the addition on activated alkene.^{4,7} While the interest of such dimers might be of limited interest, their synthesis establishes a proof of concept that C=C double bond can be generated from their parent aminoarylcarbenes.

The main objective of this PhD thesis was to achieve a novel family of poly(phenylene vinylene)s, namely, consisting of side amino groups, *via* repeated dimerization reactions involving acyclic bis-aminoarylcarbenes as monomeric building blocks. We reasoned that a preliminary investigation into the understanding of the selectivity of the elementary dimerization reaction was required, *i.e.* using monofunctional analogues (Scheme II.12).

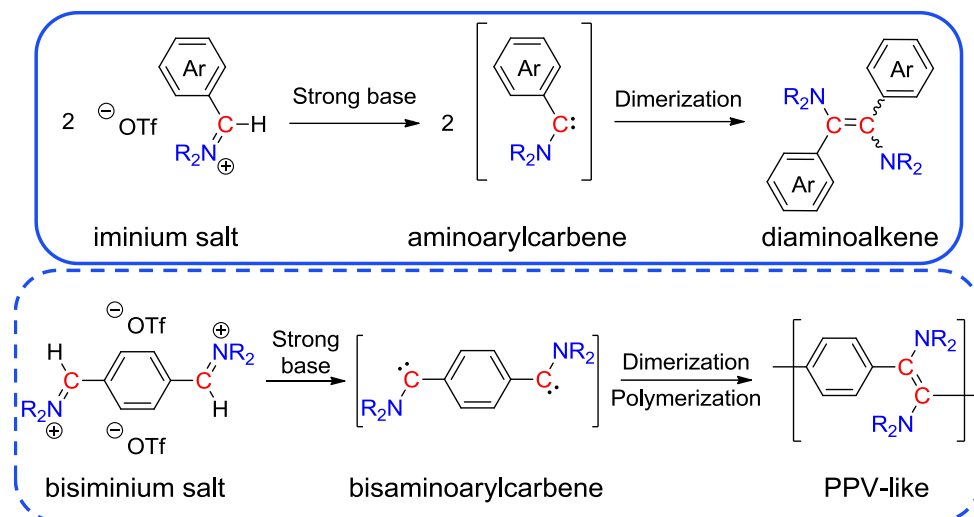
As emphasized both in the bibliographic chapter I and in the state-of-the-art of this chapter (II.1), acyclic monoaminocarbenes (MACs) exhibit peculiar physico-chemical properties.^{3,11,5} They indeed show a more basic character, but are also more electrophilic than diaminoalkenes, such as *N*-heterocyclic carbenes (NHCs).¹⁸ They can thus potentially undergo a specific reactivity such as, migration, insertion, addition and dimerization. Of particular interest, they can selectively self-dimerize into the corresponding diaminoalkenes under specific conditions,¹³⁻¹⁵ as discussed in detail further in this chapter.

In the next parts (II.2-II.5), we describe the synthesis of precursors, namely, in the form of their iminium salts, of monoaminoarylcarbenes following two different synthetic strategies. This will be followed by the thorough characterization of these iminium salts. The latter will then be subjected to a deprotonation with the help of various strong bases to trigger the selective dimerization of the corresponding carbene. We will examine how the selection of the base can affect the stereochemistry, *i.e.* the E/Z isomer ratio of the resultant diaminoalkene dimer.

The dimerization mechanism will then be investigated both experimentally and theoretically through density functional theory (DFT) calculations. Attempts to trap the transient aminoarylcarbenes will be also studied, *via* addition of electrophilic species, including S₈, CS₂, and specific alkenes. Finally, attempts to isomerize the E/Z mixture of diaminoalkenes

Chapter II: Selective dimerization of monoaminoarylcarbenes by deprotonation of aldiminium salts

resulting from the dimerization reaction will be evaluated either by addition of an organic acid or by irradiation in the visible domain.



Scheme II.12. Synthesis and deprotonation of mono-iminium salts (translation of this chemistry towards the synthesis of N-containing PPV-like polymers is described in the next chapter).

II.2 Synthesis of carbene precursors

This PhD work started with the synthesis, following two different pathways, of the iminium carbene precursor salts, in order to study the selective dimerization of their corresponding acyclic monoaminocarbenes.

II.2.1. Transition-metal-free pathway

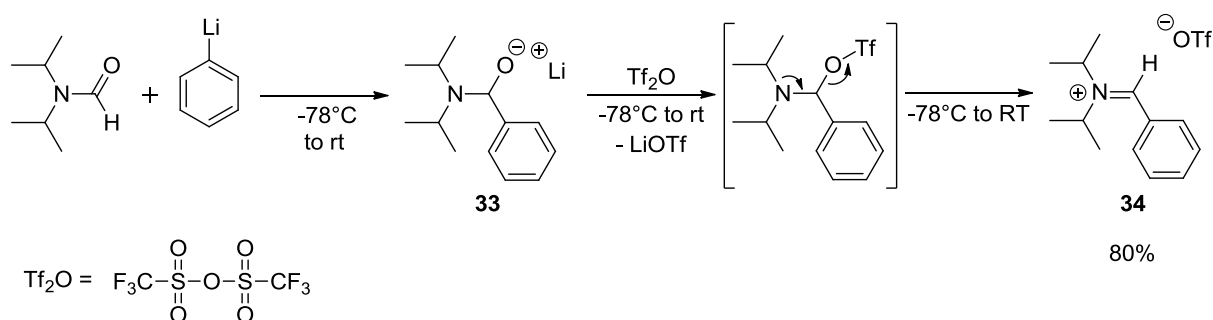
As emphasized above, deprotonation of iminium salts is by far the most popular way to generate aminoarylcarbenes.^{12,7} Here, the iminium precursor of carbene **5** was synthesized in a two-step process, involving the condensation of a primary amine with benzaldehyde, followed by methylation of the resulting imine.³ However, the methyl group affects the reactivity of the carbene, as the latter can readily isomerize into an azomethine ylide intermediate.⁶

Therefore, two different strategies allowing the introduction of two bulky groups at the nitrogen atom were implemented. One strategy (see Scheme II.13) was inspired by works reported by Alder *et al.*,¹⁹ and involved an aryl lithium that was added onto a formamide-type

Chapter II: Selective dimerization of monoaminoarylcarbenes by deprotonation of aldiminium salts

substrate. The resulting lithium alkoxide was trapped with triflic anhydride to give an iminium precursor with bulky substituents. The other strategy was reported by Schroth *et al.*²⁰ and utilized a trimethylsilylamine bearing bulky groups on the nitrogen atom, in presence of trimethylsilyltriflate at room temperature (see Scheme II.14). This yielded the same iminium salt to that obtained in the Alder's strategy.

In the former case, synthesis of the iminium precursor **34** was achieved in a two-step, one-pot process, involving firstly the nucleophilic addition of phenyllithium on diisopropylformamide at -78°C in Et_2O . Secondly, lithium alkoxide **33** was formed upon warming to room temperature. Compound **34** was thus obtained by trapping **33** with triflic anhydride at -78°C , followed by elimination of lithium triflate when heating up to room temperature. After washing with dry ether, the highly hygroscopic iminium salt **34** was isolated in 80% yield (Scheme II.13).¹⁹



Scheme II.13. Synthesis of iminium salt **34** via the Alder's route.

Analysis by ^1H and ^{13}C NMR spectroscopy of iminium salt **34** gave spectra in perfect agreement with data reported in the literature.¹⁹ For instance, in the ^1H NMR spectrum, the characteristic singlet signal at 9.5 ppm could be attributed to the iminium proton. Because of the planarity of the amino group, CHiPr protons appeared as two different septets, namely, at 4.58 and 4.94 ppm ($^3J_{\text{H-H}} = 6.4$ Hz). Note, however, that the two CH_3iPr could be barely distinguished at 1.49 and 1.54 ppm ($^3J_{\text{H-H}} = 6.4$ Hz) (Figure II.2).

Chapter II: Selective dimerization of monoaminoarylcarbenes by deprotonation of aldiminium salts

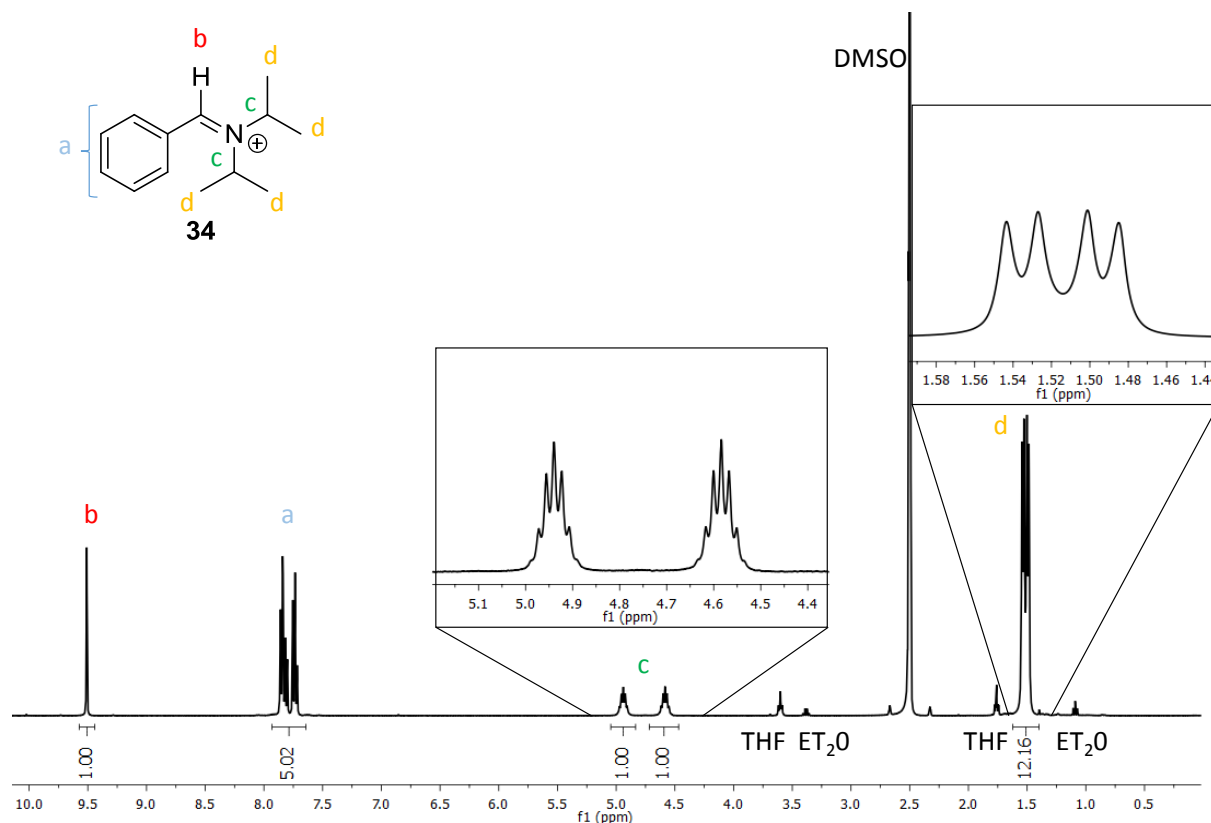


Figure II.2. ^1H NMR (400 MHz) in DMSO-d_6 of iminium salt **34**.

Most notably, the ^{13}C NMR spectrum showed the characteristic signal for the carbon iminium at 171.3 ppm. As expected, two different signals were observed for the CHiPr at 54.4 and 56.9 ppm, as well as two signals for the CH_3iPr at 19.2 and 23.9 ppm. A quartet at 120.9 ppm with a large coupling constant of $J_{\text{C-F}} = 322.5$ Hz was detected. This large coupling was due to the C-F bond between the carbon and the fluorine atom of the CF_3 group present in the triflate counter anion (Figure II.3). These spectra are representative of the various iminium salt precursors synthesized during this PhD thesis (other examples are provided in the Annex of this chapter).

Chapter II: Selective dimerization of monoaminoarylcarbenes by deprotonation of aldiminium salts

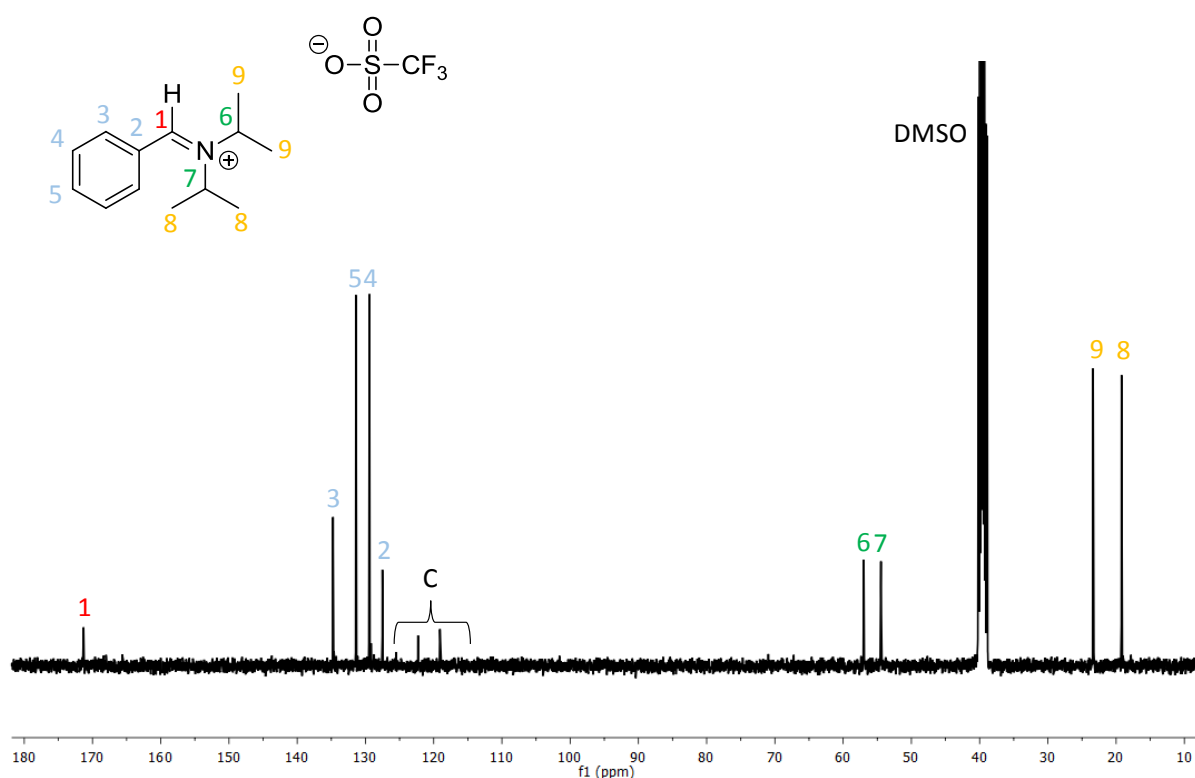


Figure II.3. ¹³C NMR (101 MHz) spectrum in DMSO_{d6} of the iminium salt **34**.

In this way, iminium salts **34** and **35** were synthesized in 80% yield, starting from commercially diisopropylformamide and formylpiperidine, respectively (Figure II.4).

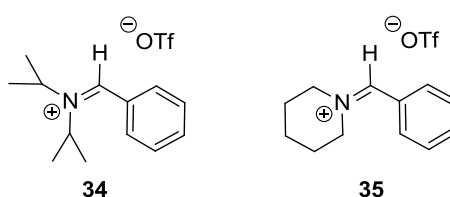
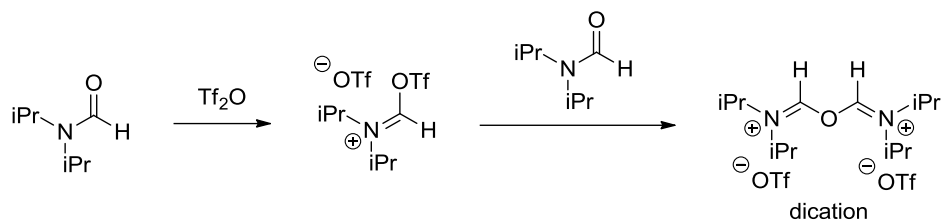


Figure II.4. Aminoaryliminium salt synthesized by Alder's route.¹⁹

Advantages of this methodology include the commercial availability of all starting materials and the fact that the reaction can be carried out one pot. However, it is important to note that the reaction requires highly pure reagents that must be handled in drastic oxygen- and moisture-free conditions and at very low temperature (-78°C). In addition, stoichiometric conditions should be fulfilled, otherwise side reactions between formamide and triflic anhydride might occur, forming a dication salt that can be separated from the targeted iminium

Chapter II: Selective dimerization of monoaminoarylcarbenes by deprotonation of aldiminium salts

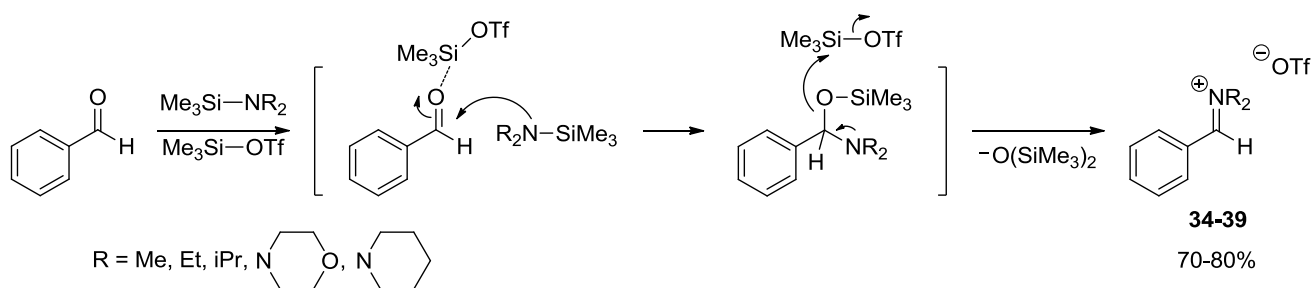
salt (Scheme II.14). We therefore investigated another strategy that could use neutral and less drastic conditions.



Scheme II.14. Side reactions between formamide and triflic anhydride leading to dications.

II.2.2 Metal-free synthetic pathway

In 1994, Schroth *et al.*²⁰ has reported a different iminium salt forming reaction, free of any lithium, to achieve similar iminium salts as shown above. The reaction involves the nucleophilic addition of a trimethylsilylamine,²¹ **36**, onto benzaldehyde in presence of a stoichiometric amount of trimethylsilyltriflate at room temperature. For this purpose, various silylamines were synthesized to access the corresponding iminium salts, **34-39** (Figure II.5). With this procedure in our hands, compounds **34-39**, were obtained after 6 hours. After washing with dry diethyl ether, these precursors were isolated in rather good yields (70-80%) (Scheme II.15).



Scheme II.15. Metal-free synthetic route towards iminium salt **34-39**.²⁰

Chapter II: Selective dimerization of monoaminoarylcarbenes by deprotonation of aldiminium salts

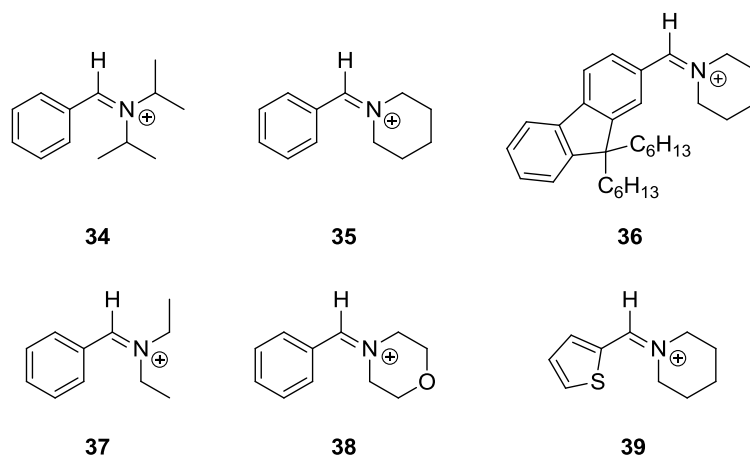
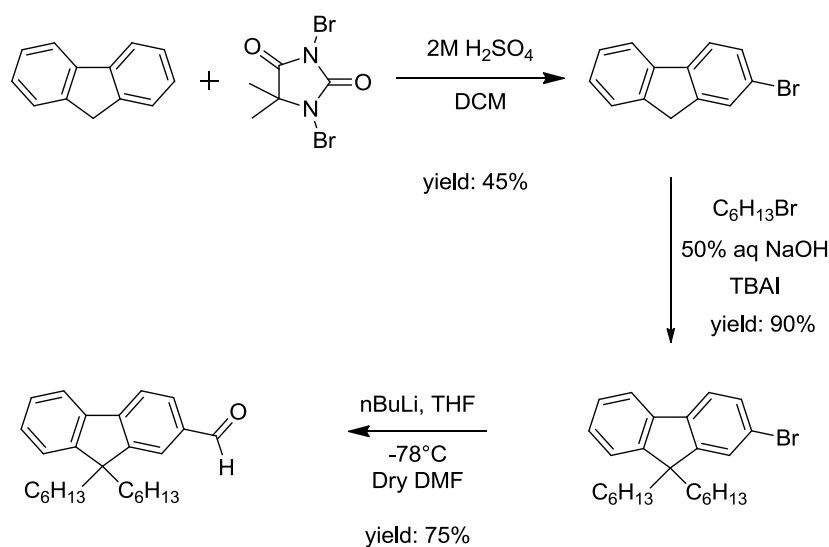


Figure II.5. Scope of iminium salts synthesized by metal-free way.

For instance, benzaldehyde could be replaced with thiophenylaldehyde, another commercially available substrate, to give the corresponding iminium salt **39** in 80% yield. As for the iminium **36** featuring a fluorene carboxaldehyde moiety, it was synthesized by a bromination reaction of a fluorene moiety, followed by an alkylation and further by a bromide/lithium exchange of the fluorene carboxaldehyde compound (Scheme II.16).^{22,23}



Scheme II.16. Synthesis of the fluorene-aldehyde precursor inspired from ref.^{22,23}

II.3 Deprotonation of iminium salts

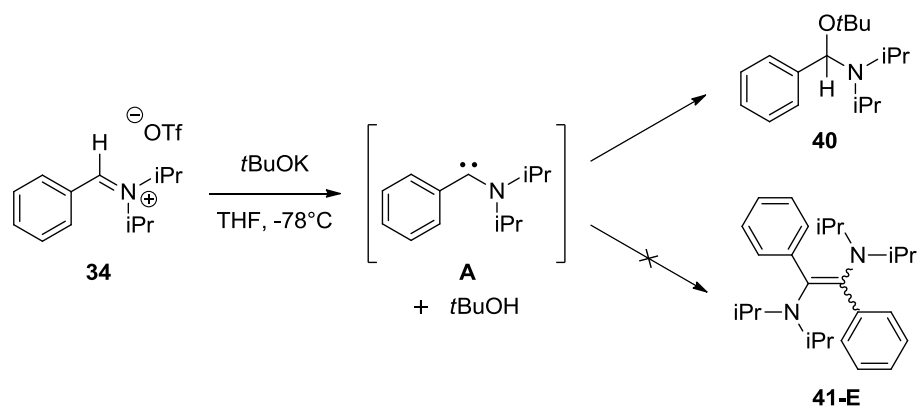
Deprotonation of the different iminium salts was accomplished using different bases, such as sodium methoxide (MeONa), potassium *tert*-Butoxide (*t*-BuOK), lithium

Chapter II: Selective dimerization of monoaminoarylcarbenes by deprotonation of aldiminium salts

bis(trimethylsilyl)amide (LiHMDS), and neutral strong bases, namely, P₄-*t*Bu phosphazene, 1,8-Diazabicyclo[5.4.0]undéc-7-ène (DBU) and 1,5,7-Triazabicyclo[4.4.0]dec-5-ene (TBD).

II.3.1 Use of *t*-BuOK

The reaction was performed by slowly adding cold THF (-78°C) onto a mixture of the iminium salt, **34**, and solid *t*-BuOK. The reaction mixture was slowly warmed to room temperature and extracted with dry diethylether, which quantitatively led to a white solid (**40**) (Scheme II.17).



Scheme II.17. Deprotonation of iminium salt **34** in presence of the strong *t*-BuOK base in THF at -78°C.

Analysis by ¹H NMR spectroscopy revealed the complete disappearance of the CH proton due to the iminium signal, as expected. A singlet assignable to the protons of the CH₃, appearing at 1.06 ppm and integrating for 9 protons, is indicative of the presence of a *t*-Bu group. A singlet due to the CH proton at 5.40 ppm was also detected. Finally, only one type of CH*i*Pr was noted, with a septuplet peak at 3.22-3.16 ppm (integrating for two protons), with a coupling constant of ³J_{H-H} = 6.80 Hz. From these signals, the structure of aminal **40** could be postulated. In other words, the *in-situ* generated carbene would selectively react with *t*-BuOK instead of dimerizing, and no dimer was eventually formed (Figure II.6).

Chapter II: Selective dimerization of monoaminoarylcarbenes by deprotonation of aldiminium salts

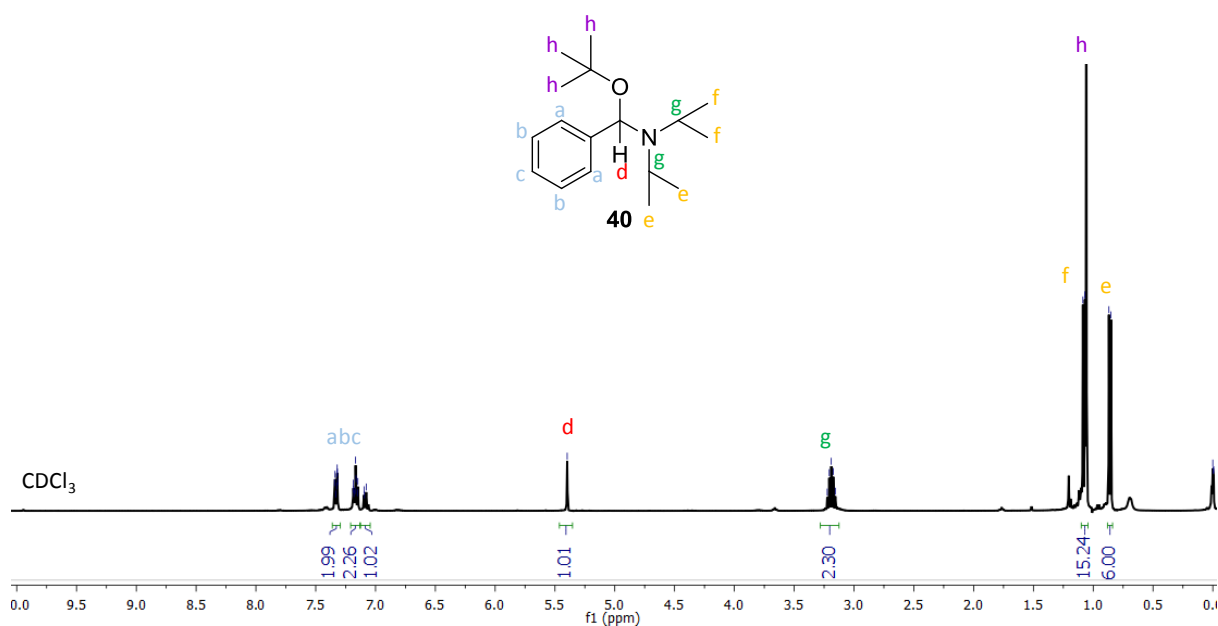
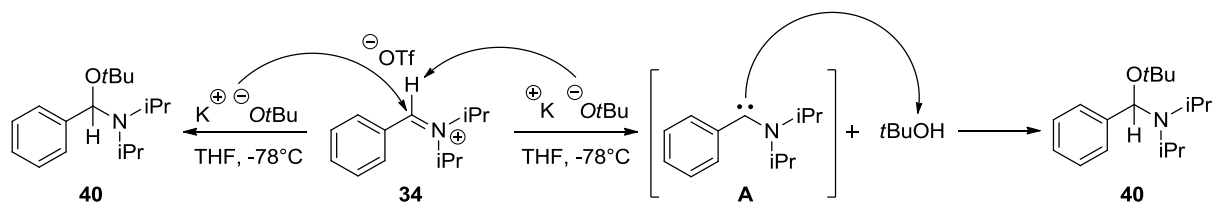


Figure II.6. ^1H NMR (400 MHz) in CDCl_3 of adduct **40**.

Two different mechanisms can be put forward to explain the formation of iminal **40**, from the reaction between **34** and *t*-BuOK. The first mechanism would involve the direct nucleophilic addition of *t*-BuOK onto the iminium salt **40**, while the other would be *via* deprotonation of the iminium **34** by *t*-BuOK, generating the corresponding carbene, which would then insert into the O-H bond of *t*-BuOH. The latter mechanism is based on the analogy with the reaction observed by Bertrand *et al.*⁷, involving an aminoanthryl carbene and *t*-BuOK (Scheme II.18).



Scheme II.18. Plausible mechanisms for the synthesis of iminal **40**.

Such adducts have been reported to behave as masked carbenes upon heating, releasing ROH.^{24,25} To test whether or not **40** could release *t*-BuOH, a solution of **40** was heated in THF at 70°C for 24 hours. According to the results observed by ^1H NMR, a novel product was formed in 45% yield, which could be identified as the targeted diaminoalkene **41** (see below). No further increase in conversion with time was noted, limiting the interest of **40** as a precursor of **41** (Figure II.7).

Chapter II: Selective dimerization of monoaminoarylcarbenes by deprotonation of aldiminium salts

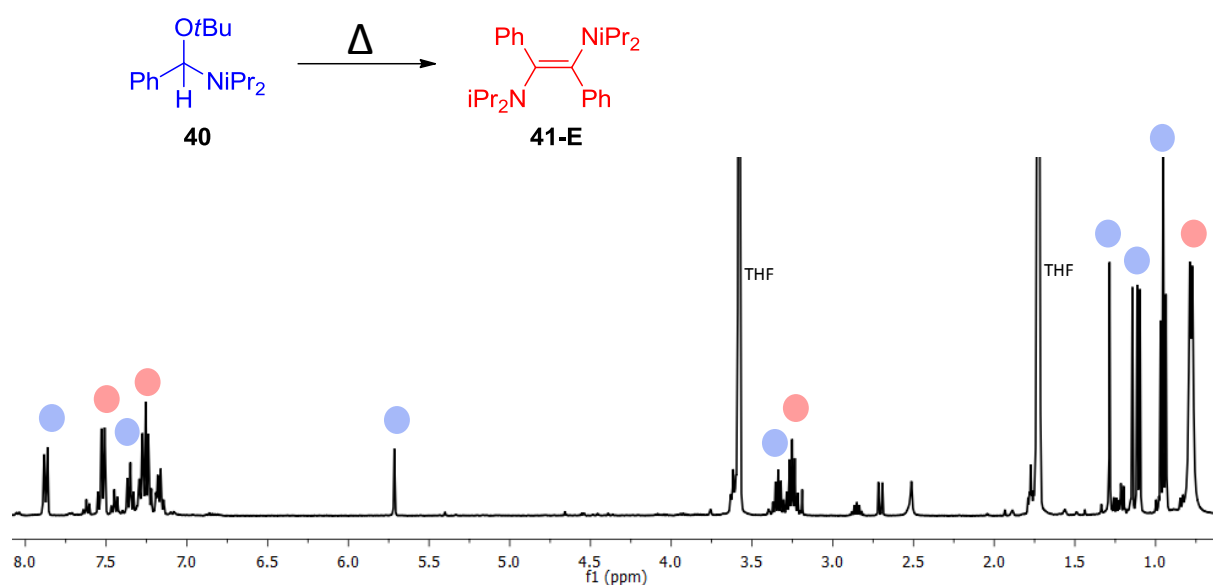


Figure II.7. ¹H NMR (400 MHz) in THF-d₆ of diaminoalkene **41-E** by heating carbene precursor adduct **40**.

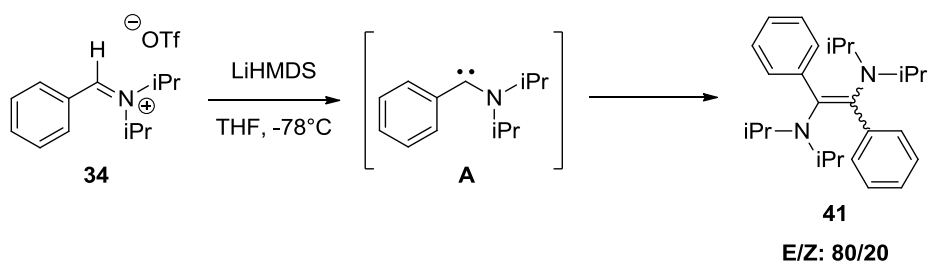
Use of another metallic base, namely, MeONa led to the same conclusion that was an absence of any dimer formation and the presence in quantitative yield of an aminal with a methoxy group. This is again explained by the fact that either the base is nucleophilic enough to add onto the iminium **34**, or the generated carbene can insert in the O-H bond of the released MeOH. MeOH being easier to remove upon heating, the new aminal could be a better carbene precursor, the dimerization of which would lead to the targeted dimer.

As we were also aiming to use a base that could selectively generate a dimerizable carbene, and thus avoid the insertion reaction, the deprotonation step was performed using the lithium salt of hexamethyldisilazane (LiHMDS). Such a base is indeed less nucleophilic and less prone to N-H insertion.²⁶

II.3.2 Use of LiHMDS

Under an inert atmosphere, slow addition of a stoichiometric amount of LiHMDS onto a THF solution of **34** at -78 °C led, after purification, to the desired dimer **41**, which was obtained as a yellow solid (Scheme II.19).

Chapter II: Selective dimerization of monoaminoarylcarbenes by deprotonation of aldiminium salts



Scheme II.19. Deprotonation of iminium salt **34** with LiHMDS leading to a mixture of dimers **41**.

The ^1H NMR spectrum of the resulting compound indeed revealed the complete disappearance of signals belonging to **34**, along with the appearance of a CHiPr peak as a septuplet at 3.30-3.20 ppm, with a constant of $^3J_{\text{H-H}} = 6.80$ Hz integrating for four protons. The latter septuplet was paired with a CH_3iPr signal as a doublet at 0.79-0.77 ppm with a $^3J_{\text{H-H}} = 6.50$ Hz integrating for 24 protons. These signals attested to the pyramidalization of the nitrogen atoms in the newly formed molecule. The same signals were observed though with different small chemical shifts (0.43-0.68 ppm), but integrate for the same amount of protons. Such signals evidenced the presence of a mixture of isomers for the new product, **41**, obtained from the dimerization of the *in-situ* generated carbenes. Moreover, integration of two similar signals revealed a 80/20 ratio in favor of the E isomer (Figure II.8), as discussed in more details in section II.3.2.

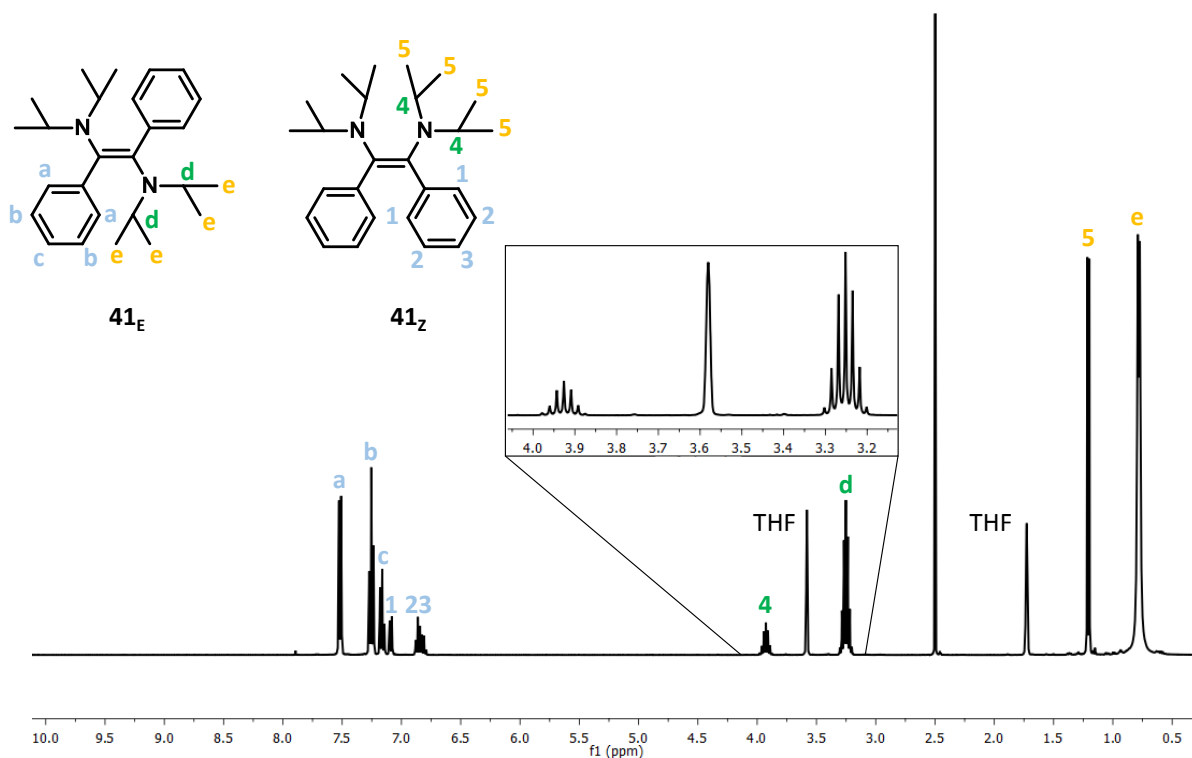


Figure II.8. ^1H NMR (400 MHz) in $\text{THF}_{\text{d}8}$ of E and Z dimer **41**.

Chapter II: Selective dimerization of monoaminoarylcarbenes by deprotonation of aldiminium salts

The ^{13}C NMR spectrum of **41** confirmed the presence of the two isomers. The structure of the dimeric compound showed a C=C bond signal appearing at 140.6 ppm for the E-configuration, and at 135.0 ppm for the Z-configuration, which was close to the C=C of stilbene signal at 137 ppm.²⁷

In the case of the E-isomer, the CHiPr signal was found at 52.04 ppm and that of the CH₃iPr signal at 23.48 ppm. As for the Z-isomer, the CHiPr signal appeared at 48.31 ppm along with a peak due to the methyl carbon atoms at 24.33 ppm (Figure II.9). These results are eventually in good agreement with those reported in the literature.¹⁵

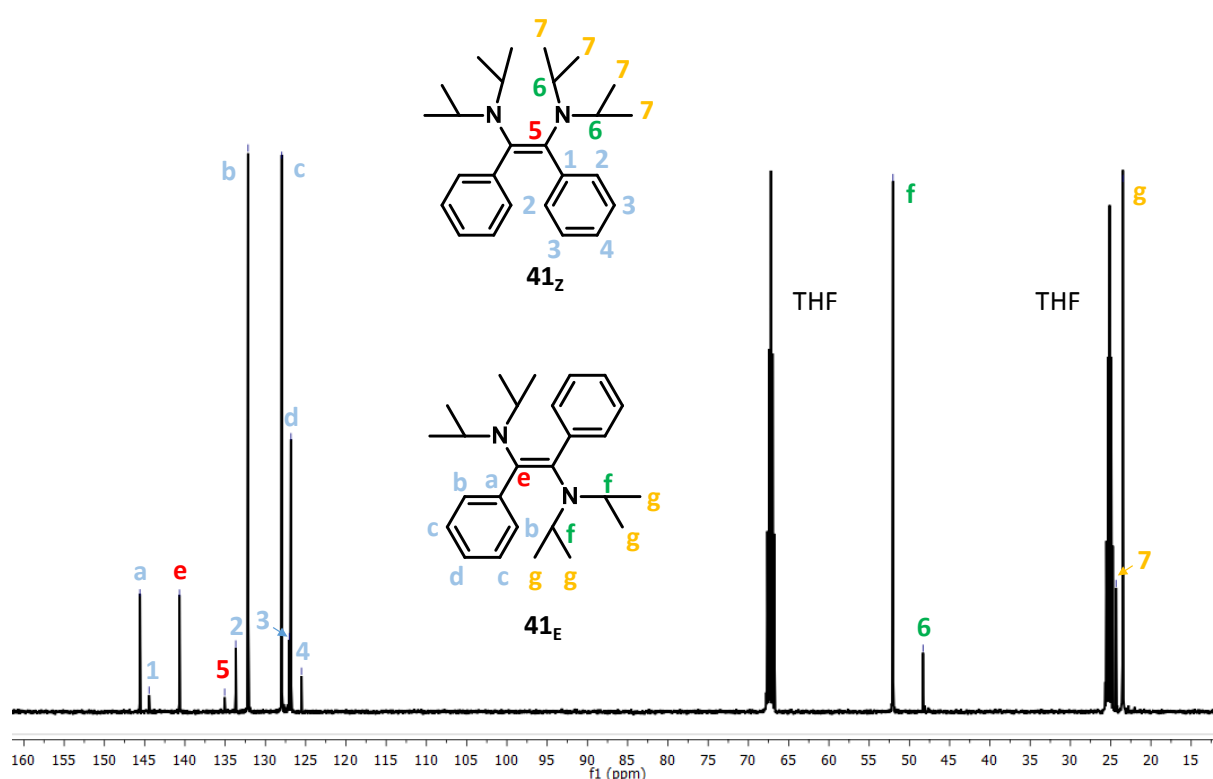


Figure II.9. ^{13}C NMR (101 MHz) in THF_{d8} of isomers E/Z of dimer **41**.

Single crystals of the isomer with the E-configuration could be successfully obtained by slow evaporation of a pentane solution containing **41** at -20°C , which by X-Ray analysis confirmed the identity of the **41-E** isomer. X-Ray analysis of crystal **41-E** indeed showed a C₁=C₂ bond of 1.359 Å, *i.e.* slightly longer than the trans-stilbene double bond with 1.34 Å, which might be attributed to the interaction of amino group with the C=C bond.²⁸ Comparison with an enamine showing a C=C bond length of 1.349 Å,²⁹ the length of **41-E** was almost

Chapter II: Selective dimerization of monoaminoarylcarbenes by deprotonation of aldiminium salts

similar. This indicated a weak influence of the presence of the second amino group onto the C=C double bond.

The C₁-N₁ and C₂-N₂ bond lengths were found equal to 1.421 Å, which was shorter than a single C-N bond length (1.469 Å), but longer than a C=N double bond length (1.279 Å). In fact, this value fitted closely with that of a regular enamine dCN= 1.416 Å.³⁰ The N₁ atom exists in a planar environment, as evidenced by the sum of angles around the nitrogen atom of 359.4°, which likely results from the packing of the molecules in the crystal. Finally, the dihedral angle C₄-C₃-C₁-C₂ that is equal to 68.8° indicates that the phenyl group is tilted relative to the C₂C₁C₃ plan, thus preventing its interaction with the C=C bond. This result is reflected with the C₁-C₃ bond length of 1.50 Å, as compared to a conjugated double bond with an aryl C_{Ar}-C=C with 1.47 Å (Figure II.10).

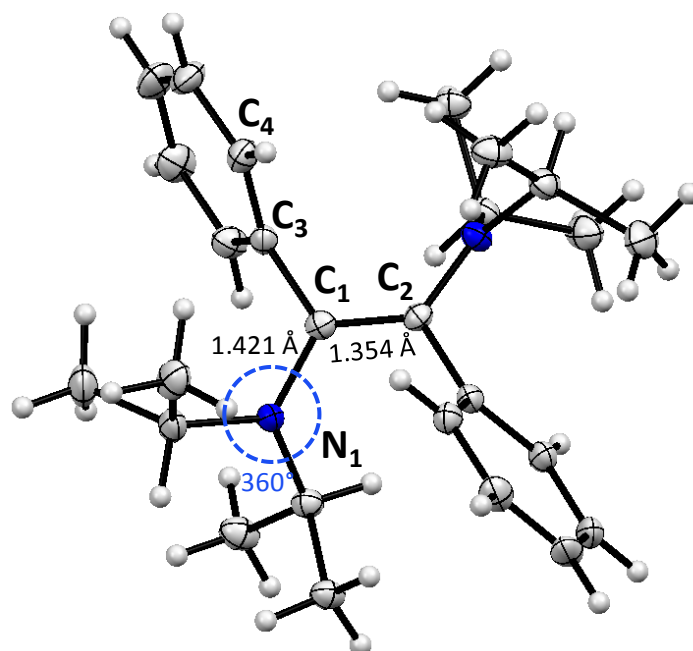


Figure II.10. X-ray of compound 41-E.

UV-Vis analysis was then performed to evaluate the impact of the amino groups on the π -conjugated system. Corresponding spectra of **41** showed a π - π^* transition at a wavelength $\lambda_{\max} = 229$ nm, and a n - π^* transition at a wavelength $\lambda_{\max} = 388$ nm. Compared to the trans-stilbene model showing two π - π^* transitions, at 228 nm and 294 nm, respectively, the π - π^* at 229 nm was similar in both products, which could be ascribed to the presence of the phenyl moiety. However, adding an amino group onto the double bond in compound **41** proved to enhance the absorption wavelength. This was due to the n - π^* transition from the free lone pair of electrons of the amino group on the π^* of the conjugated system, as illustrated in Figure

Chapter II: Selective dimerization of monoaminoarylcarbenes by deprotonation of aldiminium salts

II.11. It can thus be concluded that the addition of two amino groups on the double bond has a bathochromic effect on the UV absorption of the Z- and the E-diaminoalkenes **41**.

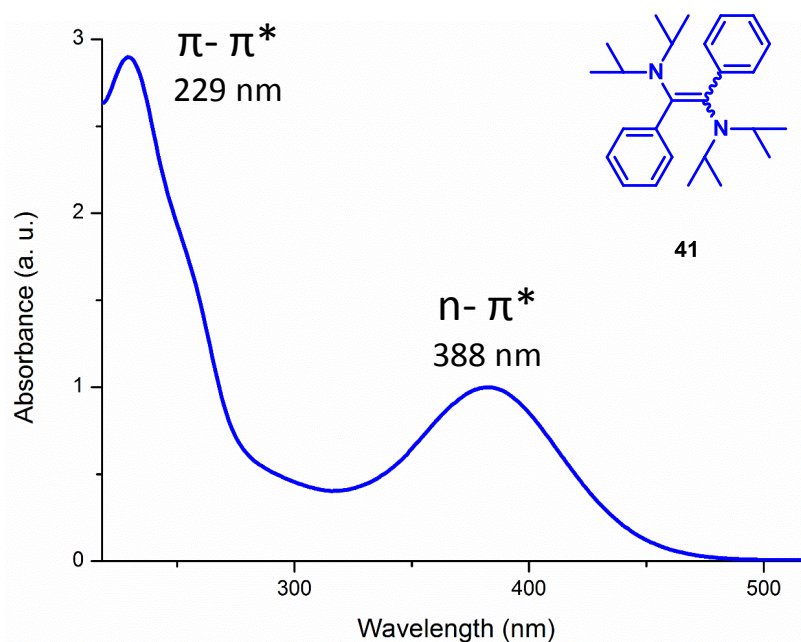


Figure II.11. UV-Vis spectrum of compound **41** in CHCl_3 .

In order to better assess this $n-\pi^*$ transition, modelling of the HOMO and LUMO of compound **41** was achieved at B3LYP/def2-SVP level of theory (Figure II.12). It was thus found that the HOMO was mainly localized on the $\pi_{\text{C}=\text{C}}$ and n_{N} orbitals, while the LUMO was localized on the combination of the orbitals $\pi^*_{\text{C}=\text{N}}$ and $\pi^*_{\text{C}=\text{C}}$ on the phenyl.

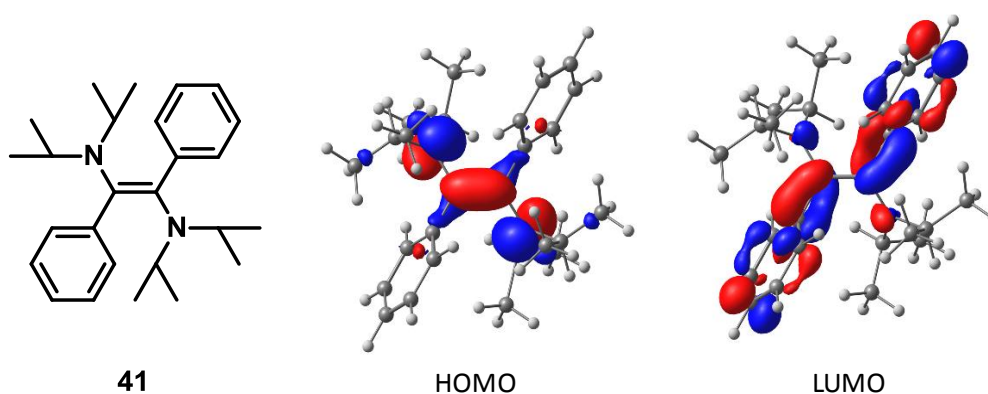


Figure II.12. Frontier orbital for the E isomer of dimer **41**.

II.3.3 Use of a neutral base

Chapter II: Selective dimerization of monoaminoarylcarbenes by deprotonation of aldiminium salts

After LiHMDS, *t*-BuOK and MeONa were used as metallic bases, strong and neutral bases were also tested, including 1,8-diazabicyclo[5.4.0]undec-7-ene (DBU), 1,5,7-Triazabicyclo[4.4.0]dec-5-ene (TBD) and phosphazene (P_4 -*t*-Bu; Figure II.13).

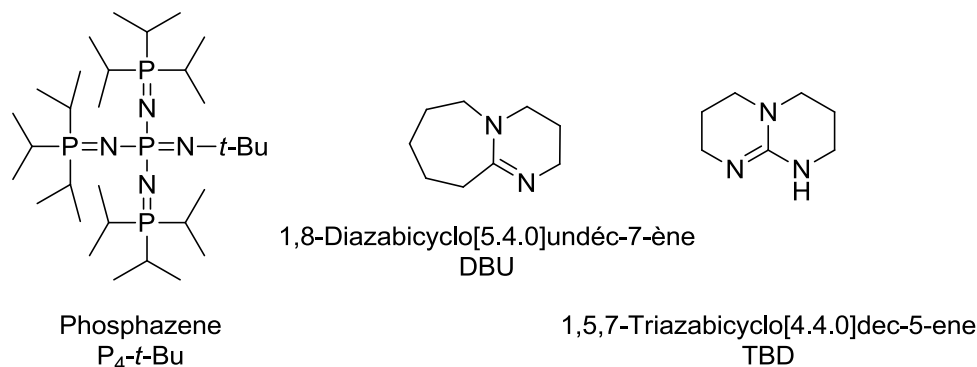


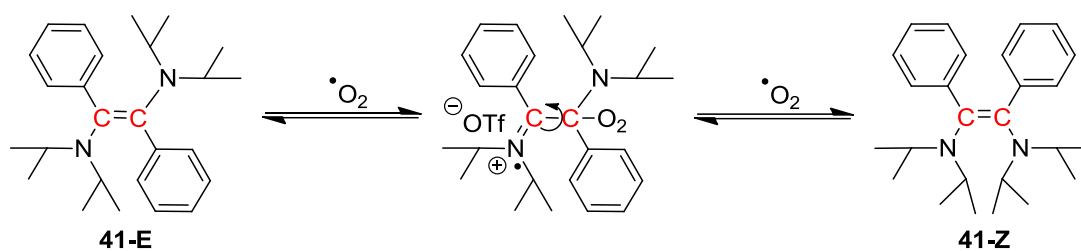
Figure II.13. P_4 -*t*-Bu, DBU and TBD bases selected for the dimerization of aminoarylcarbenes.

Such neutral bases were expected to facilitate the purification step of the dimer. After deprotonation indeed, the salt formed could be easily removed by simple filtration. Although all bases gave full conversion of the iminium salt precursor (**34**), different E/Z isomer ratios were obtained for the crude reactions. It also appeared that the stronger the neutral base was, the more E-isomer formation was favored. After purification, however, the ratio was always found equal to 80/20 in favor of **41-E** (Table II.2). These values were eventually reached when the dimer was manipulated in air. Therefore, we hypothesized that dimers **41** could react with triplet oxygen in a reversible manner, as shown in scheme II.20. Indeed, the radical cation generated upon addition of O_2 could rotate about the central C-C bond, ultimately leading to the E/Z interconversion.

Table II.2. E/Z ratio of crude dimer **41** according to the strength of the charged or neutral base.

Base	pKa (DMSO)	E/Z ratio of crude 41	Conversion
Phosphazene P_4 - <i>t</i> Bu	42,7	97/3	100 %
LiHMDS	30	100/0	100 %
TBD	21 (THF)	85/15	100 %
DBU	12	78/22	100 %

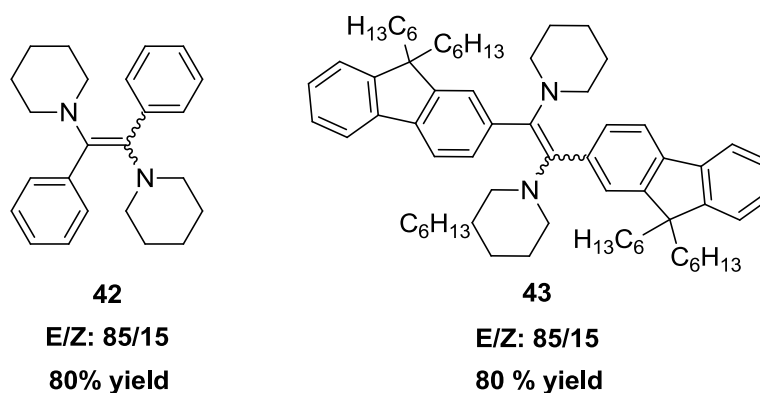
Chapter II: Selective dimerization of monoaminoarylcarbenes by deprotonation of aldiminium salts



Scheme II.20. Isomerization of dimer **41** through reversible addition of triplet oxygen.

II.3.4 Scope of the deprotonation reaction

Finally, the scope of this reaction was investigated by using the different iminium salts **35-39** synthesized above. For the iminium salts **35** and **36**, the deprotonation in presence of LiHMDS successfully and selectively led to the corresponding dimer **42** and **43**, in 80% yield (Scheme II.21). Interestingly, the E/Z ratio observed changed from 80/20 to 85/15, compared to dimer **41** (80/20 E/Z), evidencing that the alkyl group on the amino functionality had an influence on this ratio. In contrast, the aryl moiety did not seem to show any significant impact on the reaction outcomes.



Scheme II.21. Dimerization carbene generated *in-situ* from deprotonation of iminium salts **35** and **36** by addition of LiHMDS leading to a E/Z mixture in favor of the E isomer for dimers **42** and **43**.

Deprotonation of iminium salts **37-39** gave rise to rather complex ^1H NMR spectra. No characteristic peak that could be attributed to the presence of the dimer could be detected, making impossible the accurate characterization of the products. In the case of iminium salt **37**, the reason could be due to the lower steric hindrance provided by the ethyl group, compared to the isopropyl group, which could not stabilize enough the *in-situ* generated carbene for selective dimerization. In the case of precursor **39** (Figure II.5), the aryl moiety was replaced with a thiophene group, hence it could be hypothesized that the reactivity of the molecule got changed

Chapter II: Selective dimerization of monoaminoarylcarbenes by deprotonation of aldiminium salts

with the presence of a sulfur atom. Thus, upon addition of a strong base, the deprotonation may not be selective for the iminium proton, leading to side reactions and products. Similarly, for precursor **38**, the presence of an oxygen in the morpholine moiety might change the proton acidity leading to side reactions upon deprotonation.

II.4 Investigation into the dimerization mechanism

As discussed in the bibliographic chapter, the carbene dimerization reaction can go through two different pathways, including a direct dimerization of free carbenes or *via* an electrophilic-catalyzed mechanism.²⁶ The non-catalyzed dimerization eventually follows a non-least motion pathway and involves the attack of the occupied in-plane σ orbital of one carbene on the out-of-plane p_π orbital of a second carbene. Although this reaction is exergonic for non-aromatic, cyclic and acyclic diaminocarbenes,^{31,32} the calculated energy barrier is prohibitively high, making this path unlikely. As for the proton-catalyzed mechanism, protonation of the carbene considerably decreases the energy of the LUMO, facilitating the dimerization reaction (Figure II.14). Studies reported by the Alder's group have shown that dimerization of diaminocarbenes takes place mostly by the proton-catalyzed mechanism.²⁶ It is only in 2014 that the direct dimerization has been observed in the case of a cross-coupling between a cyclopropenylidene and a seven-membered diamidocarbene (see chapter I, section 6).³³

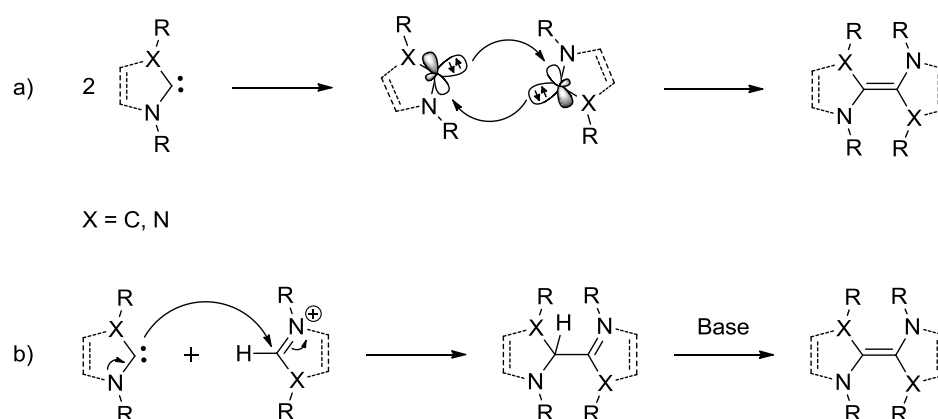


Figure II.14. Two mechanisms for the carbene dimerization reaction. a) direct proton-free dimerization, b) proton catalyzed dimerization.^{13,14,26,34}

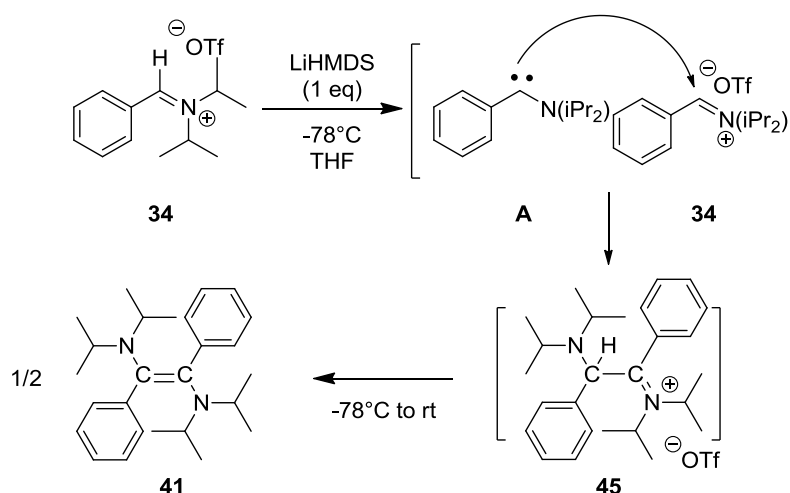
Chapter II: Selective dimerization of monoaminoarylcarbenes by deprotonation of aldiminium salts

Monoaminocarbenes (MACs) have a higher HOMO and a lower LUMO level, as explained in chapter I. Therefore, one can wonder whether the LUMO level is low enough to observe the direct dimerization in the case of aminoarylcarbenes **A**. A piece of evidence of the direct dimerization of MACs has been reported by Bertrand *et al.*¹⁴, with the generation of an *in-situ* aminoarylcarbene, free from any proton (using the reductive dechlorination route), which dimerizes into the corresponding diaminoalkene. It was thus of interest in our case to investigate the dimerization mechanism of our system.

II.4.1 Experimental investigation of the mechanism of dimerization

The reaction was monitored at -80°C by ¹³C NMR spectroscopy. Unfortunately, no carbene formation could be evidenced, as deduced from the absence of characteristic signal around 300 ppm.^{5,11,35} Nevertheless, the deprotonation did occur, as shown by ¹H NMR spectroscopy with the disappearance of the CH-iminium signal and apparition of signals characteristic of **41-E** (Figure II.15). Interestingly, another set of signals attributed to **45** was also observed (only signals between 6 and 3.5 ppm were identified, because analysis was performed on the crude mixture). Two CHiPr septets down-fielded, compared to that of the dimer **41** at 4.64 and 5.04 ppm, and integrating for one proton each, attested to the presence of an iminium group. Two other CHiPr multiplets observed at 2.95 and 2.84 ppm and integrating for one proton each could be attributed to a pyramidal amino group (Fig II.15 in blue). From these two types of isopropyl groups, we proposed that the adduct **45** was formed by reaction between a transient carbene and its iminium salt, as described in scheme II.22. The CH singlet observed at 5.89 ppm, and integrating for one proton, is in agreement with such structure (Figure II.15).

Chapter II: Selective dimerization of monoaminoarylcarbenes by deprotonation of aldiminium salts



Scheme II.22. Proposed intermediate **45** during the dimerization of **34** into **41** via addition of one equivalent of LiHMDS.

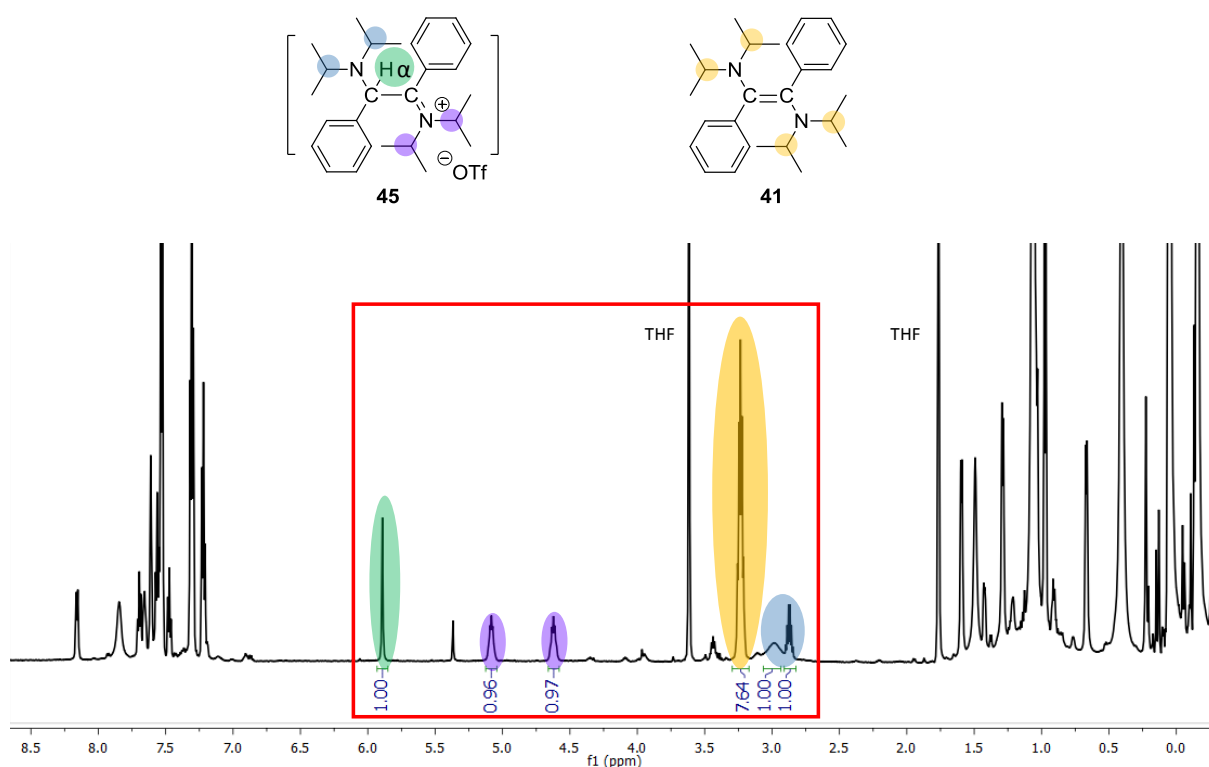
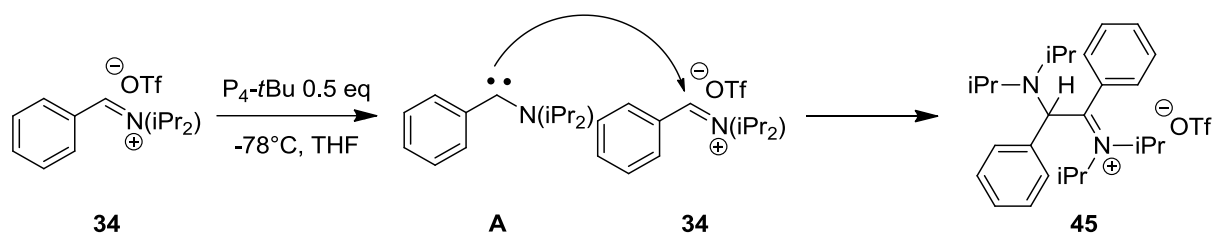


Figure II.15. ^1H NMR (400MHz) in THF_{d6} at -80°C of a mixture of compounds **45** and **41**.

Compound **45** proved however unstable, hampering its further characterization by ^{13}C NMR spectroscopy. Upon heating to room temperature, indeed, the intermediate disappeared in favor of the isomer **41-E**. As a mean to isolate this intermediate, half equivalent of base was used in presence of the iminium **34**. Addition at -78°C of 0.5 eq. of P_4 -*t*-Bu phosphazene on one equivalent of iminium salt **40** was thus carried out (Scheme II.23).

Chapter II: Selective dimerization of monoaminoarylcarbenes by deprotonation of aldiminium salts



Scheme II.23. Proposed mechanism to isolate compound **45** with the use of 0.5 eq of P_4-tBu .

The intermediate **45** was successfully obtained as a light yellow powder. Characterization by 1H NMR spectroscopy in CD_3CN was directly performed at ambient temperature, revealing clear signals assignable to compound **45** (Figure II.15). For instance, two clear down-fielded septets at 4.88 and 4.35 ppm ($^3J_{H-H} = 7.1$ Hz) integrating for one proton each could be detected and were assigned to the He iminium function. In contrast to the low temperature analysis, only one Hc septet appearing at 2.94 ppm ($^3J_{H-H} = 6.6$ Hz) was observed, due to the presence of a pyramidal amino group. Finally, the CH_α singlet at 5.64 ppm confirmed the hypothesis of an addition of a carbene molecule onto an iminium salt forming the compound **45**. Also, two doublet signals at 0.57 and 0.70 ppm ($^3J_{H-H} = 6.6$ Hz), integrating for 6 protons each, were assigned to the Hb amino function and the doublet signals at 0.74, 1.04, 1.19 and 1.48 ppm ($^3J_{H-H} = 7.0$ Hz), integrating for 3 protons each, represented the Hd iminium function. Finally, and Hd signals integrated each for twelve protons. Finally, Ha atoms integrating for ten protons were assigned for the aromatics protons. All these signals matched with the proposed structure of **45**, as summarized in Figure II.16.

Chapter II: Selective dimerization of monoaminoarylcarbenes by deprotonation of aldiminium salts

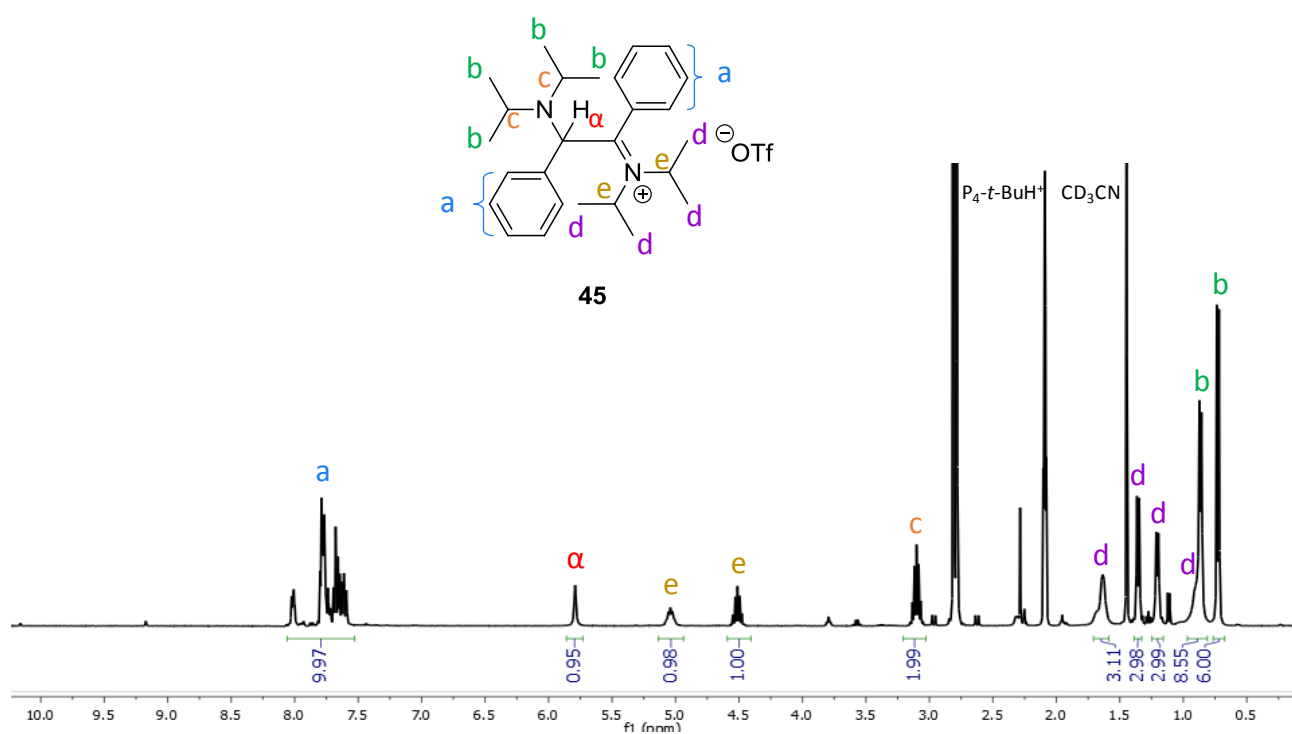


Figure II.16. ¹H NMR (400 MHz) in CD₃CN of the intermediate **45** obtained by deprotonation of **34** with 0.5 eq of P₄-*t*-Bu base on iminium salt **34**.

When **45** was left at ambient temperature for 12 hours in THF or CH₃CN as solvent, its characteristic signals progressively vanished, while new signals corresponding to a mixture of dimer **41-E/Z** and starting material **34** were observed (Figure II.17).

Chapter II: Selective dimerization of monoaminoarylcarbenes by deprotonation of aldiminium salts

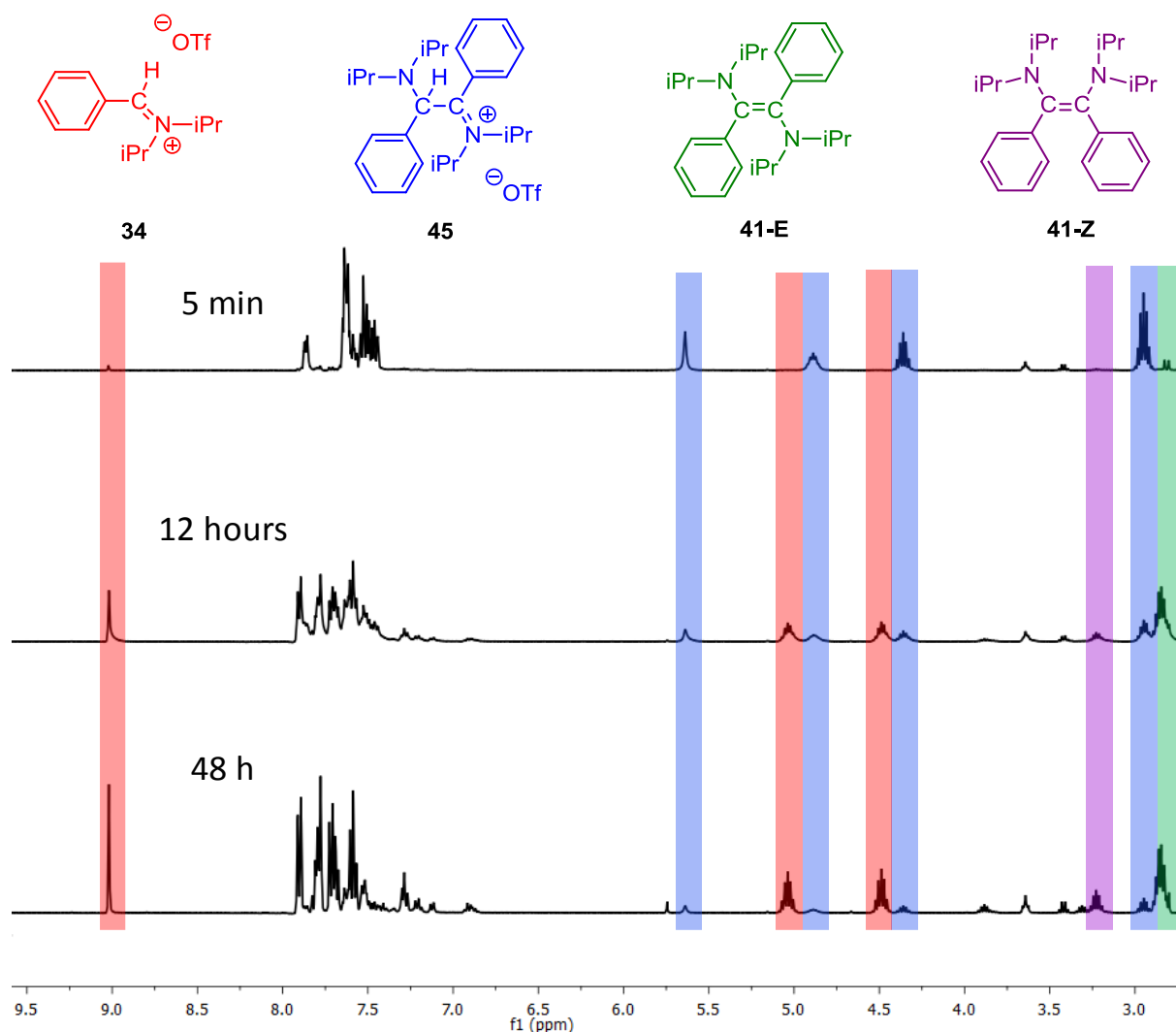
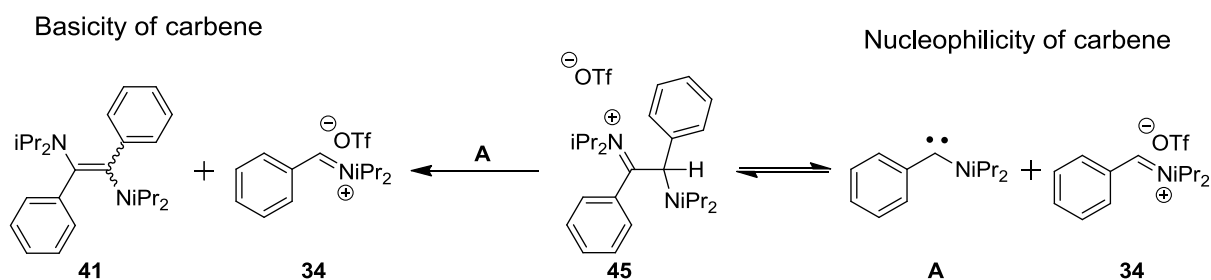


Figure II.17. Stability study of **45** over time monitored by ^1H NMR (400 MHz) in CD_3CN at rt.

These results suggested that the intermediate **45** could readily dissociate in solution to reform the starting iminium **34**, along with the corresponding carbene, which was basic enough to deprotonate the intermediate **45** and to generate the final diaminoalkene **41**, as depicted in scheme II.24.



Scheme II.24. Mechanism of the evolution of **45** over time.

Chapter II: Selective dimerization of monoaminoarylcarbenes by deprotonation of aldiminium salts

The structure of **45** could be confirmed by recrystallization by diffusing Et₂O into a solution of **45** in CH₃CN at -40°C in a glovebox. X-Ray analysis indeed confirmed the structure established for compound **45** by NMR. For instance, the C₁-N₁ distance of 1.29 Å and the sum of angles around the N₁ atom of 360° is characteristic of a double C=N bond. The C₂-N₂ bond distance of 1.45 Å (typical of a single bond) coupled with a sum of angle around N₂ of 352° certified the pyramidalization of the the amino group. Finally, the C₁-C₂ distance of 1.56 Å is a simple bond (Figure II.18).

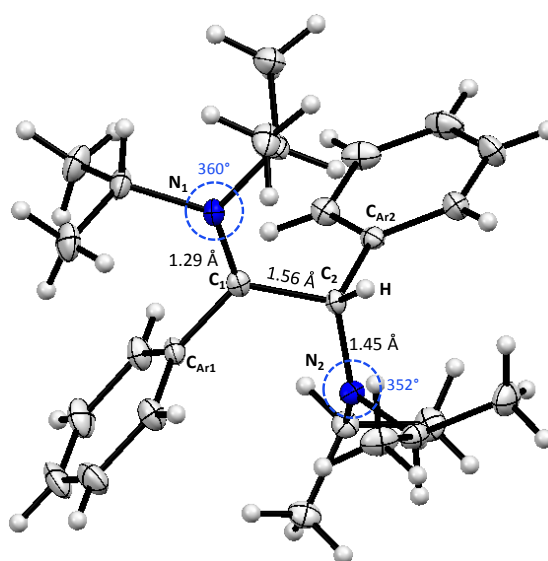


Figure II.18. X-ray analysis of intermediate **45**.

The isolation and unambiguous characterization of intermediate **45** thus evidenced that aminoarylcarbenes undergo dimerization through a proton-catalyzed mechanism. However, a direct dimerization pathway cannot be totally ruled out.

II.4.2 Attempt to trap the aminoarylcarbene

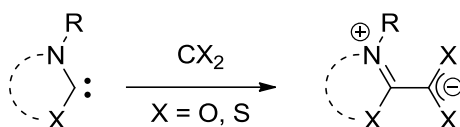
Despite the unsuccessful observation of aminoarylcarbenes by NMR spectroscopy, upon deprotonating the iminium precursor at -78°C, attempts to trap this putative carbene through its reaction with different electrophiles were envisaged, in particular using CS₂ and S₈. The reactivity of this carbene was also investigated in cyclopropanation and insertion reactions.

Chapter II: Selective dimerization of monoaminoarylcarbenes by deprotonation of aldiminium salts

II.4.2.1 Trapping reaction with organic compounds

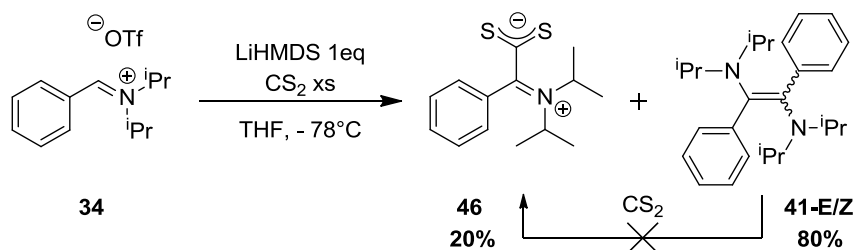
II.4.2.1.1 Addition to heterocumulenes

Addition of carbenes to heterocumulenes, such as carbon dioxide, carbon disulfide or isocyanate, has been mainly reported for NHCs,³⁶ but also in the case of acyclic diaminocarbenes (ADACs),³⁷ diaminocarbenes incorporating a pyramidalized nitrogen atom,³⁸ and CAACs³⁹ as well as all giving the corresponding stable betaines (Scheme II.25).⁴⁰⁻⁴³



Scheme II.25. Addition of DAC and MAC to heterocumulenes giving the corresponding betaines.

The reaction was tested with our acyclic diisopropylaminoarylcarbene. LiHMDS was thus slowly added onto a THF solution of **34**, in presence of an excess of CS₂ at -78°C (Scheme II.26).



Scheme II.26. Addition of *in-situ* generated diisopropylaminoarylcarbene **A** on CS₂ by deprotonation in cold THF of iminium salt **34**.

Characterization by ¹H NMR spectroscopy of the resulting compound revealed the complete disappearance of signals due to the starting iminium salt, **34**, along with signals corresponding to three different compounds in a 20/80 ratio. Signals corresponding to the major compounds could be attributed to the E/Z dimer (80/20) **41**, which again resulted from the dimerization of diisopropylaminoarylcarbene **A**. The minor product exhibited two CHiPr septets downfielded at 4.20 and 5.18 ppm, integrating for one proton, characteristic of the iminium function (see experimental part). Both compounds were separated by extraction with ether of the major product.

Chapter II: Selective dimerization of monoaminoarylcarbenes by deprotonation of aldiminium salts

To gain further insight into the structure of the latter reaction product, ^{13}C NMR was performed. The signals at 238.7 ppm and 179.3 ppm, corresponding to the CS_2 carbon and $\text{C}_{\text{iminium}}$ carbon allowed the unambiguous attribution of the expected betaine **46** resulting from the trapping of the carbene with CS_2 (Figure II.19).

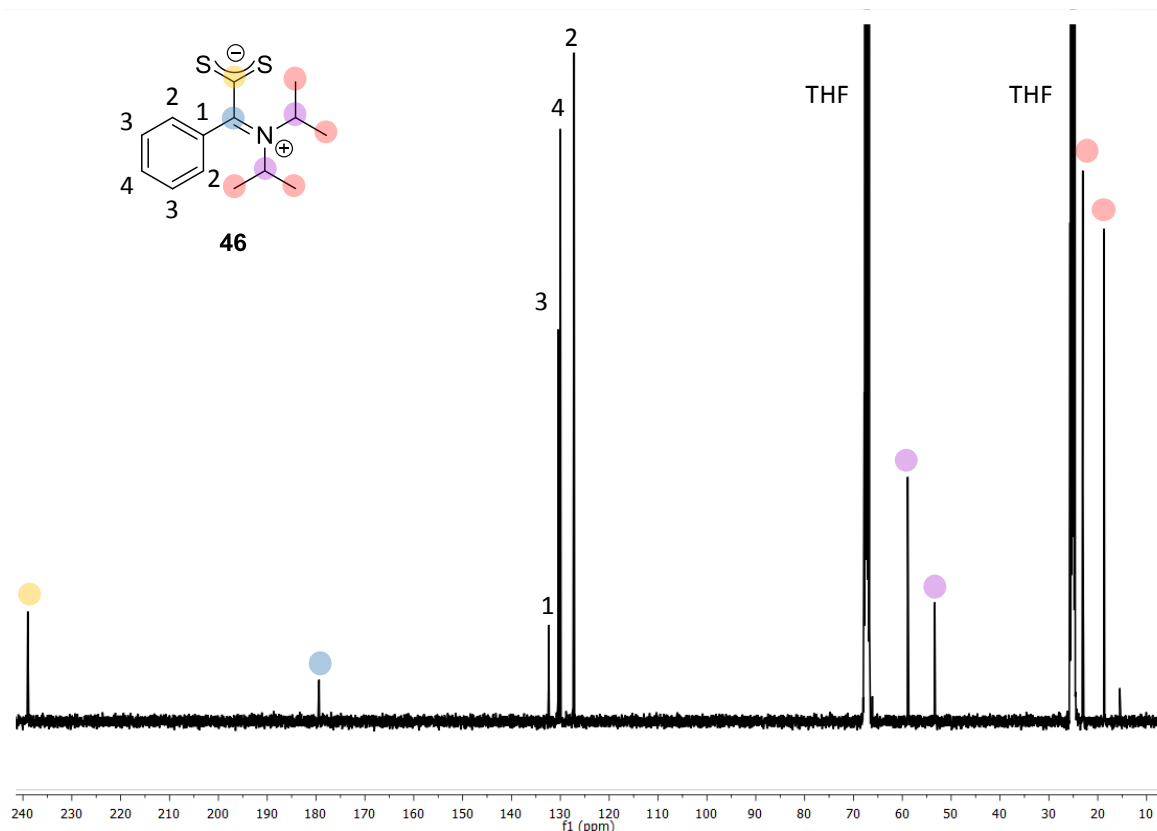


Figure II.19. ^{13}C NMR (101 MHz) in THF_{d8} of recrystallized betaine **46**.

The dimeric alkene **41** could form even though excess of CS_2 was used, meaning that iminium **34** was likely more electrophilic than CS_2 , so that aminoarylcarbene **A** preferentially reacted with iminium **34** (Scheme II.26). A control reaction with dimer **41** and CS_2 was also carried out, but no reaction was observed, thus confirming the carbene pathway to achieve the betaine **46**.

Successful recrystallization of **46** further confirmed the structure of the first stable betaine resulting from the addition of an acyclic aminoarylcarbene onto CS_2 . X-ray analysis showed a planar nitrogen atom ($\Sigma\text{N} = 360^\circ$) and a short $\text{C}_1\text{-N}$ bond (1.30 Å) corresponding to a C-N iminium bond. Moreover, a dihedral angle between the CS_2 group and the iminium group ($\text{S}_1\text{-C}_2\text{-C}_1\text{-N}$) of 90° is observed. However, despite this dihedral angle, no significant interaction between the sulfur atoms and the C_1 atom was noted, as observed by a planar C_1 atom

Chapter II: Selective dimerization of monoaminoarylcarbenes by deprotonation of aldiminium salts

($\Sigma_{C1} = 360^\circ$), a planar N atom ($\Sigma_N = 360^\circ$), a short C₁-N bond distance (1.30 Å) and a rather long C₁-C₂ bond distance (1.49 Å). Finally, C₂-S₁/ C₂-S₂ bond distances were found almost equivalent (~1.67 Å), indicating that the negative charge is symmetrically delocalized (Figure II.20).

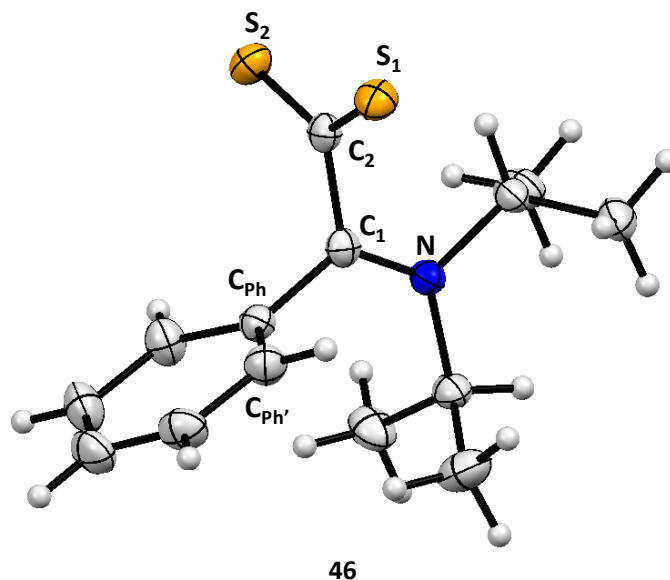
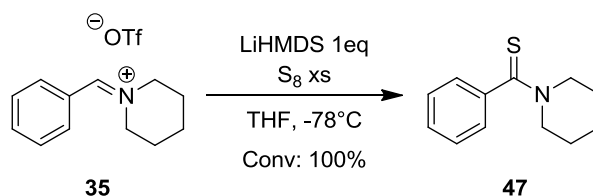


Figure II.20. X-Ray of isolated betaine **46**.

II.4.2.1.2 Addition to elemental sulfur (S₈)

Another way to establish the generation of transient carbenes is to trap them with elemental sulfur (S₈).⁴⁴⁻⁴⁷ The reaction was attempted through the slow addition of LiHMDS onto a mixture of the iminium salt **34**, in presence of an excess of elemental sulfur in THF at -78°C. When the salt precursor bearing the diisopropyl group was employed, only dimerization was observed. In contrast, when iminium **35** featuring a piperidine substituent was deprotonated with LiHMDS at -78°C, thioamide **47** could be isolated with full conversion (Scheme II.27).



Scheme II.27. Synthesis of thioamide **47** through addition of piperidinearylcarbene onto S₈.

Chapter II: Selective dimerization of monoaminoarylcarbenes by deprotonation of aldiminium salts

Signals of the crude reaction obtained for **47** by ^1H NMR spectroscopy were indeed in accordance with data found in the literature, as reported by Krishna Nand Singh *et al.*⁴⁸ (see Figure II.21). In particular, the CH_{arom} signals at 7.25 ppm integrating for 5 protons could be detected, along with the two different H_{α} signals at 4.31 and 3.51 ppm, and the 6 protons in β - and γ -positions in the piperidine group, appearing as multiplets between 1.2 and 1.5 ppm. Also by ^{13}C NMR, the characteristic signal at 199 ppm of the thione function was observed.

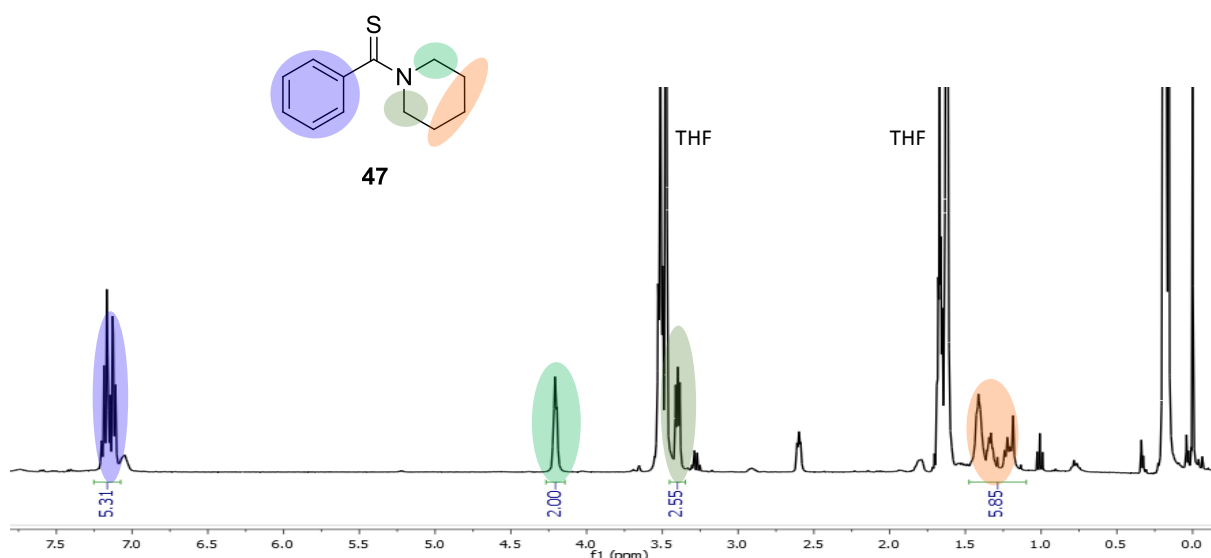


Figure II.21. ^1H NMR (400 MHz) in THF_{d_6} of the crude reaction leading to thioamide **47**.

II.4.2.1.3 Addition to alkenes (cyclopropanation) and coupling reactions with isonitriles.

Diamidocarbene, coumaraz-2-on-4-ylidene, and amino-*tert*-butylcarbene are the only three examples of carbenes that were reported to cyclopropanate alkenes, such as methyl acrylate or styrene (Figure II.22).^{4,49,50}

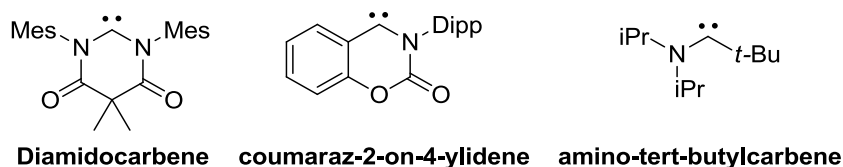
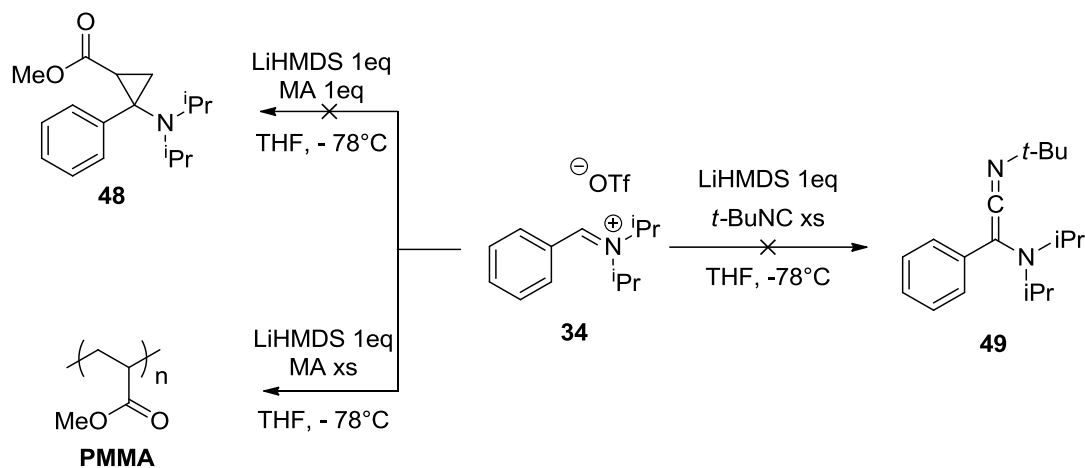


Figure II.22. Aminocarbenes that can perform cyclopropanation.

In the case of aminoarylcarbenes **A**, the deprotonation at -78°C in THF of the iminium salt **34** with LiHMDS, followed by addition of methyl acrylate did not lead to the targeted

Chapter II: Selective dimerization of monoaminoarylcarbenes by deprotonation of aldiminium salts

compounds. Instead, only the dimer **41** was identified as the main reaction product. Therefore, it can be again concluded that the transient carbene preferably reacts with the iminium salt rather than with the added electrophile. When methyl acrylate (MA) was used in excess, polymerization was observed, leading to poly(methylacrylate) (PMA; Scheme II.28).



Scheme II.28. Reactivity of the transiently generated carbene with Ma and *t*-BuNC.

The reaction of carbene with *t*-BuNC to afford the corresponding ketenimine has only been observed with ambiphilic carbene, such as diamidocarbene, coumaraz-2-on-4-ylidene, and amino-*tert*-butylcarbene (Figure II.22),^{4,49,50} which possess a low lying LUMO. The deprotonation of **34** with LiHMDS in presence of *t*-BuNC was performed. However, no trace of the corresponding ketenimine **49** was observed.

In summary, in this part, we attempted to trap the *in-situ* generated transient aminoarylcarbenes with the help of electrophiles. In presence of CS₂, for instance, the trapping was partial, with only 20% of the carbene being trapped to form the related betaine product, the other 80% corresponding to the dimer issued from the dimerization reaction. This result evidenced that the carbene formed would preferably react with the more electrophilic iminium salt than with CS₂. Using the electrophile S₈ in excess did not lead to any trapping with the carbene **A**. However, when the piperidine substituent was introduced onto the amino group of the aminoarylcarbene, the reaction with S₈ showed a full conversion of the carbene into the thioamide.

Chapter II: Selective dimerization of monoaminoarylcabenenes by deprotonation of aldiminium salts

The reactivity of aminoarylcabene **A** was then investigated and a similar result as with the trapping was obtained. Indeed, comparing the dimerization reaction with cyclopropanation with methyl acrylate or with the coupling with isocyanide, the transient aminoarylcabene **A** was observed performing only dimerization over the other reactions. These results thus demonstrate that aminoarylcabenenes can indeed be generated upon deprotonation of the iminium salt. However, in those cases, the dimerization reaction is the dominant reaction pathway prevailing over the insertion, coupling and addition reactions.

II.4.3 Investigation of the dimerization mechanisms by DFT calculation

The direct and proton-catalyzed mechanisms were computationally investigated by DFT calculations. Besides, the high selectivity of the dimerization reaction prompted us to consider a common side reaction of MAC, namely, the intramolecular CH-insertion reactions.^{3,10,11} These calculations were conducted by Dr. Daiann Sosa Carrizo, under the supervision of Dr. Karinne Miqueu and Dr. Jean-Marc Sotiropoulos, at the “Institut Pluridisciplinaire de Recherche sur l'Environnement et les matériaux (IPREM)” at the Université de Pau & des Pays de l'Adour (UPPA). Density Functional Theory (DFT) calculations were carried out at the B3LYP/def2-SVP level of theory.

II.4.3.1 Optimization of the geometry of the starting (cabene) and final compound (dimer)

The geometry of cabene **I** was first optimized for both triplet and singlet ground states. As expected, the singlet state was found 19.8 kcal.mol⁻¹, more stable than the triplet state. In the singlet state, the N₁-C₁ bond is short (1.30 Å) and the nitrogen atom in a planar environment ($\Sigma N = 360^\circ$), indicating a strong interaction between the nitrogen lone pair and the p_π cabene empty orbital. In addition, the acute N₁-C₁-C_{Ph} angle (124°) and the long C_{cabene}-C_{Ph} bond distance (1.46 Å) indicate that the phenyl group merely behaves as a spectator toward the cabene center. In contrast, the triplet state possesses a longer N₁-C₁ bond (1.37 Å), a

Chapter II: Selective dimerization of monoaminoarylcabenenes by deprotonation of aldiminium salts

pyramidalized nitrogen atom ($\Sigma N = 355^\circ$), a wider $N_1-C_1-C_{Ph}$ angle (130°) and a shorter $C_{carbene}-C_{Ph}$ bond distance (1.41 Å).

The geometries of both the **E**- and **Z**- isomers of dimer **II** were then investigated. In **II-E**, both nitrogen atoms are in a planar environment as deduced from the sum of angles, $\Sigma N_1 = 359.8^\circ$ and $\Sigma N_2 = 359.8^\circ$. While this parameter may suggest an interaction between the nitrogen lone pair and the central $C_1=C_2$ double bond, the long C_1-N_1 of 1.42 Å (1.41 Å for a simple C-N bond), the short $C_1=C_2$ bond of 1.37 Å (1.35 Å for a C=C double bond) and the dihedral angle θ of 52° do not attest of any noticeable interaction. Furthermore, no interaction between the phenyl and the $C_1=C_2$ is observed as judged by the long C_1-C_{Ph} bond distance of 1.50 Å (1.48 Å for a single $C_{sp^2}-C_{Ph}$ bond) and the large $C_4-C_3-C_2-C_1$ dihedral angle of 64° .

For **II-Z**, a slight pyramidalization of both nitrogen atoms ($\Sigma N_1 = 353.6^\circ$ and $\Sigma N_2 = 353.6^\circ$) allows the steric hindrance between the iPr_2N groups to be better accommodated in the **Z** configuration. . Similarly to **II-E**, no interaction is observed between the nitrogen lone pair and the $C_1=C_2$ double bond, as deduced from the C_1-N_1 bond length of 1.42 Å, the $C_1=C_2$ bond length of 1.38 Å and the $N_{1orbital}-N_1-C_1-C_{p\pi}$ dihedral angle (θ) of 41° . Furthermore, no interaction between the phenyl and the $C_1=C_2$ is observed, as attested by the long C_1-C_{Ph} bond distance (1.52 Å) and the large $C_4-C_3-C_2-C_1$ dihedral angle of 76° .

It is worth noting that all values of the calculated parameters are in good agreement with those determined experimentally by XRay diffraction analysis.

II.4.3.2 Direct dimerization investigation

The direct dimerization of carbene **I** into the corresponding diaminoalkene was next computed for both **Z**- and **E**-configuration. Both reactions were found strongly exergonic, with a Gibbs free energy of $-35 \text{ kcal.mol}^{-1}$ for **II-Z** and $-45 \text{ kcal.mol}^{-1}$ for **II-E**. **II-E** is thus thermodynamically more stable by 10 kcal.mol^{-1} than **II-Z**, which could explain the **E/Z** ratio in favor of the **E**-isomer observed experimentally.

Next, the potential energy surfaces of the transformations **I** into **II-E** and **I** into **II-Z** were scrutinized. A single transition state connecting **I** and **II-E**, namely **TS-II-E**, and **I** and **II-Z**, namely **TS-II-Z**, could be localized for each transformation, leading to moderate activation barriers of 18.5 and 17.3 kcal.mol^{-1} respectively.

For **TS-II-E**, the $C_1 \cdots C_2$ bond (2.43 Å) is strongly elongated compared to its corresponding dimer **II-E** (76 %). Moreover, the short C_1-N_1 bond of 1.30 Å, the planar nitrogen and carbon

Chapter II: Selective dimerization of monoaminoarylcarbene by deprotonation of aldiminium salts

atoms ($\Sigma N_1 = 360^\circ$ and carbon $\Sigma C_1 = 360^\circ$, respectively) found in the carbene on the left part of **TS-II-E** are in agreement with the geometrical parameters of the starting carbene **I**. Similar geometrical parameters are observed for the carbene on the right part of **TS-II-E**, with a C_2-N_2 bond distance of 1.32 Å, and a ΣN_1 of 359.9° and a ΣC_1 of $\sim 359.0^\circ$. Thus, **TS-II-E** can be considered as an early transition state.

For **TS-II-Z**, the $C_1 \cdots C_2$ bond (2.379 Å) is strongly elongated compared to its corresponding dimer **II-Z** (72 %) but less than the one in **TS-II-E**, suggesting a slightly stronger interaction between the two carbene carbons in **TS-II-Z**. As a result, $C_{1,2}$ and $N_{1,2}$ are moderately pyramidalized (353° and 359.7° for $\Sigma C_{1,2}$ and $\Sigma N_{1,2}$ respectively) and $C_{1,2}-N_{1,2}$ bonds are slightly longer (1.33 Å for each C-N bond). Although those data are in agreement with an early transition state (Figure II.23), **TS-II-Z** is relatively later than **TS-II-E**.

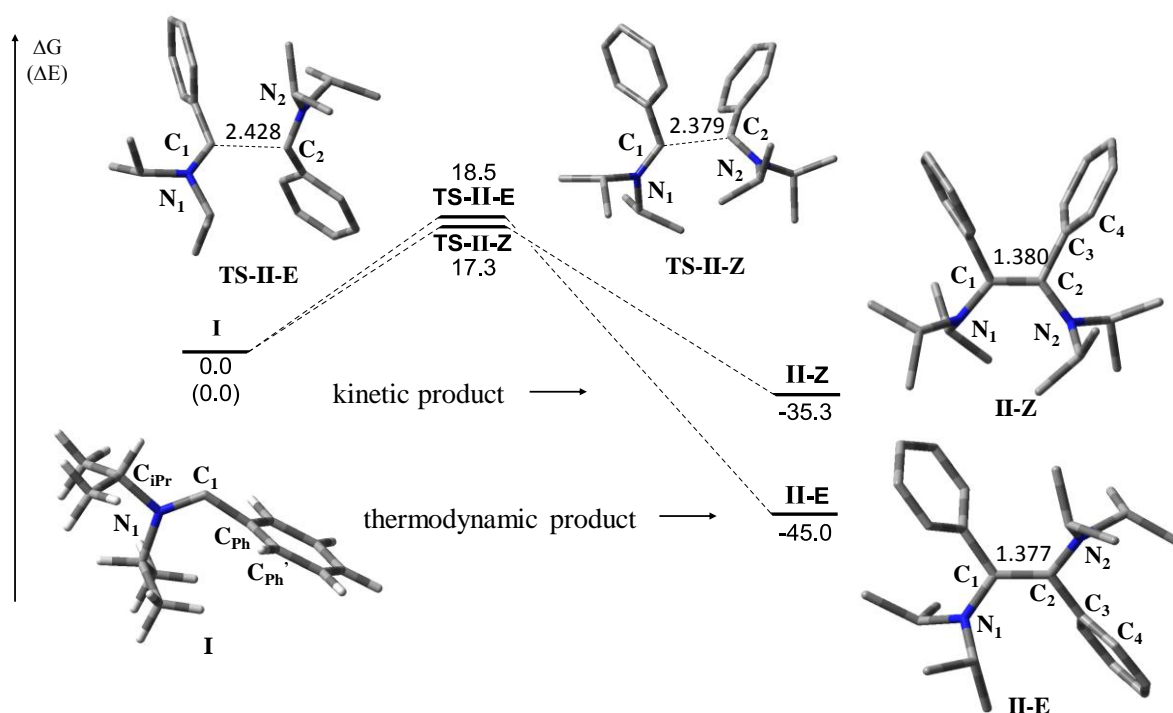


Figure II.23. Energy profiles computed for the dimerization of diisopropylamino aryl carbene, using B3LYP/def2-SVP level theory. Gibbs free energies in kcal.mol⁻¹.

II.4.3.3 Indirect dimerization

The indirect dimerization pathway, involving carbene **I** and its corresponding conjugated acid **I'**, was then investigated by first computing the transformation of **I+I'** into

Chapter II: Selective dimerization of monoaminoarylcarbenes by deprotonation of aldiminium salts

carbene-iminium intermediates **IV-E/Z**, followed by the deprotonation of **IV-E/Z** (by **I**) to yield the final diaminoalkenes **II-E/Z**. For the first transformations, both reactions were found moderately exergonic, with a Gibbs free energy of $-14.4 \text{ kcal.mol}^{-1}$ for **IV-Z** and $-13.5 \text{ kcal.mol}^{-1}$ for **IV-E**, respectively. Note also that because both carbene-iminium adducts **IV-E** and **IV-Z** are isoenergetic (1 kcal.mol^{-1} difference), a single intermediate could be identified by ^1H NMR at -80°C , highlighting the facile rotation about the central C-C bond at this temperature. Note also that the geometrical parameters of compound **IV** determined by XRay diffraction are well reproduced by calculation.

Analysis of the potential energy surface of the transformation **I+I'** into **IV-E/Z** revealed the initial formation of a hydrogen-bound carbene-iminium pre-complex **int-III-E** and **int-III-Z**, in the case of the E and Z isomer respectively. Those intermediates evolved *via* the nucleophilic addition of **I** onto the iminium salt precursor **I'**, generating the experimentally observed carbene-iminium adduct **IV-E/Z**. A transition state, connecting **int-III-E** and **IV-E**, but also **int-III-Z** and **IV-Z**, could be localized on the PES, leading to very low activation barriers of $0.8 \text{ kcal.mol}^{-1}$ and $2.4 \text{ kcal.mol}^{-1}$, respectively.

For the **E**-configuration, the transformation goes first through a pre-organized complex (**int-III-E**), where carbene **I** is H-bonded to its conjugated acid **I'**. This interaction slightly stabilizes the complex compared to the initial reactants ($\Delta G = -3.6 \text{ kcal.mol}^{-1}$). According to the $\text{C}_I\cdots\text{H}$ and $\text{C}_I\cdots\text{H}$ bond distances (1.10 \AA and 2.26 \AA , respectively), this adduct is unsymmetrical and can be considered as a carbene H-bound to an iminium (C_I , C_I and H are aligned), rather than two carbenes bridged by a H^+ . In **TS-IV-E**, the iminium moiety is tilted so as to maximize the interaction between the $\pi^*_{\text{C}_I\text{-N}_I}$ and the sp_2 orbital centered on the C_I carbon atom. The $\text{C}_I\cdots\text{C}_I$ bond (2.07 \AA) is moderately elongated compared to its corresponding carbene-iminium adduct **IV-E** (32 %). Moreover, the double bond character of the $\text{C}_I\text{-N}_I$ bond (1.30 \AA and the planarity of both nitrogen and carbon atoms ($\Sigma\text{N}_I = 360^\circ$ and $\Sigma\text{C}_I = 360^\circ$, respectively) in the carbene moiety are in agreement with the geometrical parameters of the starting carbene **I**. In the iminium moiety, the $\text{C}_I\text{-N}_I$ is slightly elongated (1.37 \AA), while the nitrogen and carbon are remained planar ($\Sigma\text{N}_I = 359.9^\circ$ and $\Sigma\text{C}_I \sim 359^\circ$, respectively).

For the **Z**-configuration, a pre-organized complex (**int-III-Z**), similar to that observed for the **E**-pathway, was also computed. Again, this hydrogen bond slightly stabilizes the complex compared to the initial reactants, with a ΔG value equal to $-2.6 \text{ kcal.mol}^{-1}$. According

Chapter II: Selective dimerization of monoaminoarylcarbenes by deprotonation of aldiminium salts

to the C_F-H and $C_I\cdots H$ bond distances (1.10 Å and 2.30 Å, respectively), this adduct is unsymmetrical, as observed in **int-III-E**. In **TS-IV-Z**, the iminium moiety is tilted similarly to **TS-IV-E**, to favor the interaction between the C_F and C_I carbon atoms. The $C_F\cdots C_I$ bond (2.18 Å) is moderately elongated compared to its corresponding dimer **IV-Z** (39 %) but more than in **TS-IV-E**, which likely results from the steric congestion between iPr_2N_F and iPr_2N_I . While the geometrical parameters of the carbene moiety ($C_I-N_I = 1.30$ Å, $\Sigma N_I = 360^\circ$ and $\Sigma C_I = 360^\circ$) are in perfect agreement with those of the starting carbene **I**, the carbon atom of the iminium moiety (C_F) is seriously pyramidalized ($\Sigma C_F \sim 348^\circ$) because of the $sp_2 \rightarrow sp_3$ re-hybridization. Accordingly, the C_F-N_F bond is slightly elongated (1.36 Å) compared to that in **I'**.

The second step of the proton-catalyzed mechanism is the deprotonation of the carbene-iminium intermediate **IV-E/Z** by the carbene **I**, leading to the desired diaminoalkenes **II-E/Z**. The deprotonation of **IV-E** and **IV-Z** were found highly exergonic by -31.5 and -20.9 kcal.mol⁻¹ respectively (Figure II.25). From all these theoretical investigations, it can be concluded that the indirect dimerization mechanism is kinetically favored over the direct mechanism, but direct dimerization remains plausible under our experimental conditions and cannot be totally ruled out.

Chapter II: Selective dimerization of monoaminoarylcarbenes by deprotonation of aldiminium salts

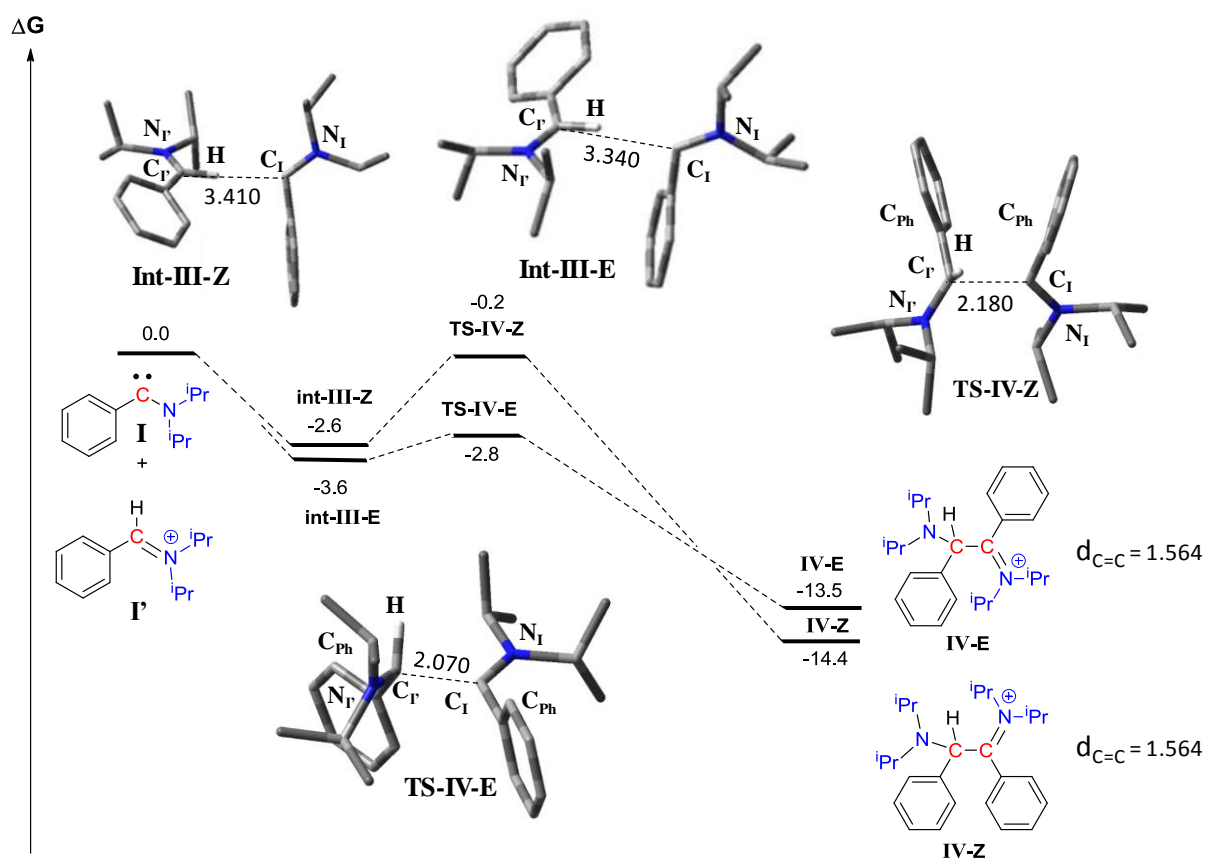


Figure II.24. Energy profiles computed for the proton catalyzed dimerization of diisopropylaminoarylcarbene at B3LYP/def2-SVP level of theory. Gibbs free energies in kcal.mol⁻¹.

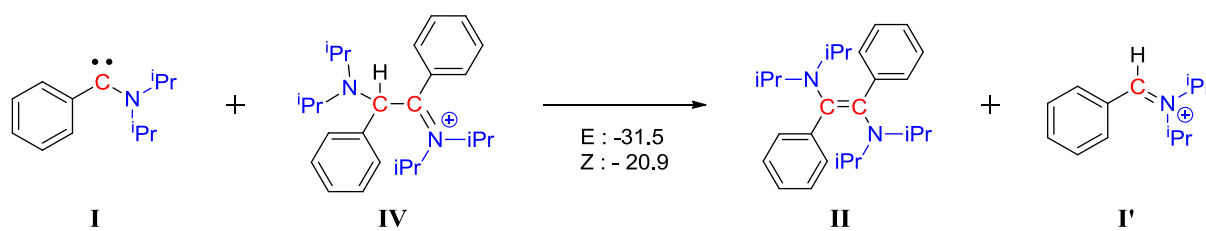


Figure II.25. Deprotonation of the protonated dimer computed at B3LYP/def2-SVP level of theory. Gibbs free energy in kcal.mol⁻¹.

II.4.3.4 Investigation of side reactions

As emphasized in the bibliographic chapter, carbenes might undergo side reactions, in particular C-H insertion reactions.^{10,11,51,36} Intramolecular C-H insertion reactions of aminoarylcarbene **I** into CHiPr or CH₃iPr were thus carried out by DFT calculations (see Figure

Chapter II: Selective dimerization of monoaminoarylcarbenes by deprotonation of aldiminium salts

II.26). Although both reactions were predicted to be exergonic ($\Delta G = -16$ and -30.6 kcal.mol⁻¹ respectively), prohibitive activation barriers of 39.4 kcal.mol⁻¹ and 45.6 kcal.mol⁻¹ respectively, were calculated, in agreement with the high selectivity observed experimentally for the dimerization reaction.

Insertion of carbene **I** into the **CH₃iPr** was first investigated. A single transition state connecting **I** and the cyclobutane **V**, namely **TS-V**, could be localized on the potential energy surface. Analysis of the geometrical parameters of **TS-V** revealed that the disruptive **H₃-C_{iPr}** bond was elongated by only 18 % compared to that of **I** (1.29 Å vs 1.09 Å) and that the forming **C_I-H** bond was also elongated by 18 % compared to the **C_I-H** bond of **V** (1.32 Å vs 1.11 Å). In parallel, the forming **C_I-C_{iPr}** bond was moderately elongated by 37 % compared to that of cyclobutane **V** (2.12 Å vs 1.54 Å). As a consequence of the **C_I-C_{iPr}** interaction, both **C_I** and **N_I** atoms are strongly pyramidalized ($\Sigma N_I = 332^\circ$ and $\Sigma C_I = 333^\circ$, respectively), and the **C_I-N_I** bond length of 1.43 Å is characteristic of a C-N single bond (1.42 Å). Therefore, **TS-V** can thus be considered as a late transition state. Overall, these data suggest that this insertion reaction is a concerted but asynchronous process, where the C-C formation event precedes the proton transfer.

The insertion of carbene **I** into **CHiPr** was next investigated. In contrast to **CH₃iPr** insertion, insertion of carbene **I** into **CHiPr** involves a stepwise process, where the **CHiPr** proton of **I** is transferred to the carbene center (**C_I**) with a high activation barrier of 39.4 kcal.mol⁻¹ for the first step (**I**→**VI**); the resulting azomethine ylide intermediate **VI** then undergoes a ring closure in the second step (**VI**→**VII**) with a very low activation barrier of 5.1 kcal.mol⁻¹. Two transition states, connecting **I** and **VI**, namely **TS-VI**, and **VI** and **VII**, namely **TS-VII**, could be located on the PES. .

Analysis of **TS-VI** allows some insight into the nature of this proton transfer step to be gained. The breaking **CHiPr** bond in **TS-VI** is strongly elongated by 48 % compared to that of the starting carbene **I** (1.62 Å vs 1.09 Å), while the forming **C_I-H** bond is only moderately elongated (21 %), compared to the **C_I-H** of compound **VI** (1.30 Å vs 1.09 Å). In parallel, the **C_I-C_{iPr}** bond distance remains long (2.26 Å) in comparison with that of the azomethine ylide **VI** (2.56 Å). Besides, the short **C_I-N_I** bond distance of 1.30 Å, the sum of angles around **C_I** and **N_I** of 360° attest of the absence of any re-hybridization of those atoms between **I** and **VI**. From those data, it can be concluded that **TS-VI** is a late transition state.

Chapter II: Selective dimerization of monoaminoarylcarbenes by deprotonation of aldiminium salts

The cyclopropane final compound is formed in the last step of this process by ring closure of the zwitterionic azomethine ylide **VI**. This step proceeds via **TS-VII**, where the forming C_I-C_{iPr} is strongly elongated by 40 % compared to that of the final compound **VII** (2.12 Å vs 1.51 Å). The long C_I-N_I bond distance of 1.43 Å (characteristic of a single C-N bond) associated with the pyramidal N_I atom ($\Sigma N_I = 339^\circ$) and the planar C_I atom ($\Sigma C_I = 360^\circ$) suggest a zwitterionic structure for **TS-VII**, where both the negative and positive charges are localized at C_{iPr} and C_I, respectively.

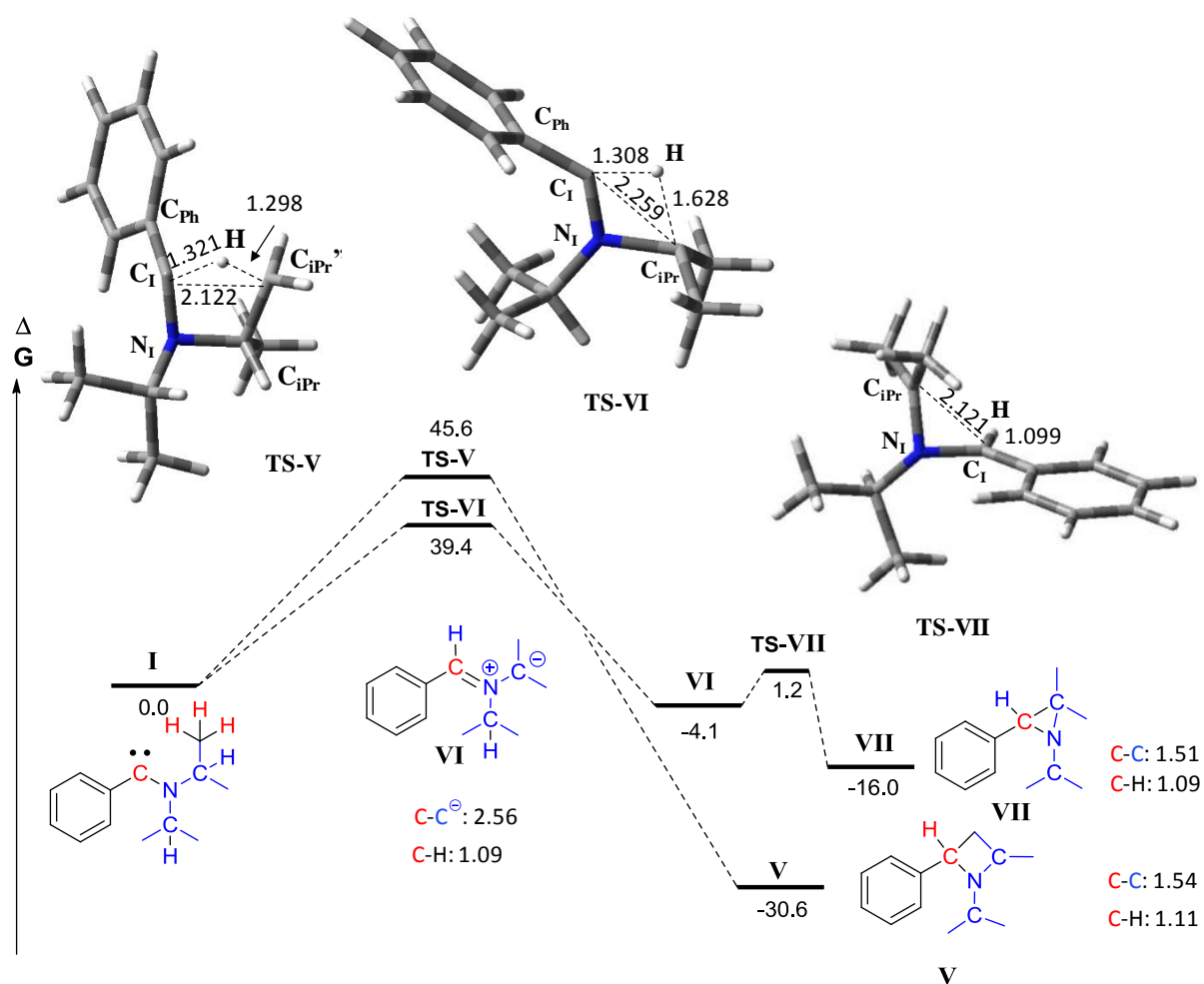


Figure II.26. Energy profiles computed for the CH insertion reactions of diisopropylaminoarylcarbene at the B3LYP/def2-SVP level of theory. Gibbs free energies in kcal.mol⁻¹ and bond distance in Å.

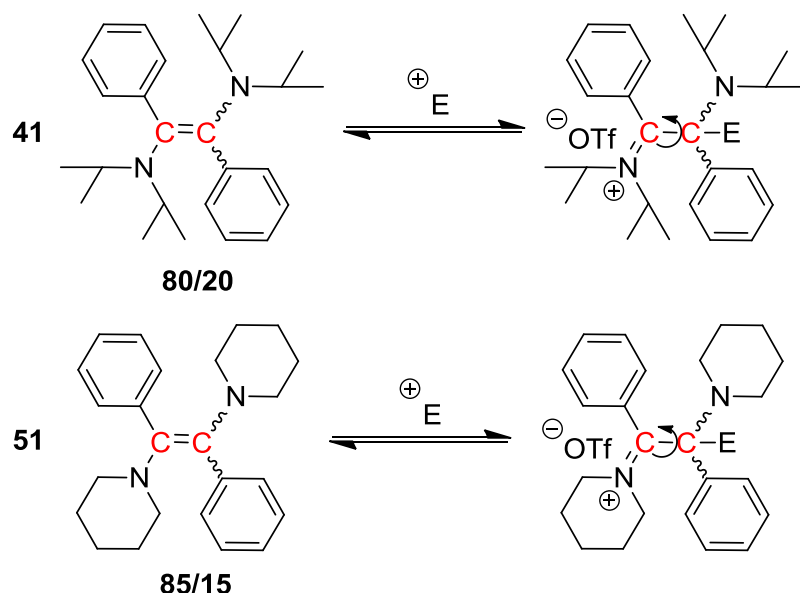
In summary, investigation of the dimerization and CH-insertion reactions of aminoarylcarbenes **I** by DFT calculations allowed rationalizing experimental data, especially concerning the high selectivity of the desired dimerization reaction, as well as its corresponding

Chapter II: Selective dimerization of monoaminoarylcarbenes by deprotonation of aldiminium salts

mechanism. In particular, dimerization of **I** into the corresponding diaminoalkenes appeared to be kinetically favored over intramolecular CH insertion reactions.

II.5 Isomerization of diaminoalkenes

During the synthesis of diaminoalkene **41**, various ratio E/Z of isomers were achieved depending on the base employed. After purification of **41**, however, the ratio was always found equal to 80/20 in favor of the E-isomer (even if 100% of the E-isomer could form at the early stage of the reaction; see II.3.3). It thus appeared that one type of isomer could be quantitatively isomerized to the other. As highlighted in the previous section, dimerization of our aminoaryl carbenes involves a protonated intermediate that can rotate around the C₁-C₂ axis, which is believed to be the cause of the change in the E/Z ratio. We thus attempted to isomerize the diaminoalkene-type dimer **41** in presence of weak acid. We indeed hypothesized that the acid species could reversibly add onto the amino-containing double bond, enabling its free rotation as a means to change the E/Z ratio which at his equilibrium is 80/20 E/Z (Scheme II.29).



Scheme II.29. Proposed mechanism for the isomerization of dimer **41** and **51** via addition of catalytic amounts of an electrophile.

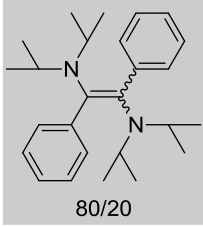
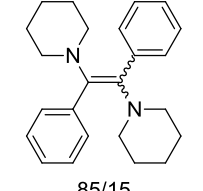
However, no change in the E/Z ratio was observed by ¹H NMR spectroscopy, even upon heating the reaction mixture. In the field of photochemistry, isomerization of stilbene has been

Chapter II: Selective dimerization of monoaminoarylcabenenes by deprotonation of aldiminium salts

reported by irradiation under different conditions.⁵²⁻⁵⁴ Using similar conditions, irradiation of dimers **41** and **51** was attempted to change the 80/20 ratio. A solution of **41** and **51** was irradiated at three different wavelengths in THF. Irradiation for 24h at 256nm and 325 nm did not enable any isomerization of **41** and **51**. Using a solar lamp (200 nm to 800 nm), however, some isomerization of **51** was observed, changing the E/Z ratio, from 85/15 to 58/42. Use of pentane as an apolar solvent allowed increasing further the isomerization to 50/50. These preliminary experiments thus established a standard procedure for the further attempts. Use of catalytic amounts of electrophilic species under irradiation was also evaluated. For instance, addition of HMDS, which was a side product of the deprotonation process of iminium salt **34** to form dimer **41**, did not lead to any isomerization of **41**. In contrast, HMDS enabled to isomerize **51** giving a 57/43 E/Z ratio. Addition of the phosphazanium side product issued from the deprotonation of iminium salt **34** by the P₄-*t*Bu phosphazene base led to an absence of isomerization for **41**. In contrast, its use with **51** gave the best result with a ratio of 36/64 E/Z. Addition of the more electrophilic carbon disulfide led to the observation of isomerization for both dimers **41** and **51**. In the latter case, a E/Z ratio of 58/42 was achieved, while for **41** the ratio changed to only 42/58. Finally, when specific catalyst 2-iodo-9-fluorenone was used to transform the E- to the Z-isomer, no reaction took place for any dimer (Table II.3).⁵³ These results show that for diisopropyl dimer **41**, which is the more sterically hindered, the isomerization is more difficult to achieve, requiring stronger electrophiles. However, for dimer **51**, which readily isomerizes in absence of any electrophile, the presence of electrophilic species enables to increase the E/Z ratio in favor of the Z-isomer, but is not correlated to their electrophilicity. It is worth mentioning that the electrophilicity of the compounds has to be weak enough to favor their reversible addition on the double bond. In presence of a stronger acid, indeed, protonation on the nitrogen atoms proves irreversible (see next chapter). Therefore, further investigation on the selection of an electrophile which has the good properties to be reversibly added on the diaminoalkene and allows an isomerization to a better E/Z ratio has to be investigated more scarcely.

Table II.3. Ratio E/Z of dimers by irradiation with a solar lamp for 24h in pentane

Chapter II: Selective dimerization of monoaminoarylcarbenes by deprotonation of aldiminium salts

Dimer Ratio E/Z	Pure dimer	P ₄ -t-BuH ⁺	HMDS	CS ₂	Cata 1 mol% (2-iodo-9-fluorenone)
 80/20	80/20	80/20	80/20	58/42	80/20
 85/15	50/50	36/64	57/43	42/58	85/15

II.6 Conclusion

This chapter describes the synthesis of novel aminoarylcarbene-type precursors and their corresponding diaminoalkenes generated by selective dimerization. Only a few aminoarylcarbenes had been previously isolated before, and their dimerization had been only reported for compounds where the carbene center was not sufficiently protected, *i.e.* compounds with no substituents in the ortho-position in the aryl moiety. While different synthetic routes exist, they usually involve either rather sophisticated precursors or toxic reagents.^{13,14} Instead, here we developed a method based on the deprotonation of aldiminium salts in presence of a strong base. The precursors used for this route were first designed by methylation of an imine. However, the presence of the methyl group strongly influenced the reactivity of the precursor. Upon deprotonation, indeed the product was found to isomerize into an ylide showing different reactivity compared to the carbene.⁶ To avoid this problem, iminium salts featuring two bulky substituents on the nitrogen atoms were purposely synthesized, the deprotonation of which was studied using a strong base at low temperature. A mixture of the E- and the Z-isomers with a higher proportion of the former compound could thus be achieved. This reaction was further investigated computationally through DFT calculations, which enabled to shed light on the dimerization involving aminoarylcarbenes. Although carbene dimerization was proposed to occur following a non-least motion pathway, involving the attack of the occupied in-plane σ orbital of one carbene onto the out-of-plane p_{π} orbital of a second carbene,⁵⁵⁻⁵⁷ such a mechanism was evidenced in our case. Instead, both dimerization and the reverse process appeared to be most generally catalyzed by electrophilic impurities.^{58,59,26,60}

Chapter II: Selective dimerization of monoaminoarylcarbenes by deprotonation of aldiminium salts

From an experimental viewpoint, the first intermediate obtained by addition of an acyclic aminoarylcarbene to its iminium salt precursor could be successfully isolated, crystallized and characterized. This is an important result as it establishes that the dimerization mechanism involves a proton-catalyzed pathway. The latter mechanism was supported by DFT calculations, which also showed that the E-isomer was the thermodynamic product.

Further attempts to trap the putatively *in situ* generated aminoarylcarbenes using various reagents, including CS₂, and S₈, silanes, isocyanide or methyl acrylate met with very limited success. In most cases, the dimerization product, *i.e.* the diaminoalkene, was observed instead. This could be explained by lesser energetic barrier required for the self-dimerization, which was confirmed by computational studies. In other words, the dimerization process proved very selective relatively to many other addition reactions. However, some reactions such as the addition on CS₂ and S₈ could be successfully achieved, demonstrating that aminoarylcarbenes could indeed be *in situ* generated upon deprotonation of their parent iminium salts.

The dimerization reaction process, and relatedly, the E/Z ratio, was found to depend on the base. For instance, metal alkoxides did not lead to any dimer, but instead to the formation of a stoichiometric adduct at low temperature. The latter finding appears interesting as it could be exploited to protect/mask aminoaryl carbenes. One could expect, indeed, that dimerization could be triggered upon heating such an adduct, *i.e.* without the need for any metallic base. However, this method would require further optimization.

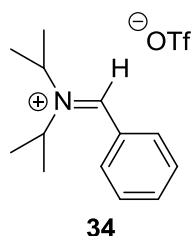
Finally, the configuration of the resulting dimers could be manipulated by isomerization, namely, using catalytic amounts of an electrophile under UV irradiation. At this stage of our study, however, full conversion from one isomer to the other was not achievable, requiring also here more investigations.

This dimerization strategy developed in this chapter was further translated to purposely designed bifunctional iminium salt precursors. As described in the next chapter, this allowed us to achieve unprecedented amino-containing poly(*para*-phenylene vinylene)s (*N*-PPV) by a step-growth polymerization process.

II.7 Experimental Part

For general information, see the corresponding section at the end of the manuscript.

Fluorene precursor was synthesized following the procedure of Fang²² and Ball.²³



Benzylidenediisopropyliminium triflate 34:

Alder's route: To a stirred solution of diisopropylformamide (1.38 mL, 9.5 mmol) in dry ether (50 mL) cooled at -78°C was added phenyllithium (1.9M, 7.9 mL) dropwise and the resulting mixture was stirred at this temperature for 30 min then at room temperature for 1h. Then, to the reaction mixture cooled at -78°C was added trifluoromethanesulfonic anhydride and the mixture was stirred for 1h at this temperature then for 2h at room temperature. The precipitated solid was filtered under argon and washed with dry ether (3x5 mL) and THF (3x5mL) and dried under vacuum to obtain the compound **34**, as white crystals (2.1 g, 70%).

Schroth's route: To a stirred solution of benzaldehyde (1 mL, 10 mmol) and 1-(trimethylsilyl) diisopropylamine (1.45 g, 10 mmol) in dry ether (50 mL), TMSOTf (1.8 mL, 10 mmol) was added dropwise at room temperature and the resulting mixture was stirred at the same temperature for 6h under inert atmosphere. The precipitated solid was filtered under inert atmosphere and dried under vacuum to obtain the compound **34** as white crystals (2.32 g, 70%).

^1H NMR (DMSO-*d*₆, 400 MHz): δ 1.49 (d, 6H, $^3J = 6.6$ Hz), 1.54 (d, 6H, $^3J = 6.6$ Hz), 4.59 (m, 1H), 4.95 (m, 1H), 7.73 (t, 2H, $^3J = 6.6$ Hz), 7.81 (t, 1H, $^3J = 6.6$ Hz), 7.85 (d, 2H, $^3J = 6.6$ Hz), 9.51 (s, 1H);

^{13}C NMR (DMSO-*d*₆, 101 MHz): δ 19.16, 23.33, 54.50, 56.98, 120.70 (q, $^1J_{\text{C-F}} = 322.6$ Hz), 127.49, 29.38, 131.36, 134.71, 171.31;

^{19}F NMR (DMSO-*d*₆, 377 MHz): δ -77.76 ;

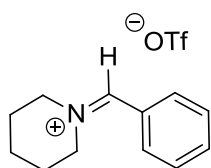
IR (ATR) ν_{max} (cm^{-1}): 2990, 2947, 2885, 2116, 1650, 1600, 1470, 1303, 1275, 1226, 1158, 1033, 972, 832;

HRMS (TOFMS, m/z): Calcd. For $\text{C}_{12}\text{H}_{20}\text{N}^+$ 190,1596, found 190.1607;

λ_{max} (ACN): 278 nm;

Chapter II: Selective dimerization of monoaminoarylcarbenes by deprotonation of aldiminium salts

Pf: 155-160°C.



35

Benzylidenepiperidineiminium triflate 35:

To a stirred solution of benzaldehyde (1.0 mL, 10 mmol) and 1-(trimethylsilyl)piperidine (1.57 g, 10 mmol) in dry ether (50 mL), TMSOTf (1.8 mL, 10 mmol) was added dropwise at room temperature and the resulting mixture was stirred at the same temperature for 6h under inert atmosphere. The precipitated solid was filtered under inert atmosphere and dried under vacuum to obtain the compound **35** as yellow crystals (2.62 g, 80%).

^1H NMR (CDCl_3 , 400 MHz): δ 1.89 (m, 4H), 2.04 (m, 2H), 4.23 (t, 2H, $^3J = 5.6$ Hz), 4.29 (t, 2H, $^3J = 5.6$ Hz), 7.57 (t, 2H, $^3J = 7.6$ Hz), 7.67 (t, 1H, $^3J = 7.6$ Hz), 7.78 (t, 2H, $^3J = 7.6$ Hz), 9.34 (s, 1H);

^{13}C NMR (CDCl_3 , 101 MHz): δ 22.26, 26.43, 26.58, 52.63, 61.49, 120.67 (q, $^1J_{\text{C-F}} = 322.3$ Hz), 126.69, 129.51, 131.19, 134.84, 171.21;

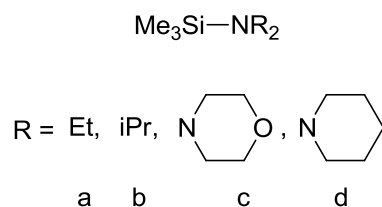
^{19}F NMR (CDCl_3 , 377 MHz): δ -78.38.

IR (ATR) ν_{max} (cm^{-1}): 2962, 2942, 2873, 2115, 1663, 1600, 1400, 1303, 1275, 1226, 1158, 1032, 972, 832;

HRMS (TOFMS, m/z): Calcd. For $\text{C}_{12}\text{H}_{16}\text{N}^+$ 174.1283, found 174,1281;

λ_{max} (ACN): 272 nm,

Pf: 57-62°C.



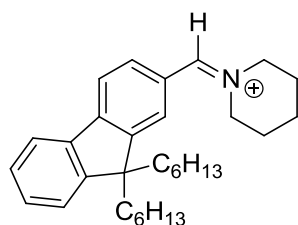
Aminosilanes:

To a THF solution (6 mL) of an amine **a-d** (6.0 mmol) was added $n\text{BuLi}$ (2.5 M solution in n -hexane, 2.4 mL, 6.0 mmol) at 0°C. The mixture was stirred at 0°C for 30 min then to this mixture was added chlorotrimethylsilane (6.0 mmol), and the resulting mixture was stirred at room temperature overnight before the removal of the solvent in vacuum. The residue was

Chapter II: Selective dimerization of monoaminoarylcarbenes by deprotonation of aldiminium salts

treated with dry *n*-hexane (20 mL), and the insoluble materials were filtered through a Celite pad. Evaporation of the solvent gave an aminosilane of sufficient purity to be used directly.

Yield: **34.b**: 15%, **35.a**: 26%, **35.b**: 10%, **35.c**: 10%, **35.d**: 25%.



9,9'-dihexyl-9H-fluorenylidene-piperidinium triflate 36:

36

To a stirred solution of fluorene-aldehyde (1.81 g, 5 mmol) and 1-(trimethylsilyl)piperidine (0.79 g, 5 mmol) in dry ether (25 mL), TMSOTf (0.9 mL, 5 mmol) was added dropwise at room temperature and the resulting mixture was stirred at the same temperature for 14h under inert atmosphere. After the solvent was removed under reduced pressure, the resulting mixture was washed with dry cyclohexane (3x20 mL). The resulting solid was filtered under inert atmosphere to obtain the desired compound **36** as a purple solid (2.25 g, 78%).

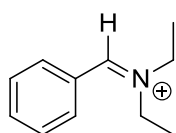
^1H NMR (THF- d_8 , 400 MHz): δ 0.60 (m, 4H), 0.73 (t, 6H, $^3J = 7.2$ Hz), 1.06 (m, 12H), 1.87 (m, 2H), 1.97 (m, 2H), 2.06 (m, 4H), 2.17 (m, 2H), 4.33 (dt, 4H, $^3J = 5.8$ Hz), 7.42 (m, 3H), 7.86 (d, 1H, $^3J = 7.8$ Hz), 7.97 (m, 2H), 8.11 (s, 1H), 9.46 (s, 1H);

^{13}C NMR (THF- d_8 , 101 MHz): δ 14.30, 23.39, 24.72, 25.31, 27.20, 27.50, 27.75, 30.45, 32.42, 40.64, 53.35, 56.57, 61.95, 121.21, 122.22, 122.29 (q, $^1J_{\text{C-F}} = 321.8$ Hz), 124.07, 126.82, 128.17, 128.58, 130.26, 121.82, 140.26, 148.76, 152.51, 153.23, 171.88;

^{19}F NMR (THF- d_8 , 377 MHz): δ -79.00.

IR (ATR) ν_{max} (cm^{-1}): 2960, 2932, 2858, 2112, 1654, 1603, 1448, 1273, 1223, 1155.

Compounds 37-39 were synthesized following the same protocol as **34**.

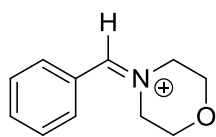


Benzylidenediethyliminium triflate 37:

37

Yield: 74%. ^1H NMR (DMSO- d_6 , 400 MHz): δ 1.44-1.50 (m, 6H), 4.05-4.11 (m, 4H), 7.72-7.76 (m, 2H), 7.82-7.86 (m, 1H), 7.90-7.92 (m, 2H), 9.24 (s, 1H)

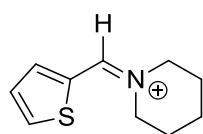
Chapter II: Selective dimerization of monoaminoarylcarbenes by deprotonation of aldiminium salts



Benzylidenemorpholineiminium triflate 38:

38

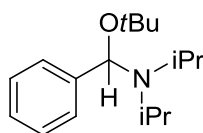
Yield: 70%. $^1\text{H NMR}$ (DMSO-d_6 , 400 MHz): δ 3.88-4.04 (dt, 4H, $J = 52.3$ and 5.0 Hz), 4.19-4.29 (dt, 4H, $J = 31.1$ and 5.0 Hz), 7.70-7.74 (m, 2H), 7.80-7.84 (m, 1H), 7.85-7.87 (m, 2H), 9.40 (s, 1H)



Thiophenyldenepiperidineiminium triflate 39:

39

Yield: 73%. $^1\text{H NMR}$ (DMSO-d_6 , 400 MHz): δ 1.73-1.77 (m, 2H), 1.88-1.95 (m, 4H), 4.04-4.19 (dt, 4H, $J = 48.6$ and 5.8 Hz), 7.54-7.57 (dd, 1H, $J = 5.0$ and 3.9 Hz), 8.25-8.27 (dd, 1H, $J = 4.0$ and 1.4 Hz), 8.65-8.67 (dt, 1H, $J = 4.9$ Hz and 1.1 Hz), 9.28 (s, 1H).



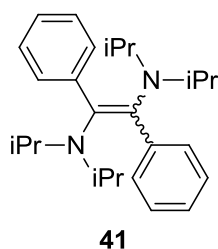
1-phenyl-1-tert-butoxy-1-diisopropylamine-methane 40:

40

To a mixture of diisopropyliminium **34** (0.210 g, 0.62mmol) and solid *t*-BuOK (0.077 g, 0.68 mmol) was added dropwise THF at -78°C . The reaction mixture was stirred at this temperature until it reached room temperature overnight. The reaction was washed with dry ether, then the solvent was evaporated under reduced pressure to give compound **40** (0.138 g, 85%) as a yellow solid.

Yield: 85%. $^1\text{H NMR}$ (CDCl_3 , 400 MHz): δ 0.85-1.09 (d, 12H, $J = 6.7$ Hz), 1.06 (s, 9H), 1.07-1.09 (d, 6H, $J = 6.7$ Hz), 3.14-3.24 (hept, 2H, $J = 6.7$ Hz), 5.40 (s, 1H), 7.08-7.10 (m, 1H), 7.15-7.19 (m, 1H), 7.32-7.34 (m, 1H).

Chapter II: Selective dimerization of monoaminoarylcabenenes by deprotonation of aldiminium salts



1,2-bis(diisopropylamino)stilbene 41:

With P₄-^tBu base:

To a stirred solution of **34** (0.1 g, 0.3 mmol) in THF (6 mL) cooled at -78°C, P₄-^tBu base (0.38 mL, 0.3 mmol, 0.8M in hexanes) was added and the resulting mixture was stirred at this temperature for 1h followed by 24h at room temperature. The solvent was evaporated under reduced pressure and the reaction mixture was diluted with pentane (20 mL) and passed through a short column of basic alumina. The final compound **41** (0.034 g, 60%) was obtained as a yellow solid. Single crystals were grown from the slow diffusion of a pentane solution of **41** at -20°C.

With LiHMDS base:

34 (0.1 g, 0.3 mmol) and LiHMDS (50 mg, 0.3 mmol) were dissolved in cold THF (6 mL, -78°C). The resulting mixture was stirred at this temperature for 1h followed by 24h at room temperature. The solvent was evaporated under reduced pressure and the reaction mixture was diluted with pentane (20 mL) and passed through a short column of basic alumina. The final compound **41** (0.034 g, 60%) was obtained as a yellow solid. Single crystals were grown from the slow diffusion of a pentane solution of **41** at -20°C.

¹H NMR (THF-*d*₈, 400 MHz): [*E*-isomer] δ 0.77 (d, 24H, ³*J* = 6.5 Hz), 3.25 (m, 4H), 7.16 (m, 2H), 7.25 (m, 4H), 7.51 (m, 4H) ; [*Z*-isomer] δ 1.20 (d, ³*J* = 6.8 Hz, 24H), 3.93 (m, 4H), 6.81 (m, 4H), 6.86 (m, 4H), 7.09 (m, 4H);

¹³C NMR (THF-*d*₈, 101 MHz): [*E*-isomer] δ 23.48, 52.04, 126.82, 127.97, 132.16, 140.68, 145.59; [*Z*-isomer] δ 24.33, 48.31, 125.52, 127.04, 133.68, 135.06, 144.45;

IR (ATR) ν_{max} (cm⁻¹): 3054, 3018, 2964, 2928, 2866, 1595, 1465, 1441, 1377, 1219, 1193, 1113, 753, 641;

HRMS (TOFMS): Calcd. for C₂₆H₃₈N₂ 378.3029, found 378.3030;

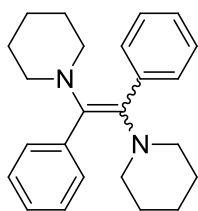
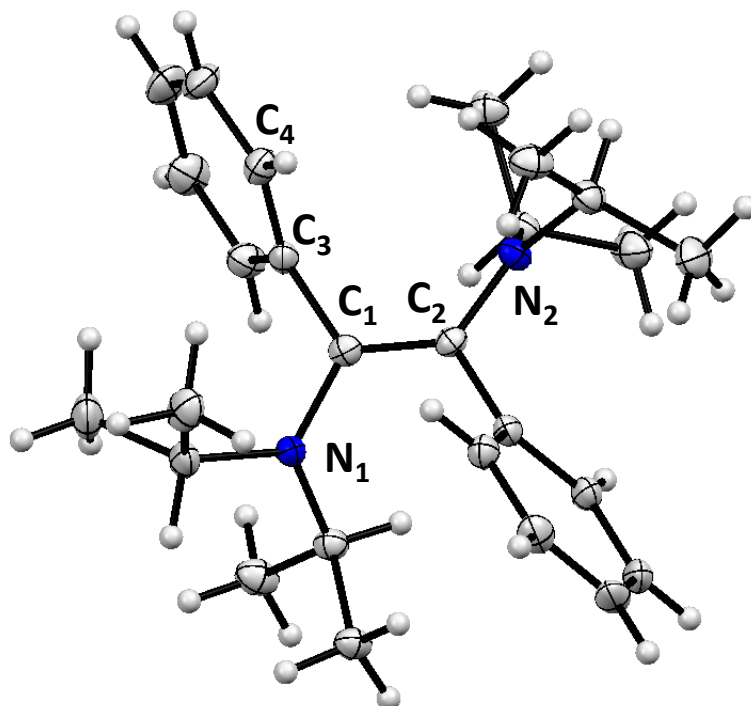
λ_{max} (CHCl₃): 245, 388 nm, Pf: 47.22°C.

Crystal data :

Chapter II: Selective dimerization of monoaminoarylcarbenes by deprotonation of aldiminium salts

Identification code	1,2-bis(diisopropylamino)stillbene
Empirical formula	C ₂₆ H ₃₈ N ₂
Formula weight	378.58
Temperature/K	373(2)
Crystal system	monoclinic
Space group	P2 ₁ /c
a/Å	14.677(3)
b/Å	17.737(2)
c/Å	19.322(3)
α/°	90
β/°	112.105(4)
γ/°	90
Volume/Å ³	4660.0(13)
Z	8
ρ _{calc} /cm ³	1.079
μ/mm ⁻¹	0.465
F(000)	1664.0
Crystal size/mm ³	0.200 × 0.200 × 0.200
Radiation	CuKα (λ = 1.54178)
2θ range for data collection/°	6.5 to 136.48
Index ranges	-17 ≤ h ≤ 17, -21 ≤ k ≤ 20, -23 ≤ l ≤ 23
Reflections collected	34019
Independent reflections	8527 [R _{int} = 0.0120, R _{sigma} = 0.0112]
Data/restraints/parameters	8527/0/521
Goodness-of-fit on F ²	1.252
Final R indexes [I ≥ 2σ (I)]	R ₁ = 0.0599, wR ₂ = 0.1524
Final R indexes [all data]	R ₁ = 0.0637, wR ₂ = 0.1537
Largest diff. peak/hole / e Å ⁻³	0.27/-0.28

Chapter II: Selective dimerization of monoaminoarylcarbenes by deprotonation of aldiminium salts



1,2-bis(piperidine)stilbene 42:

42

To a stirred solution of **35** (0.32 g, 1 mmol) in THF (3 mL) cooled at -78°C , $\text{P}_4\text{-}^t\text{Bu}$ base (1.38 mL, 1.1 mmol, 0.8M in hexanes) was added and the resulting mixture was stirred at this temperature for 1h followed by 24h at room temperature. The solvent was evaporated under reduced pressure and the reaction mixture was diluted with pentane (20 mL) and passed through a short column of basic alumina. The final compound **42** (0.108 g, 62%) was obtained as a yellow solid. Single crystals were grown from the slow diffusion of a pentane solution of **42** at -20°C .

^1H NMR (THF- d_8 , 400 MHz): [*E*-isomer] δ 1.36 (s, 12H), 2.38 (br, 8H), 7.16 (m, 2H), 7.31 (m, 8H); [*Z*-isomer] δ 1.60 (m, 12H), 3.00 (m, 8H), 6.93 (m, 6H), 7.06 (m, 4H);

^{13}C NMR (THF- d_8 , 101 MHz): [*E*-isomer] δ 25.16, 27.83, 53.56, 127.06, 128.31, 130.33, 137.30, 142.92; [*Z*-isomer] δ 25.46, 27.67, 52.63, 126.14, 127.68, 131.93, 138.54, 141.13;

Chapter II: Selective dimerization of monoaminoarylcabenenes by deprotonation of aldiminium salts

IR (ATR) ν_{\max} (cm⁻¹): 3054, 3018, 2929, 2850, 2812, 1594, 1489, 1442, 1378, 1228, 1194, 1112, 755, 670;

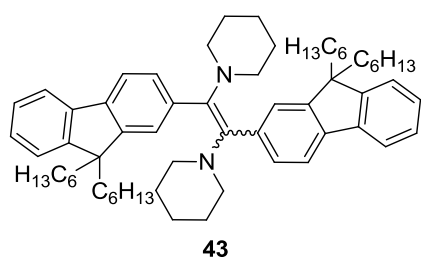
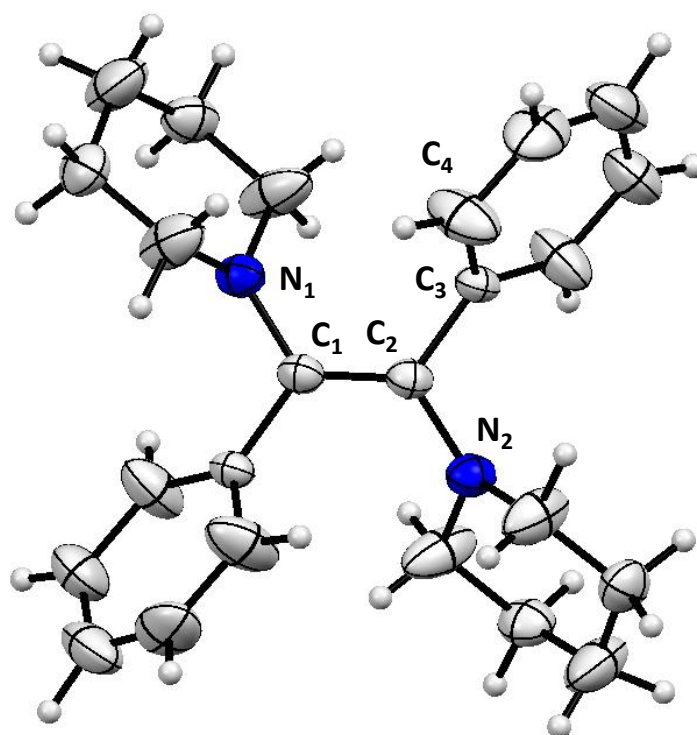
HRMS (TOFMS): Calcd. for C₂₄H₃₀N₂ 346.2403, found 346.2407;

λ_{\max} (CHCl₃): 245, 395 nm, Pf: 101°C.

Crystal data:

Identification code	1,2-bis(piperidine)stillbene
Empirical formula	C ₁₂ H ₁₅ N
Formula weight	173.25
Temperature/K	153(2)
Crystal system	monoclinic
Space group	C2/c
a/Å	18.199(8)
b/Å	5.945(3)
c/Å	18.968(13)
α /°	90
β /°	97.767(18)
γ /°	90
Volume/Å ³	2033.4(19)
Z	8
ρ_{calc} /g/cm ³	1.132
μ /mm ⁻¹	0.496
F(000)	752.0
Crystal size/mm ³	0.060 × 0.040 × 0.010
Radiation	CuK α (λ = 1.54187)
2 Θ range for data collection/°	15.696 to 136.384
Index ranges	-21 ≤ h ≤ 21, -7 ≤ k ≤ 7, -18 ≤ l ≤ 22
Reflections collected	5658
Independent reflections	1850 [R _{int} = 0.0319, R _{sigma} = 0.0337]
Data/restraints/parameters	1850/0/118
Goodness-of-fit on F ²	1.097
Final R indexes [I ≥ 2 σ (I)]	R ₁ = 0.0771, wR ₂ = 0.1858
Final R indexes [all data]	R ₁ = 0.0963, wR ₂ = 0.1954
Largest diff. peak/hole / e Å ⁻³	0.41/-0.41

Chapter II: Selective dimerization of monoaminoarylcarbenes by deprotonation of aldiminium salts



1,2-bis(9,9-dihexyl-9H-fluorene)-1,2-bis(piperidine)ethene 43:

To a stirred solution of **36** (1.16 g, 2 mmol) in THF (10 mL) cooled at -78°C , $\text{P}_4\text{-tBu}$ base (3 mL, 2.4 mmol, 0.8M in hexanes) was added and the resulting mixture was stirred at this temperature for 1h followed by 24h at room temperature. The solvent was evaporated under reduced pressure and the reaction mixture was diluted with pentane (20 mL) and passed through a short column of basic alumina. The final compound **43** (0.48 g, 56%) was obtained as an orange solid. Single crystals were grown from the slow diffusion of a pentane solution of **43** at -20°C .

^1H NMR (THF- d_8 , 400 MHz): [*E*-isomer] δ 0.57 (m, 20H+4H*), 0.95 (m, 24H+6H*), 1.30 (s, 12H), 1.94 (m, 8H), 2.39 (s, 8H), 7.15 (m, 5H), 7.25 (m, 5H+1H*), 7.59 (m, 4H); [*Z*-isomer] δ 1.52 (m, 12H), 1.74 (m, 8H), 2.98 (br, 8H), 6.99 (m, 2H), 7.05 (m, 4H), 7.39 (m, 2H);

^{13}C NMR (THF- d_8 , 101 MHz): [*E*-isomer] δ 14.35, 23.40, 24.74, 25.45, 28.24, 30.70, 32.60, 41.63, 54.00, 55.63, 119.83, 120.20, 123.43, 124.51, 127.45, 127.54, 129.55, 137.44, 140.94,

Chapter II: Selective dimerization of monoaminoarylcabenenes by deprotonation of aldiminium salts

142.43, 142.57, 151.03, 151.46; [Z-isomer] δ 14.39, 24.64, 25.71, 25.84, 27.96, 30.66, 32.55, 41.42, 52.82, 55.41, 119.29, 120.10, 123.26, 126.27, 127.20, 127.33, 131.22, 138.95, 139.90, 140.82, 142.27, 150.47, 151.50;

IR (ATR) ν_{\max} (cm^{-1}): 2930, 2848, 1457, 1371, 1122;

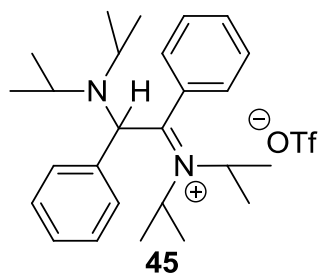
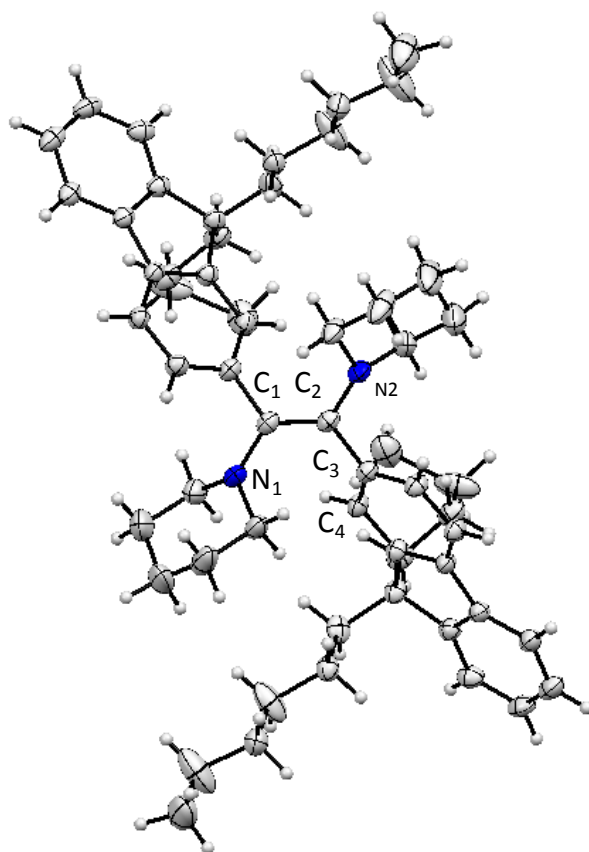
HRMS (TOFMS): Calcd. for $\text{C}_{62}\text{H}_{86}\text{N}_2$ 858.6791, found 858.6810;

λ_{\max} : 237, 305, 440 nm.

Crystal data:

Identification code	1,2-bis(9,9-dihexyl-9H-fluorene)-1,2-bis(piperidine)ethene
Empirical formula	$\text{C}_{64}\text{H}_{90.5}\text{N}_2$
Formula weight	887.88
Temperature/K	100(2)
Crystal system	monoclinic
Space group	C2/c
a/Å	26.645(3)
b/Å	10.2444(12)
c/Å	22.697(3)
$\alpha/^\circ$	90
$\beta/^\circ$	114.360(3)
$\gamma/^\circ$	90
Volume/Å ³	5643.9(12)
Z	4
$\rho_{\text{calc}}/\text{g}/\text{cm}^3$	1.045
μ/mm^{-1}	0.437
F(000)	1954.0
Crystal size/mm ³	0.200 × 0.200 × 0.200
Radiation	CuK α ($\lambda = 1.54178$)
2 Θ range for data collection/ $^\circ$	7.284 to 145.562
Index ranges	-32 ≤ h ≤ 32, -12 ≤ k ≤ 9, -28 ≤ l ≤ 25
Reflections collected	21425
Independent reflections	5547 [$R_{\text{int}} = 0.0196$, $R_{\text{sigma}} = 0.0194$]
Data/restraints/parameters	5547/7/341
Goodness-of-fit on F ²	1.103
Final R indexes [$I > 2\sigma(I)$]	$R_1 = 0.0598$, $wR_2 = 0.1821$
Final R indexes [all data]	$R_1 = 0.0711$, $wR_2 = 0.1901$
Largest diff. peak/hole / e Å ⁻³	0.58/-0.48

Chapter II: Selective dimerization of monoaminoarylcabenenes by deprotonation of aldiminium salts



1-N-(diisopropylamino)-2-N-(diisopropyliminium)-1,2-diphenylethylidene triflate **45:**

To a stirred solution of **34** (0.58 g, 1 mmol) in THF (10 mL) cooled at -78°C , $\text{P}_4\text{-}^t\text{Bu}$ base (1.34 mL, 0.5 mmol, 0.8M in hexanes) was added. The resulting mixture was stirred at this temperature for 1h. Then, the reaction mixture was dried under vacuum at -40°C . After washing the crude mixture with dry Et_2O and drying it under vacuum at -40°C , intermediate **45** was successfully obtained as a light yellow powder (0.61 g, 90 %).

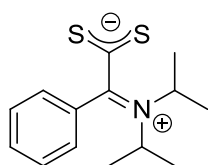
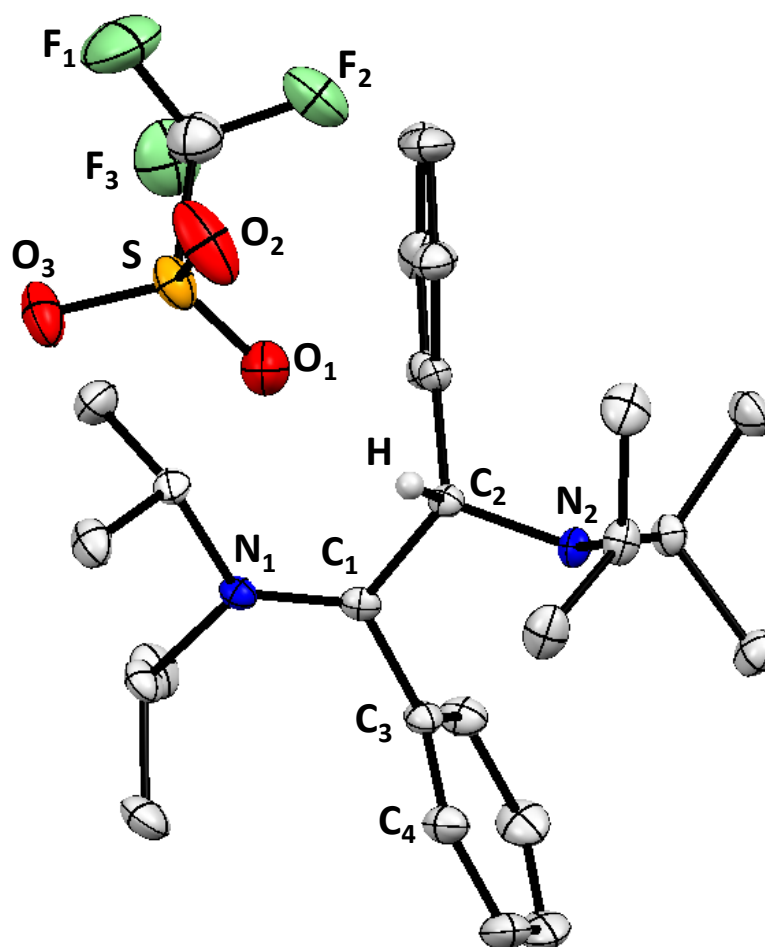
^1H NMR (CD_3CN , 400 MHz): δ 0.56-0.58 (d, 6H, $J = 6.7$ Hz), 0.70-0.71 (d, 6H, $J = 6.6$ Hz), 0.74 (m, 3H), 1.04-1.05 (d, 3H, $J = 6.77.0$ Hz), 1.18-1.20 (d, 3H, $J = 7.0$ Hz), 1.47 (m, 3H), 2.94 (hept, 2H, $J = 6.6$ Hz), 4.30-4.40 (hept, 1H, $J = 7.0$ Hz), 4.83-4.92 (hept, 1H, $J = 6.5$ Hz), 5.63 (s, 1H), 7.43-54 (m, 4H), 7.55-7.64 (m, 5H), 7.84-7.874 (m, 1H).

Chapter II: Selective dimerization of monoaminoarylcarbenes by deprotonation of aldiminium salts

Crystal data:

Identification code	1-(N,N-diisopropylamine)-2-(N,N-diisopropyliminium)-1,2-(diphenyl)ethane
Empirical formula	C ₂₇ H ₃₉ ClF ₃ N ₂ O ₃ S
Formula weight	528.66
Temperature/K	293(2)
Crystal system	monoclinic
Space group	P2 ₁ /c
a/Å	9.24720(10)
b/Å	14.32220(10)
c/Å	21.00510(10)
α/°	90
β/°	92.3560(10)
γ/°	90
Volume/Å ³	2779.57(4)
Z	4
ρ _{calc} /cm ³	1.263
μ/mm ⁻¹	1.464
F(000)	1128.0
Crystal size/mm ³	? × ? × ?
Radiation	CuKα (λ = 1.54184)
2θ range for data collection/°	7.472 to 147.932
Index ranges	-11 ≤ h ≤ 11, -17 ≤ k ≤ 17, -26 ≤ l ≤ 25
Reflections collected	19418
Independent reflections	5544 [R _{int} = 0.0116, R _{sigma} = 0.0074]
Data/restraints/parameters	5544/0/334
Goodness-of-fit on F ²	1.035
Final R indexes [I ≥ 2σ (I)]	R ₁ = 0.0392, wR ₂ = 0.0981
Final R indexes [all data]	R ₁ = 0.0394, wR ₂ = 0.0982
Largest diff. peak/hole / e Å ⁻³	0.41/-0.35

Chapter II: Selective dimerization of monoaminoarylcarbenes by deprotonation of aldiminium salts



46

Benzylidenediisopropyliminium-2-dithiocarboxylate 46:

To a stirred solution of **34** (0.146 g, 0.45 mmol) and S_8 (1.16 g, 4.5 mmol) in THF (5 mL) cooled at -78°C , LiHMDS (0.5 mL, 0.5 mmol, 1.0 M in THF) was added and the resulting mixture was stirred at this temperature for 1h then warmed to room temperature overnight. Evaporation of the solvent followed by silica-gel column chromatography (n-hexane/ethyl acetate) gave the compound **46** as a yellow powder (0.069 g, 70 %). Single crystals were grown from the slow diffusion of a solution of ether in a THF solution of **46**.

^1H NMR (THF- d_8 , 400 MHz): δ 1.32 (m, 2H), 1.44 (m, 1H), 1.52 (m, 3H), 3.50 (t, 2H, $^3J = 5.6$ Hz), 4.31 (t, 2H, $^3J = 5.6$ Hz), 7.25 (m, 5H).

Chapter II: Selective dimerization of monoaminoarylcabenenes by deprotonation of aldiminium salts

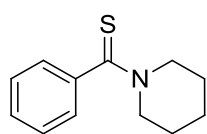
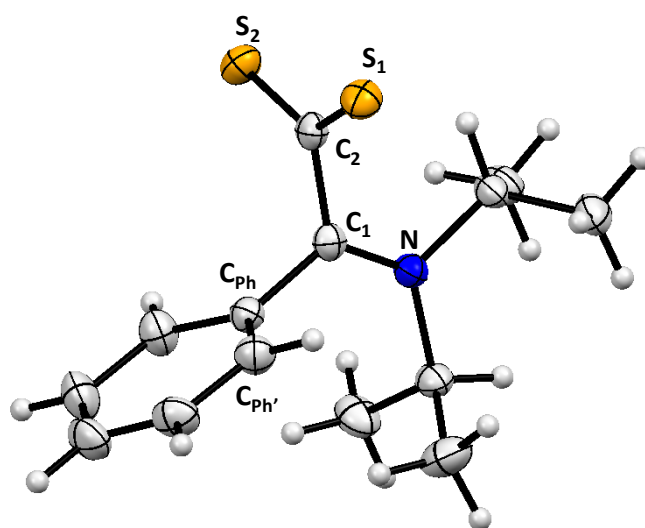
^{13}C NMR (CDCl_3 , 101 MHz): δ 199.5, 143.3, 128.3, 128.2, 125.3, 53.1, 50.5, 26.8, 25.4, 24.1.

^{13}C NMR ($\text{THF-}d_8$, 101 MHz): δ 0.90, 18.41, 22.78, 53.08, 58.61, 126.89, 129.72, 130.17, 132.12, 179.10, 238.72.

Crystal data:

Identification code	Benzylidenediisopropyliminium-2-dithiocarboxylate
Empirical formula	$\text{C}_{14}\text{H}_{19}\text{NS}_2$
Formula weight	265.42
Temperature/K	120(2)
Crystal system	triclinic
Space group	P-1
$a/\text{\AA}$	7.5701(3)
$b/\text{\AA}$	8.9559(3)
$c/\text{\AA}$	11.8979(4)
$\alpha/^\circ$	106.304(3)
$\beta/^\circ$	108.363(3)
$\gamma/^\circ$	94.556(3)
Volume/ \AA^3	722.20(5)
Z	2
$\rho_{\text{calc}}/\text{g/cm}^3$	1.221
μ/mm^{-1}	3.100
F(000)	284.0
Crystal size/ mm^3	$0.1 \times 0.01 \times 0.01$
Radiation	$\text{CuK}\alpha$ ($\lambda = 1.54178$)
2Θ range for data collection/ $^\circ$	8.274 to 136.48
Index ranges	$-7 \leq h \leq 9, -10 \leq k \leq 10, -14 \leq l \leq 14$
Reflections collected	10131
Independent reflections	2628 [$R_{\text{int}} = 0.0217, R_{\text{sigma}} = 0.0142$]
Data/restraints/parameters	2628/0/158
Goodness-of-fit on F^2	1.092
Final R indexes [$I \geq 2\sigma(I)$]	$R_1 = 0.0281, wR_2 = 0.0769$
Final R indexes [all data]	$R_1 = 0.0290, wR_2 = 0.0776$
Largest diff. peak/hole / $e \text{\AA}^{-3}$	0.28/-0.19

Chapter II: Selective dimerization of monoaminoarylcarbenes by deprotonation of aldiminium salts



Morpholino(phenyl)methanethione 47:

47

To a stirred solution of **35** (0.146 g, 0.45 mmol) and S_8 (1.16 g, 4.5 mmol) in THF (5 mL) cooled at -78°C , LiHMDS (0.5 mL, 0.5 mmol, 1.0 M in THF) was added. The reaction mixture was stirred at this temperature for 1h and warmed to room temperature overnight. The solvent was evaporated to obtain the crude reaction mixture which was purified by silica gel flash chromatography (n-hexane/ethyl acetate). Compound **47** was successfully obtained as a yellow powder (0.069 g, 70 %).

^1H NMR (THF d_8 , 400 MHz): δ 1.29-1.35 (m, 2H), 1.42-1.46 (m, 1H), 1.49-1.55 (m, 3H), 3.49-3.52 (t, 2H, $J = 5.6$ Hz), 4.30-4.32 (t, 2H, $J = 5.6$ Hz), 7.20-7.31 (m, 5H).

^{13}C NMR (CDCl $_3$, 101 MHz): δ 199.5, 143.3, 128.3, 128.2, 125.3, 53.1, 50.5, 26.8, 25.4, 24.1.

II.8 References

1. A. Igau, H. Grutzmacher, A. Baceiredo and G. Bertrand, *J. Am. Chem. Soc.*, 1988, **110**, 6463–6466.
2. A. J. Arduengo III, R. L. Harlow and M. Kline, *J. Am. Chem. Soc.*, 1991, **113**, 361–363.
3. S. Sole, *Science*, 2001, **292**, 1901–1903.
4. V. Lavallo, J. Mafhouz, Y. Canac, B. Donnadiou, W. W. Schoeller and G. Bertrand, *J. Am. Chem. Soc.*, 2004, **126**, 8670–8671.
5. M. Melaimi, R. Jazzar, M. Soleilhavoup and G. Bertrand, *Angew. Chem. Int. Ed.*, 2017, **56**, 10046–10068.
6. X. Cattoën, S. Solé, C. Pradel, H. Gornitzka, K. Miqueu, D. Bourissou and G. Bertrand, *J. Org. Chem.*, 2003, **68**, 911–914.
7. X. Cattoën, H. Gornitzka, D. Bourissou and G. Bertrand, *J. Am. Chem. Soc.*, 2004, **126**, 1342–1343.
8. S. Solé, X. Cattoën, H. Gornitzka, D. Bourissou and G. Bertrand, *Tetrahedron Lett.*, 2004, **45**, 5391–5393.
9. J. Vignolle, H. Gornitzka, B. Donnadiou, D. Bourissou and G. Bertrand, *Angew. Chem. Int. Ed.*, 2008, **47**, 2271–2274.
10. J. Vignolle, M. Asay, K. Miqueu, D. Bourissou and G. Bertrand, *Org. Lett.*, 2008, **10**, 4299–4302.
11. J. Vignolle, X. Cattoën and D. Bourissou, *Chem. Rev.*, 2009, **109**, 3333–3384.
12. S. Sole, H. Gornitzka, W. Schoeller W., D. Bourissou and G. Bertrand, *Science*, 2001, **292**, 1901–1903.
13. S. Conejero, Y. Canac, F. S. Tham and G. Bertrand, *Angew. Chem. Int. Ed.*, 2004, **43**, 4089–4093.
14. M. Otto, S. Conejero, Y. Canac, V. D. Romanenko, V. Rudzevitch and G. Bertrand, *J. Am. Chem. Soc.*, 2004, **126**, 1016–1017.
15. S. Conejero, M. Song, D. Martin, Y. Canac, M. Soleilhavoup and G. Bertrand, *Chem. – Asian J.*, 2006, **1**, 155–160.
16. K. Kobayashi and H. Konishi, *Chem. Lett.*, 1998, 87.
17. A. Ogawa, T. Nanke, N. Takami, M. Sekiguchi, N. Kambe and N. Sonoda, *Appl. Organomet. Chem.*, 1995, **9**, 461–466.
18. D. Martin, Y. Canac, V. Lavallo and G. Bertrand, *J. Am. Chem. Soc.*, 2014, **136**, 5023–5030.
19. R. W. Alder, M. E. Blake, S. Bufali, C. P. Butts, A. G. Orpen, J. Schütz and S. J. Williams, *J. Chem. Soc. Perkin 1*, 2001, **14**, 1586–1593.
20. W. Schroth, U. Jahn and D. Ströhl, *Chem. Ber.*, 1994, **127**, 2013–2022.
21. T. Morishita, H. Fukushima, H. Yoshida, J. Ohshita and A. Kunai, *J. Org. Chem.*, 2008, **73**, 5452–5457.
22. Z. Fang, R. D. Webster, M. Samoc and Y.-H. Lai, *RSC Adv.*, 2013, **3**, 17914–17917.
23. L. T. Ball, G. C. Lloyd-Jones and C. A. Russell, *J. Am. Chem. Soc.*, 2014, **136**, 254–264.
24. D. Enders, K. Breuer, G. Raabe, J. Runsink, J. H. Teles, J.-P. Melder, K. Ebel and S. Brode, *Angew. Chem. Int. Ed. Engl.*, 1995, **34**, 1021–1023.
25. D. Enders, O. Niemeier and A. Henseler, *Chem. Rev.*, 2007, **107**, 5606–5655.
26. R. W. Alder, M. E. Blake, L. Chaker, J. N. Harvey, F. Paolini and J. Schütz, *Angew. Chem. Int. Ed.*, 2004, **43**, 5896–5911.
27. M. Amini, M. Bagherzadeh, Z. Moradi-Shoeili and D. M. Boghaei, *RSC Adv.*, 2012, **2**, 12091.

Chapter II: Selective dimerization of monoaminoarylcabenenes by deprotonation of aldiminium salts

28. M. Oelgemöller, B. Brem, R. Frank, S. Schneider, D. Lenoir, N. Hertkorn, Y. Origane, P. Lemmen, J. Lex and Y. Inoue, *J Chem Soc Perkin Trans 2*, 2002, 1760–1771.
29. D. A. Bock, C. W. Lehmann and B. List, *Proc. Natl. Acad. Sci.*, 2010, **107**, 20636–20641.
30. F. H. Allen, O. Kennard, D. G. Watson, L. Brammer, A. G. Orpen and R. Taylor, *J. Chem. Soc. Perkin Trans. 2*, 1987, S1–S19.
31. M.-J. Cheng and C.-H. Hu, *Chem. Phys. Lett.*, 2000, **322**, 83–90.
32. M.-J. Cheng and C.-H. Hu, *Chem. Phys. Lett.*, 2001, **349**, 477–482.
33. C. M. Weinstein, C. D. Martin, L. Liu and G. Bertrand, *Angew. Chem. Int. Ed.*, 2014, **53**, 6550–6553.
34. D. C. Graham, K. J. Cavell and B. F. Yates, *J. Phys. Org. Chem.*, 2005, **18**, 298–309.
35. G. D. Frey, M. Song, J.-B. Bourg, B. Donnadiou, M. Soleilhavoup and G. Bertrand, *Chem. Commun.*, 2008, 4711–4713.
36. D. Bourissou, O. Guerret, F. P. Gabbaï and G. Bertrand, *Chem. Rev.*, 2000, **100**, 39–92.
37. Ai.-C. Blanrue and R. Wilhelm, 3.
38. D. Martin, N. Lassauque, B. Donnadiou and G. Bertrand, *Angew. Chem. Int. Ed.*, 2012, **51**, 6172–6175.
39. G. Kuchenbeiser, M. Soleilhavoup, B. Donnadiou and G. Bertrand, *Chem. - Asian J.*, 2009, **4**, 1745–1750.
40. L. Delaude, *Eur. J. Inorg. Chem.*, 2009, **2009**, 1681–1699.
41. L. Delaude, A. Demonceau and J. Wouters, *Eur. J. Inorg. Chem.*, 2009, **2009**, 1882–1891.
42. W. Krasuski, D. Nikolaus and M. Regitz, *Eur. J. Org. Chem.*, 1982, **1982**, 1451–1465.
43. U. Siemeling, H. Memczak, C. Bruhn, F. Vogel, F. Träger, J. E. Baio and T. Weidner, *Dalton Trans.*, 2012, **41**, 2986.
44. M. A. Schmidt and M. Movassaghi, *Tetrahedron Lett.*, 2007, **48**, 101–104.
45. H. Rodríguez, G. Gurau, J. D. Holbrey and R. D. Rogers, *Chem. Commun.*, 2011, **47**, 3222.
46. T. K. Das and A. T. Biju, *Eur. J. Org. Chem.*, 2017, **2017**, 4500–4506.
47. J. Huang, S. P. Nolan, K. B. Capps, A. Bauer and C. D. Hoff, 4.
48. T. Guntreddi, R. Vanjari and K. N. Singh, *Org. Lett.*, 2014, **16**, 3624–3627.
49. J. P. Moerdyk, D. Schilter and C. W. Bielawski, *Acc. Chem. Res.*, 2016, **49**, 1458–1468.
50. H. Song, H. Kim and E. Lee, *Angew. Chem. Int. Ed.*, 2018, **57**, 8603–8607.
51. A. J. Arduengo III, J. C. Calabrese, F. Davidson, H. V. Rasika Dias, J. R. Goerlich, R. Krafczyk, W. J. Marshall, M. Tamm and R. Schmutzler, *Helv. Chim. Acta*, 1999, **82**, 2348–2364.
52. Saltiel, J.; Sears, D. F., Jr.; Ko, D. H.; Park, K. M. *CRC Handbook of Organic Photochemistry and Photobiology; Horspool, W. M. and Song, P-S., Eds. CRC Press: Boca Raton, FL, USA, 1995; Vol. 3., .*
53. W. Cai, H. Fan, D. Ding, Y. Zhang and W. Wang, *Chem. Commun.*, 2017, **53**, 12918–12921.
54. C. Dugave and L. Demange, *Chem. Rev.*, 2003, **103**, 2475–2532.
55. J. P. Malrieu and G. Trinquier, *J. Am. Chem. Soc.*, 1989, **111**, 5916–5921.
56. H. Jacobsen and T. Ziegler, *J. Am. Chem. Soc.*, 1994, **116**, 3667–3679.
57. E. A. Carter and W. A. Goddard, *J. Phys. Chem.*, 1986, **90**, 998–1001.
58. Y. Liu, P. E. Lindner and D. M. Lemal, *J. Am. Chem. Soc.*, 1999, **121**, 10626–10627.
59. Y. Liu and D. M. Lemal, *Tetrahedron Lett.*, 2000, **41**, 599–602.
60. W. Kirmse, *Angew. Chem. Int. Ed.*, 2010, **49**, 8798–8801.

Chapter III: Synthesis of amino-PPV by metal free dimerization/polymerization of novel bis-aminoarylcaben

Chapter III: Synthesis of amino-PPV by metal free dimerization/polymerization of novel bis-aminoarylcaben

Chapter III: Synthesis of amino-PPV by metal free dimerization/polymerization of novel bis-aminoarylcarbenes

Chapter III: Synthesis of amino-PPV by metal free dimerization/polymerization of novel bis-aminoarylcarbenes

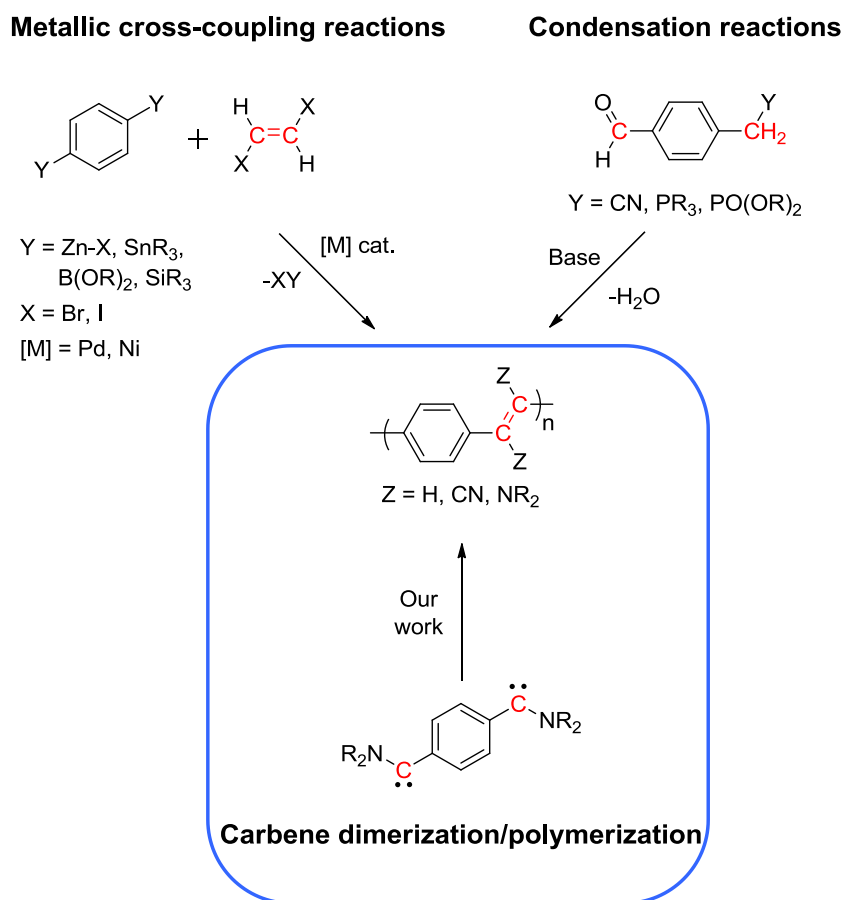
III.1. Introduction

Since 1977 and the discovery by Shirakawa that, when doped, polyacetylene displays a metallic behavior, considerable efforts have been undertaken to develop organic π -conjugated polymers.¹ In 2000, Shirakawa, together with MacDiarmid and Heeger, were awarded the Nobel prize in Chemistry for their work on “doped” polyacetylene behaving as an electronic conductor. The promising applications related to π -conjugated materials have driven the synthetic developments of semi-conducting polymers, with a special focus on the control of the C-C and C=C bonds alternation to achieve optimal performances. In most cases, related polymerization methods rely on metal-promoted cross-coupling reactions and more seldom on metal-free routes.¹⁻⁶ Alternatively, oxidative/reductive coupling *via* electrochemistry can be implemented (Scheme III.1). These methodologies have allowed accessing a wide variety of polymeric structures typically based on aryl-aryl, C \equiv C-C \equiv C and aryl-C=C linkages.

In the following introduction are discussed the synthetic strategies to specific π -conjugated polymers involving aryl-C=C repeating motifs, namely, poly(*p*-phenylenevinylene)s (PPV's). The scope and limitations of metal-based methods is discussed in section III.1.1, while metal-free alternatives are presented in section III.1.2. The self-dimerization reaction involving aminoarylcarbenes, which has been described in details in the previous chapter, has been adapted here to the synthesis of new amino-containing (*p*-phenylene vinylene) (N-PPV's). This could be achieved through the dimerization/polymerization from bis-aminoarylcarbenes used as novel monomeric building blocks, as highlighted in Scheme III.1. The discussion includes both the synthesis and the characterization of bis-iminium salts used as precursors, as well as the properties of the resulting N-PPV's. Finally, as both dimers and polymers feature two amino functions in alpha-position of the C=C double bond, they could be readily modified, for instance by protonation or methylation as a means to vary their physicochemical properties. This strategy based on the post-chemical modification of the amino groups will be discussed in the last section.

Chapter III: Synthesis of amino-PPV by metal free dimerization/polymerization of novel bis-aminoarylcarbenes

Main methodologies to access PPV-like polymers



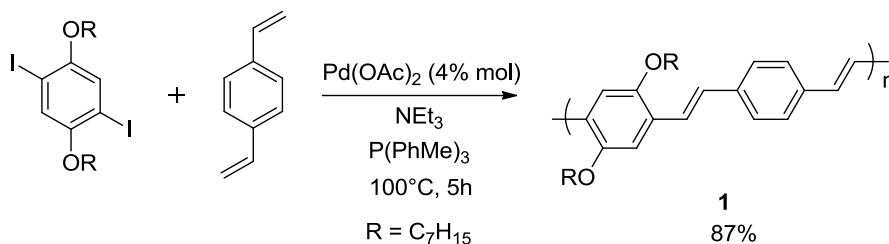
Scheme III.1. Main synthetic routes to PPV-like polymers using organometallic cross-coupling, metal-free polycondensation reactions and lastly the novel methodology developed in this work based on the dimerization/polymerization of bis-aminoarylcarbenes.

III.1.1 PPV synthesized from metal-based strategies

PPV-derivatives are usually synthesized using metal-based strategies.^{7,8} Incorporation of alkoxy groups in *ortho* position of the aryl motifs represents a general means in order to increase the solubility of the resulting polymers (OR-PPV). In this way also, higher molar mass can be achieved. OR-PPV derivatives polymers were first synthesized by Yu *et al.* in 1993, using the Heck coupling reaction between diiodobenzene derivatives (R = alkyl groups) and divinylbenzene in presence of a palladium-based catalyst (Scheme III.2).^{9,10} The reaction was performed at 100 °C for 5h, leading to OR-PPV **1** in 87% yield, with a \overline{M}_n of 18.5 kg.mol⁻¹ (\mathcal{D}

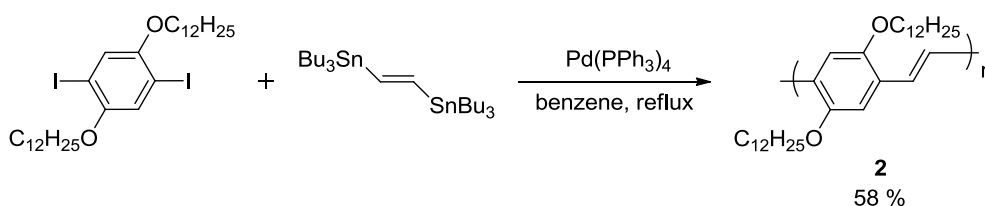
Chapter III: Synthesis of amino-PPV by metal free dimerization/polymerization of novel bis-aminoarylcabenenes

= 2.66) for R = C₇H₁₅. UV-Vis spectrum showed a strong absorption at $\lambda_{\text{max}} = 459$ nm, corresponding to the π - π^* transition. This value was eventually red-shifted in comparison to the parent PPV (400 nm), which was explained with the electronic effects of the alkoxy groups. However, the reaction was not fully regioselective, a majority of E-type linkages being produced under the aforementioned conditions.



Scheme III.2. Synthesis of OR-PPV **1** via Heck coupling.¹⁰

The Stille cross-coupling between a diiodobenzene derivative and *E*-distannylalkene, employing a palladium-type catalyst, also led to OR-PPV polymers, as displayed in Scheme III.3.¹¹⁻¹⁴ The reaction was heated at reflux in benzene for seven days, leading to OR-PPV **2** in 58% yield with a dispersity of 1.4 and a \overline{M}_n of 2230 g.mol⁻¹. As in the case of polymer **1**, **2** showed a strong absorption at 446 nm. One benefit of the latter strategy was that the *E*-isomer could be exclusively obtained. However, this required the use of a toxic ditin reagent and only PPV oligomers could be obtained in this way.



Scheme III.3. PPV derivatives obtained from Stille coupling.¹²

Both the Heck and the Stille coupling reactions are the main metal-based strategies to achieve PPV-derivatives, although other methodologies have been reported such as the ring opening metathesis polymerization using ruthenium metal.^{7,15} However, despite the great diversity of PPV-derivatives accessible through substitution on the aryl moiety, the substitution

Chapter III: Synthesis of amino-PPV by metal free dimerization/polymerization of novel bis-aminoarylcarbenes

pattern at the double bond can rarely be modified, which is inherent to the nature of the coupling methods. Another drawback of such strategies is the use of transition metal-based catalysts that are most often toxic and expensive. Moreover, their presence even as traces in the final material has a negative impact on the optoelectronic performances.^{16,17} The complete removal of metallic residues requires several tedious and lengthy purification steps, which is the main limitation for their large-scale industrialization.¹⁶⁻²⁰ To overcome this issue, transition metal-free polymerization reactions have been developed to access PPV-like polymers free of any metallic residues.

III.1.2 Synthetic access to PPV from transition metal-free routes

While different methodologies have been exploited, they can be classified into two distinct groups depending on their direct (electrochemistry,²¹⁻²⁵ condensation reactions,^{26-28,2,29} direct aryl-aryl coupling³⁰⁻³²) or stepwise preparation,^{1,3,4,33,34} where conjugation occurs during the polymerization or from a non-conjugated pre-polymer, respectively. The pre-polymer strategy has the advantage of synthesizing longer polymer chains, in comparison to the direct polymerization strategy. However, chemical treatment of the pre-polymers may not generate the double bonds quantitatively, so that the final PPV-like polymers may include some defaults along the polymer chains, contributing to the “breaking of the conjugation”.

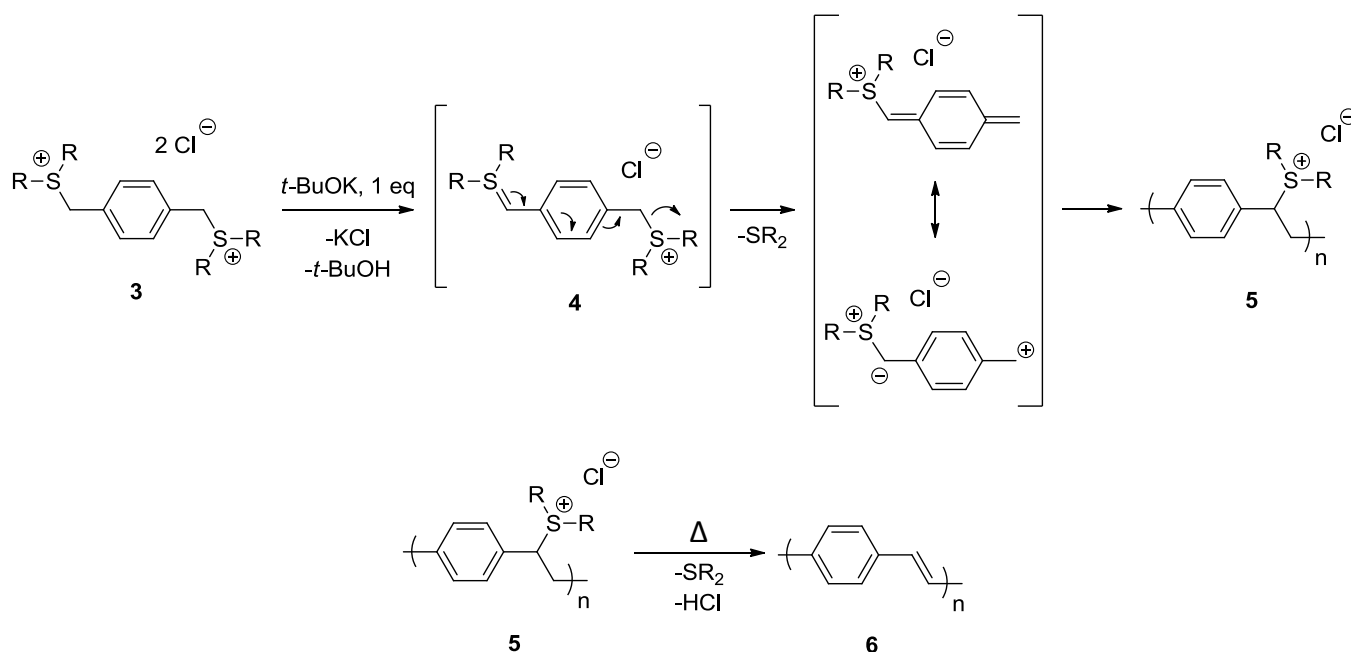
III.1.2.1 Synthesis of PPV from non-conjugated pre-polymers (*via* precursor routes)

- From polysulfonium (poly-S⁺)

Conjugation along the polymer chain may result from the generation of π -conjugation from suitable pre-polymers, for instance **5** or **8**, in the reaction developed by Wessling *et al.* and Rämberg-Bäcklung *et al.*, respectively. In the former route,^{3,33} treatment of a bis-sulfonium with one equivalent of a base (*t*-BuOK), leads to the formation of the transient sulfonium ylide **4**, which further self-polymerizes *via* poly-addition to afford the corresponding polysulfonium **5**. Conjugation between phenyl moieties arises from the elimination of both the sulfonium groups and the proton under thermal conditions, leading to the PPV **6**, as depicted Scheme III.4. Polymer **6** was obtained with a high dispersity of 5.7 and a molar mass $\overline{M}_n = 57\text{-}100 \text{ kg}\cdot\text{mol}^{-1}$.

Chapter III: Synthesis of amino-PPV by metal free dimerization/polymerization of novel bis-aminoarylcarbenes

However, some defects and impurities causing a breaking of conjugation in polymers **6** was suspected to take place *via* side reactions or incomplete elimination of the sulfonium groups. UV-Vis analysis showed that **6** exhibited a maximum of absorption at $\lambda_{\max} = 427$ nm.

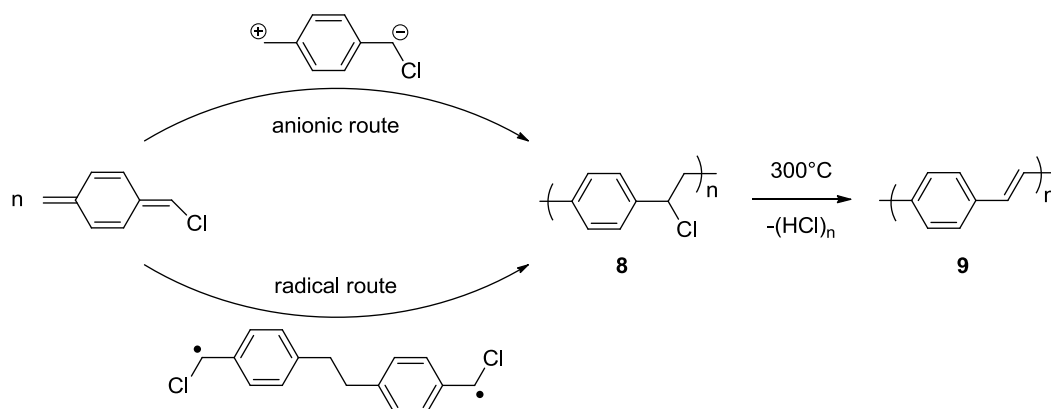
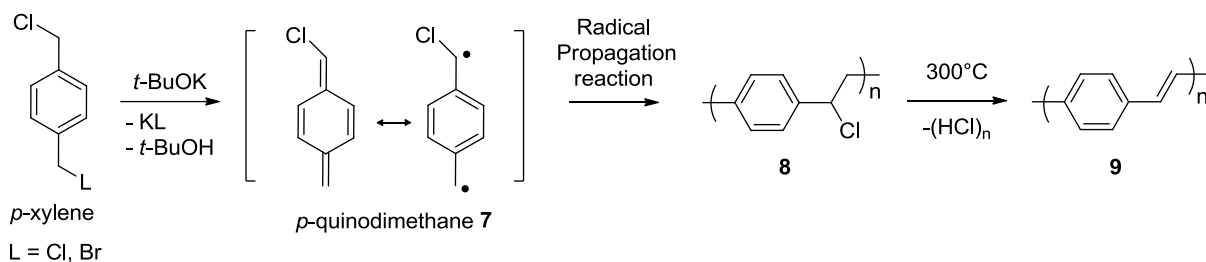


Scheme III.4. Synthesis of PPV **6** *via* Wessling route through intermediate polysulfonium **5**.^{3,33}

- From chlorine precursor polymer

The coupling of two halogenated compounds to access PPV-like polymers was developed by Gilch in 1966.¹ Two different pathways were proposed. In the first one, a base was used to eliminate the leaving group, initiating an anionic-like polymerization. The second route involved the self-dimerization of monomer **7**, which was followed by a radical polymerization leading to the chlorinated pre-polymer **8**. The final PPV **9** was then obtained by elimination of HCl upon heating (Scheme III.5).^{35,36} The polymer **9** was obtained with a $\overline{M}_n = 200.000$ g.mol⁻¹ and a dispersity around 2.5-3.5 (PS calibration). The main advantage of this technique, compared to the Wessling and Ramberg-Bäcklund (see next paragraph) reactions is that the monomer only requires to be halogenated and can bear various alkyl functions on the phenyl moiety. However, because of the self-dimerization of **7**, the center of the polymer chain is not conjugated (Scheme III.5).

Chapter III: Synthesis of amino-PPV by metal free dimerization/polymerization of novel bis-aminoarylcarbenes



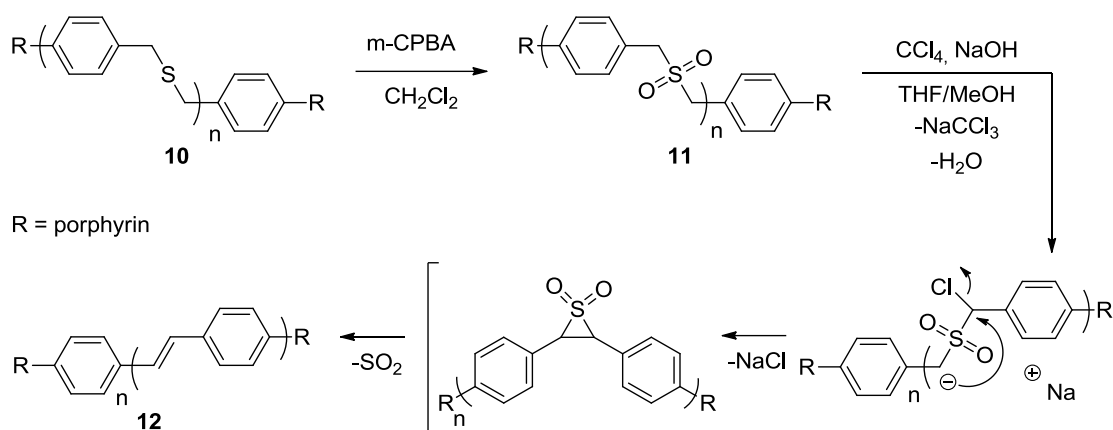
Scheme III.5. The Gilch reaction mechanisms enabling the synthesis of PPV derivatives.^{35–37}

- From polysulfone

Polysulfone **11**, resulting from the oxidation of polysulfide **10** with *m*-CPBA, was found to undergo the so-called Ramberg-Bäcklund reaction to afford the corresponding oligo-PPV **12**. The Ramberg-Bäcklund reaction involves a stepwise mechanism, where chlorination of **11** and deprotonation of the resulting α -chlorosulfone, generates the unsaturation by extrusion of sulfur dioxide (SO_2) from the thiirane dioxide intermediate (Scheme III.6).⁴ In this work, the reaction leads to oligomers ($n = 4$) in 73 % yield.

Surprisingly, the Ramberg-Bäcklund reaction has never been applied to the synthesis of PPV-type polymers using polysulfones as precursor. This strategy, in opposition to the Wessling and Gilch routes, also allows for the preparation of PPV-like polymers with different aryl groups, such as the fluorene moiety used in the synthesis of poly(fluorene vinylene), as recently reported by Landais, Taton *et al.*³⁸

Chapter III: Synthesis of amino-PPV by metal free dimerization/polymerization of novel bis-aminoarylcabenenes



Scheme III.6. Synthesis of PPV derivative **12** via Ramberg-Bäcklund route.^{4,38}

III.1.2.2 Formation of PPV-like derivatives via direct routes

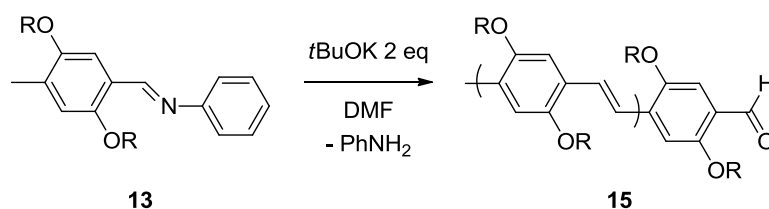
Conjugation in PPV-like polymers may be obtained directly by the condensation of suitable (AA + BB) or AB-type monomers. Most representative examples include the Siegrist, Wittig/ Wittig-Horner and Knoevenagel condensations. In general, those reactions involve neutral or anionic carbon-centered nucleophiles and an aldehyde as an electrophilic partner (or the corresponding Schiff base, *i.e.* **13** in Scheme III.7). PPV-like polymers can also be obtained by electrochemistry, which is a versatile technique not only giving PPV, but also aryl-aryl and heteroaryl-containing polymers (see section III.1.2.3).

III.1.2.2.1 Siegrist condensation

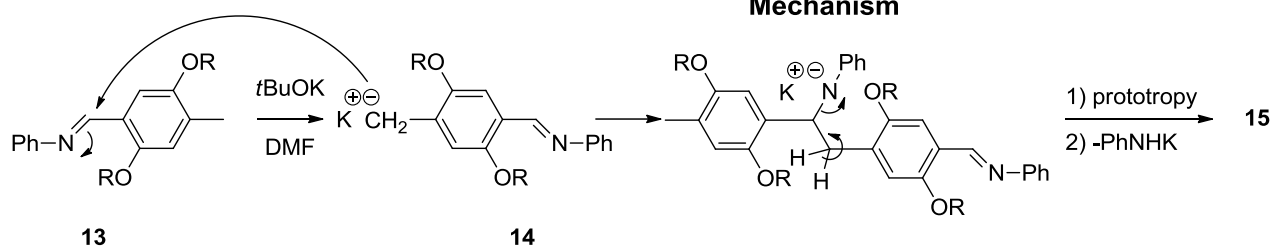
In 1969, Siegrist *et al.* developed an original reaction involving an imine **13** as an AB-type monomer precursor. Deprotonation of the CH₃ of **13** with *t*-BuOK generated the corresponding carbanion **14**, followed by reaction onto the imine moiety **13**. The C=C bond was generated upon release of ArNH₂ (see Scheme III.7).^{2,39} Polymer **15** was obtained in 70-90% yield, with a DP_n = 9. The reaction was found to be dependent on the acidity of the proton on the methyl group. As the polymer increases in size, indeed, the anionic chain-end becomes less reactive because of the increased delocalization, leading to a decrease of the reactivity of the proton. Consequently, relatively low molecular weight and low dispersity PPVs were achieved in this way.

Chapter III: Synthesis of amino-PPV by metal free dimerization/polymerization of novel bis-aminoarylcarbenes

Siegrist reaction



Mechanism

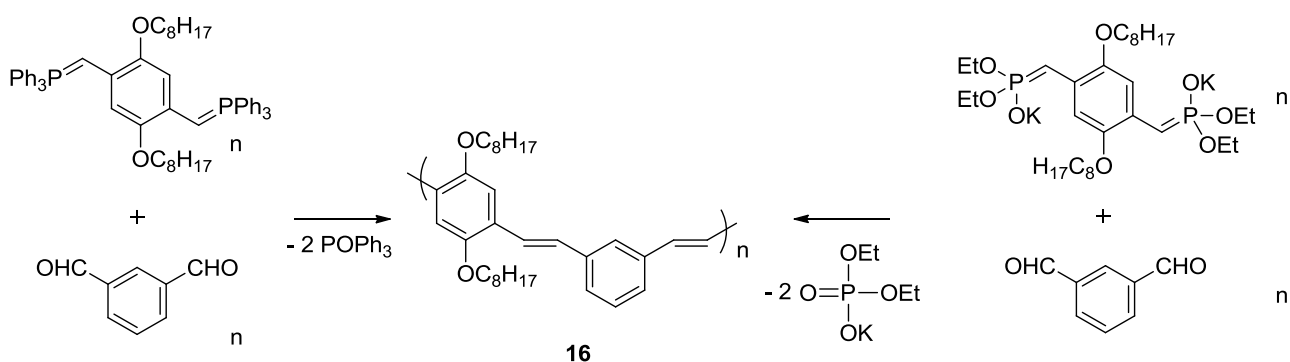


Scheme III.7. Synthesis of MeH-PPV derivatives based on Siegrist condensation.^{2,39} R = Methylhexyl

III.1.2.2.2 Wittig/Wittig-Horner reactions

Other elementary condensation reactions employed for PPV synthesis include the Wittig²⁶ and Wittig-Horner²⁷ reactions. Both involve the addition of either an ylide or a stabilized carbanion onto an aldehyde monomer substrate. The first PPV-like synthesized by adaptation of such routes was reported by Campbell *et al.*, as summarized in Scheme III.8.⁴⁰ Through the Wittig reaction, polymer **16** was obtained with a $\overline{M}_n = 8.800 \text{ g.mol}^{-1}$ ($D = 1.70$). Using the Wittig-Horner (WH) reaction, the more nucleophilic carbanion led to polymer **16** with a higher molar mass ($\overline{M}_n = 30.000 \text{ g.mol}^{-1}$; $D = 1.16$). While the reaction proved efficient with both *meta* and *para*-terephthalaldehyde, no polymerization occurred with *ortho* derivatives for steric reasons. Polymerization could not only be achieved using AA + BB-type monomers, but also from an AB-type monomer. In the latter case, the resulting polymer was characterized by a molar mass, $\overline{M}_n = 33.000 \text{ g.mol}^{-1}$ and a dispersity $D = 2.3$.⁵

Chapter III: Synthesis of amino-PPV by metal free dimerization/polymerization of novel bis-aminoarylcarbenes



a) Wittig Reaction

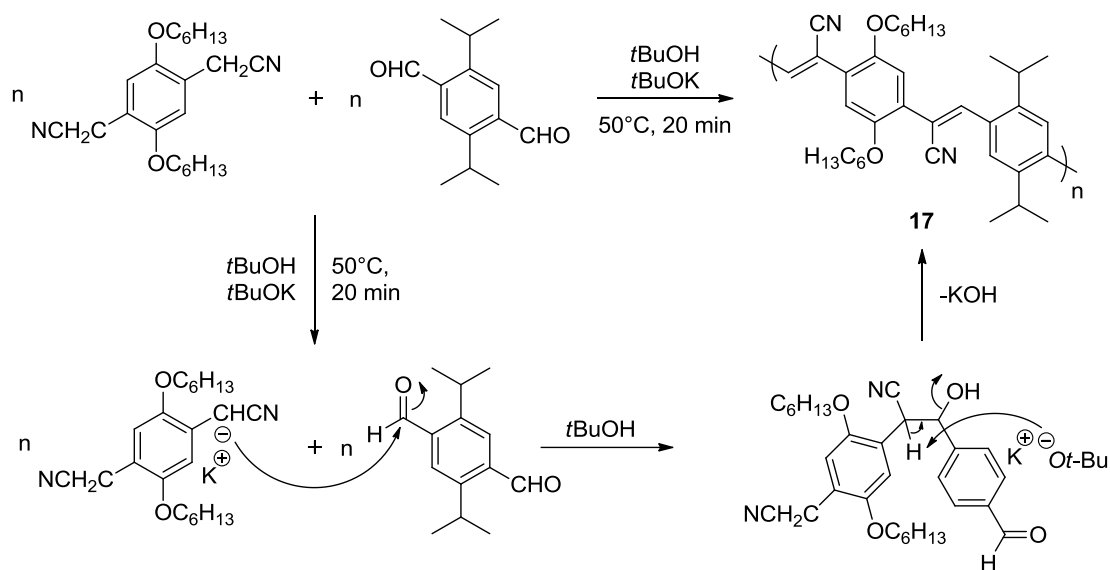
b) Wittig-Horner Reaction

Scheme III.8. PPV derivatives **16** synthesized by a) Wittig b) WH routes.⁴⁰

III.1.2.2.3 Knoevenagel condensation

The Knoevenagel reaction was adapted to the PPV synthesis by Hamer *et al.*,⁴¹ using bis-benzonitrile and bis-aldehyde derivatives as AA- and BB-type monomers. This method specifically introduces a substituent onto the repeating C=C double bonds. Use of a strong base, *e.g.* *t*-BuOK, enables the deprotonation of the acidic CH₂CN, yielding the corresponding stabilized anion, which in turn reacts by nucleophilic addition with the electrophilic partner. Upon elimination of KOH, the corresponding PPV **17** could be prepared in this way in 78% yield, with a $\overline{M}_n = 3700 \text{ g}\cdot\text{mol}^{-1}$ ($D = 3.59$), as shown in Scheme III.9. Because of the presence of electron-withdrawing cyano groups, the λ_{max} absorption was found to be blue shifted ($\lambda_{\text{max}} = 355 \text{ nm}$), as compared to the parent non-substituted PPV. Interestingly, PPV **17** behaved as an n-type material, *i.e.* showing an electron-acceptor behavior.

Chapter III: Synthesis of amino-PPV by metal free dimerization/polymerization of novel bis-aminoarylcarbenes



Scheme III.9. Synthesis of CN-PPV **17** derivative *via* Knoevenagel condensation.⁴¹

III.1.2.3 Electrochemistry

Electrochemical polymerization represents a common and efficient and low cost synthetic strategy to semiconducting polymers, such as poly(*p*-phenylene), polythiophene, poly(carbazole), polypyrrole and polyaniline (see Figure III.1). PPV-type compounds can also be accessed following this pathway. This method provides a high degree of process control in particular regarding polymer thickness, through the control over the number of cycles applied and the current of the electrode.^{21,25,42–50}

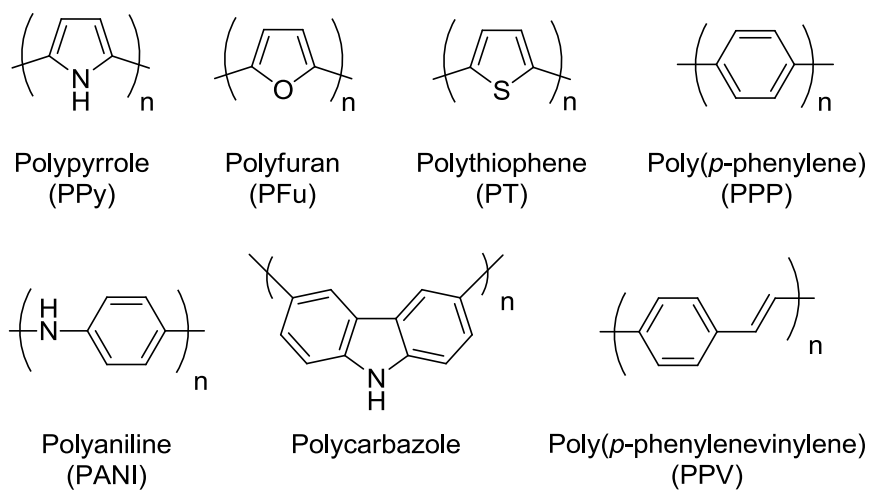
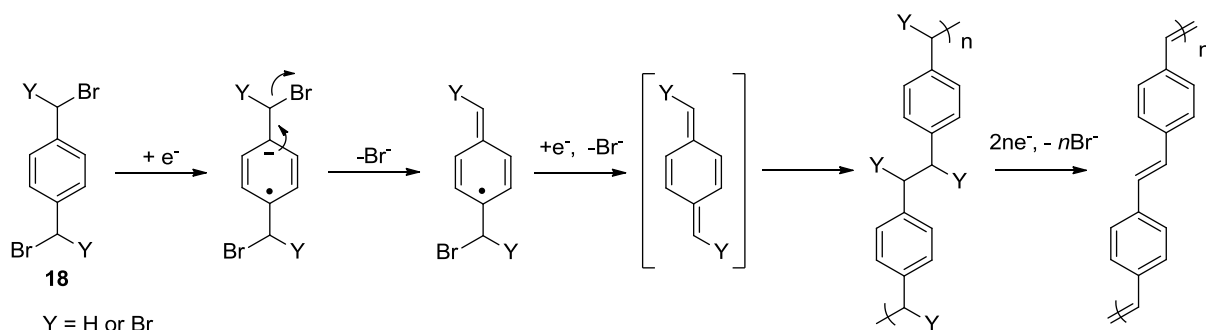


Figure III.1. Polymers synthesized by electrochemistry.^{21,25,45–51}

Chapter III: Synthesis of amino-PPV by metal free dimerization/polymerization of novel bis-aminoarylcarbenes

This methodology allows elaborating polymer films that could not be obtained otherwise. Moreover, it does not require the use of stoichiometric amounts of the oxidant through the application of a potential between the two electrodes to trigger the polymerization. However, this strategy cannot be applied for bulk conditions. It also requires relatively high potentials to oxidize the monomer. As such conditions could dissolve some metallic parts of the electrodes, it is not so often implemented in industry.

Polymerization can be achieved either by oxidation or by reduction, e.g. for PPV and for PT synthesis, respectively, depending on the nature of the monomer. PPV synthesis by electropolymerization of bis-bromomethylbenzene monomers was first reported in 1987 by Nishihara *et al.*²² The reaction proceeded through the application of a potential of -3V vs. Ag/Ag⁺ for 6 hours at an indium tin oxide (ITO) electrode immersed into a THF solution of monomer **18**, in *n*-Bu₄NBF₄ used as electrolyte (Scheme III.10). Using appropriate potential, electrode, monomer and electrolyte, the protocol could be applied to access most of the polymers shown in Figure III.1. It is worthy of note that polymers were most often synthesized following the oxidation route.

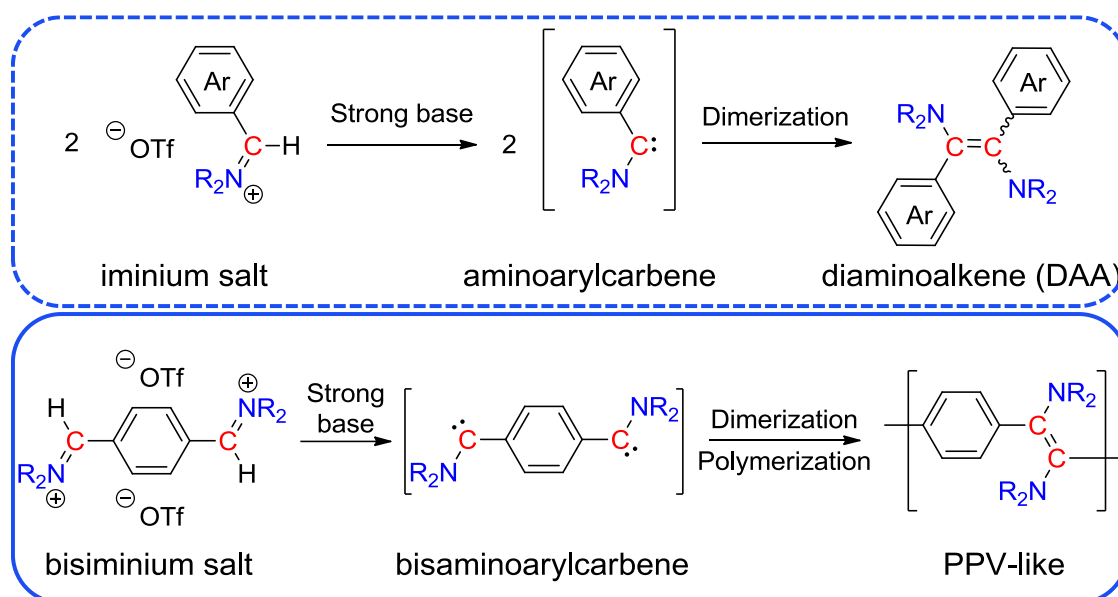


Scheme III.10. Synthesis of PPV by electropolymerization of bis(dibromomethyl)arenes.²¹

While carbenes are among the most extensively investigated reactive species in chemistry,⁵² their use as true monomer substrates in polymer synthesis has received very little attention. Bielawski *et al.* have reported that bis-benzimidazol-2-ylidene-type NHCs can be subjected to a “dimerizing polymerization”, forming thermally reversible (dynamic) covalent π -conjugated polymers.^{53,54} However, the as-obtained polymers display an inherent low conjugation across the aryl spacer, in addition of being relatively air-sensitive and unstable. One can therefore believe that there is still plenty of room to employ the carbene dimerization as an important C=C bond skeleton forming process in polymer synthesis.

Chapter III: Synthesis of amino-PPV by metal free dimerization/polymerization of novel bis-aminoarylcabenenes

Carbenes targeted in this project are acyclic aminoaryl carbenes that can self-dimerize into the corresponding diaminoalkenes,^{55,56} as emphasized in the previous chapter. Our hypothesis is that amino-containing poly(p-phenylene vinylene)s (NPPV's) may be accessible from a “dimerizing polymerization” of bis-aminoarylcabenenes serving as original monomeric building blocks. Of particular interest, amino groups adjacent to C=C bonds can be subjected to a post-modification through protonation/deprotonation reactions, in contrast to classical PPV's. In this chapter, the synthesis and characterization of the new bis-iminium salt precursors, as well as the study of their deprotonation will be first presented (Scheme III.11). Then, synthesis and characterization of corresponding N-PPV's obtained by dimerizing polymerization will be discussed. The last section will be devoted to the post-chemical modification of N-PPV's by protonation/methylation as a means to tune their photophysical properties.



Scheme III.11. Synthesis of diaminoalkenes *via* deprotonation of the corresponding monoiminium salts (dashed blue line) and amino-PPVs by deprotonation of bis-iminiums (blue line).

III.2 Synthesis of bis-iminium precursors

By analogy with the monofunctional iminium salts studied in chapter 2, bis-iminium **21**, **22** and **23** were purposely synthesized. Thus, depending on the substituent pattern, either the Alder or the Schroth method was implemented (Figure III.2).^{57,58}

Chapter III: Synthesis of amino-PPV by metal free dimerization/polymerization of novel bis-aminoarylcabenenes

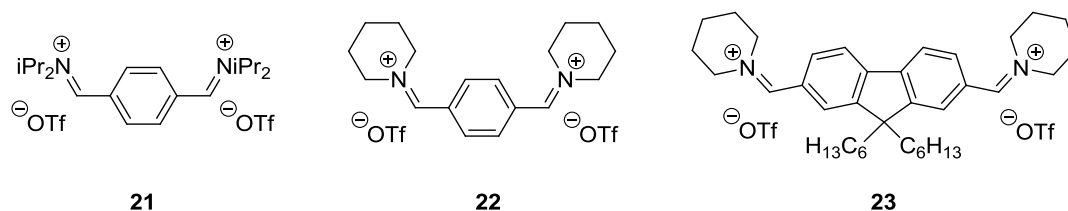
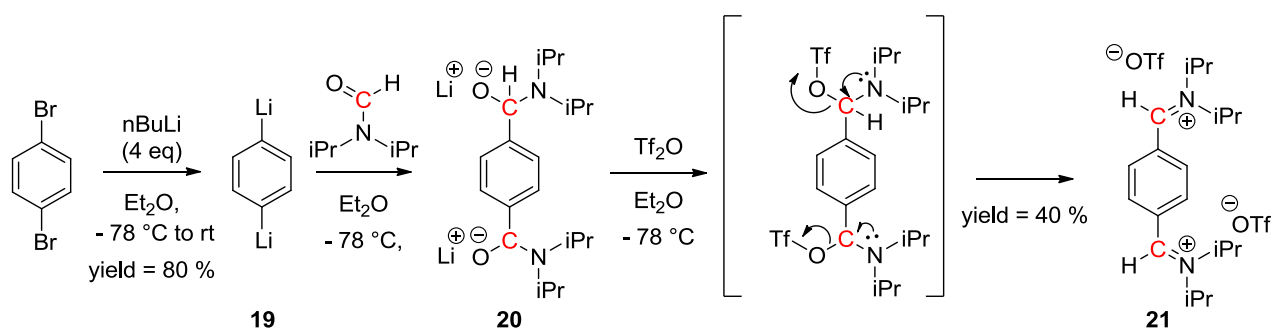


Figure III.2. Bis-iminium synthesized through Alder or Schroth routes.^{57,58}

III.2.1 Alder's route

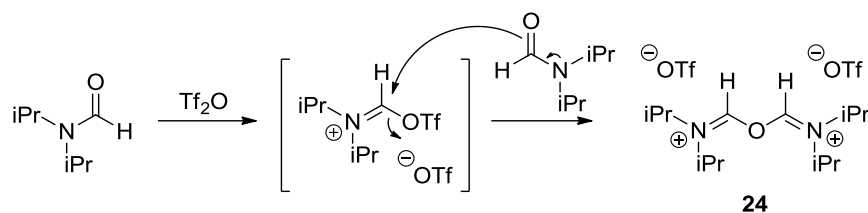
The Alder's route is especially suitable for the one-pot synthesis of iminium salts featuring bulky amino substituents, such as in **21** (Scheme III.12).



Scheme III.12. Synthesis of bis-iminiumaryl salt **21** via adapted Alder's methodology.⁵⁸

The reaction was initially performed with the *in-situ* generated bis-lithium **19**. Under these conditions, however, **21** was contaminated with dication **24**, as a result of the reaction between N,N-diisopropylformamide and triflic anhydride (Tf₂O). Unfortunately, **21** could not be purified because of the dicationic nature of both compounds. Nevertheless, this result highlights the importance of controlling the 1,4-dilithiobenzene:diisopropylformamide stoichiometry (Scheme III.13). The singlet due to the CH iminium proton and the two CHiPr septet signals for **24** were clearly observed by ¹H NMR, in agreement with data from the literature.⁵⁸

Chapter III: Synthesis of amino-PPV by metal free dimerization/polymerization of novel bis-aminoarylcarbenes



Scheme III.13. Formation of dication **24** by reaction between Tf_2O and diisopropylformamide.

To avoid this contamination, the 1,4-dilithiobenzene was isolated and diisopropylformamide and triflic anhydride were added in stoichiometric amounts. To generate the bis-lithiated compound **19**, 4 equivalents of $n\text{-BuLi}$ were added to 1,4-dibromobenzene for the bromide-lithium exchange to proceed on both functions. After purification, 1,4-bis-lithiobenzene **19** was isolated as a yellow powder in 80% yield. It is worth noting that this compound had to be handled with care under an inert atmosphere, as it reacted violently and ignited in contact with air.

Then, 2 equivalents of diisopropylformamide were added onto a suspension of **19** in Et_2O at -78°C . The solution was warmed to room temperature to generate the intermediate bis-lithium alkoxide **20**. Finally, triflic anhydride was added at -80°C to a solution of **20**; as the mixture slowly reached room temperature, elimination of triflate generated the desired bis-iminium **21**. After washing with dry ether and THF, **21** was obtained as a white powder in moderate yield (40%; Scheme III.13). The low yield obtained might be explained by the high sensitivity of compound **21** which is rapidly hydrolyzed upon contact with air and water and during the purification steps because of its dicationic structure.

The chemical structure of compound **21** was confirmed by ^1H NMR spectroscopy in $\text{DMSO-}d_6$, which showed the appearance of a new set of signals. As expected from its symmetry, only six signals were observed with the most deshielded proton signal at 9.26 ppm integrating for two protons, corresponding to the CH-type iminium. Two CHiPr septet signals at 4.91 ppm and 4.57 ppm ($^3J_{\text{H-H}} = 6.7$ Hz) integrating for 2 protons each, two CH_3iPr doublet signals at 1.53 and 1.63 ppm ($^3J_{\text{H-H}} = 6.5$ Hz) integrating for 12 protons each, and the $\text{CH}_{\text{aromatics}}$ singlet signal at 7.96 ppm integrating for 4 protons, were also observed (Figure III.3). ^{13}C NMR spectroscopy also confirmed the symmetry of compound **21** with only seven signals being

Chapter III: Synthesis of amino-PPV by metal free dimerization/polymerization of novel bis-aminoarylcabenenes

observed. The most characteristic ^{13}C signal of the iminium carbon appeared at 171.9 ppm (see experimental part).

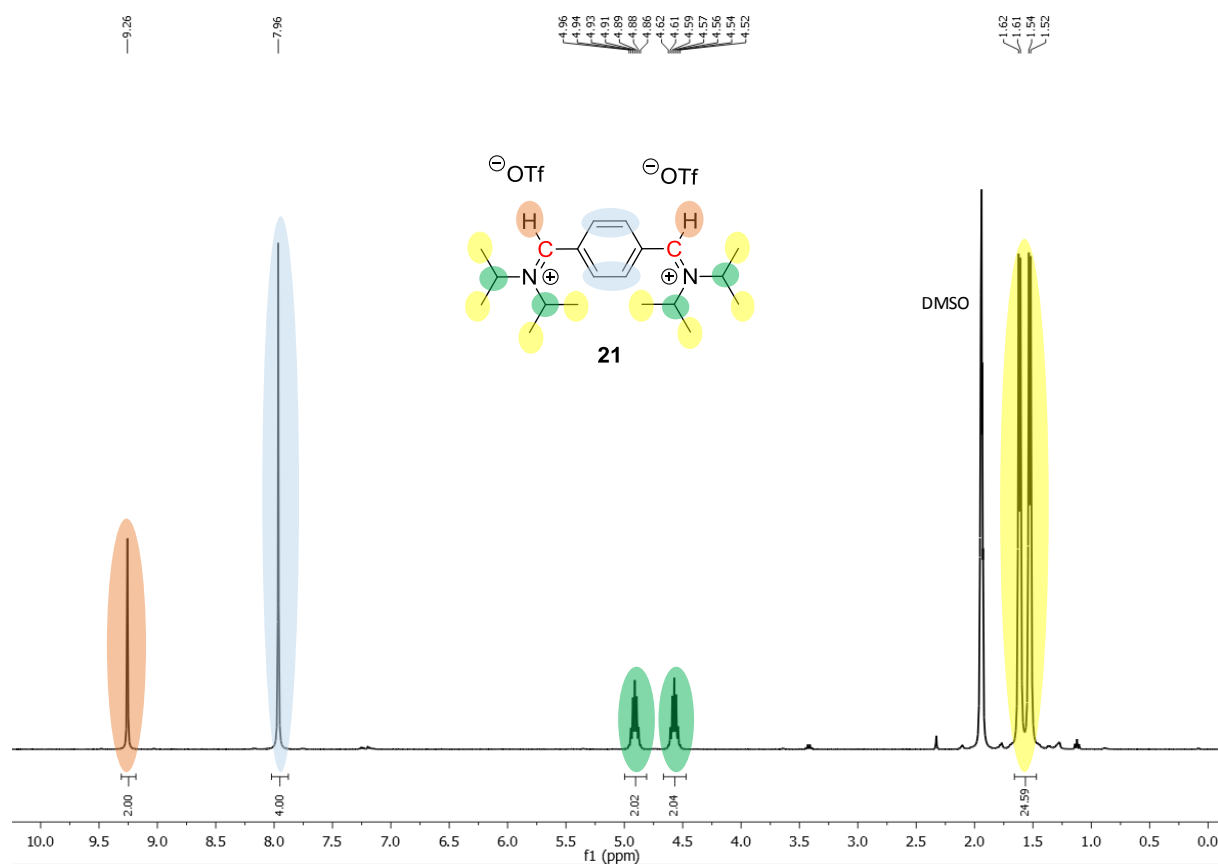


Figure III.3. ^1H NMR (400 MHz) in DMSO-d_6 of symmetrical compound **21**.

Single crystals could be successfully grown by vapor diffusion of Et_2O into a THF solution of **21**. X-Ray analysis further confirmed the identity of **21**, the different bond lengths and bond angle being in the range expected for such a structure. Unexpectedly, compound **21** showed the two iminium protons pointing toward the same triflate counter anion (Figure III.4).

Chapter III: Synthesis of amino-PPV by metal free dimerization/polymerization of novel bis-aminoarylcarbenes

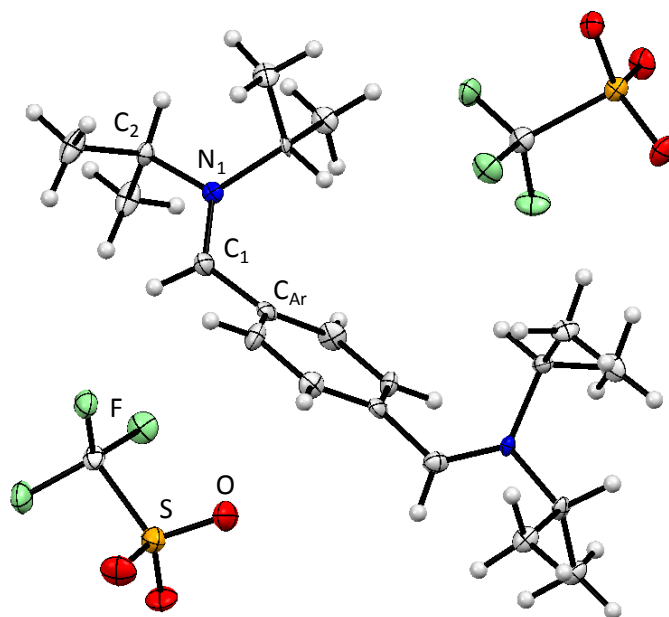
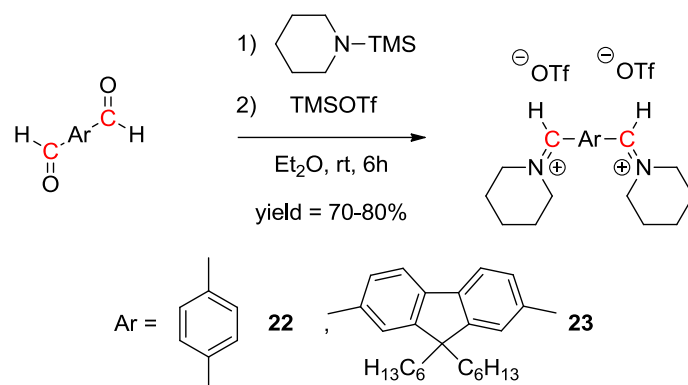


Figure III.4. X-Ray analysis of compound **21**. $C_1-C_{Ar} = 1.48 \text{ \AA}$; $N_1-C_1 = 1.29 \text{ \AA}$; $N_1-C_2 = 1.50 \text{ \AA}$ and $\Sigma_{N1} = 360^\circ$.

III.2.2 The Schroth's route

Access to sterically less hindered bis-iminium salts, such as **22** and **23**, may be achieved following the “Schroth’s route”, involving neutral conditions at room temperature. By analogy with the mono-iminium analogue prepared in chapter 2, two equivalents of piperidinetrimethylsilyl amine (synthesized accordingly to Morishita *et al.*⁵⁹) and two equivalents of trimethylsilyltriflate were successively added to an ether solution of either terephthalaldehyde or fluorene-bis-carboxaldehyde. This protocol led to the formation of bis-iminium salts, **22** and **23**, respectively in 70-80% yield (Scheme III.14). The synthesis of fluorene-bis-carboxaldehyde was performed by analogy with the synthesis of fluorencarboxaldehyde.^{60,61} Both compounds were fully characterized by ¹H, ¹³C and ¹⁹F NMR spectroscopy. In particular, corresponding ¹H NMR and ¹³C NMR spectra showed the presence of signals due to CH-type iminium proton at 9.11 and 9.02 ppm and 170.8 and 171.1 ppm for **22** and **23**, respectively.

Chapter III: Synthesis of amino-PPV by metal free dimerization/polymerization of novel bis-aminoarylcabenenes



Scheme III.14. Synthesis of bis-iminium salt **22** and **23** using Schroth methodology.⁵⁷

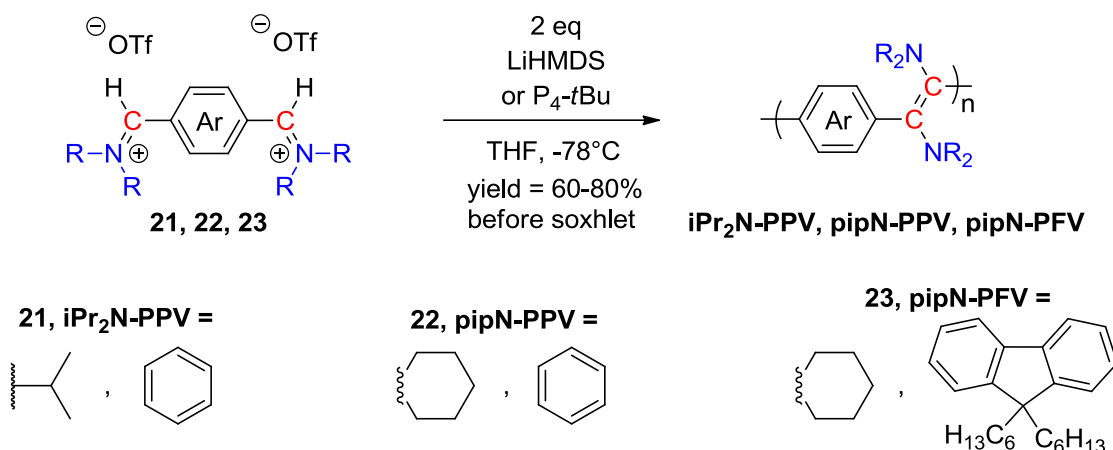
The following section discusses the polymerization through repeated dimerization of bis-aminoarylcabenenes, as well as the characterization of as-obtained N-PPV's.

III.3 Synthesis of new amino-containing PPV derivatives through dimerization/polymerization of *in-situ* generated bis-aminoarylcabenenes

III.3.1 Synthesis of N-PPV's

The dimerization/polymerization was performed by deprotonation of a suspension of bis-iminium salts **21**, **22** or **23** in THF, in presence of two equivalents of a strong base (LiHMDS, P₄-*t*Bu) at -78°C (Scheme III.15). Upon warming the reaction to room temperature, the color of the solution radically changed from yellowish to deep red, suggesting the effective extension of the conjugation. N-PPV's thus formed were thoroughly purified and led to red powders, with yields between 60-80%.

Chapter III: Synthesis of amino-PPV by metal free dimerization/polymerization of novel bis-aminoarylcarbenes



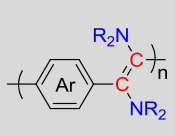
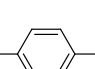
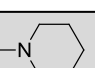
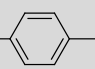
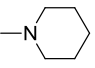
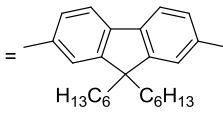
Scheme III.15. Synthesis of new PPV-derivatives **iPr₂N-PPV**, **pipN-PPV** and **pipN-PFV** through the deprotonation of their corresponding bis-iminium salts.

III.3.2 N-PPV characterizations

Crude polymers, denoted as **iPr₂N-PPV**, **pipN-PPV** and **pipN-PFV**, were analyzed by size-exclusion chromatography. The SEC trace of each polymer showed the appearance of discrete peaks at low molar masses, attesting to the occurrence of the step-growth polymerization. The series of peaks was attributed to oligomers of different degree of polymerization. For polymer **iPr₂N-PPV**, the \overline{Mn} obtained was 3000 g.mol⁻¹, along with a $\overline{DP}_n = 10$ and a typical dispersity for a step-by-step polymerization of $D = 2.08$. The formal replacement of iPr₂N by pipN substituent led to a slight increase of the \overline{Mn} value (3900 g.mol⁻¹; $\overline{DP}_n = 14$) with a dispersity of 2.05. Finally, changing the phenyl moiety by 9,9'-dihexyl-9H-2,7-fluorene led to the polymer **pipN-PFV** with a higher \overline{Mn} (5200 g.mol⁻¹; $\overline{DP}_n = 10$), a dispersity of 2.05 (Table III.1 and figure III.5).

Table III.1. Characteristics of polymers **iPr₂N-PPV**, **pipN-PPV** and **pipN-PFV**. \overline{Mn} is given in g.mol⁻¹.

Chapter III: Synthesis of amino-PPV by metal free dimerization/polymerization of novel bis-aminoarylcabenenes

	\overline{M}_n (g.mol ⁻¹)	\overline{D}	\overline{DP}_n	E/Z ratio (%)
$NR_2 = -NiPr_2$ $Ar =$  iPr₂N-PPV	3000	2.1	10	80/20
$NR_2 =$  $Ar =$  pipN-PPV	3900	2.1	14	85/15
$NR_2 =$  $Ar =$  pipN-PFV	5200	2.1	10	85/15

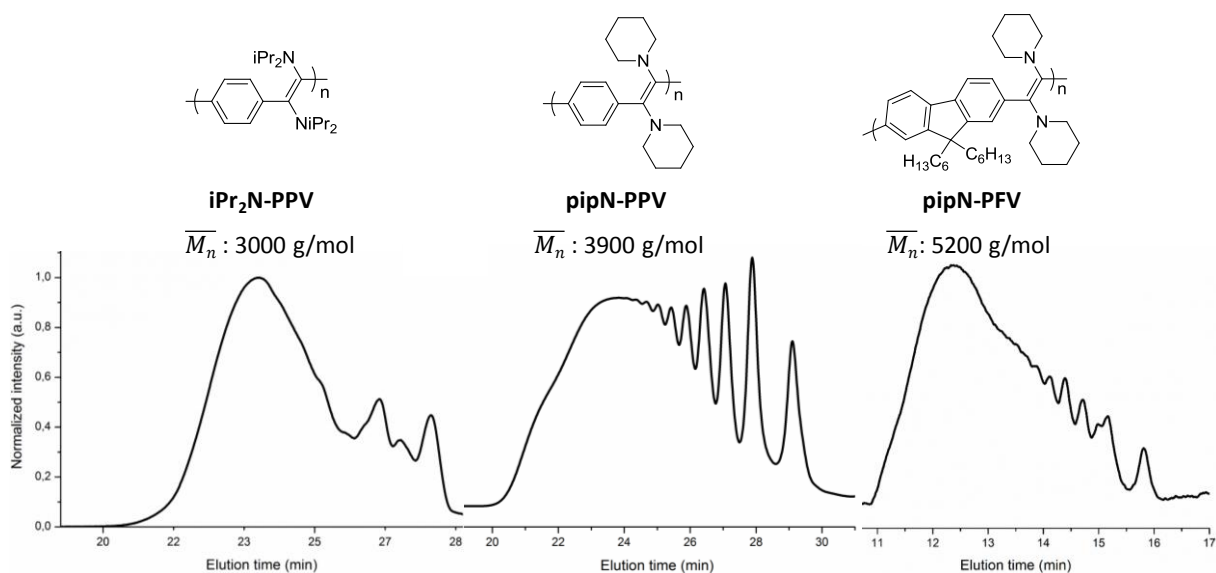


Figure III.5. SEC in THF with polystyrene calibration of polymers **iPr₂N-PPV**, **pipN-PPV** and **pipN-PFV**.

All polymers were analyzed by NMR spectroscopy. However, only **iPr₂N-PPV** will be described as it is characterized by the presence of well resolved multiplets due to the iPr

Chapter III: Synthesis of amino-PPV by metal free dimerization/polymerization of novel bis-aminoarylcabenenes

substituents, as compared to piperidine groups. In comparison with the diisopropyl dimer **iPr₂N-DAA** described in the previous chapter and, as expected, the ¹H NMR spectrum of **iPr₂N-PPV** displayed similar but broader signals for all types of protons. The same E/Z ratio of 80/20 to that already determined for the corresponding dimer was obtained (Figure III.6, in green).

Of particular interest, and in contrast to **iPr₂N-DAA**, a novel signal, corresponding to an aldehyde chain end, was observed at 10 ppm. (Figure III.6). The presence of a second aldehyde signal at 9.75 ppm could be due to the presence of the two isomer conformations. Indeed, in the Z-isomer the aldehyde proton might be near the shielding cone of an aromatic moiety explaining the signal at a higher field. The presence of such an aldehyde group can be explained by the hydrolysis of the carbenic chain-end during workup, *i.e.* when the reaction vessel is open to air during the purification steps (Scheme III.16).

Chapter III: Synthesis of amino-PPV by metal free dimerization/polymerization of novel bis-aminoarylcarbenes

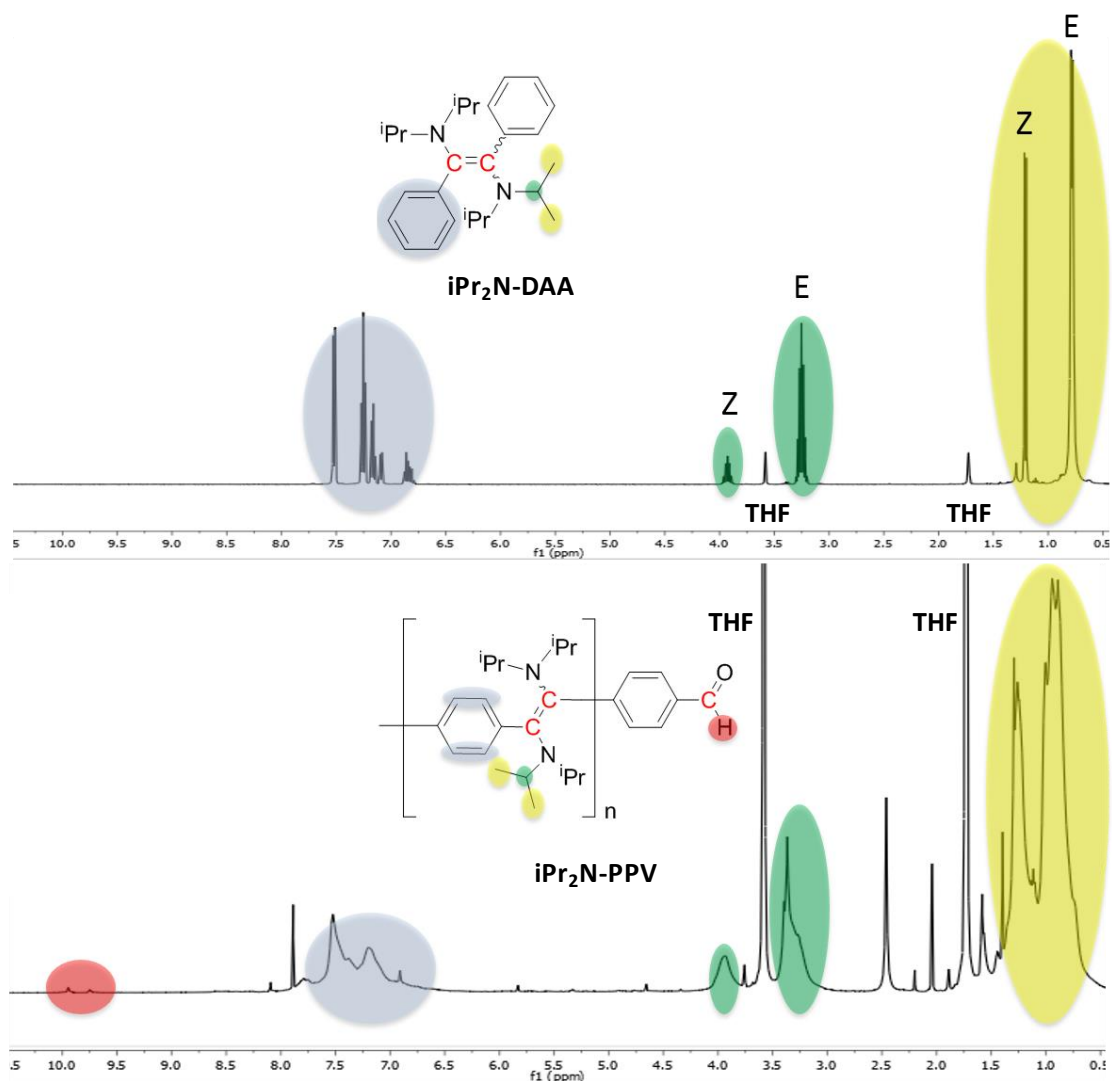
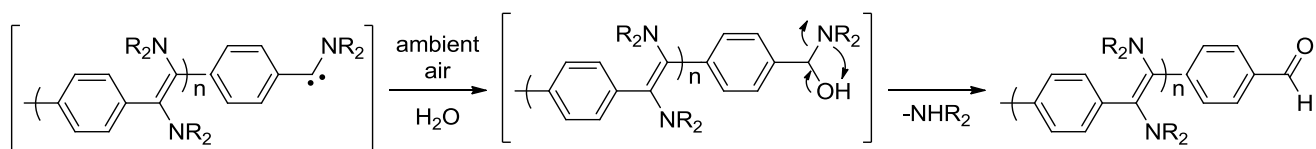


Figure III.6. ¹H NMR (400 MHz) in THF_d₆ of polymer **iPr₂N-PPV** and its corresponding dimer **iPr₂N-DAA**.



Scheme III.16. Hydrolysis of the carbene end-chain leading to the aldehyde end-chain function.

The degree of polymerization, \overline{DP}_n , as thus determined by ¹H NMR spectroscopy was found equal to 48, that was, a different value to that obtained by SEC ($\overline{DP}_n = 10$). This discrepancy might be explained by an underestimation of the SEC value because of the PS standards used

Chapter III: Synthesis of amino-PPV by metal free dimerization/polymerization of novel bis-aminoarylcarbenes

for calibration. Nevertheless, NMR values might be also overestimated, as the above calculation is based on the integration of the small signals of aldehyde chain-ends.

III.3.3 Optoelectronic properties

a) Absorption properties

Analysis by UV/Vis of all polymer compounds showed two absorption maxima, namely in the range $\lambda_{\max} = 240\text{-}273$ nm and $\lambda_{\max} = 460\text{-}483$ nm, respectively. These maxima can be attributed to the $\pi\text{-}\pi^*$ and $n\text{-}\pi^*$ transitions (Table III.2). It is worthy of note that the $n\text{-}\pi^*$ transition corresponds to the HOMO-LUMO level of the polymer. The HOMO is a combination of the n_N and $\pi_{C=C}$ orbitals and the LUMO is delocalized over the whole π -system ($\pi_{C=C}$ and $\pi_{\text{aromatics}}$). The $\pi\text{-}\pi^*$ transition corresponds to the gap between the π -system of the double bond and the aromatics moieties. These results were obtained for the **iPr₂N-DAA** discussed in section III.4.1.4, with the help of Dr. K. Miqueu and J. M. Sotiropoulos from IPREM in Pau.

Table III.2. Maximum of absorption (λ_{\max} in nm) of polymers **iPr₂N-PPV**, **pipN-PPV** and **pipN-PFV** depending on their electronic transitions.

Polymers \ Electronic transition (λ_{\max} in nm)	$\pi\text{-}\pi^*$	$n\text{-}\pi^*$
iPr ₂ N-PPV	255	462
pipN-PPV	273	476
pipN-PFV	240	483
iPr ₂ N-DAA	229	388

The extension of conjugation was also investigated by measuring the red shifts observed for both absorption maxima of **iPr₂N-PPV**, in comparison to the dimer homologue, **iPr₂N-DAA** (26 nm and 74 nm for the $\pi\text{-}\pi^*$ and $n\text{-}\pi^*$ respectively; Figure III.7). These red shifts were also observed for polymers **pipN-PPV** and **pipN-PFV** relatively to their respective dimers. The higher maximum of absorption of **pipN-PFV** compared to **pipN-PPV** might be due to, in the one hand, the planarization effect brought by the fluorene moiety and, on the other hand, to the extended π -system of the fluorene moiety, in comparison to the phenyl moiety.

Chapter III: Synthesis of amino-PPV by metal free dimerization/polymerization of novel bis-aminoarylcarbenes

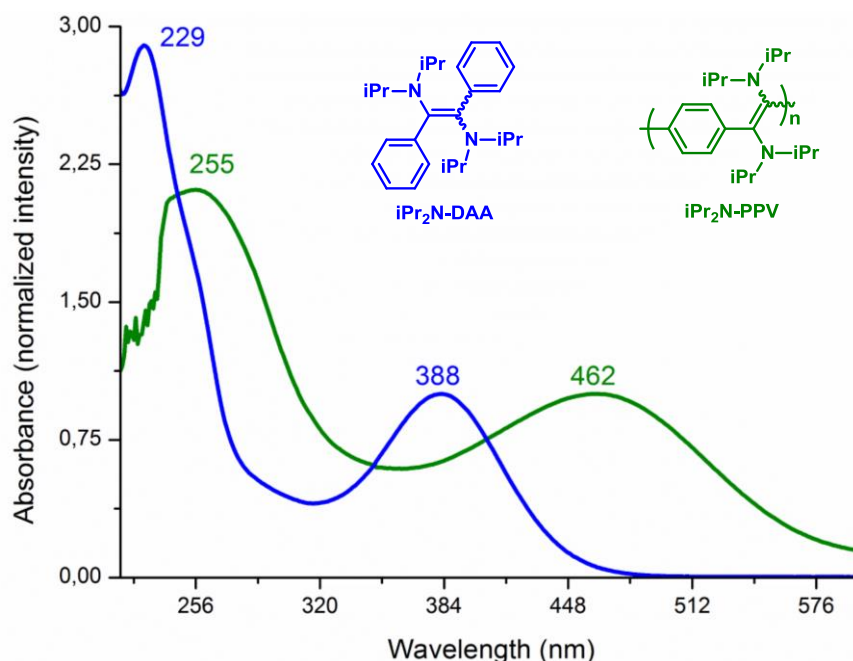


Figure III.7. UV/Vis spectra in CHCl₃ showing the maximum of absorption in polymer **iPr₂N-PPV** and its dimer **iPr₂N-DAA**.

Moreover, the presence of nitrogen atoms on the double bond also impacts the maximum of absorption of the polymers ($n-\pi^*$ transition), as shown by a red shift of ~ 35 nm as compared to similar neutral PPV **7** (~ 427 nm) (see scheme III.4).⁶²

b) Emission properties

The emission properties were investigated by irradiation of thin films and solution of polymers **iPr₂N-PPV**, **pipN-PPV** and **pipN-PFV** at their maximum of absorption. In thin films, λ_{max} (emission) were recorded at 666, 685 and 640 nm for **iPr₂N-PPV**, **pipN-PPV** and **pipN-PFV**, respectively. In solution, however, those polymers emitted at shorter wavelengths because of the multiple ways to relax ($\lambda_{\text{max}} = 592, 528$ and 561 for **iPr₂N-PPV**, **pipN-PPV** and **pipN-PFV**, respectively). Importantly, all these values were red shifted as compared to their respective dimeric model compounds (see experimental part chapter II and Figure III.8).

Chapter III: Synthesis of amino-PPV by metal free dimerization/polymerization of novel bis-aminoarylcabenenes

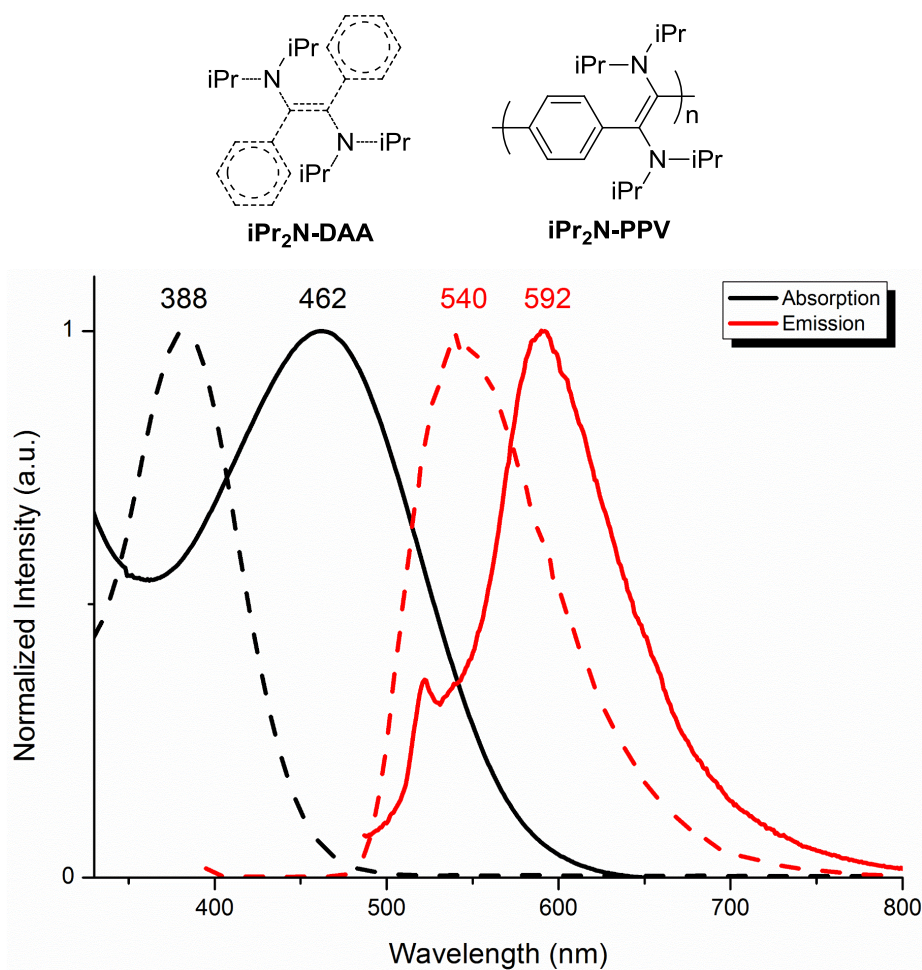
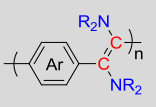
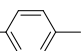
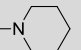
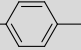
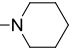
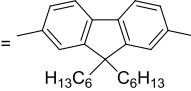


Figure III.8. Maximum of absorption and emission of polymer **iPr₂N-PPV** (plain) and its dimer **iPr₂N-DAA** (dashed) in solution (CHCl₃).

Overall, a large stoke shift (160-209 nm), an emission on a large array of the visible spectra and a λ_{max} absorption and emission, which moderately overlap, would make these novel amino-PPV polymers of interest for the development of OLED (Organic light-emitting diode) devices (Table III.3). For such devices indeed, it is an advantage that the energy absorbed and then released by the polymers is not reabsorbed by itself. Moreover, if the large emission goes to the infrared region it would be a strong advantage for these polymers when integrated in OLED devices, as only few polymers can emitted in this infra-red area and most of them are hetero-aromatic conjugated polymers.⁴¹ Among the polymers synthesized in this work, polymer **iPr₂N-PPV** appears as the most qualified to be used in such OLED devices (Figure III.8 in solution, Figure III.9 in thin film).

Chapter III: Synthesis of amino-PPV by metal free dimerization/polymerization of novel bis-aminoarylcarbenes

Table III.3. Absorption, emission, stoke shift and array of emission of polymers **iPr₂N-PPV**, **pipN-PPV** and **pipN-PFV**. Red = in thin film, black = in CHCl₃ solution

	Absorption (λ_{\max} in nm) n- π^*	Emission (λ_{\max} in nm)	Stoke Shift (nm)	Emission window (nm)
NR ₂ = —NiPr ₂ Ar =  iPr₂N-PPV	457 462	666 592	209 130	>300 300
NR ₂ =  Ar =  pipN-PPV	480 476	685 528	205 52	175 250
NR ₂ =  Ar =  H ₁₃ C ₆ C ₆ H ₁₃ pipN-PFV	480 483	640 561	160 78	≈300 <200

The electronic influence of the aryl and amino groups on the three polymers can be appreciated by comparing their λ_{\max} . Based on the thin film results, an overall bathochromic effect in the absorption and emission is observed, by changing the amino group from diisopropylamino to piperidine in the polymers. This effect may be due to the bulkiness of the diisopropyl groups, which prevents interaction of the amino lone pair of electrons with the $\pi_{C=C}$ double bond. Another bathochromic shift is observed in emission and absorption when the aryl moiety is changed from phenyl to fluorene. This may be due to the structure of the fluorene that induces higher planarity along the polymer chains and has a longer π -system, which thus increases the conjugation along the polymer backbone.

Chapter III: Synthesis of amino-PPV by metal free dimerization/polymerization of novel bis-aminoarylcarbenes

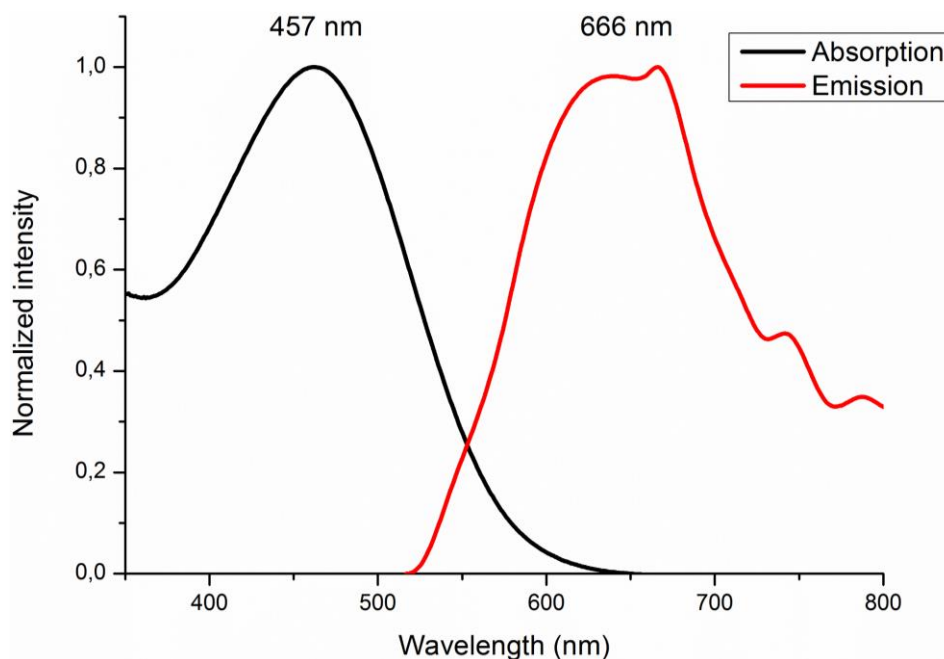


Figure III.9. Absorption and emission of polymer **iPr₂N-PPV** in thin film.

The synthetic methodology to our amino-PPV's gave polymers with rather low molar masses (\overline{Mn} between 3000-5900 g.mol⁻¹) as compared to RO-PPV obtained from methodologies discussed in the introduction (\overline{Mn} between 30-200 x 10³ g.mol⁻¹). However, N-PPV's are characterized by a lower dispersity ($D = 2$), as compared to the RO-PPV (2.5-5.7). Looking at their spectroscopic characteristics, the new polymers **iPr₂N-PPV**, **pipN-PPV** and **pipN-PFV** showed red shifted maximum of absorption and emission because of the presence of the amino groups in α position of the double bonds. Indeed, a n- π^* transition was involved in the λ_{\max} of the N-PPV, differing from the π - π^* of the RO-PPV (absorption: $\lambda_{\max} = 462$ vs. 427 nm and emission: $\lambda_{\max} = 592$ vs. 551 nm for **iPr₂N-PPV** and OR-PPV **6**, respectively).

Finally, the presence of nitrogen atoms (adjacent to the C=C double bond) should allow the tuning of their properties by protonation/methylation. The influence of the protonation is investigated in the following part. This was achieved not only on the amino-PPV's but also on the corresponding dimeric model compounds in order to get some insight into the origin of the effects observed in the polymers.

III.4 Physicochemical properties of polymers and their model compounds.

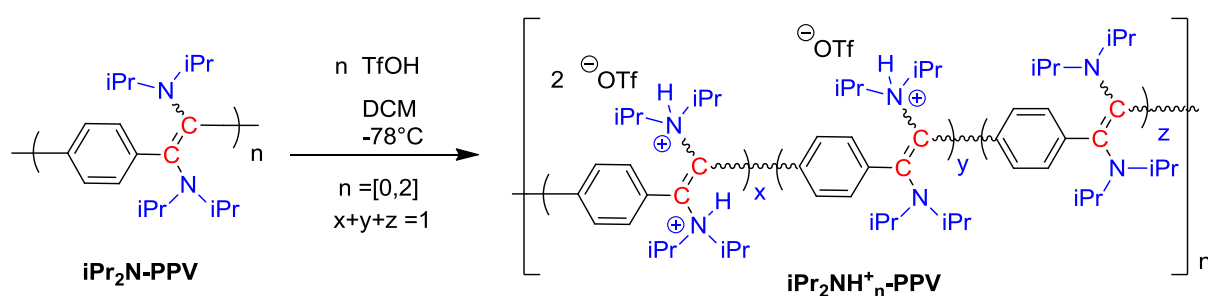
III.4.1 Chemical modifications on the iPr_2N -PPV and iPr_2N -DAA

Amino groups adjacent to C=C bonds were thus subjected to a post-modification through protonation/deprotonation and alkylation reactions, which cannot be achieved with more classical PPV's. Such chemical post-treatments provide an additional mean to vary the properties of the dimeric/polymeric platform.

Protonation of iPr_2N -PPV and iPr_2N -DAA was investigated by UV-Vis following the λ_{max} associated with the $n-\pi^*$ transition using increasing amount of triflic acid.

III.4.1.1 Modification of Polymer iPr_2N -PPV

Addition of one equivalent of triflic acid (TfOH) per nitrogen atom of iPr_2N -PPV in $CHCl_3/ACN$ 50/50 solution (Scheme III.17) induced a hypsochromic effect on the maximum of absorption at $\lambda_{max} = 446$ nm ($n-\pi^*$). A new maximum of absorption at $\lambda_{max} = 352$ nm ($\pi-\pi^*$) also appeared.



Scheme III.17. Synthesis of protonated $iPr_2NH^+_n$ -PPV by addition of increasing amount of triflic acid.

Adding another equivalent of TfOH led to the complete disappearance of the λ_{max} at 446 nm, only the new λ_{max} at 352 nm being observed. Further addition of TfOH did not change the absorption properties of the protonated polymer $iPr_2NH^+_n$ -PPV. As expected, the $\pi-\pi^*$ transition was not affected by the protonation, the $\lambda_{max} = 252$ nm remaining unchanged. Thus, increasing the amount of triflic acid led to an hypsochromic shift of the $n-\pi^*$ maximum of

Chapter III: Synthesis of amino-PPV by metal free dimerization/polymerization of novel bis-aminoarylcabenenes

absorption, with the disappearance of absorption at 446 nm and the appearance of a novel λ_{\max} at 352 nm (π - π^* transition; Figure III.10).

Use of a Brønsted acid, such as trifluoroacetic acid (CF_3COOH), for protonation of **iPr₂N-PPV** did not lead to any change of the λ_{\max} observed by UV/Vis spectroscopy. This could be explained by the fact that CF_3COOH is a too weaker acid to protonate **iPr₂N-PPV** under those conditions.

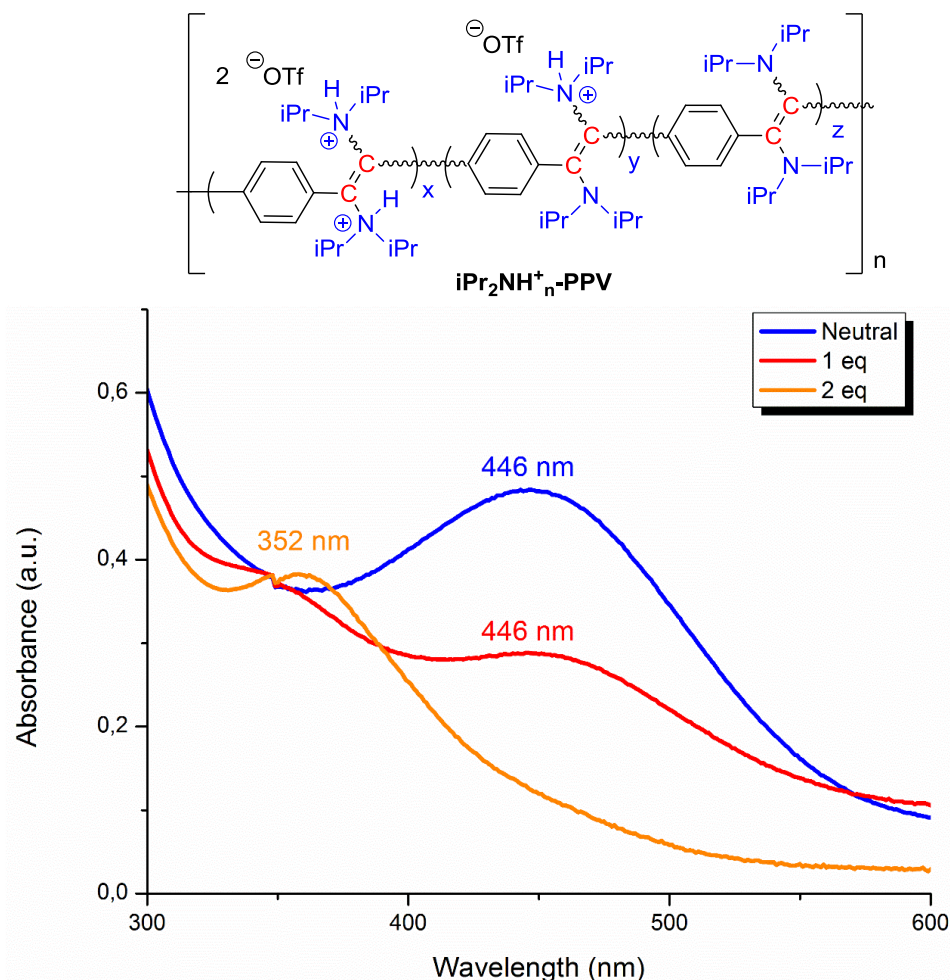


Figure III.10. UV/Vis in $\text{CHCl}_3/\text{CH}_3\text{CN}$ of polymer **iPr₂N-PPV** before and after protonation with 1 or 2 equivalents of triflic acid.

Emission spectroscopy was carried out to evaluate the effect of such modifications. By comparison with the parent neutral polymer **iPr₂N-PPV**, which after irradiation at 462 nm gave a maximum emission peak at $\lambda_{\max} = 592$ nm, compound **iPr₂NH⁺_n-PPV** gave, after irradiation at 352 nm, a blue shifted peak at $\lambda_{\max} = 446$ nm. This might be due to the loss of conjugation

Chapter III: Synthesis of amino-PPV by metal free dimerization/polymerization of novel bis-aminoarylcabenenes

between the double bond and the amino lone pair and to the increased HOMO-LUMO gap upon changing electronic environment of the amino group (from +M to -I).

Further addition of 2.1 equivalents of a strong base, such as *t*-BuOK, to a solution of polymer **iPr₂NH⁺_n-PPV** in chloroform and acetonitrile (50/50) at 0°C did not allow to restore the neutral polymer. In other words, the protonation/deprotonation reaction did not prove reversible. Indeed, only λ_{\max} corresponding to **iPr₂NH⁺_n-PPV** was observed after deprotonation, suggesting the absence of the deprotonation reaction under the employed conditions.

The same sequence of protonation with one equivalent and an excess of acid and deprotonation reactions was also performed with the corresponding dimer **iPr₂N-DAA**.

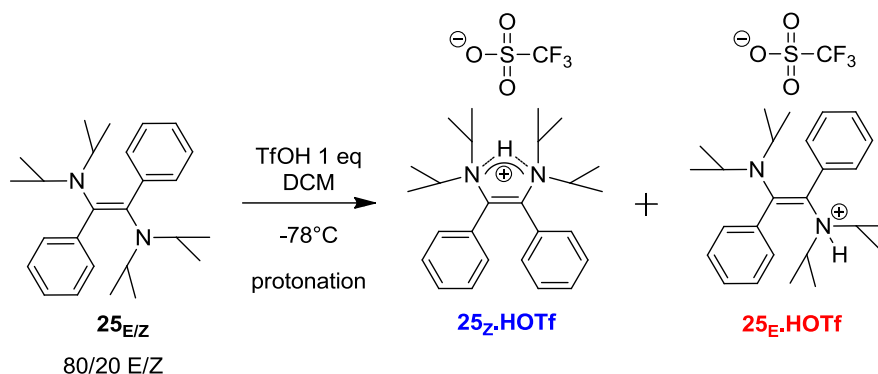
III.4.1.2 Modification of dimer **iPr₂N-DAA**

For better clarity dimer **iPr₂N-DAA** will be denoted as **25**, and the letter Z or E next to the number specifies which isomer is obtained. When **25** is protonated, the notation is as followed: **25_{ZorE}.HOTf** or **25_{ZorE}.(HOTf)₂** for the addition of 1 and 2 eq. of TfOH, respectively.

Addition of one eq. of TfOH onto a DCM solution of **25** at -78°C led to a mixture of two products, according to results obtained by ¹H NMR spectroscopy (Scheme III.18). Protonation of the Z-isomer yielded the corresponding symmetric cationic compound **25_Z.HOTf**, which was notably characterized by a single set of signals for the CH and CH₃iPr protons at 3.83 ppm (³J_{H-H} = 6.6 Hz) and 1.41 ppm, respectively. Due to the C_{2v} symmetry, a highly downfielded signal, corresponding to the acidic N₂H⁺ proton, was also observed at 9.69 ppm.

In contrast, the monoprotonated **25_E.HOTf** isomer was characterized by multiple signals due to the absence of symmetry. In particular, a doublet of septet at 4.30 ppm (³J_{H-H} = 6.5 Hz, ⁵J_{H-H} = 13.0 Hz) and a septet at 3.47 ppm (³J_{H-H} = 6.8 Hz) were observed for the CHiPrN⁺ and CHiPrN, respectively. A doublet of doublet at 1.24 ppm and a doublet at 0.73 ppm were detected for the CH₃iPrN⁺ and CH₃iPrN protons, respectively. A downfielded signal corresponding to the acidic NH⁺ proton was also noted at 5.98 ppm (Figure III.11).

Chapter III: Synthesis of amino-PPV by metal free dimerization/polymerization of novel bis-aminoarylcarbenes



Scheme III.18. Synthesis of **25_{ZorZ}.HOTf** via protonation of **25_{E/Z}** with TfOH (1 eq).

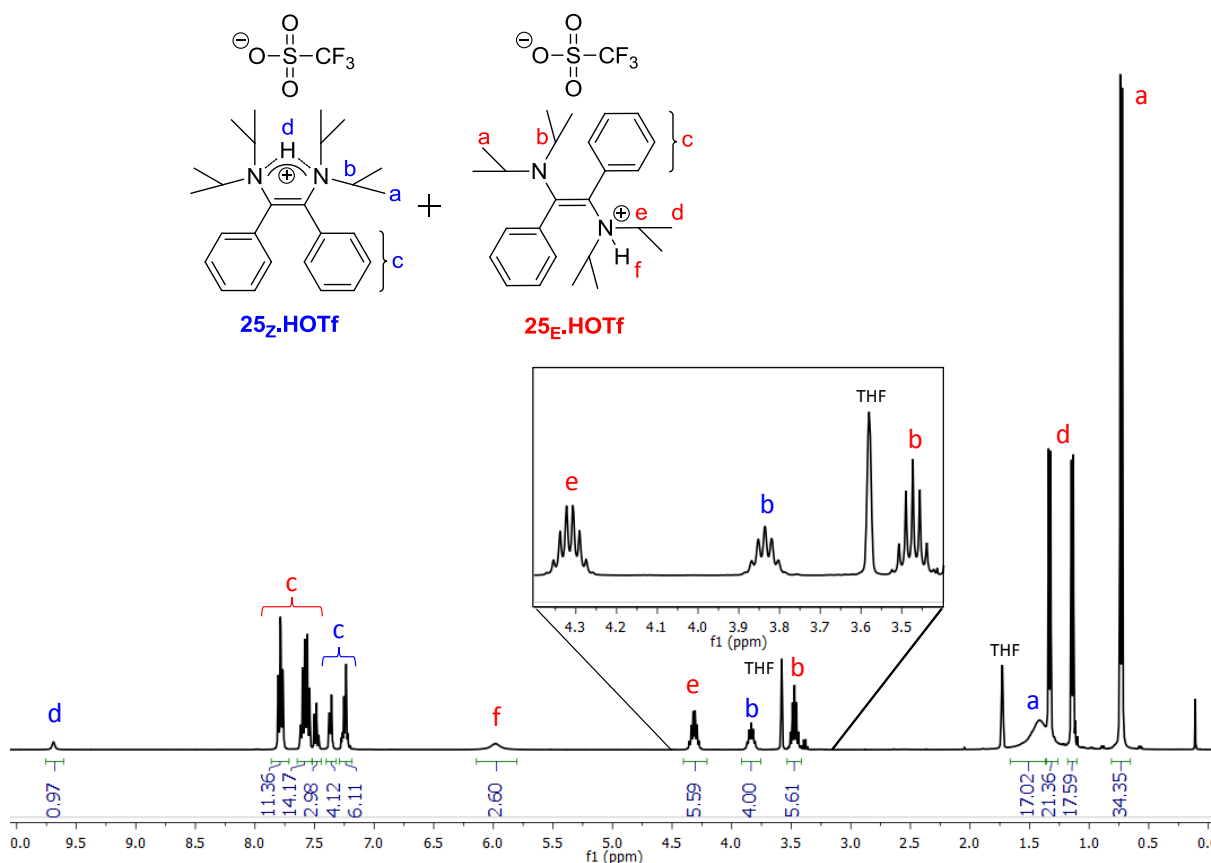


Figure III.11. ¹H NMR (400 MHz) in THF*d*₆ of protonated dimers **26_E.HOTf** and **26_Z.HOTf**.

Vapor diffusion of ether into a CH₃CN solution of protonated **25** led only to crystals of **25_E.HOTf**. The X-Ray analysis gave a N-H bond of 0.83 Å confirming the protonation of one nitrogen atom. The protonation did not influence the structural parameters of the crystal, as compared to free-**25** (C₁-C₂ = 1.35 Å), except for the N₁-C₁ bond longer in **25_E.HOTf** (1.50 Å for **25_E.HOTf** and 1.42 Å for **25**) which might be due to the electron-withdrawing effect of the

Chapter III: Synthesis of amino-PPV by metal free dimerization/polymerization of novel bis-aminoarylcarbenes

ammonium group (Figure III.12). The θ angle corresponds to the angle between the lone pair of nitrogen and the π orbital of the double bond. The more acute the angle was, the better the conjugation between these orbitals was.

Despite several attempts to crystallize **25_Z.HOTf**, no single crystals could be grown. However, the identity of **25_Z.HOTf** could be indirectly confirmed with the synthesis of **25_Z.HNTf₂** using a similar protonation procedure, utilizing Tf₂NH instead of TfOH. X-Ray analysis confirmed the structure of the Z-isomer and revealed that the parameters found were similar to **25** and **25_E.HOTf**, indicating that the protonation had virtually no structural influence. Indeed, the C=C bond length proved similar to **25** (1.35 Å). Protonation was evidenced on one nitrogen atom (N₁-H = 0.98 Å). Moreover, the Z-isomer showed a θ angle of 90° preventing any interaction between the amino groups and the C=C double bond (Figure III.13).

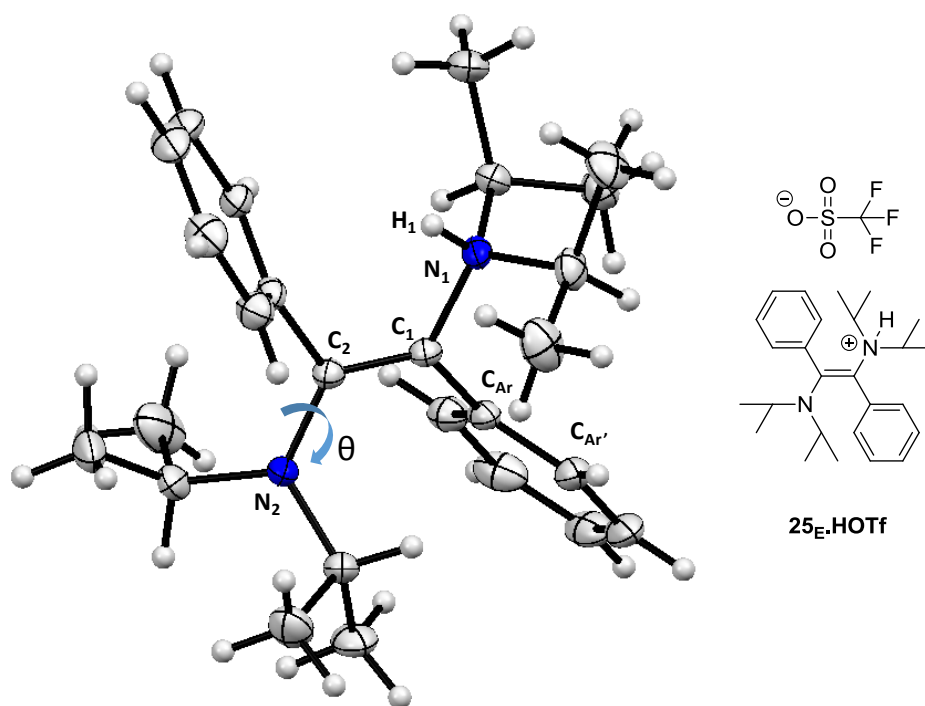


Figure III.12. X-Ray diffraction studies on compound **25_E.HOTf**; the counter anion triflate (TfO⁻) was omitted for clarity.

C₁-C₂ = 1.35 Å; C₁-C_{Ar} = 1.49 Å; C₂-C_{Ar} = 1.50 Å; N₁-H = 0.83 Å; N₁-C₁ = 1.50 Å; N₂-C₂ = 1.39 Å;
C_{Ar}'-C_{Ar}-C₁-C₂ = 70°; Σ N₂ = 360°; θ = 52°.

Chapter III: Synthesis of amino-PPV by metal free dimerization/polymerization of novel bis-aminoarylcarbenes

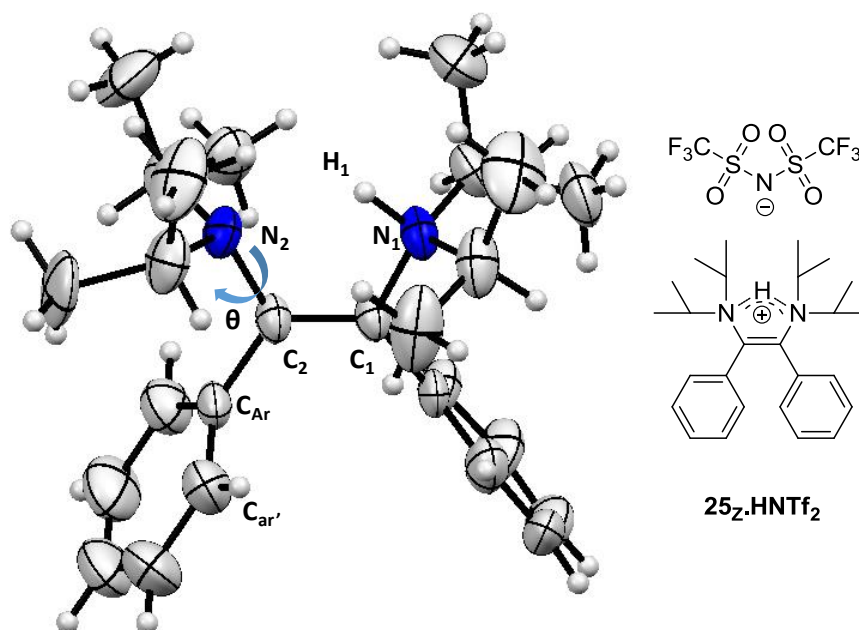
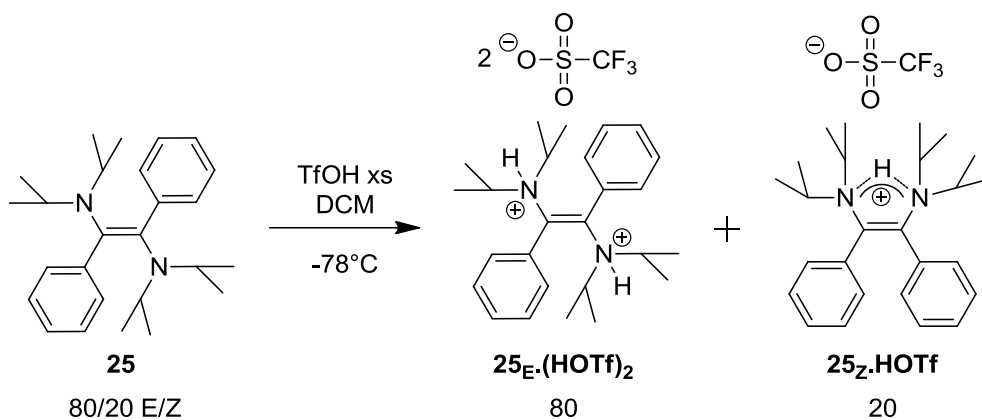


Figure III.13. X-Ray diffraction studies on compound **25_z.HNTf₂**; the counter anion trifluoromethanesulfonimide (NTf_2^-) was removed for clarity. The proton modeled was shown on nitrogen N_1 but calculations indicate that the probability of its presence on each nitrogen atoms is equivalent. $\text{C}_1\text{-C}_2 = 1.34 \text{ \AA}$; $\text{C}_1\text{-C}_{\text{Ar}} = 1.50 \text{ \AA}$; $\text{C}_2\text{-C}_{\text{Ar}} = 1.50 \text{ \AA}$; $\text{N}_{1\text{or}2}\text{-H} = 0.98 \text{ \AA}$; $\text{N}_1\text{-C}_1 = 1.47 \text{ \AA}$; $\text{N}_2\text{-C}_2 = 1.46 \text{ \AA}$; $\text{C}_{\text{Ar}'}\text{-C}_{\text{Ar}}\text{-C}_1\text{-C}_2 = 73^\circ$; $\theta = 90^\circ$; $\Sigma\text{N}_2 = \Sigma\text{N}_1 = 340$.

Addition, dropwise, of an excess of TfOH to a dichloromethane solution of compound **25** (which exists as a 80/20 mixture of E/Z isomer) at -78°C led to the clean formation of two compounds (Scheme III.19). According to ^1H NMR analysis, the fraction soluble in THF contains the **25_z.HOTf** isomer. The ^1H NMR spectrum of the fraction insoluble in THF is shown in Figure III.14. The compound likely corresponds to the symmetric doubly protonated E-isomer, given the few signals observed. The characteristic broad singlet signal at 6.74 ppm corresponds to the NH^+ groups. The CH_3iPr doublet at 1.29 ppm ($^3\text{J}_{\text{H-H}} = 6.9 \text{ Hz}$) and the CHiPr at 4.03 ppm ($^3\text{J}_{\text{H-H}} = 6.6 \text{ Hz}$) can be attributed to the four isopropyl groups on the molecule. These signals further confirmed the symmetry of **25_E.(HOTf)₂** (see Figure III.14). Moreover, analysis by ^{13}C NMR spectroscopy revealed the carbon signal of the $\text{C}=\text{C}$ bond at 123.16 ppm, which was actually shielded by 20 ppm in comparison to compound **25_E** (140.68 ppm; Figure III.15).

Chapter III: Synthesis of amino-PPV by metal free dimerization/polymerization of novel bis-aminoarylcarbenes



Scheme III.19. Protonation in DCM of a dimer **25** with an excess of TfOH leading to two clear compounds **25_E.(HOTf)₂** and **25_Z.HOTf**.

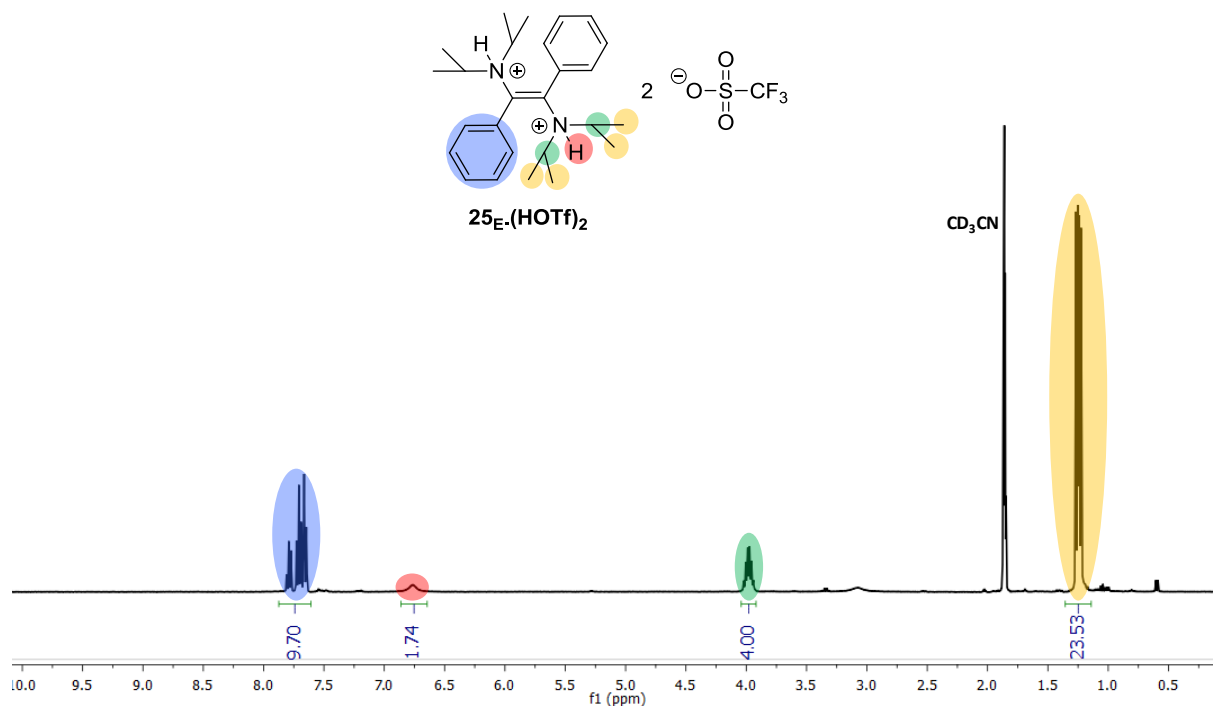


Figure III.14. ^1H NMR (400 MHz) spectra in CD_3CN of compound **25_E.(HOTf)₂** after extraction.

Chapter III: Synthesis of amino-PPV by metal free dimerization/polymerization of
novel bis-aminoarylcarbenes

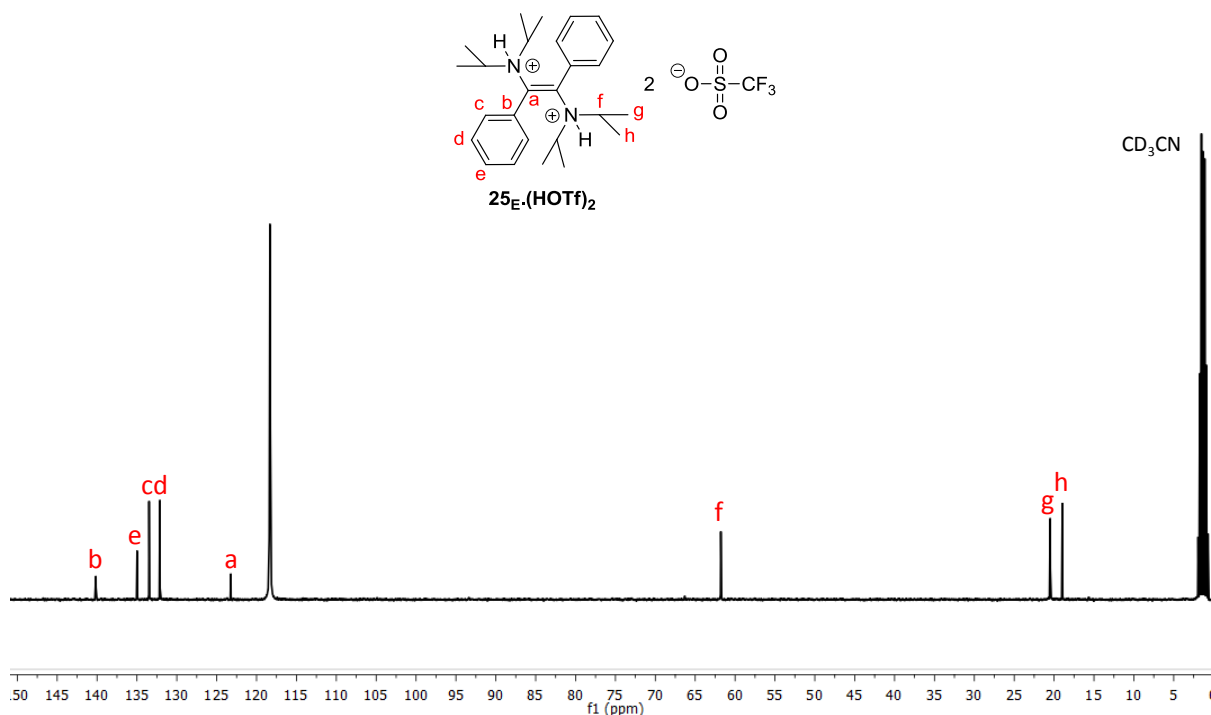


Figure III.15. ^{13}C NMR (101 MHz) in CD_3CN of isolated compound $25_{\text{E}}\cdot(\text{HOTf})_2$.

Single crystals of $25_{\text{E}}\cdot(\text{HOTf})_2$ could be grown by vapor diffusion of THF into a CH_3CN solution of protonated $25_{\text{E}}\cdot(\text{HOTf})_2$. X-Ray analysis confirmed the structure of $25_{\text{E}}\cdot(\text{HOTf})_2$, in particular with both amino groups protonated in a *E*-configuration ($\text{C}=\text{C}$ bond of 1.34 Å). The structural parameters were found similar to those of **25** (Figure III.16).

Chapter III: Synthesis of amino-PPV by metal free dimerization/polymerization of novel bis-aminoarylcarbenes

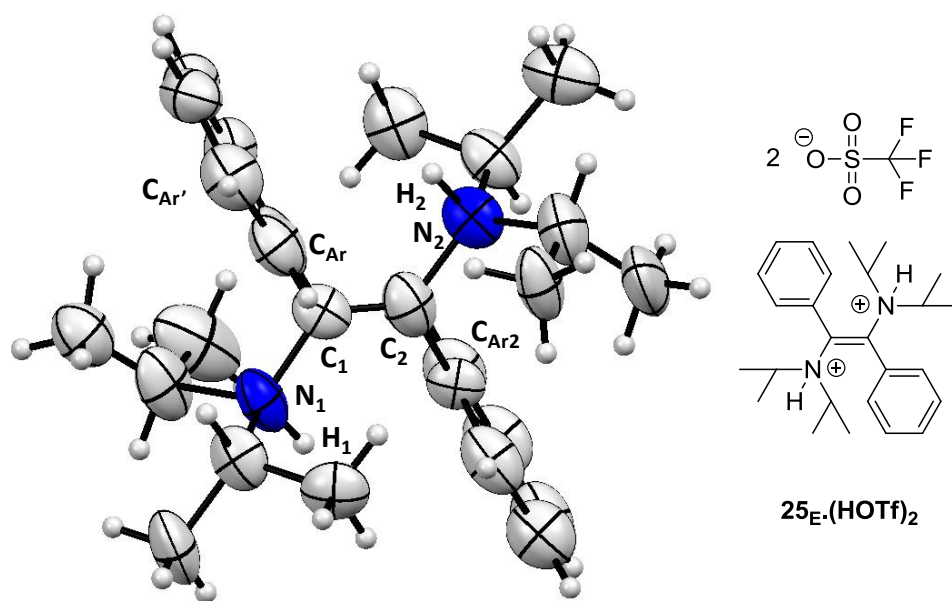
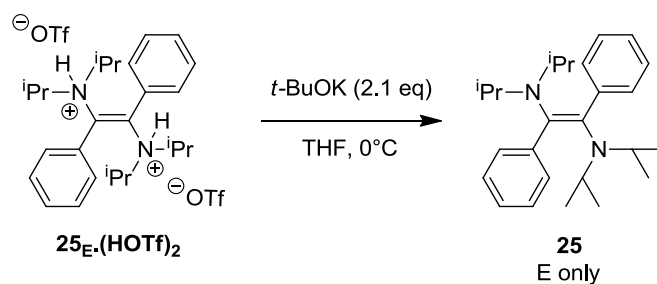


Figure III.16. X-Ray diffraction studies of compound **25_E.(HOTf)₂**; the counter anion triflate (⁻OTf) was omitted for clarity. C₁-C₂ = 1.34 Å; C₁-C_{Ar} = 1.56 Å; C₂-C_{Ar} = 1.40 Å; N_{1or2}-H = 0.98 Å; N₁-C₁ = 1.49 Å; N₂-C₂ = 1.49 Å; C_{Ar'}-C_{Ar}-C₁-C₂ = 80°.

The reversibility of the protonation reaction was investigated on **25_E.(HOTf)₂** under the same experimental conditions than those used for protonated polymers **iPr₂NH⁺-PPV**. For this purpose, *t*-BuOK was added on compound **25_E.(HOTf)₂** in THF at 0°C (Scheme III.20). The initial white powder of **25_E.(HOTf)₂** turned yellow upon drying. However, the resulting compound showed only signals of the *E*-isomer of the starting diaminoalkene **25** (Figure III.17) by ¹H NMR spectroscopy in THF_{d6}.



Scheme III.20. Deprotonation of bis-protonated **25_E.(HOTf)₂** via addition of *t*BuOK (2.1 eq).

Chapter III: Synthesis of amino-PPV by metal free dimerization/polymerization of novel bis-aminoarylcarbenes

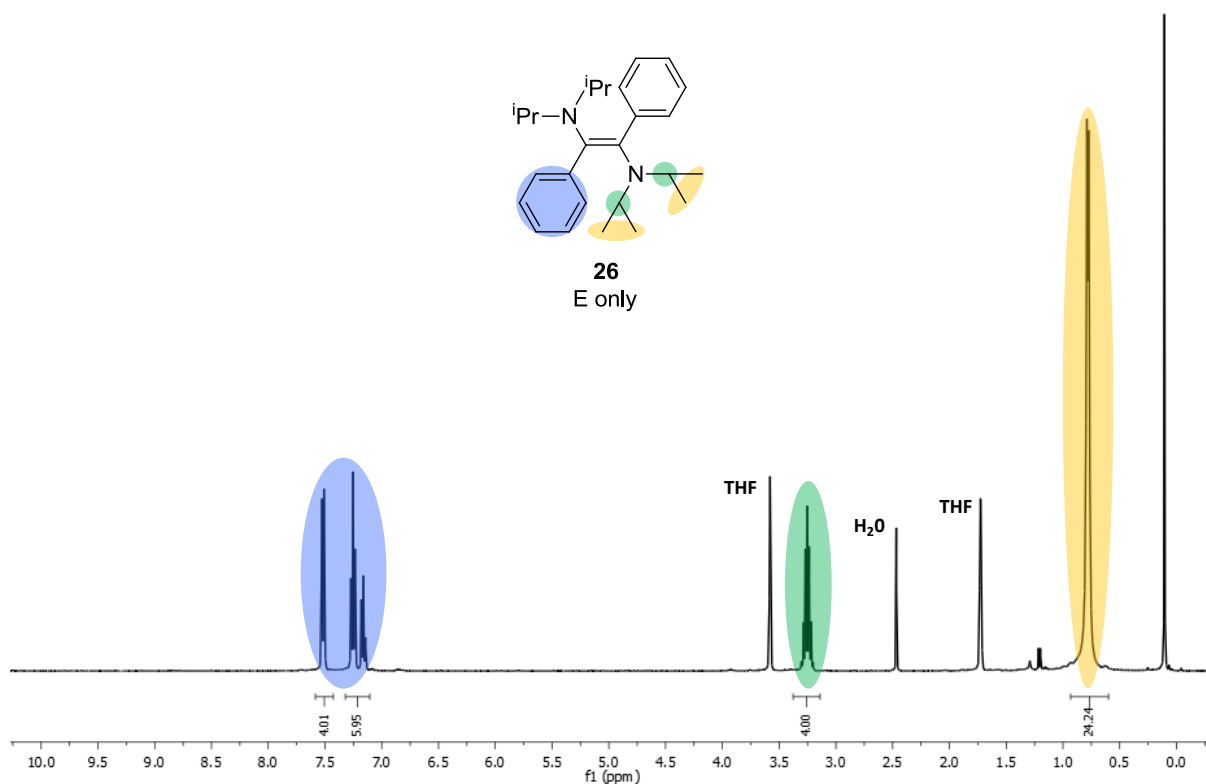


Figure III.17. ^1H NMR (400 MHz) in THF_{d6} of clean E -isomer 25_E after deprotonation of $25_E \cdot (\text{HOTf})_2$ by a strong base $t\text{-BuOK}$.

The protonation/deprotonation reaction sequence could also be followed by UV-Vis spectrometry in CH_3CN . After deprotonation of $25_E \cdot (\text{HOTf})_2$, the maximum of absorption of compound 25 was recovered with $\lambda_{\text{max}} = 386$ nm, supporting that the process was indeed reversible (Figure III.18). This result suggests that, in the case of the polymer $i\text{Pr}_2\text{NH}^+\text{-PPV}$ discussed above, deprotonation could not be achieved likely to a particular conformation adopted by the polymer chains. Such a behavior has already been reported by Schwartz *et al.* with the experiment on protonated poly(2,5-bis[N-methyl-N-hexyl amino]phenylenevinylene) (Figure III.19), on the basis of dynamic light scattering measurements.⁶³

Chapter III: Synthesis of amino-PPV by metal free dimerization/polymerization of novel bis-aminoarylcarbenes

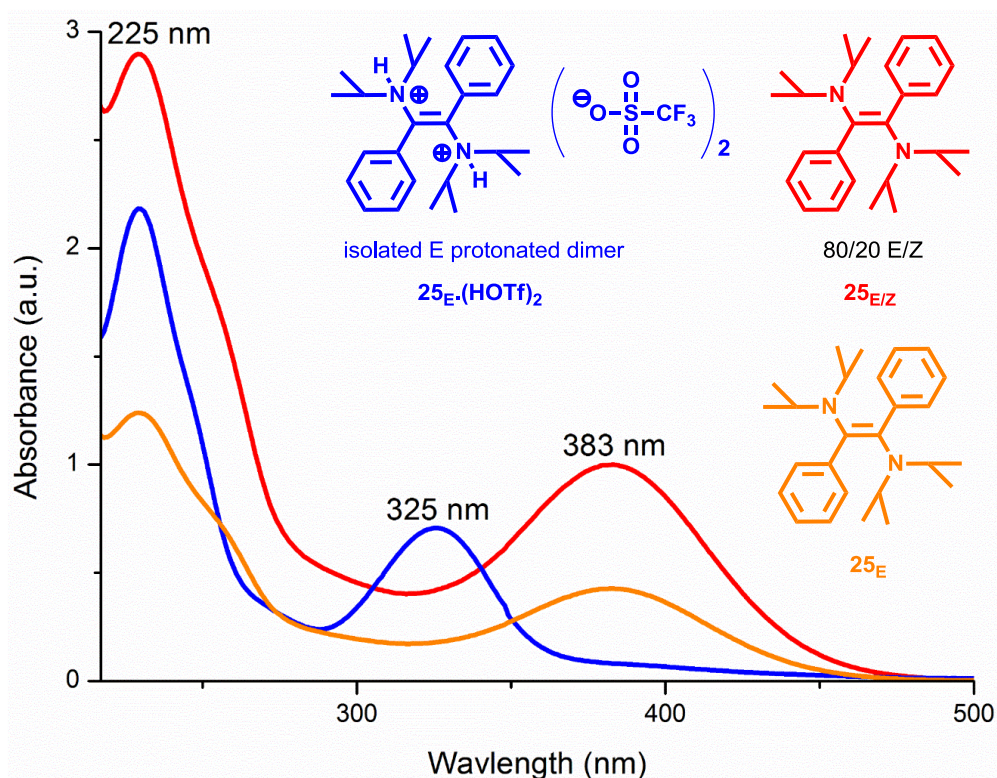


Figure III.18. UV-Vis experiments in CH_3CN of compounds **25** before protonation (red curve), after deprotonation (orange curve), and **26_E.(HOTf)₂** (blue curve). The curves in orange and red have the same maximum of absorptions with $\lambda_{\text{max}} = 225$ and 383 nm.

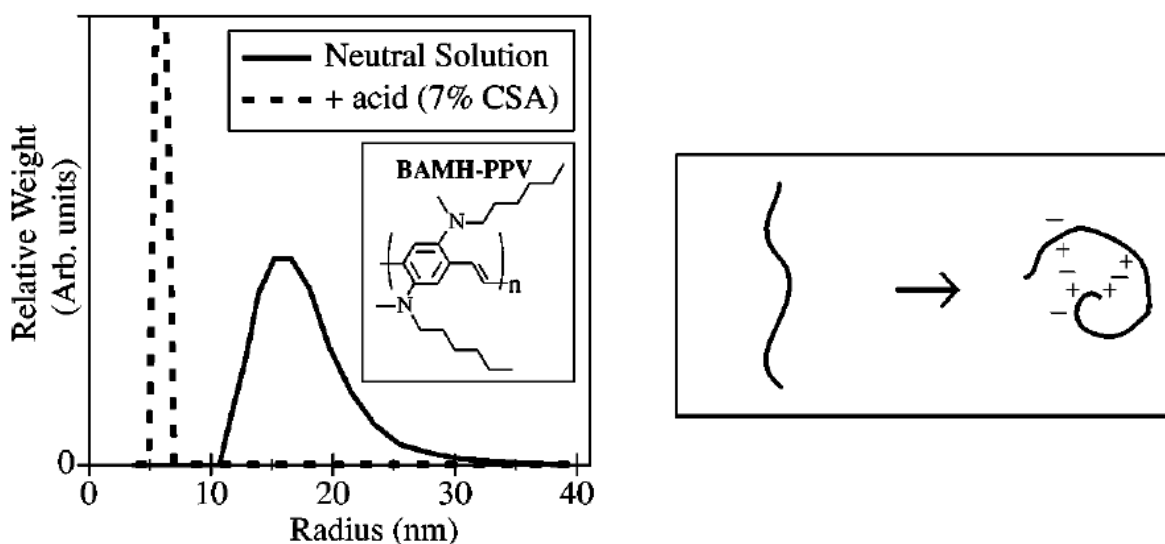


Figure III.19. Relationship between protonation and chain conformation in solution. Top panel: Dynamic light scattering size distributions \sim hydrodynamic radii for dilute neutral (solid curve) and protonated (7% w/w CSA, dashed curve) solutions of BAMH-PPV. The inset shows the chemical structure of BAMH-PPV. Lower panel: Schematic illustration of the conformational change of a charged

Chapter III: Synthesis of amino-PPV by metal free dimerization/polymerization of novel bis-aminoarylcarbenes

ionomer in nonpolar solution. Protonation increases the charge along the backbone of the open chain coil, causing the coil to collapse to minimize exposure of the both the backbone charges and counter ions to the nonpolar environment (reproduced from Schwartz *et al.*).⁶³

III.4.1.3 Optical properties

Experimental investigation of the electronic properties of the protonated compounds

Protonated compounds were analyzed by UV-Vis spectroscopy in acetonitrile in an inert atmosphere of argon at 5×10^{-2} M. Changing the neutral amino group, having a +M effect (donor group), to an electron-withdrawing group (-I) was expected to modify the intrinsic properties of these compounds. As expected, the π - π^* transition ($\lambda_{\max} = 259$ nm) associated to the aryl moiety was evidenced for all compounds. No change was noted from the neutral diaminoalkene **25** to the monoprotinated **25_Z.HOTf**, **25_E.HOTf**, and to the bis-protonated **25_E.(HOTf)₂**. In the latter case, the UV/Vis spectra showed the disappearance of the maximum of absorption at $\lambda_{\max} = 383$ nm in **25** (n - π^*) with a novel blue shifted maximum of absorption at $\lambda_{\max} = 325$ nm (π - π^* ; Figure III.20).

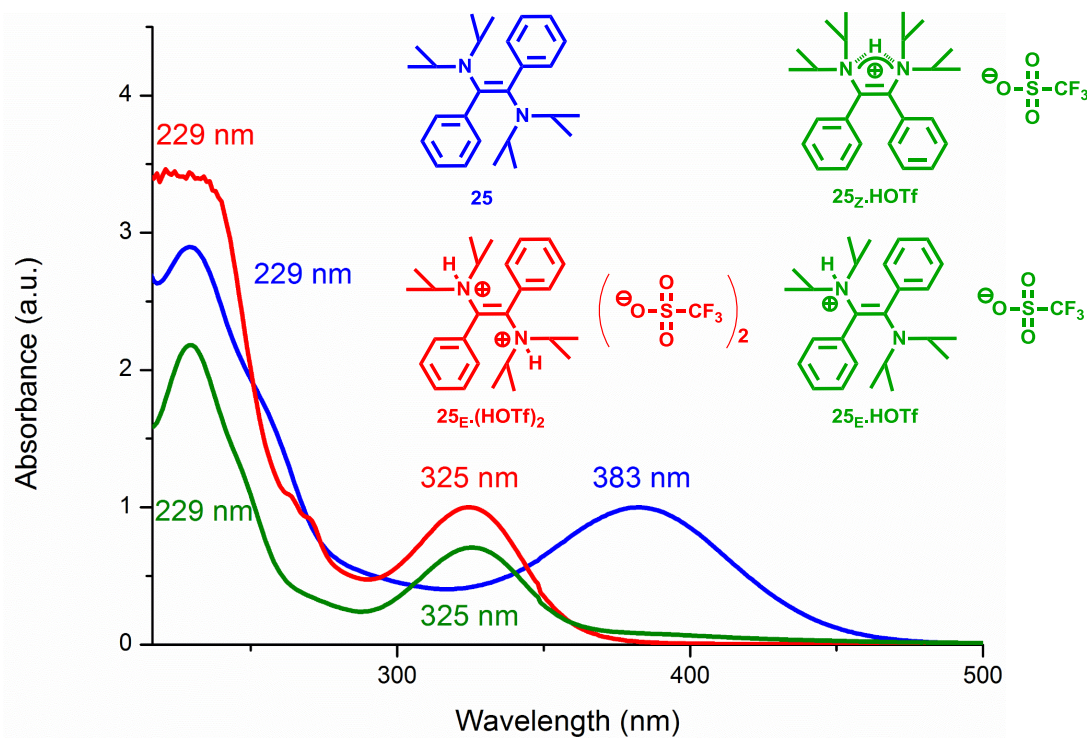


Figure III.20. UV-Vis in CH₃CN of neutral dimer **25** and protonated compounds **25_Z.HOTf**, **25_E.HOTf** and **25_E.(HOTf)₂** in solution.

Chapter III: Synthesis of amino-PPV by metal free dimerization/polymerization of novel bis-aminoarylcarbenes

For compounds **25_Z.HOTf** and **25_E.HOTf**, the same phenomenon to that of **25_E.(HOTf)₂** was observed despite the presence of one neutral amino group. This result means that there is no apparent interaction between the neutral amino group (n) and the π_{c-c} system, which might come from the very weak overlapping between the n and π_{c-c} due to tilting of the amino group around the N₂-C₂ bond ($\theta = 90^\circ$ for **25_Z.HOTf**, 52° for **25_E.HOTf** and 52° for **25**; Figure III.21). Surprisingly, the θ angle proved to be similar in the solid state for **25_E.HOTf** and **25** despite a different maximum of absorption observed experimentally. It can be proposed that, in the liquid state, **25_E.HOTf** cannot reach a lower value of θ by rotation around the N₂-C₂ bond compared to **25**, which would allow the conjugation and thus the n- π^* transition (Figure III.21). However, the interaction between the lone pair of the nitrogen atom and the p π orbitals of the double bond seems feasible as shown by calculation (see next part). The comparison is hard to be made though because of the different conditions used to perform the calculations compared to the experimental ones (*i.e.* the molecule is in the void, the counter anion is omitted and solvation effect is not included).

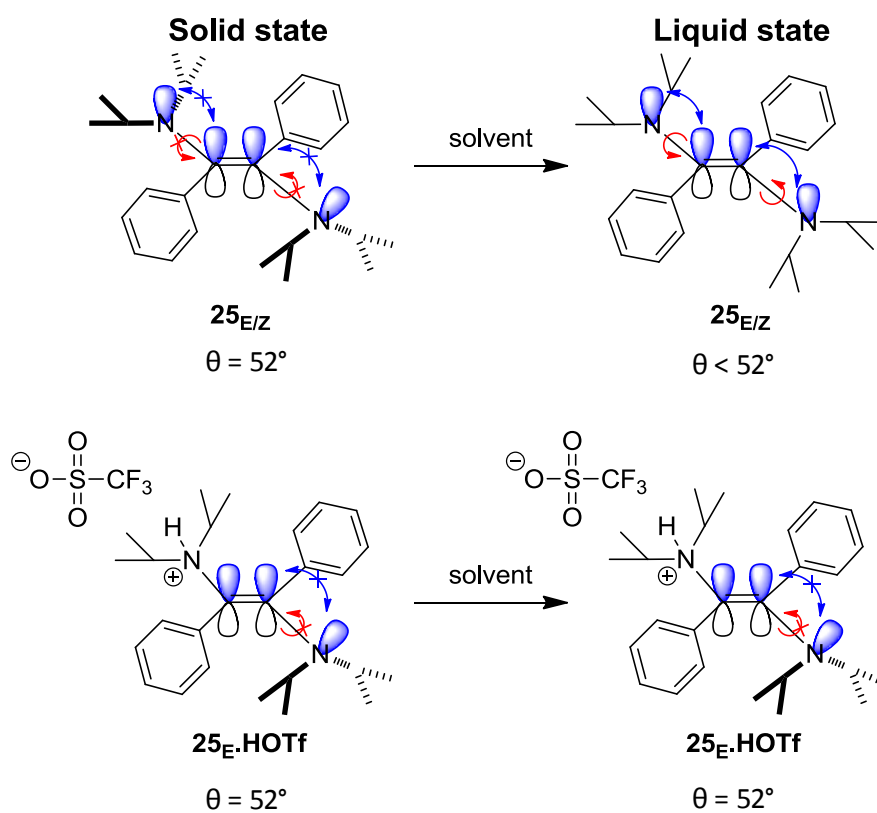


Figure III.21. Proposed mechanism to explain the absence of n- π^* star transition based on the absence of θ rotation in solution of **25_E.HOTf**. The interaction between the lone pair of the nitrogen atoms and

Chapter III: Synthesis of amino-PPV by metal free dimerization/polymerization of novel bis-aminoarylcarbenes

the $p\pi$ orbitals of the double bond is represented by a blue arrow. The rotation around the $C_{C=C}$ carbon atom and the nitrogen atom is represented by a red arrow. The dihedral angle $n_N-N-C_{C=C}-\pi_{C=C}$ is the θ angle.

The effect of protonation on the fluorescence properties on dimer **25** was also assessed using emission spectroscopy. Irradiation of **25**_E·(HOTf)₂ at its maximum of absorption ($\lambda_{max} = 325$ nm) gave a blue shifted emission peak at 446 nm, compared to the neutral dimer **25** ($\lambda_{max} = 540$ nm) (Figure III.22). Although the protonation of dimer **25** did not impact the geometrical parameters, as shown by X-ray diffraction studies, both absorption and emission properties are deeply affected.

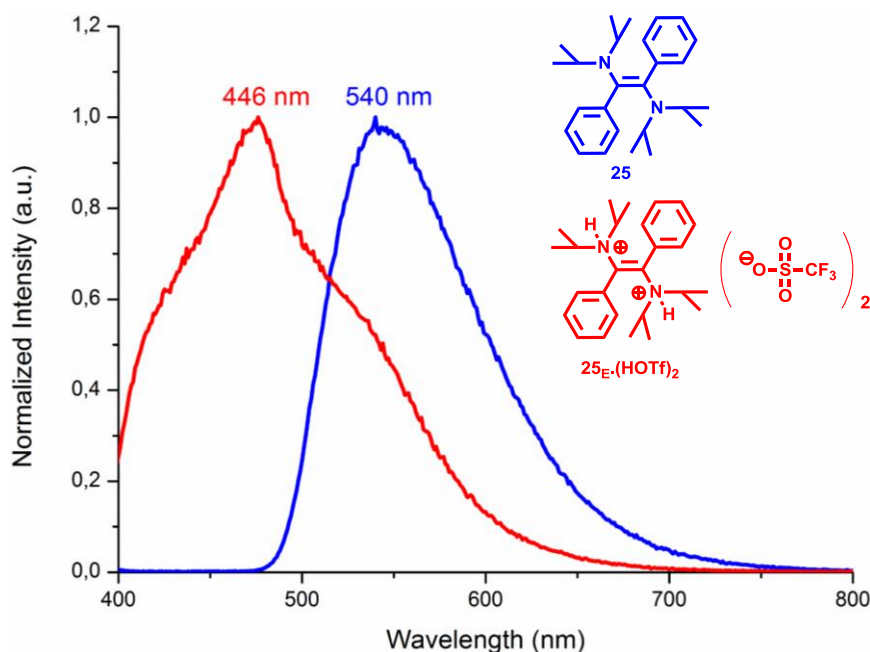


Figure III.22. Emission spectroscopy in CH_3CN of neutral compound **25** and protonated compound **25**_E·(HOTf)₂ in solution.

Theoretical investigation on the electronic properties of the protonated diisopropyl dimer by DFT calculations

To gain more insight into the influence of protonation over electronic properties, DFT calculations were performed, in collaboration with Dr. K. Miqueu and Dr. J. M. Sotiropoulos (IPREM, Pau) at the CAM-B3LYP/6-311++G** level of theory, while the geometry of all compounds was optimized with B3LYP/def2-SVP.

Chapter III: Synthesis of amino-PPV by metal free dimerization/polymerization of novel bis-aminoarylcarbenes

All structural parameters of compounds **XXV_E**, **XXV_E.HOTf** and **XXV_E.(HOTf)₂** proved to fit with parameters obtained experimentally, *i.e.* bond lengths (*e.g.* $d_{C=C} = 1.37 \text{ \AA}$) and angles (dihedral, $\Sigma N = 360^\circ$, $\theta = 53^\circ$). DFT calculations thus allowed us to gain more information about the nature of HOMO and LUMO orbitals and the energy gap (λ_{max}).

Firstly, the LUMO of all compounds was found to be localized on the same orbitals ($\pi_{C=C}$ and π_{ary}), hence with an energy that was virtually the same. Therefore, the energy gap (λ_{max}) was thus, only influenced by the position of the HOMO.

For the bis-protonated **XXV_E.(HOTf)₂**, the HOMO was localized only on the $\pi_{C=C}$ orbitals, as each nitrogen atom had its lone pair of electrons engaged in bonding with an hydrogen atom. Thus the HOMO was characterized by lowest energy gap calculated with a λ_{max} at 254 nm.

For the mono-protonated **XXV_E.HOTf**, the HOMO was localized on one nitrogen lone pair and on the $\pi_{C=C}$ orbitals ($n_N-\pi_{C=C}$). Thus, the gap should decrease slightly, as confirmed by calculations with a λ_{max} at 317 nm.

For **XXV_E**, the HOMO was localized on the nitrogen lone pairs and the C=C bond orbital ($n_N-\pi_{C=C}$). The contribution of the two nitrogen atoms should affect the gap by lowering it even more. This was confirmed by the lowest gap found with a λ_{max} at 371 nm.

Those results, however, are in contradiction with experimental results, since both the mono and the bis-protonated dimers showed the same gap ($\lambda_{\text{max}} = 325 \text{ nm}$). This could be explained by the poor overlapping between the n_N orbital and the $\pi_{C=C}$ of **XXV_E.HOTf** in solution, as highlighted in Figure III.23.

Chapter III: Synthesis of amino-PPV by metal free dimerization/polymerization of novel bis-aminoarylcarbenes

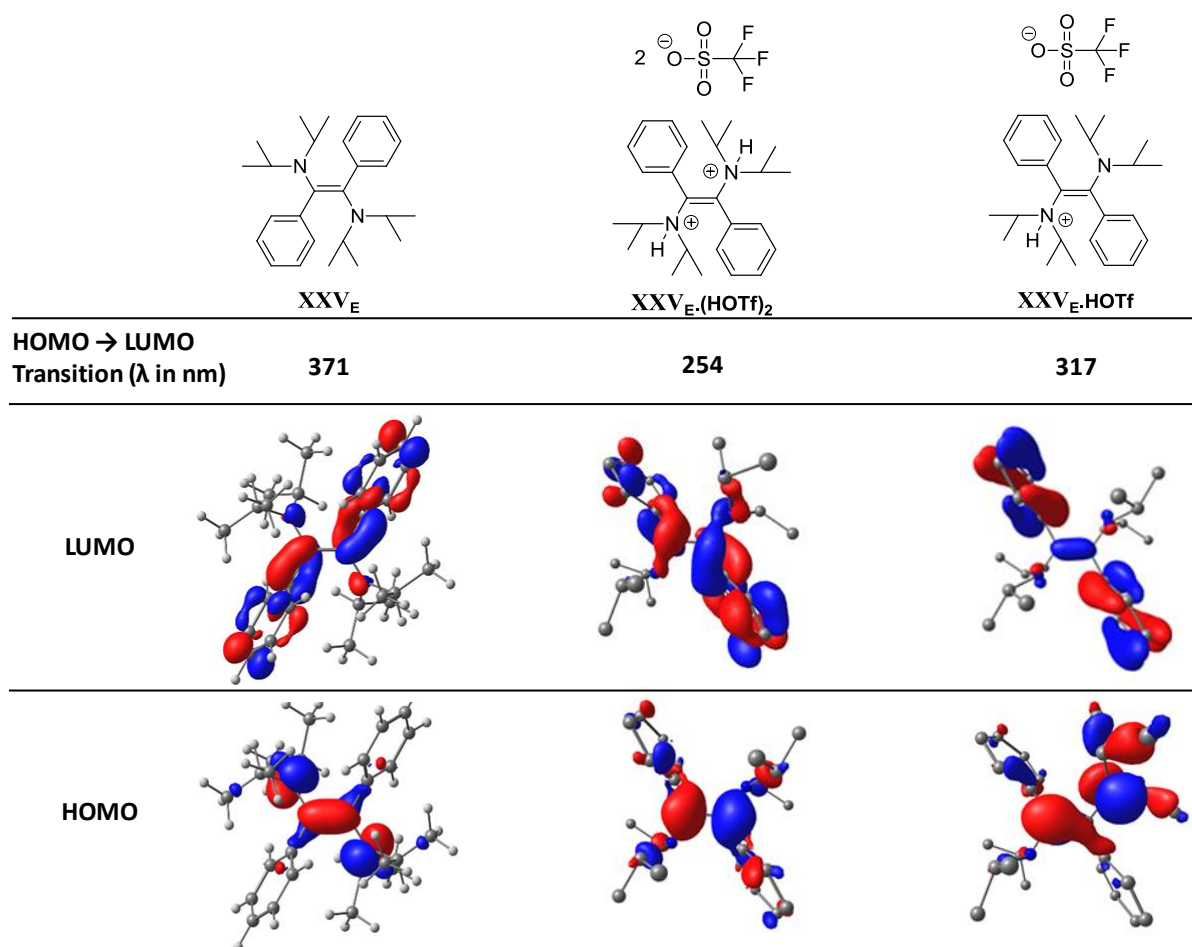
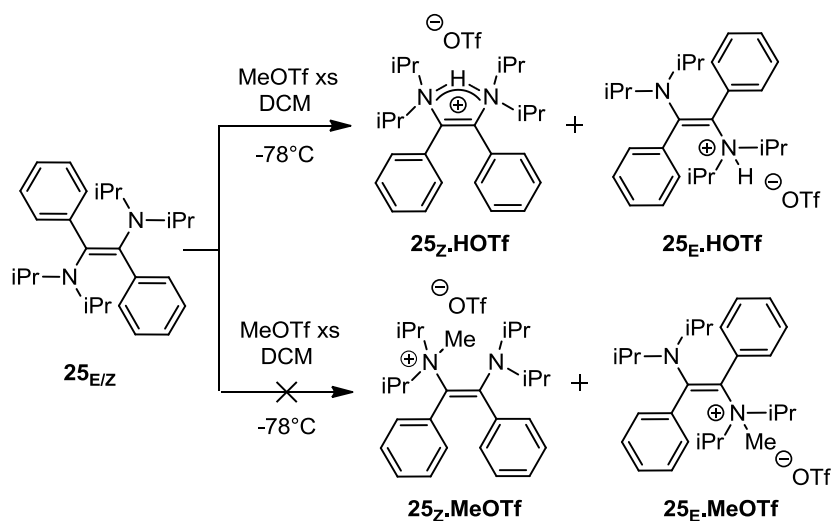


Figure III.23. HOMO → LUMO excitation energy (λ) at CAM-B3LYP/6-311++G** level of theory on the geometry optimized at B3LYP/def2-SVP of compound **XXV_E**, **XXV_E.HOTf** and **XXV_E.(HOTf)₂** and their electronic density structure.

III.4.1.4 Methylation of dimer **iPr₂N-DAA**

To explore the possible generality of the chemical transformation of amino groups, methylation of **25** was investigated. Addition of excess MeOTf (10 eq) on dimer **25** in DCM at -78°C to room temperature led to a white powder. Instead of the expected methylated product **25_{Z/E}.MeOTf**, however, only the mono-protonated **25_Z.HOTf** and **25_E.HOTf** isomers were isolated, according to the results obtained by ¹H NMR spectroscopy. This result suggests that diisopropyl substituents on the amino groups are too bulky to enable the methylation. Protonation in this case likely resulted from a slow hydrolysis of MeOTf into TfOH (Scheme III.21).

Chapter III: Synthesis of amino-PPV by metal free dimerization/polymerization of novel bis-aminoarylcabenenes



Scheme III.21. Attempted methylation with excess MeOTf, leading to product **25_e.HOTf** and **25_z.HOTf** instead of methylated compound **26_{Ez}.MeOTf**.

In summary, UV/Vis analysis evidenced significant changes of the physicochemical properties of polymer **iPr₂N-PPV** and dimer **iPr₂N-DAA** upon protonation with one equivalent or an excess of triflic acid. Protonation of **iPr₂N-PPV** led to a blue shift with a maximum absorption starting from $\lambda_{\text{max}} = 446$ nm to 352 nm. The same reaction was performed on the dimer homologue to understand such a behavior. A similar blue shift was observed ($\lambda_{\text{max}} = 383$ nm to 325 nm). Both the mono and the bis-protonated dimers could be crystallized giving insight in the structural parameters. It could be concluded that if protonation did not affect the structural parameters, it had a significant impact on the absorption and emission parameters. Indeed, loss of the $n-\pi^*$ transition was noted for the bis-protonated dimer, while the remaining neutral amino group does not seem to interact with the π_{cc} system in the case of the mono-protonated dimer, which may be due to a wide θ angle. These experimental results were supported by DFT calculations. In contrast experimental findings were distinct from results determined theoretically regarding the maximum of absorption of both the bis- and the mono-protonated dimers. In the latter case, a lower maximum of absorption was calculated in comparison to that found experimentally.

Protonation proved a reversible process only in the case of the dimer, as the protonated polymer homologue could not be restored into its neutral form in presence of a strong base. To explain this distinct behavior between the dimer and the polymer, we hypothesized that the

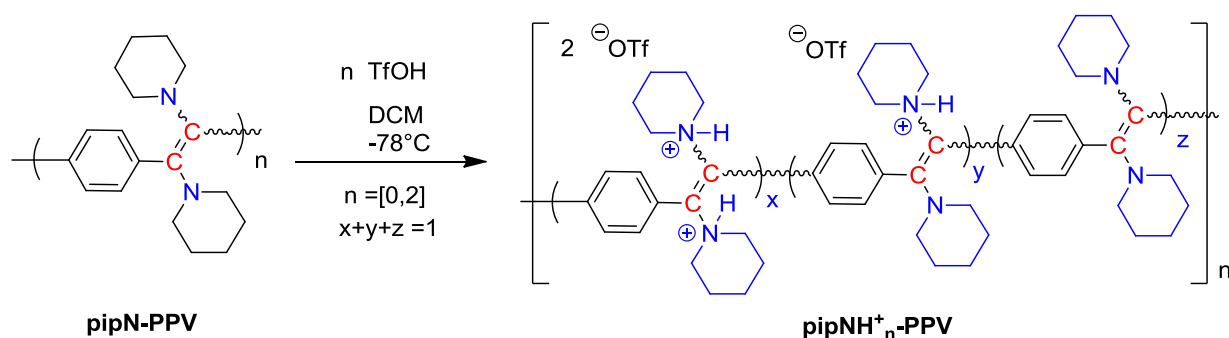
Chapter III: Synthesis of amino-PPV by metal free dimerization/polymerization of novel bis-aminoarylcabenenes

polymer might adopt a peculiar conformation preventing the access of the base to the protonated amino groups. Finally, attempts to methylate the dimer was not successful, likely because of some steric hindrance brought by the diisopropyl substituents. The next section discusses similar investigations performed on NPPV's featuring the piperidine substituent on the nitrogen atom.

III.4.2 Chemical modifications on the pipN-PPV and pipN-DAA

III.4.2.1 Modification of Polymer pipN-PPV

Physicochemical modifications on the polymer **pipN-PPV** with piperidine substituents in α -position of the C=C bond was also investigated. The same protocol for **iPr₂N-PPV** was applied on **pipN-PPV** (Scheme III.22). Remarkably, an entirely distinct behavior was observed for **pipN-PPV** upon gradually adding triflic acid. In this case, indeed, the direct disappearance of the $n-\pi^*$ transition ($\lambda_{\max} = 484$ nm) was observed by UV/Vis analysis. Moreover, no novel λ_{\max} could be observed as in the case of **iPr₂N-PPV**, suggesting a loss of conjugation in **pipN-PPV**. In fact, only the $\pi-\pi^*_{\text{arom}}$ transition remained, with a maximum of absorption around 255 nm (Figure III.24).



Scheme III.22. Synthesis of **pipNH⁺_n-PPV** by addition of increasing amount of triflic acid.

Chapter III: Synthesis of amino-PPV by metal free dimerization/polymerization of novel bis-aminoarylcaben

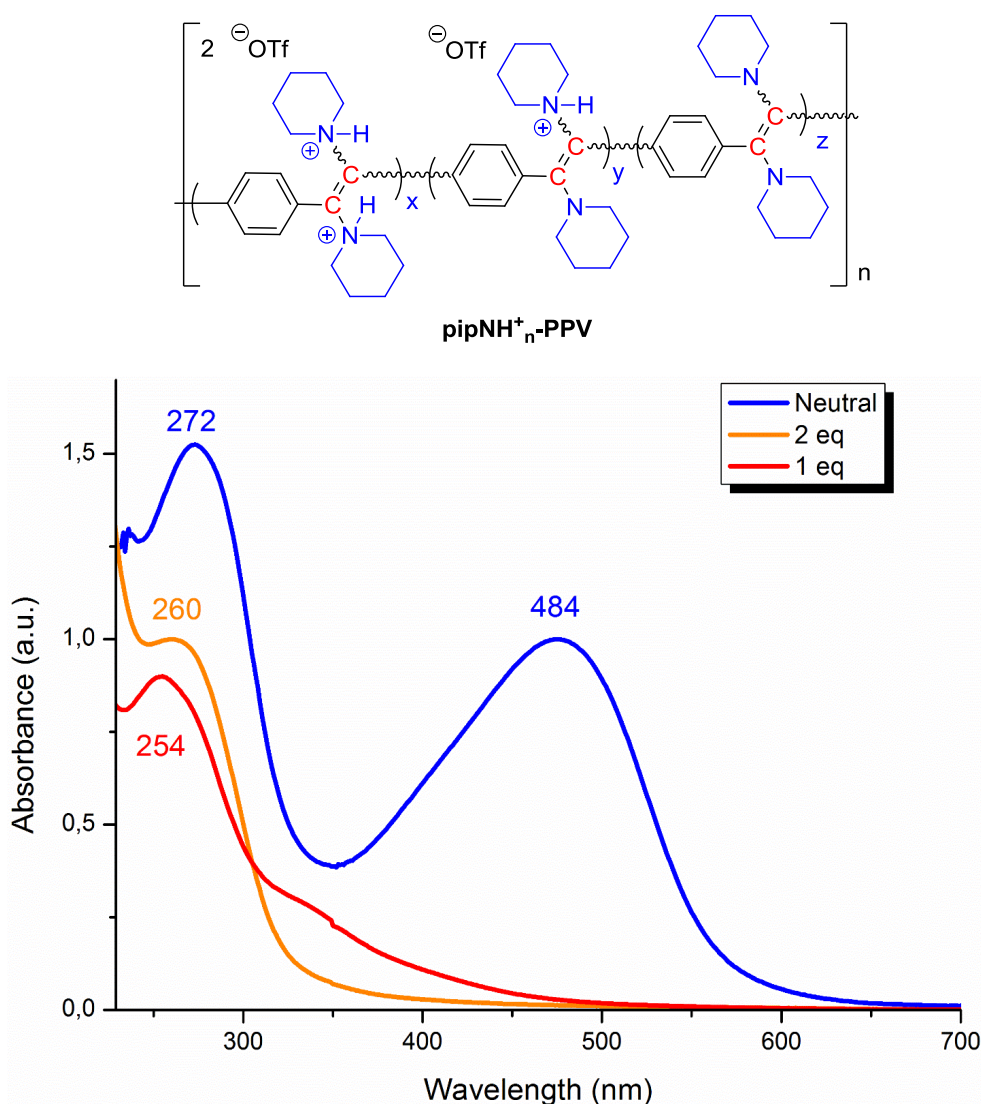
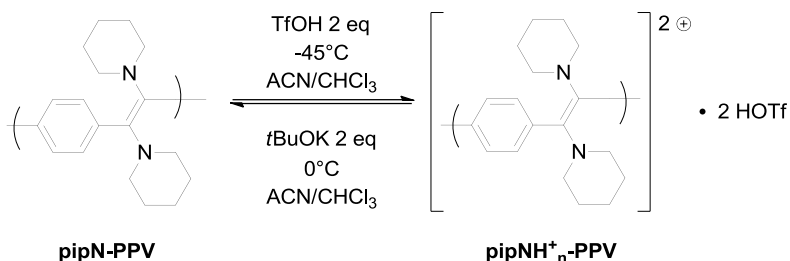


Figure III.24. UV/Vis analysis of polymer **pipN-PPV** in $\text{CHCl}_3/\text{CH}_3\text{CN}$, before and after protonation with 1 or 2 equivalents of triflic acid.

Then, **pipNH⁺_n-PPV** was subjected to the deprotonation reaction using *t*-BuOK. Addition of 2.1 equivalents of *t*-BuOK at 0°C on a solution of **pipNH⁺_n-PPV** in $\text{CHCl}_3/\text{CH}_3\text{CN}$ (50/50) led to a polymer with a maximum of absorption $\lambda_{\text{max}} = 460$ nm (Scheme III.23), *i.e.* close to that of the parent **pipN-PPV** ($\lambda_{\text{max}} = 476$ nm). This result suggested that the parent **pipN-PPV** could be restored and the protonation process was reversible. The decreased value for the maximum of absorption was partially caused by the UV-Vis analysis that was performed in a mixture of $\text{CH}_3\text{CN}/\text{CHCl}_3$ solvent, which induced a blue shift compared to the UV-vis analysis in CHCl_3 . However, it might also come from an incomplete deprotonation of the polymer, which would

Chapter III: Synthesis of amino-PPV by metal free dimerization/polymerization of novel bis-aminoarylcarbenes

reduce the conjugation along the polymer backbone and thus its maximum of absorption (Figure III.25).



Scheme III.23. Protonation and deprotonation reactions of **pipN-PPV** and **pipNH⁺_n-PPV**, respectively.

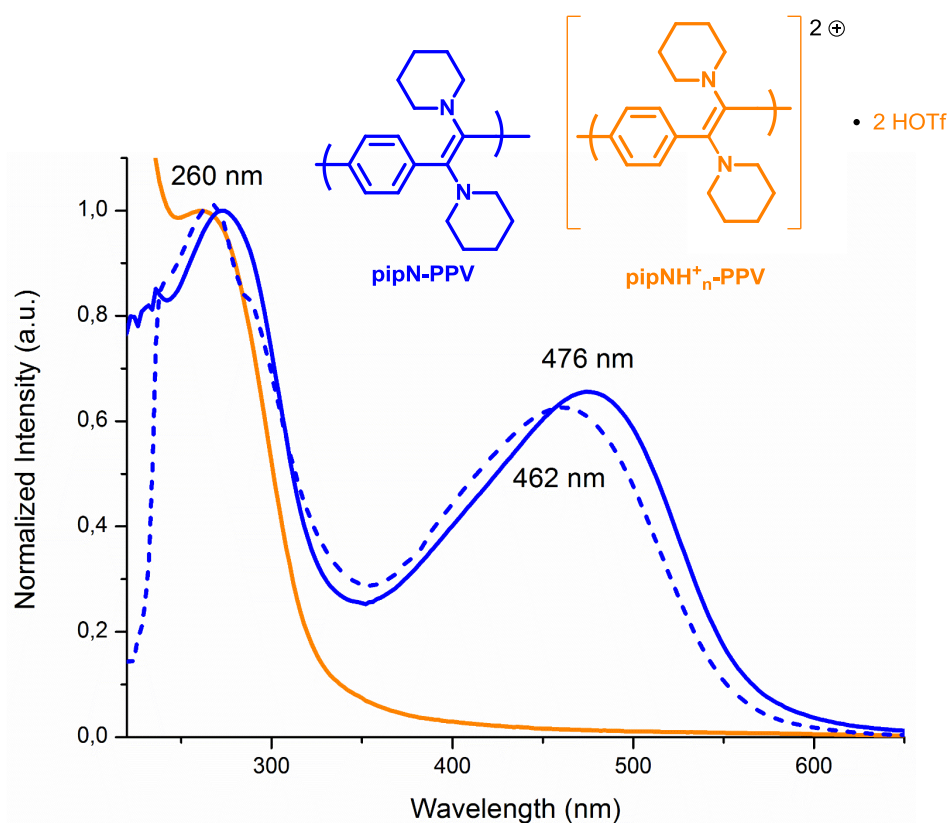


Figure III.25. UV-Vis analysis of protonated **pipNH⁺_n-PPV** (orange) and neutral **pipN-PPV** (blue) in $\text{CHCl}_3/\text{CH}_3\text{CN}$ before protonation reaction (continue blue) and after deprotonation of **pipNH⁺_n-PPV** (dashed blue).

In order to understand this difference in behavior between the protonation of **iPr₂N-PPV** and **pipN-PPV**, protonation of the dimer **pipN-DAA** homologue is discussed hereafter.

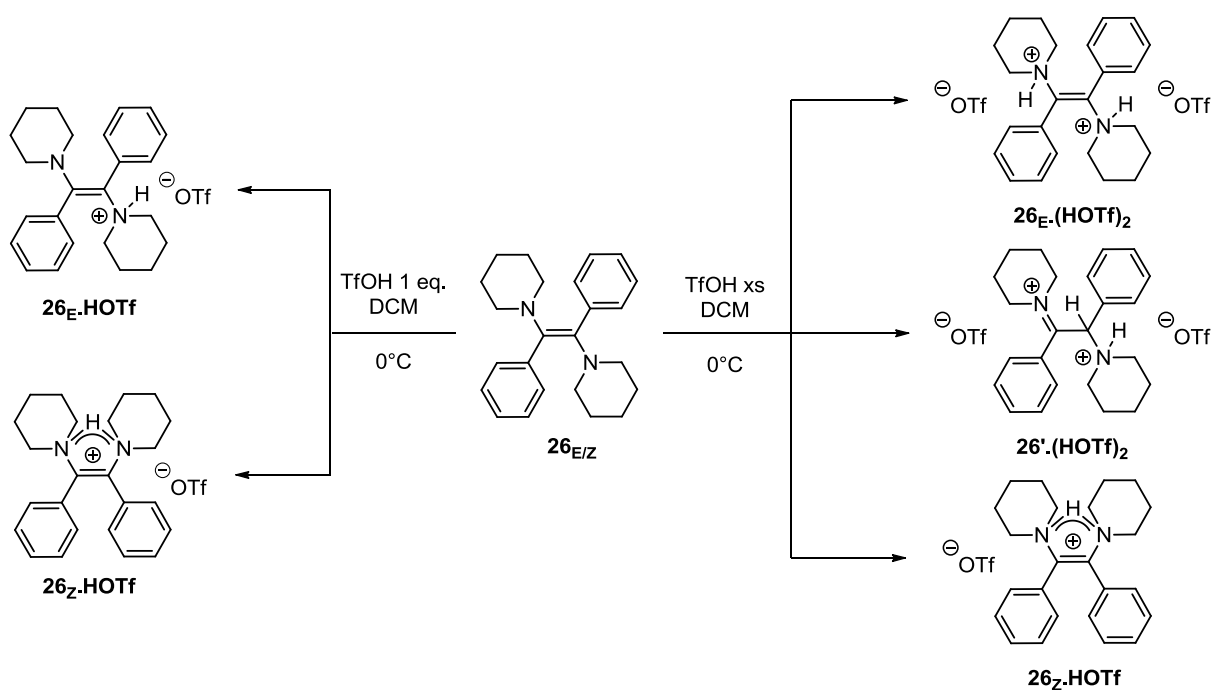
Chapter III: Synthesis of amino-PPV by metal free dimerization/polymerization of novel bis-aminoarylcarbenes

III.4.2.2 Modification of dimer with piperidine groups

Similarly to the discussion made with the dimer with isopropyl substituents in the previous section, compound **pipN-DAA** will be denoted with the number **26**. Protonation of **26** was thus carried out following the same protocol to that implemented for **25**.

Addition of one equivalent of TfOH in DCM led to a mixture of compounds that could not be analyzed by ^1H NMR spectroscopy, due to the complexity of the signals, and the presence of multiple species. Despite several attempts to crystallize **26_{E/Z}.HOTf**, no single crystals could be grown precluding the identification of the reaction products.

Protonation of **26** was next investigated with an excess of TfOH. Again, compounds obtained could not be analyzed by ^1H NMR spectroscopy. One might suspect that different compounds including isomers **26_Z.HOTf**, **26_E.(HOTf)₂** along with compound denoted as **26'.(HOTf)₂**, might have formed (see Scheme III.24).



Scheme III.24. Protonation of dimer **26_{E/Z}** with one equivalent or an excess of triflic acid leading to potentially either protonated compounds **26_E.HOTf**, **26_Z.HOTf**, **26_E.(HOTf)₂** and **26'.(HOTf)₂**.

Chapter III: Synthesis of amino-PPV by metal free dimerization/polymerization of novel bis-aminoarylcarbenes

In this case, single crystals of **26'**·(HOTf)₂ could be grown by slow evaporation of THF into a solution of protonated **26E/Z**·(HOTf)₂ in CH₃CN at -20°C. X-Ray diffraction analysis revealed the structure of one of the protonated compound *i.e.* **26'**·(HOTf)₂. In contrast to **25E**·(HOTf)₂ with the iPr₂N groups, and for which both nitrogen atoms were protonated, protonation here occurred both on nitrogen and carbon atoms (C₁-H: 0.98 Å and N₁-H: 0.86 Å). This resulted in the formation of the non-symmetrical molecule **26'**·(HOTf)₂. The C₁-C₂ bond length measured was found to be increased (1.53 Å), compared to **26** (1.35 Å), confirming the C-C single bond. The shorter C₂-N₂ (1.30 Å) corresponding to a C=C double bond and the planarity of the amino atom N₂ (Σ_{N2} = 360°) was in agreement with the formation of an iminium moiety (Figure III.26).

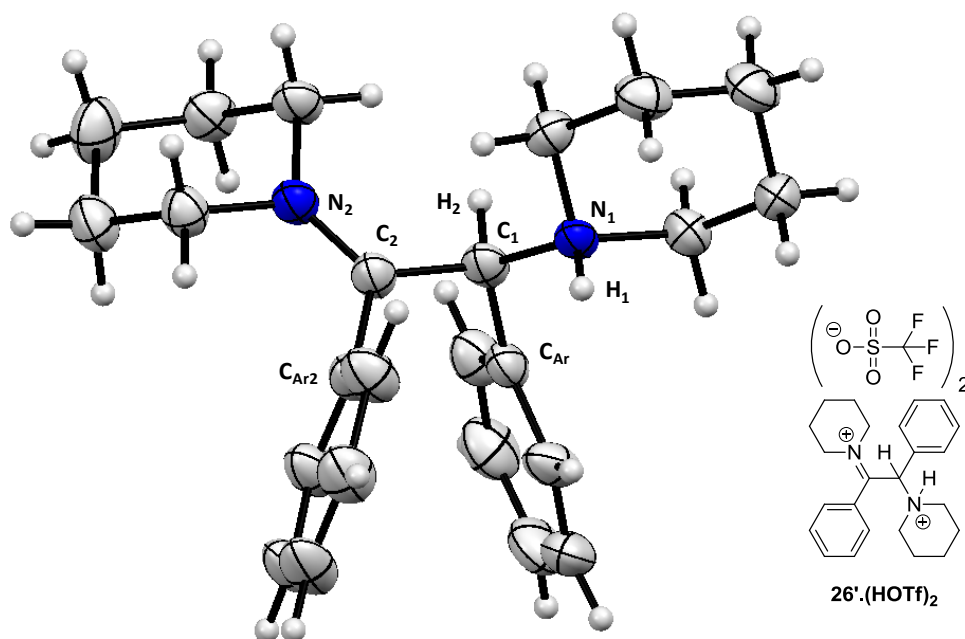
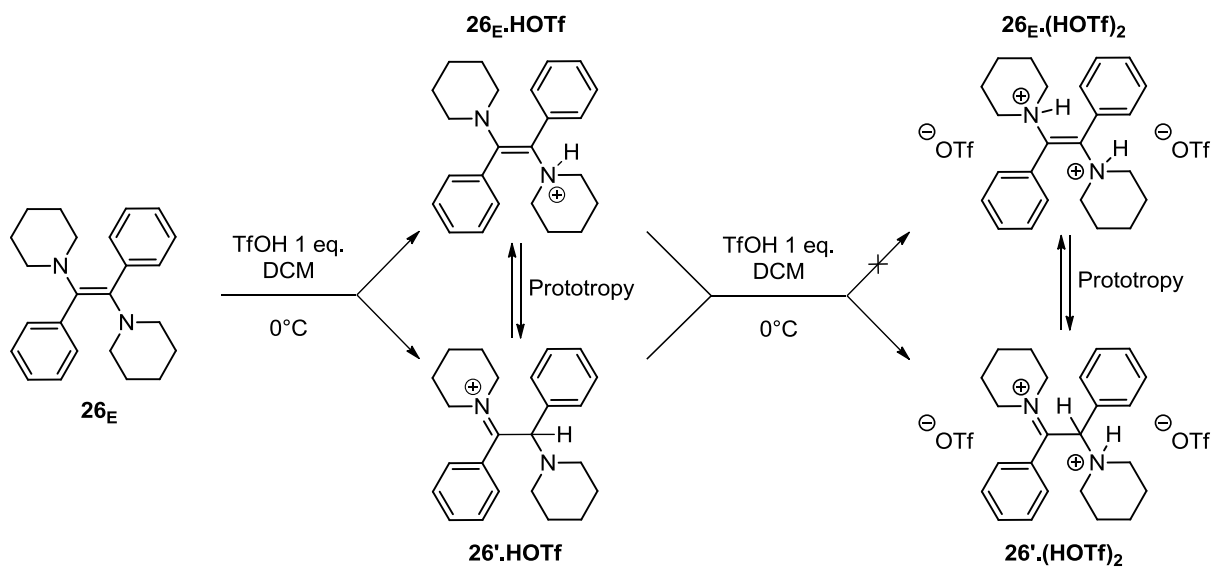


Figure III.26. X-Ray diffraction studies of compound **26'**·(HOTf)₂; the counter anion triflate (TfO⁻) was omitted for clarity. C₁-C₂ = 1.53 Å; C₁-C_{Ar} = 1.50 Å; C₂-C_{Ar2} = 1.49 Å; N₁-H₁ = 0.86 Å; N₁-C₁ = 1.51 Å; N₂-C₂ = 1.30 Å; C₁-H₂ = 0.98 Å.

This compound could be formed *via* different pathways. Following the theory of HSAB (Hard and soft acid and bases), the first protonation should happen on the nitrogen atom, forming the kinetically favored **26E**·HOTf which, by prototropy, could lead to the thought thermodynamic compound **26'**·HOTf. Then, the second protonation of **26E**·HOTf or **26'**·HOTf should also happen on the second nitrogen atom leading for **26E**·HOTf to **26E**·(HOTf)₂; which

Chapter III: Synthesis of amino-PPV by metal free dimerization/polymerization of novel bis-aminoarylcarbenes

could (as it was not isolated experimentally) lead by prototropy to the final $26'.(\text{HOTf})_2$; and for $26'.\text{HOTf}$ to $26'.(\text{HOTf})_2$ directly (Scheme III.25).



Scheme III.25. Proposed mechanisms to rationalize the formation of compound $26'.(\text{HOTf})_2$.

Compound **26** and $26'.(\text{HOTf})_2$ were analyzed by UV-Vis spectroscopy. As expected, no maximum of absorption was observed at $\lambda_{\text{max}} = 386 \text{ nm}$ ($n-\pi^*$ transition) for the bis-protonated dimer $26'.(\text{HOTf})_2$, because of the lack of conjugation. Only the $\pi-\pi^*$ transition remained, showing a maximum of absorption at 255 nm (Figure III.27).

Chapter III: Synthesis of amino-PPV by metal free dimerization/polymerization of novel bis-aminoarylcarbenes

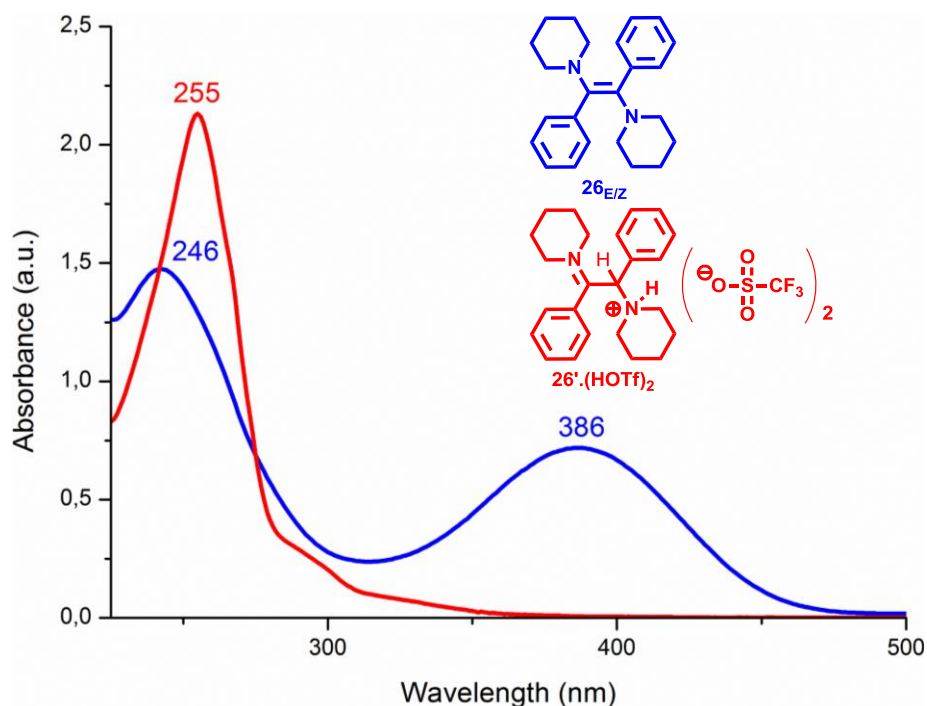
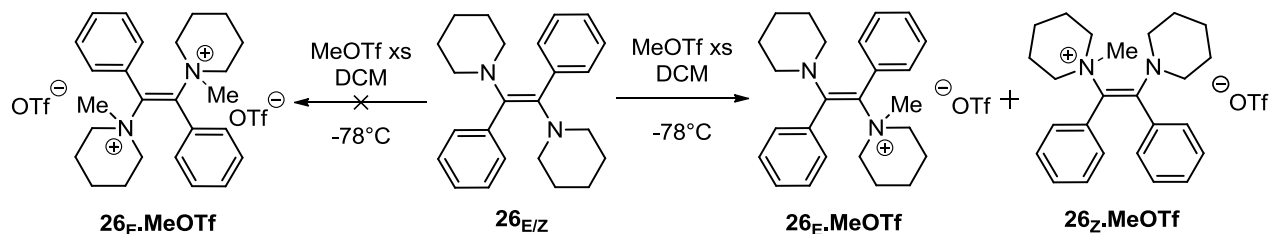


Figure III.27. UV-Vis spectra in CH₃CN of neutral dimer **26** and protonated dimer **26'**·(HOTf)₂.

The reaction of *E/Z*-diaminoalkene **26** with MeOTf was then investigated. Addition of MeOTf in excess, between -78°C and room temperature, on a solution of **26** in DCM led to the precipitation of a brown solid (Scheme III.26). Recrystallization by diffusion of a diethyl ether solution of methylated **26**_{*E/Z*} in THF led to orange/red crystals. X-Ray diffraction analysis confirmed the structure of **26**_{*Z*}·MeOTf showing a *Z*-configuration in the solid state. The C₁=C₂ bond length of 1.33 Å confirmed the C=C double bond and the methylation was confirmed with a N₂-C_{methyl} bond length of 1.50 Å (Figure III.28). Unfortunately, only the *Z*-isomer could be recrystallized.



Scheme III.26. Methylation of dimer **26** by addition at -78°C of an excess of MeOTf.

Chapter III: Synthesis of amino-PPV by metal free dimerization/polymerization of novel bis-aminoarylcabenenes

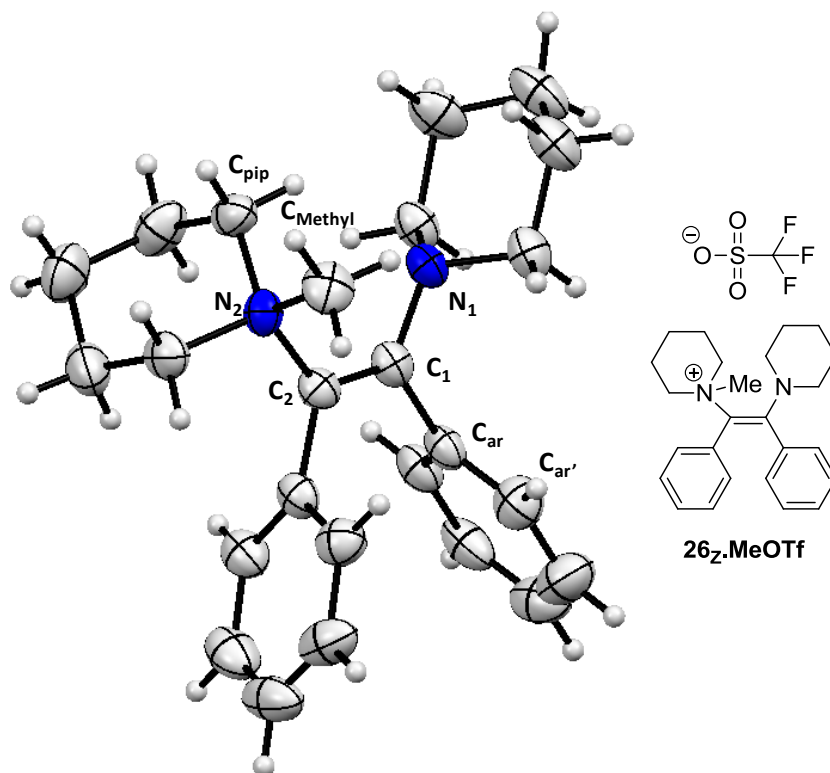


Figure III.28. X-Ray diffraction analysis of methylated compound **26_z.MeOTf**. For better clarity, the triflate counter anion was omitted. $C_1-C_2 = 1.33 \text{ \AA}$; $C_1-C_{Ar} = 1.51 \text{ \AA}$; $C_2-C_{Ar} = 1.51 \text{ \AA}$; $N_1-C_1 = 1.43 \text{ \AA}$; $N_2-C_2 = 1.52 \text{ \AA}$; $N_1-\text{Me} = 1.50 \text{ \AA}$, $\Sigma_{N1} = 337^\circ$, $\Sigma_{N2} = 333^\circ$ and $C_{Ar'}-C_{Ar}-C_1-C_2 = 85.5^\circ$.

The ^1H NMR spectrum of recrystallized **27_z.MeOTf** in THF- d_8 showed the appearance of new signals along with the disappearance of signals due to the neutral piperidine dimer **26**. The characteristic CH_3 singlet signal integrating for three protons at 3.17 ppm attested to the successful methylation reaction. The CH_2 pip signals, in α -position of the piperidine group, were found at 4.11 ppm and 3.97 as triplets. The CH_2 pip signal in α -position of the piperidinium group was observed at 3.85 ppm as a triplet. These signals are in agreement with the X-Ray diffraction analysis of **26_z.MeOTf**. Note, however, that the NMR spectrum did not give any information about the stereochemistry of **26_z.MeOTf** (Figure III.29). Relying on those results, the reactivity with MeOTf further confirmed the least bulky nature of piperidine diaminoalkene **26**, compared to diisopropyl diaminoalkene **25**.

Chapter III: Synthesis of amino-PPV by metal free dimerization/polymerization of novel bis-aminoarylcarbenes

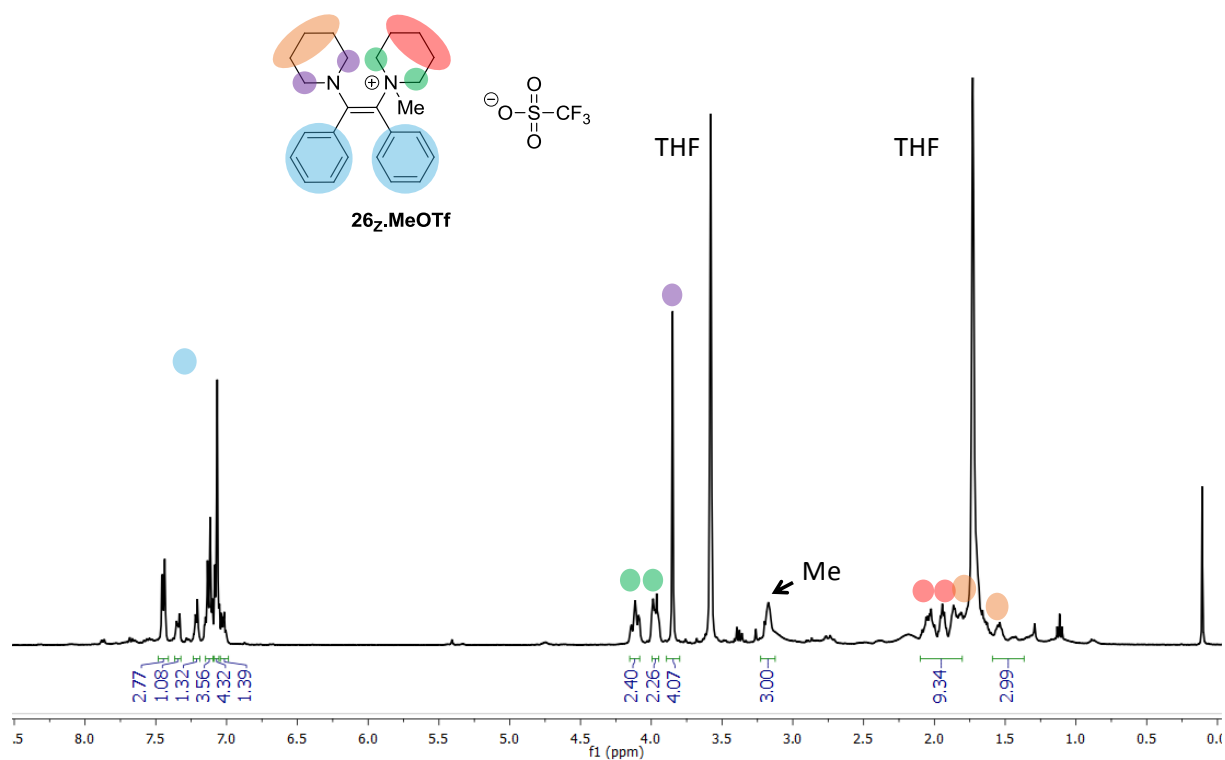


Figure III.29. ¹H NMR (400 MHz) in THF_d₆ of methylated dimer **26_z.MeOTf**.

UV-Vis analysis was performed on dimer **27_z.MeOTf**. Surprisingly, no $n-\pi^*$ transition and only the $\pi-\pi^*$ transition at $\lambda_{\text{max}} = 267$ nm was observed. The crystal structure might provide some information to explain this result. Indeed, the neutral N₁ lone pair was found orthogonal to the C₁-C₂ double bond ($\theta = 90^\circ$) in the solid state, this conformation preventing any overlapping and thus conjugation, explaining the absence of $n-\pi^*$ transition (Figure III.30).

Chapter III: Synthesis of amino-PPV by metal free dimerization/polymerization of novel bis-aminoarylcarbenes

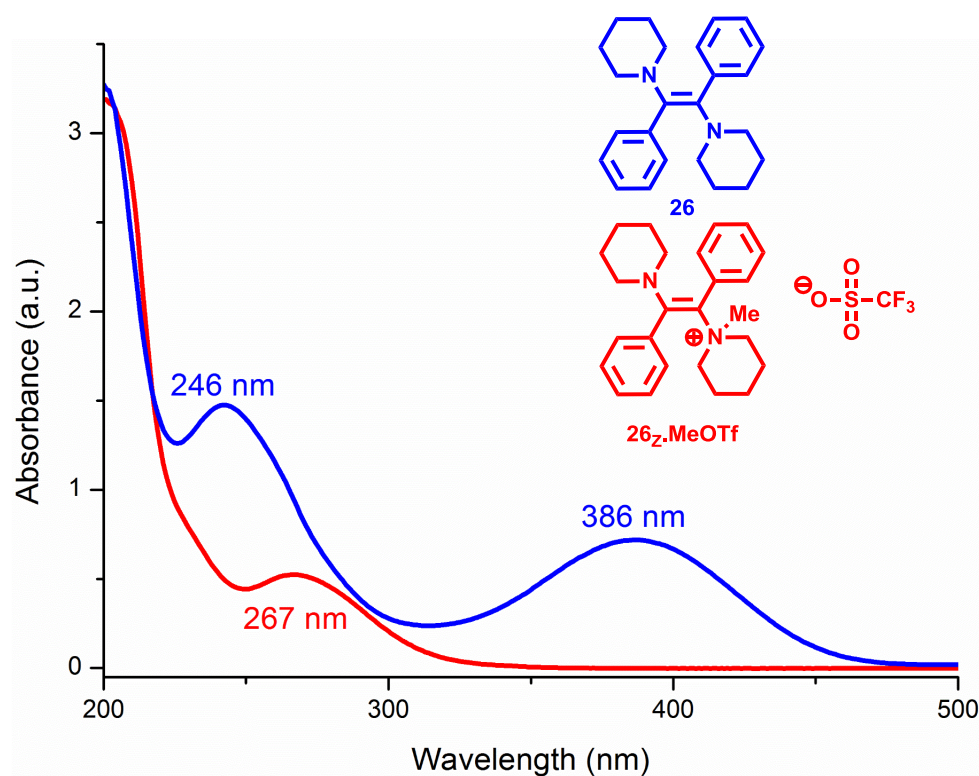


Figure III.30. UV-Vis spectra of neutral dimer **26_{E/Z}** and methylated dimer **26_Z.MeOTf** in CH₃CN.

In summary, this part showed characteristic changes of the physicochemical properties of the polymer **pipN-PPV** and **pipN-DAA** upon protonation using triflic acid. Some similarities but also some key differences were observed for **pipN-PPV** and **iPr₂N-PPV**. While protonation of **iPr₂N-PPV** led to a blue shift in its maximum of absorption, protonation of **pipN-PPV** caused the disappearance of the maximum of absorption corresponding to the $n-\pi^*$ transition. To understand these differences, the post-chemical modification was performed onto their respective model dimeric compounds. In presence of an excess of triflic acid, protonation on **iPr₂N-DAA** led to a compound, where both nitrogen atoms were found to be protonated. In contrast, protonation of **pipN-DAA** led to multiple species, among which we successfully recrystallized compound where protons were eventually present on one nitrogen atom and on one carbon atom of the double bond. This peculiarity also explained the absence of the maximum of absorption owing to a lack of conjugation. This result elucidated the behavior of the **pipN-PPV** when protonated: adding protons onto the double bond causes the loss of conjugation along the polymer backbone, leading to the absence of $n-\pi^*$ transition. Finally, a methylated *Z*-configured **pipN-DAA** could be isolated by recrystallization and its by UV-Vis

Chapter III: Synthesis of amino-PPV by metal free dimerization/polymerization of novel bis-aminoarylcarbenes

analysis showed the same lack of $n-\pi^*$ transition. This result was explained by the conformation of the latter, with a θ angle of 90° resulting in an absence of overlapping between the lone pair at the nitrogen center and the C=C double bond required to observe a $n-\pi^*$ transition.

III.4.3 Conductivity measurements

Here, we first detail the step towards the integration of the polymer in optoelectronic devices by conditioning them as thin films and then, the measurement of their sheet resistance leading to their conductivity by calculations.

The protocol used to make the thin films with polymers **iPr₂N-PPV**, **iPr₂NH⁺-PPV**, **pipN-PPV**, **pipNH⁺-PPV** is first discussed, followed by the attempts to measure their conductivity.

Film preparation involved the cleaning of the glass substrates, which incorporate two electrodes (Gold electrode, 100 nm) attached to each side. A UV/ozone treatment of the glass incorporating the electrodes is performed over 30 min and 100 μL of a solution of polymers **iPr₂N-PPV**, **iPr₂NH⁺-PPV**, **pipN-PPV**, **pipNH⁺-PPV** at a concentration of 15 $\text{mg}\cdot\text{mL}^{-1}$ is added. The polymer is then spin-coated at a speed of 2000 rpm, resulting in films with a thickness around 150 nm as measured by AFM. This methodology worked for polymers **iPr₂N-PPV** and **pipN-PPV**; however, for the protonated **iPr₂NH⁺-PPV** and **pipNH⁺-PPV**, wettability issues were encountered. For **pipNH⁺-PPV**, films were of poor quality with no homogeneity, as for **iPr₂NH⁺-PPV**, no films were obtained at all. The films did not spread on all the surface, forming numerous small droplets instead; therefore, different options have been tested to avoid this problem.

Longer UV/ozone treatment was first tried, which did not fix the problem. Another solution was to change the solvent used for the deposit, substituting chloroform for methanol or acetonitrile; unfortunately, both solvents did not improve the homogeneity of the films. Hydrophobization of the glass plates by silanisation was performed in order to get better results, but this revealed to be worse. The last solution attempted was the protonation of already prepared thin films of **iPr₂N-PPV** and **pipN-PPV** polymers. Glass plates already coated with polymers **iPr₂N-PPV** and **pipN-PPV** were suspended above a crystallizer full of fuming chlorhydric acid in a desiccator. The desiccator was then closed and the air was vacuumed out

Chapter III: Synthesis of amino-PPV by metal free dimerization/polymerization of novel bis-aminoarylcabenenes

to let the acid evaporate on the substrates. A change of color was observed in only a few seconds, the films went from brown to uncolored; no other color changes were perceived over longer time of exposure (Figure III.31).

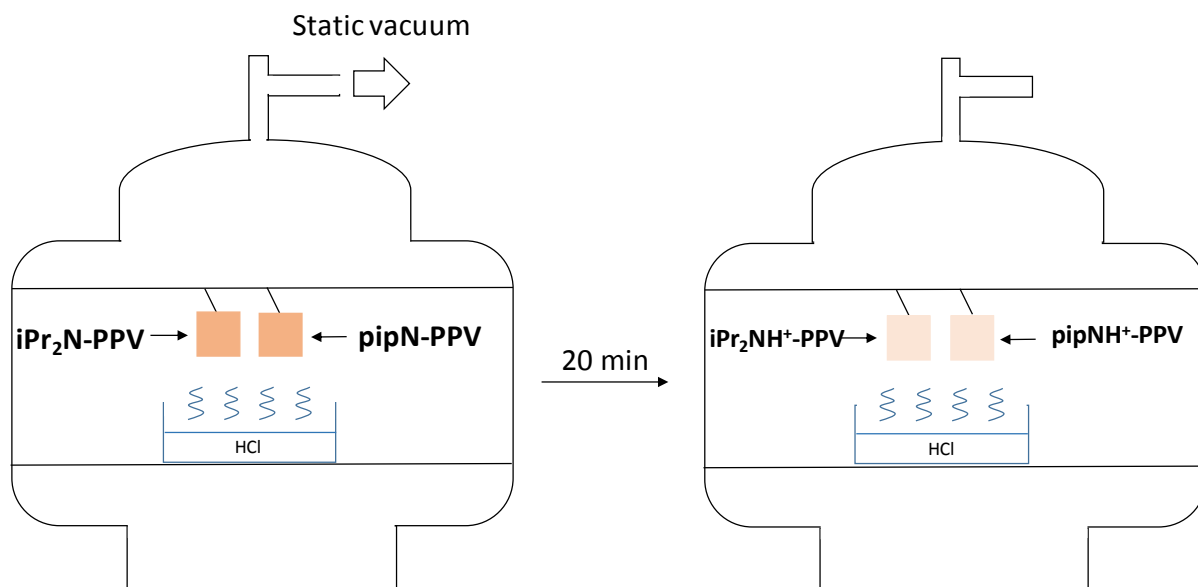


Figure III.31. Protonation of films of **iPr₂N-PPV** and **pipN-PPV** by evaporation of fuming chlorhydric acid.

The resistance of the films was measured with a 4-point probes method. In this technique, a current is applied between the two connections 1 and 4 and the tension is measured between the two connections 2 and 3. The sheet resistance could be extracted from this measurement, which multiplication by the thickness of the films gave the overall resistivity (ρ) of the materials, and allowed to calculate the conductivity ($\sigma = 1/\rho$). Polymers **iPr₂N-PPV**, **pipN-PPV** and **iPr₂NH⁺-PPV** did not give any conductivity, whereas **pipNH⁺-PPV** gave a conductivity around 10^{-6} S.cm⁻¹ (Figure 32).

Chapter III: Synthesis of amino-PPV by metal free dimerization/polymerization of novel bis-aminoarylcabenenes

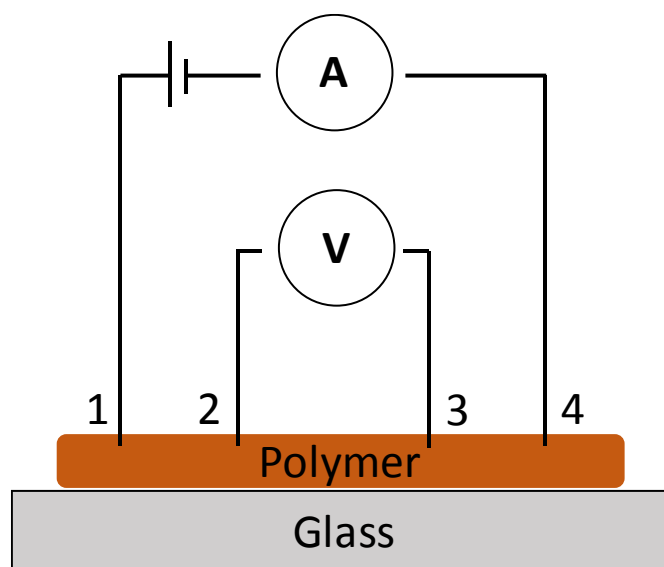


Figure III.32. Four-point probes methods set.

The Seebeck coefficient of each prepared films was also analyzed. The Seebeck effect is the property of a material to convert a temperature difference into electricity. To measure it, the substrates are first set on two Peltier plates (where temperature is controlled by applying a selected tension); then, a difference of temperature between these two plates is applied. Finally, the evolution of the open voltage (V_{oc}) created by the temperature difference is measured. A linear regression of the V_{oc} in function of time data leads to a straight line, where the coefficient gives the Seebeck coefficient (Figure III.33). If the coefficient is positive, the polymers are conducting holes and are of p-type; if it is negative, the polymers are conducting electrons and are of n-type. For polymers **iPr₂N-PPV** and **pipN-PPV**, no value could be obtained with this measurement, evidencing the non-conductivity of these undoped materials. This result is not surprising as PPV shows similar behavior when they are not doped. For polymers **iPr₂NH⁺-PPV** and **pipNH⁺-PPV** obtained from vapor deposition of acid on the neutral films, same results were obtained with absence of electrical conductivity.

Finally, on the poor quality films made with **pipNH⁺-PPV**, fluctuant negative values between -5 and $-9 \mu V.K^{-1}$ were observed. These low and inconsistent values can be explained by the heterogeneity of the films. Indeed, despite changing several parameters (concentration of the solution, time of annealing, speed during spin coating, glass treatments), no homogeneous films could be obtained. However, values obtained are negative, which might suggest that the polymer **pipNH⁺-PPV** is potentially of n-type. Those values being too low, better films need to be made by optimization of the film preparation, *i.e.* deposition technique, selection of the

Chapter III: Synthesis of amino-PPV by metal free dimerization/polymerization of novel bis-aminoarylcabenenes

type of annealing (*i.e.* solvent annealing instead of heating the glass), changing the acid used to have different counter-anions in the doped polymers, in order to make transistors that are able to measure the electronic mobility.

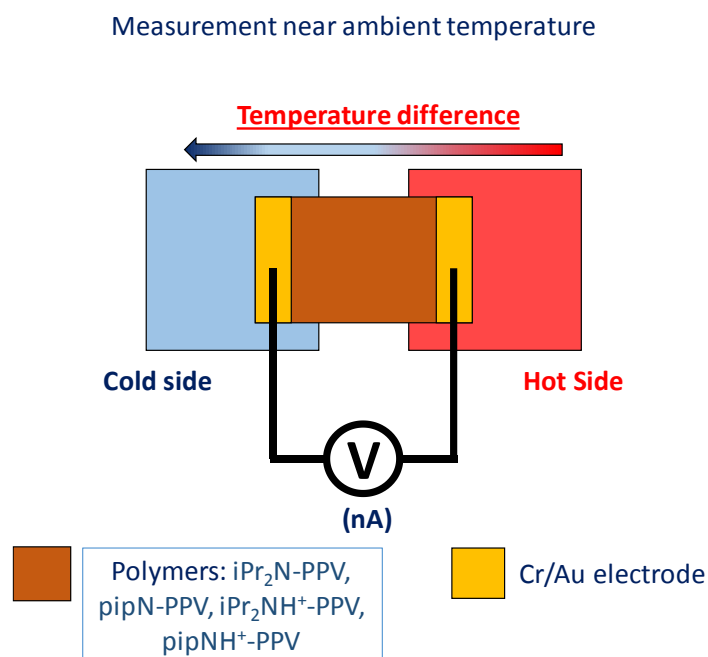


Figure III.33. Setup for the measurement set of the Seebeck effect.

III.5 Conclusions

Three distinct bis-aminoarylcabene precursors, in the form of bis-imminium salts, featuring different amino and aryl functions were synthesized *via* a transition metal-free and metal free routes. Step-growth polymerization of the *in-situ* generated bis-aminoarylcabenenes, involving a repeated dimerization reactions, was achieved by deprotonation of the salt precursors in presence of a strong base. This afforded unprecedented π -conjugated amino-containing –poly(phenylene vinylene)’s incorporating two amino groups in α -position of the double bond. An estimation of the degree of polymerization between 10 to 48 was made using both 1H NMR spectroscopy and size exclusion chromatography.

Chapter III: Synthesis of amino-PPV by metal free dimerization/polymerization of novel bis-aminoarylcabenenes

In comparison to their respective dimeric counterparts, polymers showed an overall red shift of their maximum of absorption for the $n-\pi^*$ transition, evidencing the increase of the π -conjugation. Owing to the shift between their maximum of emission and absorption, and to an emission on a large array of the visible spectra, which in some cases could even go to the infra-red, these polymers appear be good candidates in OLED devices.

Moreover, taking advantage of the two amino functions on the polymers, post-chemical modification of their optical properties was demonstrated through protonation or methylation reactions. Protonation of polymers and dimers with diisopropyl substituent an hypsochromic effect on their maximum of absorption and emission. This result probably reflected the lack of interaction between the nitrogen atom and the $\pi_{C=C}$ orbitals, as observed for the dimer counterpart where both protons were added on each amino function. Despite similarities between the **iPr₂N-PPV** and **pipN-PPV**, a totally different behavior was observed upon protonation. For **pipN-PPV**, indeed, no $n-\pi^*$ transition was noted and this compound only showed the $\pi-\pi^*$ transition of the aromatics. This result could be explained by the X-ray diffraction analysis of the dimer **pipN-DAA** homologue revealing that both a nitrogen and a carbon atom of the C=C bond were protonated, thus breaking the conjugation both in the dimer and the polymer.

Protonation also proved reversible only in the case of **iPr₂N-DAA**. In the case of **iPr₂N-PPV**, indeed, deprotonation did not occur, which might be due to specific conformation adopted by the protonated polymer. In the case of the piperidine polymer, **pipN-PPV**, deprotonation could be successfully achieved. A methylation reaction was also attempted on model compounds and was found efficient only with **pipN-DAA** featuring the piperidine substituent. This highlights the importance of steric hindrance as dimer bearing the more bulky diisopropyl substituents did not enable to achieve the methylation reaction.

Finally, thin films of the neutral polymers were obtained by spin-coating, but wettability issues were encountered for the protonated ones. However, despite the poor quality of the films made from the protonated polymer **pipNH⁺-PPV**, the measurement of its electrical conductivity showed its potential n-type nature, a quite uncommon feature in the π -conjugated polymer chemistry. However, because of the poor quality of films, optimization of the process is required to confirm the n-type nature of such polymers.

The presence of amino groups on the double bond of the synthesized dimers make them electron-rich organic molecules. It is known that analogous compounds bearing more nitrogen

Chapter III: Synthesis of amino-PPV by metal free dimerization/polymerization of novel bis-aminoarylcabenenes

atoms on the double bond, *i.e.* tetraaminoethylenes, are excellent reducing agents, which may be used as stoichiometric reagent and as organocatalysts in photo-induced atom transfer radical polymerization (OATRP). Therefore, in the next chapter, the electrochemical characterization of dimers **iPr₂N-DAA** and **pipN-DAA** and their use as stoichiometric and organocatalytic reducing agents are presented.

Chapter III: Synthesis of amino-PPV by metal free dimerization/polymerization of novel bis-aminoarylcabenenes

III.6 Experimental part



To a stirred solution of 1,4-dithiobenzene (0.456 g, 5 mmol) in Et₂O at -78°C, diisopropyl formamide (1.32 mL, 9.1 mmol) was added dropwise. The resulting mixture was stirred at -78°C for 30 minutes, followed by 1 hour at room temperature. The mixture was then cooled to -78°C before an ethereal solution of triflic anhydride (*ca.* 1.8 equivalents) was added dropwise with vigorous stirring and let to room temperature overnight. The precipitated solid was filtered, washed with dry ether (3x10 mL), DCM and THF under inert atmosphere and dried under vacuum to obtain the compound **21** as a light brown solid (1g, 33%). Single crystals were grown from the slow evaporation of a solution of ether in an acetonitrile solution of **21**.

¹H NMR (CD₃CN, 400 MHz): δ 1.54 (d, 12H, ³J = 6.6 Hz), 1.62 (d, 12H, ³J = 6.6 Hz), 4.57 (sept, 2H, ³J = 6.6 Hz), 4.91 (sept, 2H, ³J = 6.6 Hz), 7.96 (s, 4H), 9.26 (s, 2H);

¹³C NMR (CD₃CN, 400 MHz): 19.90, 24.14, 57.33, 59.64, 122.08 (q, ¹J_{C-F} = 321.1 Hz), 131.96, 132.74, 171.85 (t, 1H, J = 12.4 Hz);

¹⁹F NMR (CD₃CN, 377 MHz): δ -77.77;

IR (ATR) ν_{max} (cm⁻¹): 3090, 2987, 2885, 2115, 1655, 1467, 1340, 1275, 1225, 1158, 1033, 984, 832;

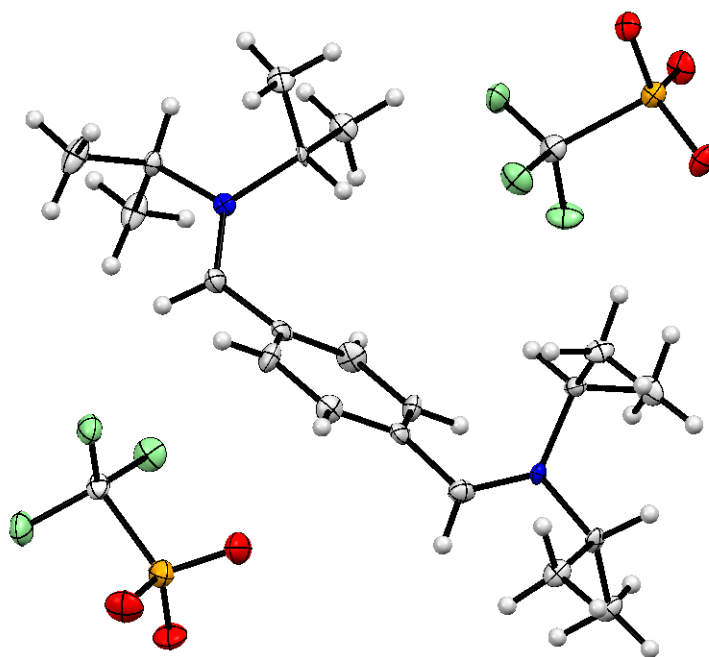
λ_{max} (ACN): 287 nm.

Structural data :

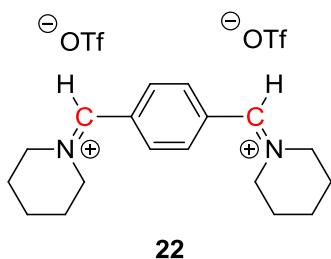
Identification code	Benzylidenebis(diisopropyliminium) triflate
Empirical formula	C ₂₂ H ₃₄ F ₆ N ₂ O ₆ S ₂
Formula weight	600.63
Temperature/K	566.3
Crystal system	orthorhombic

Chapter III: Synthesis of amino-PPV by metal free dimerization/polymerization of
 novel bis-aminoarylcarbenes

Space group	Pna2 ₁
a/Å	21.464(16)
b/Å	12.915(11)
c/Å	9.932(8)
α/°	90
β/°	90
γ/°	90
Volume/Å ³	2753(4)
Z	4
ρ _{calc} /g/cm ³	1.449
μ/mm ⁻¹	2.484
F(000)	1256.0
Crystal size/mm ³	0.2 × 0.2 × 0.2
Radiation	CuKα (λ = 1.54178)
2θ range for data collection/°	7.99 to 136.448
Index ranges	-25 ≤ h ≤ 21, -15 ≤ k ≤ 12, -11 ≤ l ≤ 11
Reflections collected	13682
Independent reflections	4304 [R _{int} = 0.0863, R _{sigma} = 0.0605]
Data/restraints/parameters	4304/1/352
Goodness-of-fit on F ²	1.055
Final R indexes [I ≥ 2σ (I)]	R ₁ = 0.0605, wR ₂ = 0.1548
Final R indexes [all data]	R ₁ = 0.0617, wR ₂ = 0.1561
Largest diff. peak/hole / e Å ⁻³	0.60/-0.45
Flack parameter	0.50(3)



Chapter III: Synthesis of amino-PPV by metal free dimerization/polymerization of novel bis-aminoarylcarbenes



Benzylidenebis(piperidineiminium) triflate 22:

To a stirred solution of terephthalaldehyde (0.27 g, 2 mmol) and 1-(trimethylsilyl) piperidine (0.63 g, 4 mmol) in dry ether (30 mL), TMSOTf (0.72 mL, 4 mmol) was dropwise added at room temperature and the resulting mixture was stirred at the same temperature overnight under inert atmosphere. The precipitated solid was filtered, washed with dry ether (2x25 mL) under inert atmosphere and dried under vacuum to obtain the compound **22** as a white solid (0.98 g, 86%).

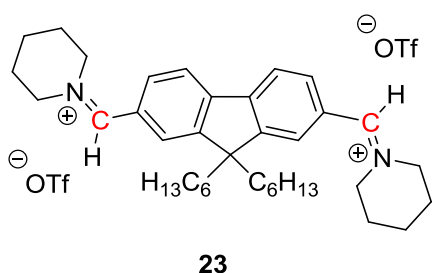
^1H NMR (CD_3CN , 400 MHz): δ 1.86 (m, 2H), 1.94 (br, 2H), 2.08 (br, 4H), 4.14 (m, 4H), 7.93 (s, 4H), 9.11 (s, 2H);

^{13}C NMR (CD_3CN , 400 MHz): δ 22.85, 26.18, 27.14, 54.39, 62.99, 68.22, 122.04 (q, $^1J_{\text{C-F}} = 321.0$ Hz), 131.97, 132.37, 170.86 (t, 1H, $J = 12.5$ Hz);

^{19}F NMR ($\text{CD}_3\text{CN}-d_6$, 377 MHz): δ -77.76.

IR (ATR) ν_{max} (cm^{-1}): 3092, 2962, 2873, 2115, 1676, 1449, 1275, 1225, 1158, 1033, 972, 832;

λ_{max} (ACN): 282 nm.



9,9'-dihexyl-9H-fluorenylidenebis-(piperidineiminium) triflate 23:

To a stirred solution of 9,9'-dihexyl-9H-fluorene-2,7-dicarbaldehyde¹ (1.17 g, 3 mmol) and 1-(trimethylsilyl) piperidine (1.04 g, 6.6 mmol) in dry ether (25 mL), TMSOTf (1.2 mL, 6.6 mmol) was dropwise added at room temperature and the resulting mixture was stirred at the same temperature overnight under inert atmosphere. The precipitated solid was filtered under

Chapter III: Synthesis of amino-PPV by metal free dimerization/polymerization of novel bis-aminoarylcarbenes

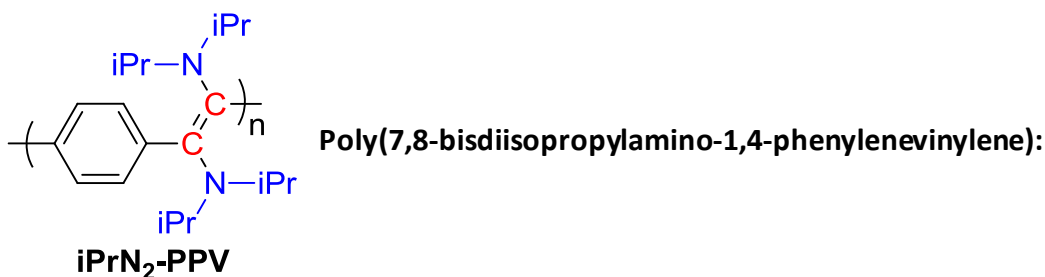
inert atmosphere, washed with dry ether (2x25 mL) and dried under vacuum to obtain the compound **23** as a yellow solid (1.97 g, 80%).

^1H NMR (CD_3CN , 400 MHz): δ 0.52-0.60 (m, 4H), 0.73 (t, 6H, $^3J = 6.8$ Hz), 1.06 (m, 12H), 1.90 (m, 4H), 2.02 (br, 8H), 2.14 (m, 4H), 4.19 (br, 8H), 7.83 (d, 2H, $^3J = 8$ Hz), 7.85 (s, 2H), 8.20 (d, 2H, $^3J = 8$ Hz), 9.02 (s, 2H);

^{13}C NMR (CD_3CN , 101 MHz): 14.21, 23.06, 23.14, 24.55, 27.22, 30.06, 32.08, 39.98, 57.34, 122.14 (q, $^1J_{\text{C-F}} = 320.6$ Hz), 123.43, 127.40K, 128.22, 132.24, 146.21, 153.84, 171.14;

^{19}F NMR (CD_3CN , 377 MHz): δ -79.27;

IR (ATR) ν_{max} (cm^{-1}): 2962, 2934, 2861, 2116, 1656, 1606, 1449, 1275, 1224, 1157, 1032.



To a stirred solution of **22** (0.300 g, 0.5 mmol) in THF (2 mL) cooled at -78°C $\text{P}_4\text{-}t\text{Bu}$ base (1.38 mL, 1.1 mmol, 0.8M in hexanes) was added and the resulting mixture was stirred at this temperature for 1h followed by 24h at room temperature. After the solvent was removed under reduced pressure, the mixture was washed with MeOH (10 mL) to remove the phosphazanium salts. The resulting mixture was dissolved in CHCl_3 (15 mL) and filtered to remove the insoluble compounds. After evaporation of the organic solvent, the mixture was purified by precipitation using CHCl_3 and MeOH at -10°C to obtain the desired polymer **iPrN₂-PPV** as a dark red solid (80 mg, 60%).

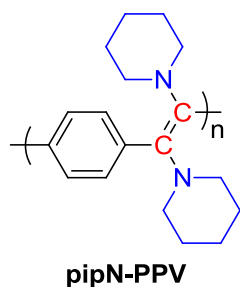
^1H NMR (THF- d_8 , 400 MHz): δ 1.05 (m, 24H), 3.32 (m, 4H, *E*-isomer), 3.91 (m, 4H, *Z*-isomer), 6.65 (m, 4H), 9.75 (s, 1H), 9.95 (s, 1H).

SEC: $\overline{M}_n = 3000$ g.mol $^{-1}$; $\overline{M}_w = 6240$ g.mol $^{-1}$; $\overline{D} = 2.08$

UV/Vis absorption : $\lambda_{\text{max}} = 255, 462$ nm;

Emission spectroscopie: $\lambda_{\text{max}}(\text{liq}) = 592$ nm, $\lambda_{\text{max}}(\text{thin film}) = 666$ nm

Chapter III: Synthesis of amino-PPV by metal free dimerization/polymerization of novel bis-aminoarylcarbenes



Poly(7,8-bispiperidine-1,4-phenylenevinylene):

To a stirred solution of **23** (0.28 g, 0.5 mmol) in THF (2 mL) cooled at -78°C $\text{P}_4\text{-}^t\text{Bu}$ base (1.38 mL, 1.1 mmol, 0.8M in hexanes) was added and the resulting mixture was stirred at this temperature for 1h followed by 24h at room temperature. After the solvent was removed under reduced pressure, the mixture was washed with MeOH (10 mL) to remove the phosphazanium salts. The resulting mixture was dissolved in CHCl_3 (15 mL) and filtered to remove the insoluble compounds. After evaporation of the organic solvent, the mixture was purified by precipitation using CHCl_3 and MeOH at -10°C to obtain the desired polymer **pip-NPPV** as a wine red solid (80 mg, 60%).

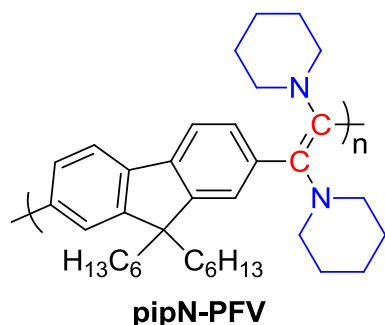
^1H NMR (THF- d_8 , 400 MHz): δ 1.48 (br, 12 H), 2.41 (br, 4H, *E*-isomer), 3.08 (br, 2H, *Z*-isomer), 3.50 (br, 2H, *Z*-isomer), 7.17 (br, 4H), 9.95 (s, 2H)

SEC: $\overline{M}_n = 3900 \text{ g}\cdot\text{mol}^{-1}$; $\overline{M}_w = 7995 \text{ g}\cdot\text{mol}^{-1}$;

$\overline{D} = 2.05$

UV/Vis absorption $\lambda_{\text{max}} = 273, 476 \text{ nm}$

Emission spectroscopie: $\lambda_{\text{max}}(\text{liq}) = 528 \text{ nm}$, $\lambda_{\text{max}}(\text{thin film}) = 685 \text{ nm}$



Poly(7,8-bispiperidine-1,4-(9,9-dihexylfluorene)vinylene):

To a stirred solution of **24** (0.83 g, 1 mmol) in THF (15 mL) cooled at -78°C $\text{P}_4\text{-}^t\text{Bu}$ base (3.0 mL, 2.4 mmol, 0.8M in hexanes) was added and the resulting mixture was stirred at this

Chapter III: Synthesis of amino-PPV by metal free dimerization/polymerization of novel bis-aminoarylcarbenes

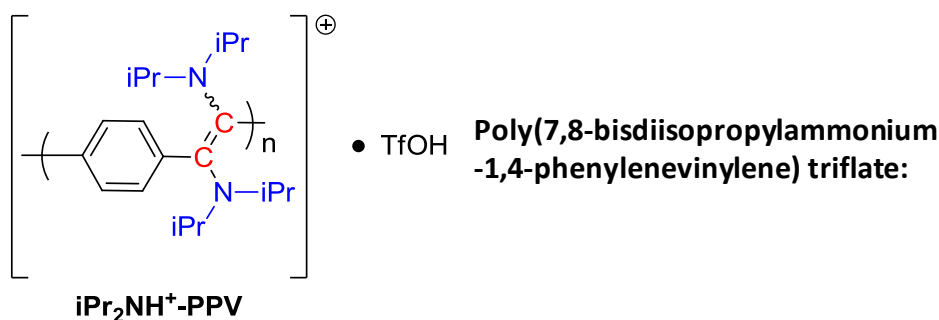
temperature for 1h followed by 24h at room temperature. After the solvent was removed under reduced pressure, the mixture was washed with MeOH (10 mL) to remove the phosphazanium salts. The resulting mixture was dissolved in CHCl₃ (15 mL) and filtered to remove the insoluble compounds. After evaporation of the organic solvent, the mixture was purified by precipitation using CHCl₃ and MeOH at -10°C to obtain the desired polymer **pip-NPFV** as a reddish-brown solid (425 mg, 81%).

¹H NMR (THF-d₈, 400 MHz): 0.78 (m, 10H), 1.12 (m, 12H), 1.44 (br, 12H, *E*-isomer), 1.68 (br, 12H, *Z*-isomer) 2.03 (m, 4H), 2.52 (br, 8H, *E*-isomer), 3.11 (br, 8H, *Z*-isomer), 7.56 (m, H), 10.02 (s, 2H).

SEC: $\overline{M}_n = 5200 \text{ g}\cdot\text{mol}^{-1}$; $\overline{M}_w = 10660 \text{ g}\cdot\text{mol}^{-1}$; $\overline{D} = 2.05$

UV/Vis absorption $\lambda_{\text{max}} = 240, 483 \text{ nm}$.

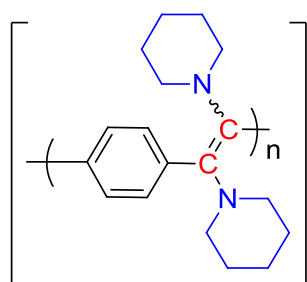
Emission spectroscopie: $\lambda_{\text{max}}(\text{liq}) = 561 \text{ nm}$, $\lambda_{\text{max}}(\text{thin film}) = 640 \text{ nm}$



To a stirred solution of **iPr₂N-PPV** (50 mg, 0.166 mmol) in a 50/50 CHCl₃/CH₃CN (4 ml_{tot}) was added TfOH (14 μL, 1.66 mmol) dropwisely at -40°C. The reaction mixture was stirred at this temperature for 10 minutes then let warmed to room temperature. The solvent was removed under vacuum to give the compound **iPr₂NH⁺-PPV** as a light brown powder in quantitative yield (49 mg).

UV/Vis analysis: $\lambda_{\text{max}} = 252 \text{ and } 352 \text{ nm}$.

Chapter III: Synthesis of amino-PPV by metal free dimerization/polymerization of novel bis-aminoarylcarbenes

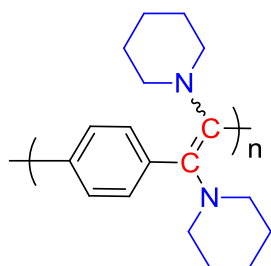


PipNH⁺-PPV

- 2 TfOH **Poly(7,8-bispiperidinium-1,4-phenylenevinylene) triflate:**

To a solution of polymer **pipN-PPPV** (0,134 g, 0.50 mmol) in CH₃CN/CHCl₃ (50/50) cooled at -40°C, TfOH (184.2 μL, 2.2 mmol) was added dropwise. The resulting mixture was warm to room temperature overnight and the organic solvent were evaporated to give the final compound **pipNH⁺-PPV** (99%, 0.245 g).

UV/Vis analysis: $\lambda_{\max} = 254$ nm.



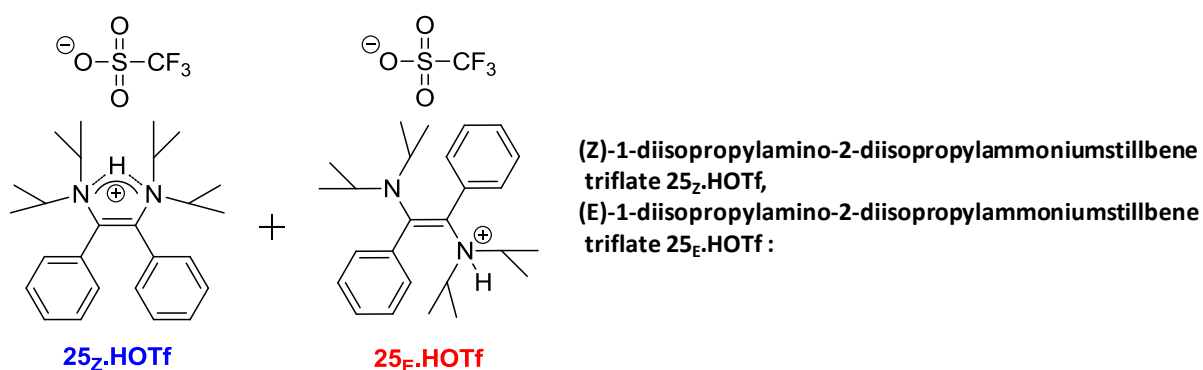
PipN-PPV

- Deprotonated Poly(7,8-bispiperidine-1,4-phenylenevinylene):**

To a stirred solution of **pipNH⁺-PPV** (0.054 g, 0.1 mmol) in CH₃CN/CHCl₃ (50/50) cooled at 0°C, *t*-BuOK (0.021 g, 0.2 mmol) was added. The reaction was warm to room temperature overnight, the solvents were removed under reduced pressure and the resulting mixture was extract with CHCl₃ leading to the final polymer **pipN-PPV** (0.048g, 89%).

UV/Vis gave $\lambda_{\max} = 462$ nm.

Chapter III: Synthesis of amino-PPV by metal free dimerization/polymerization of
novel bis-aminoarylcarbenes



To a stirred solution of **25** (0.55 g, 1.5 mmol) in DCM (1 mL) cooled at -78°C was added TfOH (0.13 mL, 1.5 mmol) dropwise. The reaction mixture was stirred at this temperature for 1h and overnight at room temperature. The solvent was evaporated under reduced pressure, the mixture washed with dry ether and dried under vacuum to obtain the desired **25_z.HOTf** and **25_e.HOTf** (0.056 g, 99%) as a white powder.

^1H NMR (ACN- d_6 , 400 MHz): [*Z*-isomer] 1.41 (br, 24H), 3.80 (hept, 4H, $J = 6.6$ Hz), 7.23-7.27 (m, 6H), 7.34-7.38 (m, 4H), 9.69 (s, 1H); [*E*-isomer] δ 0.72 (d, 12H), 1.13 (d, 6H), 1.32 (d, 6H), 3.44 (hept, 2H, $J = 6.8$ Hz), 4.27 (oct, 2H, $J = 6.5$ Hz), 5.98 (br, 1H), 7.48-7.51 (m, 1H), 7.54-7.62 (m, 5H), 7.76-7.81 (m, 4H);

^{13}C NMR (THF- d_8 , 101 MHz): [*Z*-isomer] δ 19.21, 55.22, 122.77, 129.42, 129.96, 131.78, 133.77, 143.14; [*E*-isomer] δ 19.21, 20.96, 22.95, 52.90, 60.81, 120.68, 123.89, 130.24, 130.32, 130.35, 131.75, 132.93, 134.09, 135.81, 150.97;

^{19}F NMR (CD_3CN , 377 MHz): -78.75

IR (ATR) ν_{max} (cm^{-1}): 3635, 3400, 3165, 2984, 1605, 1470, 1367, 1267, 1140, 1028, 774, 709, 633;

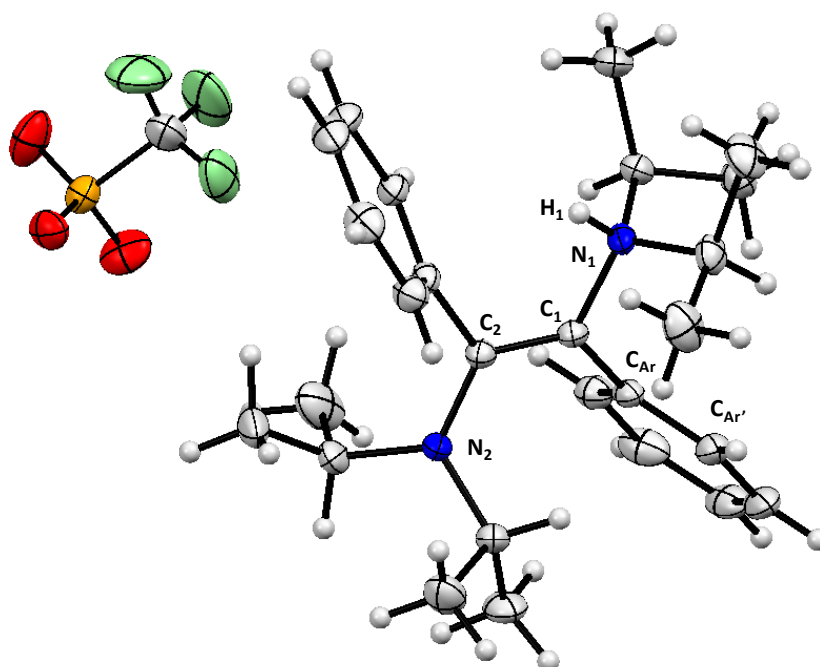
λ_{max} (ACN): 221, 325

Crystal data of the E isomer:

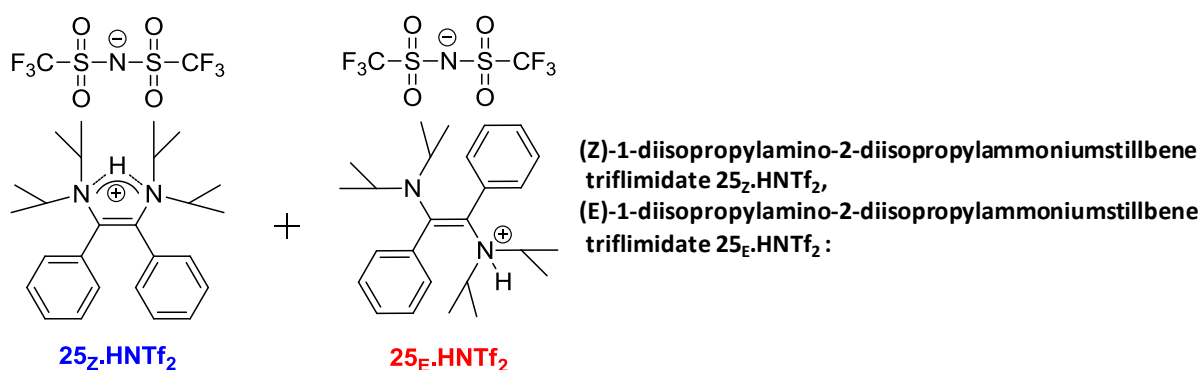
Identification code	(E)-1-diisopropylamino-2-diisopropylammoniumstilbene triflate
Empirical formula	$\text{C}_{27}\text{H}_{39}\text{F}_3\text{N}_2\text{O}_3\text{S}$
Formula weight	528.66
Temperature/K	293(2)
Crystal system	monoclinic
Space group	$\text{P2}_1/\text{n}$
$a/\text{\AA}$	11.730(2)
$b/\text{\AA}$	14.748(3)

Chapter III: Synthesis of amino-PPV by metal free dimerization/polymerization of
 novel bis-aminoarylcarbenes

$c/\text{\AA}$	16.335(4)
$\alpha/^\circ$	90
$\beta/^\circ$	101.728(7)
$\gamma/^\circ$	90
Volume/ \AA^3	2766.9(10)
Z	4
$\rho_{\text{calc}}/\text{cm}^3$	1.269
μ/mm^{-1}	1.433
F(000)	1128.0
Crystal size/ mm^3	? \times ? \times ?
Radiation	CuK α ($\lambda = 1.54187$)
2Θ range for data collection/ $^\circ$	8.154 to 146.188
Index ranges	$-14 \leq h \leq 14$, $-17 \leq k \leq 17$, $-19 \leq l \leq 20$
Reflections collected	21261
Independent reflections	5441 [$R_{\text{int}} = 0.0259$, $R_{\text{sigma}} = 0.0195$]
Data/restraints/parameters	5441/0/338
Goodness-of-fit on F^2	1.028
Final R indexes [$I \geq 2\sigma(I)$]	$R_1 = 0.0672$, $wR_2 = 0.1880$
Final R indexes [all data]	$R_1 = 0.0707$, $wR_2 = 0.1914$
Largest diff. peak/hole / $e \text{\AA}^{-3}$	1.87/-0.92



Chapter III: Synthesis of amino-PPV by metal free dimerization/polymerization of
novel bis-aminoarylcarbenes



To a stirred solution of **25** (0.55 g, 1.5 mmol) and HTFSI (0.42, 1.5 mmol) is added dropwise DCM (1 mL) at -78°C . The reaction mixture was stirred at this temperature for 1h and overnight at room temperature. The solvent was evaporated under reduced pressure, the mixture washed with dry ether and dried under vacuum to obtain the desired **25_Z.HNTf₂** and **25_E.HNTf₂** (0.97 g, 99%) as a white powder.

^1H NMR (CD_3CN , 400 MHz): [*Z*-isomer] 1.58 (br, 24H), 3.67 (dhept, 2H, $J = 6.7$ and 2.7 Hz), 7.24-7.33 (m, 10H), 9.79 (s, 1H); [*E*-isomer] δ 0.67 (d, 12H), 1.07 (d, 6H), 1.25 (d, 6H), 3.43 (hept, 2H, $J = 6.7$ Hz), 4.00 (oct, 2H, $J = 6.7$ Hz), 5.79 (br, 1H), 7.54-7.63 (m, 10H);

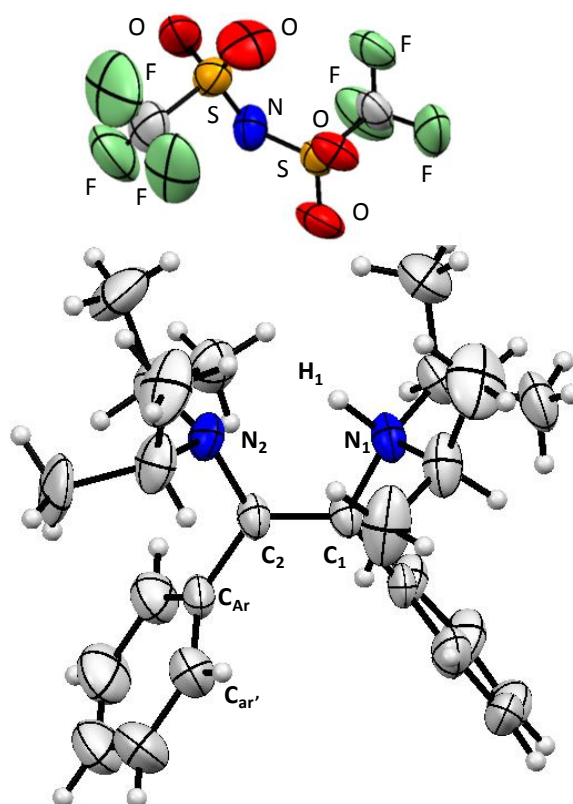
^{13}C NMR ($\text{THF-}d_8$, 101 MHz): [*Z*-isomer] δ 18.72, 57.91, 100.96, 131.59, 131.21, 133.68, 143.33; [*E*-isomer] δ 19.22, 20.81, 22.93, 53.11, 55.16, 61.04, 129.77, 130.50, 130.63, 130.67, 130.91, 131.75, 133.12, 133.97, 135.79, 151.41;

^{19}F NMR (CD_3CN , 377 MHz): -80.23

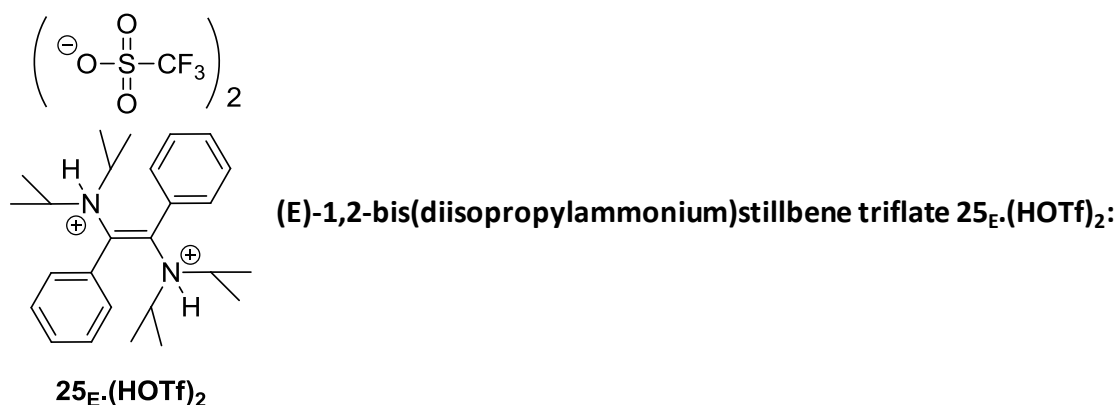
Identification code	(Z)-1-diisopropylamino-2-diisopropylammoniumstillbene triflimidate
Empirical formula	$\text{C}_{28}\text{H}_{39}\text{F}_6\text{N}_3\text{O}_4\text{S}_2$
Formula weight	659.74
Temperature/K	293(2)
Crystal system	triclinic
Space group	P-1
$a/\text{\AA}$	9.2918(11)
$b/\text{\AA}$	11.7430(9)
$c/\text{\AA}$	15.9341(7)
$\alpha/^\circ$	89.056(5)
$\beta/^\circ$	87.604(7)
$\gamma/^\circ$	70.116(9)
Volume/ \AA^3	1633.5(3)

Chapter III: Synthesis of amino-PPV by metal free dimerization/polymerization of novel bis-aminoarylcarbenes

Z	2
$\rho_{\text{calc}}/\text{cm}^3$	1.341
μ/mm^{-1}	2.107
F(000)	692.0
Crystal size/ mm^3	? \times ? \times ?
Radiation	CuK α ($\lambda = 1.54184$)
2 Θ range for data collection/ $^\circ$	13.698 to 136.5
Index ranges	$-11 \leq h \leq 11$, $-14 \leq k \leq 12$, $-19 \leq l \leq 19$
Reflections collected	21946
Independent reflections	5909 [$R_{\text{int}} = 0.1951$, $R_{\text{sigma}} = 0.1719$]
Data/restraints/parameters	5909/0/396
Goodness-of-fit on F^2	1.050
Final R indexes [$I \geq 2\sigma(I)$]	$R_1 = 0.1415$, $wR_2 = 0.3388$
Final R indexes [all data]	$R_1 = 0.1695$, $wR_2 = 0.3728$
Largest diff. peak/hole / $e \text{ \AA}^{-3}$	1.03/-0.61



Chapter III: Synthesis of amino-PPV by metal free dimerization/polymerization of novel bis-aminoarylcarbenes



To a stirred solution of **25** (0.55 g, 1.5 mmol) in DCM (1 mL) cooled at -78°C was added TfOH (0.26 mL, 3 mmol) dropwise. The reaction mixture was stirred at this temperature for 1h and overnight at room temperature. The solvent was evaporated under reduced pressure, the mixture washed with dry ether and dried under vacuum to obtain the desired **$25_E \cdot (\text{HOTf})_2$** (0.034 g, 80%) as a white powder.

^1H NMR (ACN- d_6 , 400 MHz): δ 1.29 (dd, 24H, $J = 6.9$ Hz), 4.03 (oct, 4H, $J = 6.6$ Hz), 6.83 (br, 2H), 7.74-7.81 (m, 8H), 7.85-7.89 (m, 2H);

^{13}C NMR (THF- d_8 , 101 MHz): δ 18.90, 20.43, 61.73, 123.16, 132.06, 133.41, 134.92, 140.09;

^{19}F NMR (CD_3CN , 377 MHz): -79.25;

IR (ATR) ν_{max} (cm^{-1}): 3514, 3065, 2360, 1465, 1389, 1285, 1245, 1221, 1150, 1027, 714, 628, 51;

UV/Vis analysis: $\lambda_{\text{max}}(\text{ACN}) = 229, 325$;

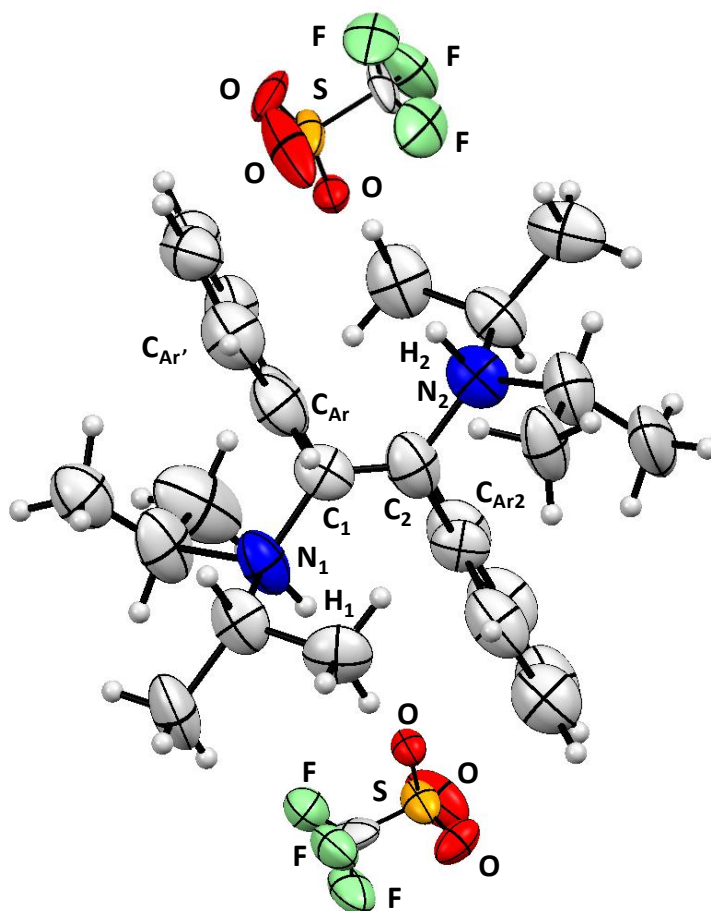
Emission spectrophotometry: irradiation at 325 nm, $\lambda_{\text{max}}(\text{ACN}) = 446$ nm

Crystal data :

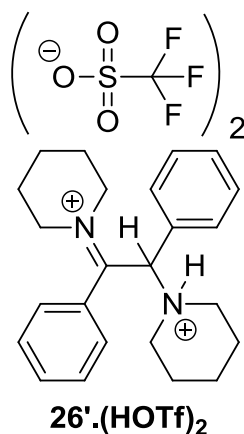
Identification code	(E)-1,2-bis(diisopropylammonium)stilbene triflate
Empirical formula	$\text{C}_{28}\text{H}_{40}\text{F}_6\text{N}_2\text{O}_6\text{S}_2$
Formula weight	678.74
Temperature/K	566(2)
Crystal system	monoclinic
Space group	Cc
a/Å	23.542(11)
b/Å	9.569(5)
c/Å	16.752(8)
$\alpha/^\circ$	90
$\beta/^\circ$	98.967(9)
$\gamma/^\circ$	90

Chapter III: Synthesis of amino-PPV by metal free dimerization/polymerization of
 novel bis-aminoarylcarbenes

Volume/Å ³	3728(3)
Z	4
$\rho_{\text{calc}}/\text{cm}^3$	1.209
μ/mm^{-1}	1.849
F(000)	1424.0
Crystal size/mm ³	0.200 × 0.200 × 0.200
Radiation	CuK α (λ = 1.54178)
2 Θ range for data collection/°	5.34 to 140.13
Index ranges	-28 ≤ h ≤ 28, -11 ≤ k ≤ 11, -20 ≤ l ≤ 20
Reflections collected	14119
Independent reflections	6105 [R_{int} = 0.0951, R_{sigma} = 0.1217]
Data/restraints/parameters	6105/20/406
Goodness-of-fit on F ²	0.820
Final R indexes [$I \geq 2\sigma(I)$]	R_1 = 0.0883, wR_2 = 0.2309
Final R indexes [all data]	R_1 = 0.1519, wR_2 = 0.2549
Largest diff. peak/hole / e Å ⁻³	0.52/-0.40
Flack parameter	0.18(8)



Chapter III: Synthesis of amino-PPV by metal free dimerization/polymerization of novel bis-aminoarylcabenenes



1-piperidinium-2-piperidineiminium-1,2-(diphenyl)ethane 26'.(HOTf)₂:

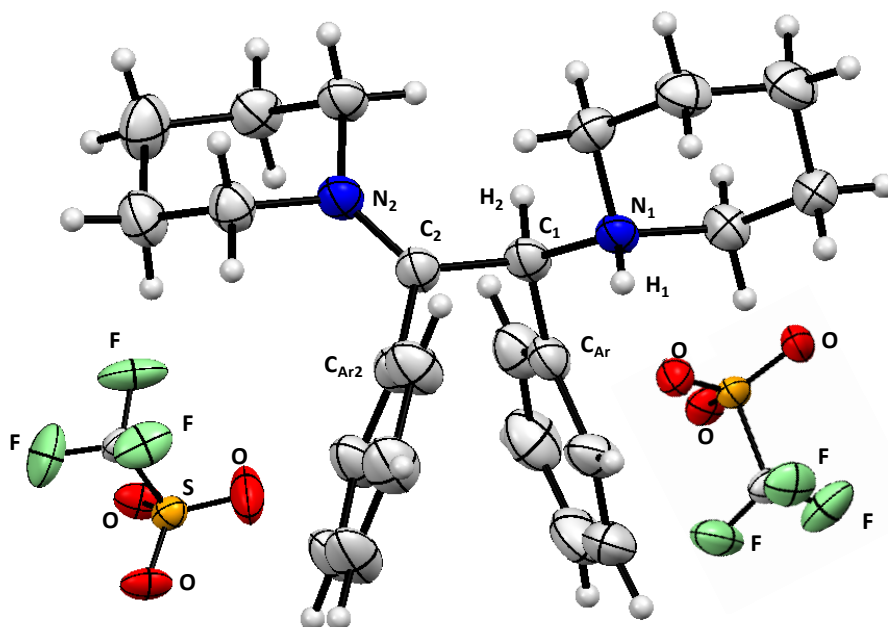
To a stirred solution of **26** (0.080 g, 0.23 mmol) in DCM (1 mL) cooled at -78°C was added TfOH (0.21 mL, 2.3 mmol) dropwise. The reaction mixture was stirred at this temperature for 1h and overnight at room temperature. The solvent was evaporated under reduced pressure, the mixture washed with dry ether and dried under vacuum to obtain the desired **26'.(HOTf)₂** (0.074 g, 50%) as a pink powder.

Crystal data:

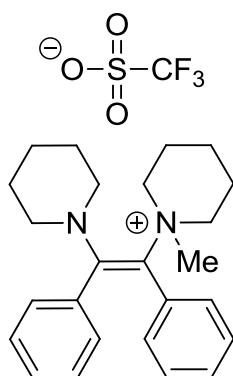
Identification code	1-piperidinium-2-piperidineiminium-1,2-(diphenyl)ethane
Empirical formula	C ₁₁ H ₁₀ FNOS
Formula weight	172.20
Temperature/K	293(2)
Crystal system	triclinic
Space group	P-1
a/Å	9.8105(4)
b/Å	11.7978(6)
c/Å	13.4042(7)
$\alpha/^{\circ}$	79.358(5)
$\beta/^{\circ}$	74.454(5)
$\gamma/^{\circ}$	76.046(4)
Volume/Å ³	1438.56(13)
Z	6
$\rho_{\text{calc}}/\text{cm}^3$	1.193
μ/mm^{-1}	0.614
F(000)	546.0
Crystal size/mm ³	? × ? × ?

Chapter III: Synthesis of amino-PPV by metal free dimerization/polymerization of novel bis-aminoarylcarbenes

Radiation	CuK α ($\lambda = 1.54184$)
2 Θ range for data collection/ $^{\circ}$	13.048 to 136.494
Index ranges	$-11 \leq h \leq 10$, $-14 \leq k \leq 14$, $-16 \leq l \leq 16$
Reflections collected	15485
Independent reflections	5200 [$R_{\text{int}} = 0.2484$, $R_{\text{sigma}} = 0.1136$]
Data/restraints/parameters	5200/0/382
Goodness-of-fit on F^2	1.723
Final R indexes [$I \geq 2\sigma(I)$]	$R_1 = 0.1616$, $wR_2 = 0.4074$
Final R indexes [all data]	$R_1 = 0.1669$, $wR_2 = 0.4236$
Largest diff. peak/hole / $e \text{ \AA}^{-3}$	1.61/-0.68



Chapter III: Synthesis of amino-PPV by metal free dimerization/polymerization of novel bis-aminoarylcarbenes



(Z)-1-piperidine-2-(N-methyl)piperidiniumstillbene triflate 26_z.MeOTf:

26_z.MeOTf

To a stirred solution of **26** (0.1 g, 0.3 mmol) in DCM (1 mL) cooled at -78°C, MeOTf (0.34 mL, 3 mmol) was added. The resulting mixture was stirred at this temperature for 1h and warmed to room temperature overnight. The solvent was evaporated under reduced pressure, and the reaction mixture was washed with dry ether (sonicated for 1h) and dried under vacuum to afford the methylated dimer **26_z.MeOTf** as a white solid (90 mg).

¹H NMR (THF-*d*₈, 400 MHz): δ 1.53-1.57 (m, 3H), 1.79-1.84 (m, 3H), 1.92-2.09 (m, 6H), “1.1è (br, 3H, Me), 3.85 (s, 4H), 3.94-4.00 (m, 2H), 4.08-4.15 (m, 2H), 7.02-7.13 (m, 6H), 7.20-7.22 (m, 1H), 7.33-7.36 (m, 1H), 7.43-7.46 (m, 2H).

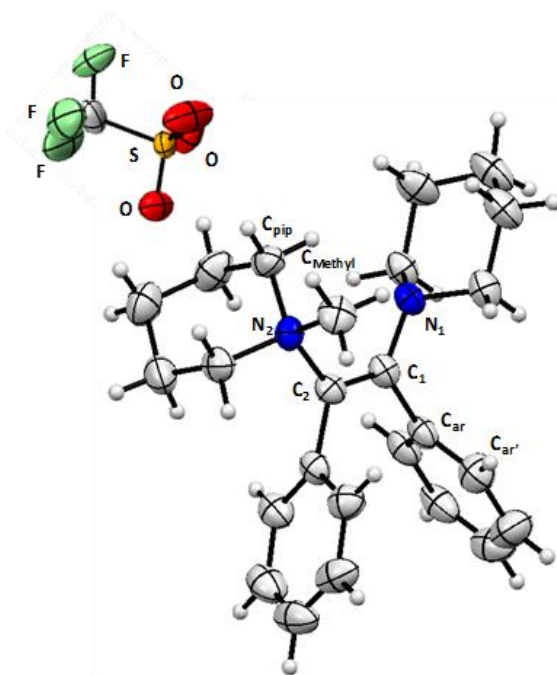
UV/Vis analysis: λ_{max} = 267 nm.

Crystal data :

Identification code	(Z)-1-piperidine-2-(N-methyl)piperidiniumstillbene triflate:
Empirical formula	C ₅₂ H ₆₆ F ₆ N ₄ O ₆ S ₂
Formula weight	1021.20
Temperature/K	373(2)
Crystal system	orthorhombic
Space group	P2 ₁ 2 ₁ 2 ₁
a/Å	10.440(3)
b/Å	17.385(5)
c/Å	28.114(9)
α/°	90
β/°	90
γ/°	90
Volume/Å ³	5103(3)

Chapter III: Synthesis of amino-PPV by metal free dimerization/polymerization of novel bis-aminoarylcarbenes

Z	4
$\rho_{\text{calc}}/\text{cm}^3$	1.329
μ/mm^{-1}	1.581
F(000)	2160.0
Crystal size/ mm^3	$0.200 \times 0.200 \times 0.200$
Radiation	$\text{CuK}\alpha$ ($\lambda = 1.54178$)
2Θ range for data collection/ $^\circ$	5.976 to 146.926
Index ranges	$-12 \leq h \leq 12, -21 \leq k \leq 21, -34 \leq l \leq 33$
Reflections collected	39265
Independent reflections	10014 [$R_{\text{int}} = 0.0581, R_{\text{sigma}} = 0.0488$]
Data/restraints/parameters	10014/0/633
Goodness-of-fit on F^2	1.024
Final R indexes [$I \geq 2\sigma(I)$]	$R_1 = 0.0641, wR_2 = 0.1749$
Final R indexes [all data]	$R_1 = 0.0692, wR_2 = 0.1782$
Largest diff. peak/hole / $e \text{ \AA}^{-3}$	0.87/-0.60
Flack parameter	0.146(9)



Chapter III: Synthesis of amino-PPV by metal free dimerization/polymerization of novel bis-aminoarylcabenenes

III.7 References

1. H. G. Gilch and W. L. Wheelwright, *J. Polym. Sci. [A1]*, 1966, **4**, 1337–1349.
2. A. E. Siegrist, P. Liechti, H. R. Meyer and K. Weber, *Helv. Chim. Acta*, 1969, **52**, 2521–2554.
3. R. A. Wessling, in *Journal of Polymer Science: Polymer Symposia*, Wiley Online Library, 1985, vol. 72, pp. 55–66.
4. N. Ono, H. Tomita and K. Maruyama, *J. Chem. Soc. Perkin 1*, 1992, **19**, 2453–2456.
5. Y. Suzuki, K. Hashimoto and K. Tajima, *Macromolecules*, 2007, **40**, 6521–6528.
6. J.-R. Pouliot, F. Grenier, J. T. Blaskovits, S. Beaupré and M. Leclerc, *Chem. Rev.*, 2016, **116**, 14225–14274.
7. F. Koch and W. Heitz, *Macromol. Chem. Phys.*, 1997, **198**, 1531–1544.
8. B. Carsten, F. He, H. J. Son, T. Xu and L. Yu, *Chem. Rev.*, 2011, **111**, 1493–1528.
9. R. F. Heck and J. P. Nolley, *J. Org. Chem.*, 1972, **37**, 2320–2322.
10. Z. Bao, Y. Chen, R. Cai and L. Yu, *Macromolecules*, 1993, **26**, 5281–5286.
11. D. Milstein and J. K. Stille, *J. Am. Chem. Soc.*, 1978, **100**, 3636–3638.
12. F. Babudri, S. R. Cicco, L. Chiavarone, G. M. Farinola, L. C. Lopez, F. Naso and G. Scamarcio, *J. Mater. Chem.*, 2000, **10**, 1573–1579.
13. F. Babudri, A. Cardone, G. Ciccarella, G. M. Farinola, F. Naso, L. Chiavarone and G. Scamarcio, *Chem. Commun.*, 2001, **19**, 1940–1941.
14. C. Cordovilla, C. Bartolomé, J. M. Martínez-Illarduya and P. Espinet, *ACS Catal.*, 2015, **5**, 3040–3053.
15. H. Katayama, M. Nagao, T. Nishimura, Y. Matsui, Y. Fukuse, M. Wakioka and F. Ozawa, *Macromolecules*, 2006, **39**, 2039–2048.
16. R. S. Ashraf, B. C. Schroeder, H. A. Bronstein, Z. Huang, S. Thomas, R. J. Kline, C. J. Brabec, P. Rannou, T. D. Anthopoulos, J. R. Durrant and I. McCulloch, *Adv. Mater.*, 2013, **25**, 2029–2034.
17. Ö. Usluer, M. Abbas, G. Wantz, L. Vignau, L. Hirsch, E. Grana, C. Brochon, E. Cloutet and G. Hadziioannou, *ACS Macro Lett.*, 2014, **3**, 1134–1138.
18. M. Urien, G. Wantz, E. Cloutet, L. Hirsch, P. Tardy, L. Vignau, H. Cramail and J.-P. Parneix, *Org. Electron.*, 2007, **8**, 727–734.
19. S. R. Cowan, W. L. Leong, N. Banerji, G. Dennler and A. J. Heeger, *Adv. Funct. Mater.*, 2011, **21**, 3083–3092.
20. M. P. Nikiforov, B. Lai, W. Chen, S. Chen, R. D. Schaller, J. Strzalka, J. Maser and S. B. Darling, *Energy Environ. Sci.*, 2013, **6**, 1513.
21. J. H. P. Utley and Y. Gao, *J Mater Chem*, 1995, **5**, 1837–1845.
22. H. Nishihara, T. M. Ohsawa, R. Y. Tateishi, Y. Company and K. Kimura, *Chem. Lett.*, 1987, 539.
23. N. Baute, L. Martinot and R. Jérôme, *J. Electroanal. Chem.*, 1999, **472**, 83–90.
24. *Handbook of Conducting Polymers: Second Edition*, .
25. J. H. P. Utley and J. Gruber, *J. Mater. Chem.*, 2002, **12**, 1613–1624.
26. G. Wittig and U. Schöllkopf, *Chem. Ber.*, 1954, **87**, 1318–1330.
27. L. Horner, H. Hoffmann, H. G. Wippel and G. Klahre, *Chem. Ber.*, 1959, **92**, 2499–2505.
28. R. N. McDonald and T. W. Campbell, *J. Am. Chem. Soc.*, 1960, **82**, 4669–4671.
29. N. C. Greenham, S. C. Moratti, D. D. C. Bradley, R. H. Friend and A. B. Holmes, *Nature*, 1993, 628–630.
30. Y. Qiu, Y. Liu, K. Yang, W. Hong, Z. Li, Z. Wang, Z. Yao and S. Jiang, *Org. Lett.*, 2011, **13**, 3556–3559.

Chapter III: Synthesis of amino-PPV by metal free dimerization/polymerization of novel bis-aminoarylcabenones

31. V. P. Mehta and B. Punji, *RSC Adv.*, 2013, **3**, 11957–11986.
32. C.-L. Sun and Z.-J. Shi, *Chem. Rev.*, 2014, **114**, 9219–9280.
33. R. A. Wessling, R. G. Zimmerman, U. S. Pats. 3,401,152 (1968); 3,404,132 (1968) 3,532,643
34. E. M. Sanford, A. L. Perkins, B. Tang, A. M. Kubasiak and J. T. Reeves, 1999, **23**, 2347–2348.
35. T. Schwalm, J. Wiesecke, S. Immel and M. Rehahn, *Macromol. Rapid Commun.*, 2009, **30**, 1295–1322.
36. J.-C. Chen, C.-J. Chiang, J.-C. Chiu and J.-J. Ju, *Chem. Commun.*, 2012, **48**, 7756–7758.
37. J. D. Nikolić, S. Wouters, J. Romanova, A. Shimizu, B. Champagne, T. Junkers, D. Vanderzande, D. Van Neck, M. Waroquier, V. Van Speybroeck and S. Catak, *Chem. - Eur. J.*, 2015, **21**, 19176–19185.
38. K. Aravindu, E. Cloutet, C. Brochon, G. Hadziioannou, J. Vignolle, F. Robert, D. Taton and Y. Landais, *Macromolecules*, 2018, **51**, 5852–5862.
39. H. Kretzschmann and H. Meier, *Tetrahedron Lett.*, 1991, **32**, 5059–5062.
40. A. P. Davey, A. Drury, S. Maier, H. J. Byrne and W. J. Blau, *Synth. Met.*, 1999, **103**, 2478–2479.
41. S. C. Morattia, R. Cervinia, A. B. Holmesa, D. R. Baigentb, R. H. Friendb, N. C. Greenhamb and J. Grtiner, *Synth. Met.*, 1995, **71**, 2117–2120.
42. T. Benincori, E. Brenna, F. Sannicolò, G. Zotti, S. Zecchin, G. Schiavon, C. Gatti and G. Frigerio, *Chem. Mater.*, 2000, **12**, 1480–1489.
43. K. Kawabata and H. Goto, *Synth. Met.*, 2010, **160**, 2290–2298.
44. J. A. Aristizabal, J. P. Soto, L. Ballesteros, E. Muñoz and J. C. Ahumada, *Polym. Bull.*, 2013, **70**, 35–46.
45. A. F. Diaz, K. K. Kanazawa and G. P. Gardini, *J. Chem. Soc. Chem. Commun.*, 1979, **14**, 635–636.
46. M. Delamar, P.-C. Lacaze, J.-Y. Dumousseau and J.-E. Dubois, *Electrochimica Acta*, 1982, **27**, 61–65.
47. Z.-B. Zhang, M. Fujiki, H.-Z. Tang, M. Motonaga and K. Torimitsu, *Macromolecules*, 2002, **35**, 1988–1990.
48. S. Komaba, A. Amano and T. Osaka, *J. Electroanal. Chem.*, 1997, **430**, 97–102.
49. G. Tourillon and F. Garnier, *J Electroanal Chem*, 1982, 173–178.
50. R. Noufi, A. J. Nozi, J. White and L. F. Warren, *J Electrochem Soc*, 1981, 2261–2265.
51. M. Leclerc, F. Martinez Diaz, G. Wegner, *Makromol. Chem*, 1989, **190**, 3105–3114.
52. M. N. Hopkinson, C. Richter, M. Schedler and F. Glorius, *Nature*, 2014, **510**, 485–496.
53. J. W. Kamplain and C. W. Bielawski, *Chem. Commun.*, 2006, 1727–1729.
54. B. M. Neilson, A. G. Tennyson and C. W. Bielawski, *J. Phys. Org. Chem.*, 2012, **25**, 531–543.
55. M. Otto, S. Conejero, Y. Canac, V. D. Romanenko, V. Rudzevitch and G. Bertrand, *J. Am. Chem. Soc.*, 2004, **126**, 1016–1017.
56. S. Conejero, Y. Canac, F. S. Tham and G. Bertrand, *Angew. Chem. Int. Ed.*, 2004, **43**, 4089–4093.
57. W. Schroth, U. Jahn and D. Ströhl, *Chem. Ber.*, 1994, **127**, 2013–2022.
58. R. W. Alder, M. E. Blake, S. Bufali, C. P. Butts, A. G. Orpen, J. Schütz and S. J. Williams, *J. Chem. Soc. Perkin I*, 2001, **14**, 1586–1593.
59. T. Morishita, H. Fukushima, H. Yoshida, J. Ohshita and A. Kunai, *J. Org. Chem.*, 2008, **73**, 5452–5457.
60. Z. Fang, R. D. Webster, M. Samoc and Y.-H. Lai, *RSC Adv.*, 2013, **3**, 17914–17917.

Chapter III: Synthesis of amino-PPV by metal free dimerization/polymerization of novel bis-aminoarylcabenenes

61. L. T. Ball, G. C. Lloyd-Jones and C. A. Russell, *J. Am. Chem. Soc.*, 2014, **136**, 254–264.
62. K. Pichler, D. A. Halliday, D. D. C. Bradley, P. L. Burn, R. H. Friend and A. B. Holmes, *J. Phys. Condens. Matter*, 1993, **5**, 7155–7172.
63. T.-Q. Nguyen and B. J. Schwartz, *J. Chem. Phys.*, 2002, **116**, 8198–8208.

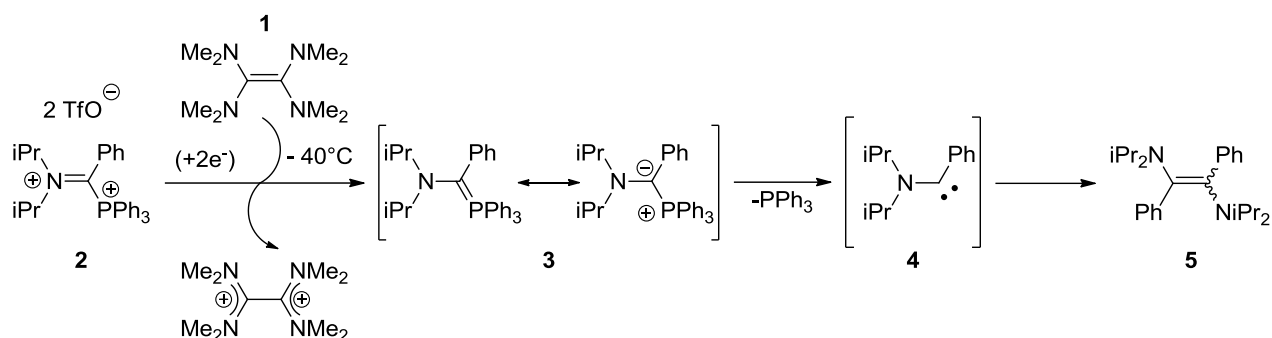
**Chapter IV: Electron-rich diaminoalkene as
potential stoichiometric electron-transfer
reagent or as organophotocatalyst**

IV.1 Introduction

Diaminoalkenes (DAA) synthesized in previous chapter are electron-rich olefins due to the interaction of the two amino groups with the central C=C double bond. They are, indeed, structurally related to tetraaminoalkenes (TAA), being well-known as powerful organic reducing agents due to the interaction of the four nitrogen atoms with the C=C double bond. Although weaker reducing properties are expected for diaminoalkenes (DAA), they have been tested in model reactions for their ability to reduce C-X (X =Br, I) bonds. They were also investigated as photocatalyst in a selected polymerization reaction, namely Organocatalyzed Atom Transfer Radical Polymerization (OATRP), where their reducing power is exacerbated through photo-irradiation. The corresponding literature about electron-transfer reagents and photocatalysts exhibiting reducing properties is thus presented first, followed by our own studies on the stoichiometric reduction of C-X bonds by our DAA and on their role as photocatalyst in OATRP.

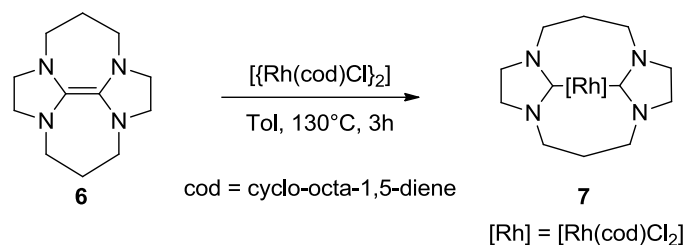
IV.1.1 Stoichiometric electron-transfer reagent

The first tetraaminoethylene, namely tetrakis(dimethylamino)ethylene **1** (TDAE), was reported by Pruett *et al.* in 1950.¹ At that time, although the authors recognized the intense luminescence of this compound when in contact with the oxygen of air, they did not examine its reactivity. The systematic study of the properties of this class of compounds only began a decade later with the work of Wanzlick on the dimerization of imidazolin-2-ylidenes, allowing a facile access to this class of compounds. Since then, tetraaminoalkenes have been mainly used as stoichiometric reducing agents,²⁻⁶ although other applications including precursor of NHC-metal complexes⁷⁻¹⁰ and organocatalysts^{11,12} have been reported (Scheme 1-3). Scheme 1 highlights how TDAE transfers two electrons to dication **2** to generate the neutral aminophosphinoylide intermediate **3**, which then fragments into the corresponding carbene. The latter instantaneously dimerizes to give the corresponding DAA **5**. This route has been presented in the previous chapter as an original way to access carbenes.



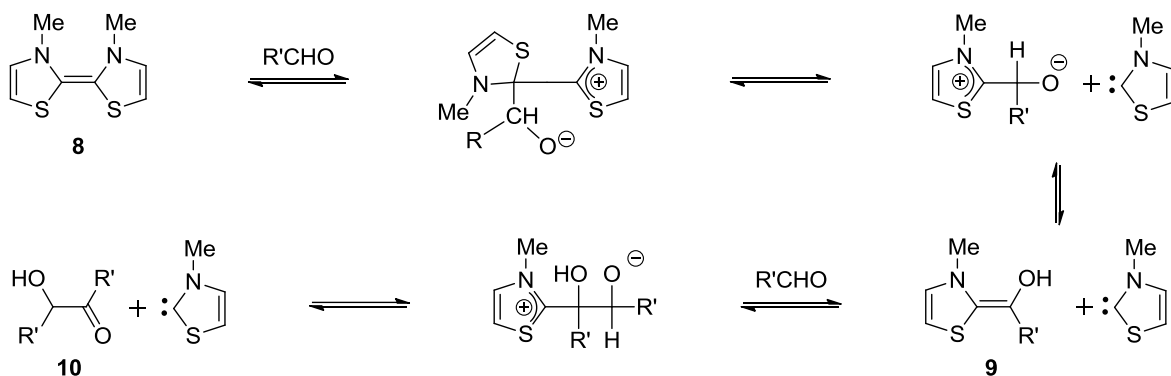
Scheme IV.1. Synthesis of DAA **5** from the reduction of dication **2** via transfer of two electrons from TDAE **1**.

In Scheme 2, the insertion of rhodium into the C=C bond of the doubly-tethered diaminoalkene **6** allows the facile access to the corresponding homoleptic bis-NHC complex **7**.



Scheme IV.2. Synthesis of bis-NHC complex **7** generated from the insertion of rhodium into the C=C bond of **6**.

The ability of analogous dithiadiazafulvalene **8** to catalyze the benzoin condensation is presented in Scheme 3. The first step illustrates the addition of the C=C double bond of **8** onto an aldehyde, leading to the Breslow intermediate **9** and a free NHC. Then, the nucleophilic aldehyde (umpolung) in **9** adds to another electrophilic aldehyde generating the final benzoin **10** and a free carbene.



Scheme IV.3. Benzoin condensation catalyzed by the dithiadiazafulvalene **8**.

Over the years, tetraaminoalkenes have mainly been used as powerful organic reducing agent, and a variety of compounds **11-16** with a range of reducing power has been reported. For each compounds **11-16**, redox potentials $E_{1/2}$, obtained through cyclic voltammetry were measured in a DMF solution, showing a two-electron redox wave (Figure 1). Therefore, the first part of this introduction will be focused on the presentation of TAA as stoichiometric reducing agent in organic synthesis.

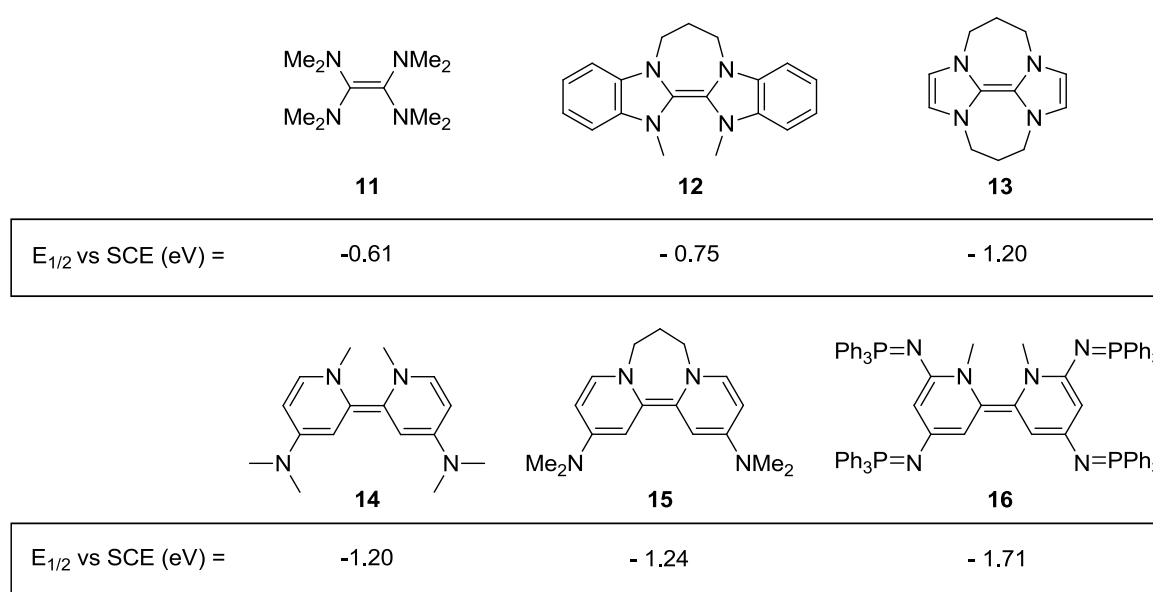
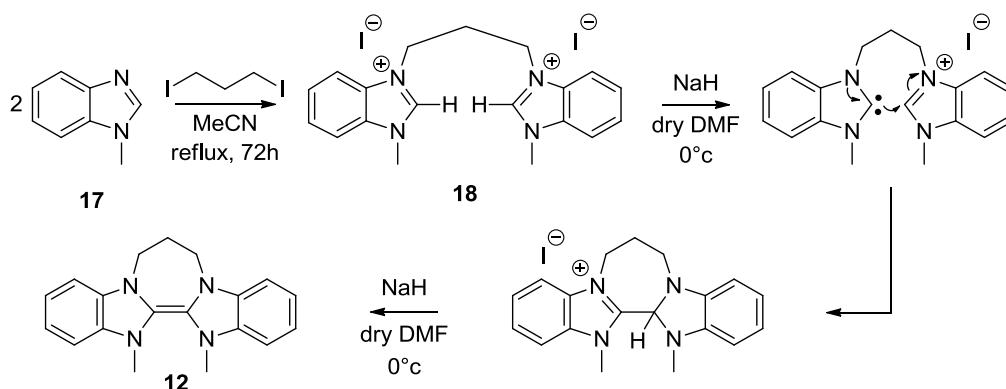


Figure IV.1. Families of super-electron donors obtained from carbene dimerization.^{3,4,13}

It is worth noticing that the presence of one or two bridges in the substrates enhance their reducing power. This is due to an increase of the planarity in the molecules induced by the bridge, allowing the radical formed to be delocalized more easily, making it more stable.

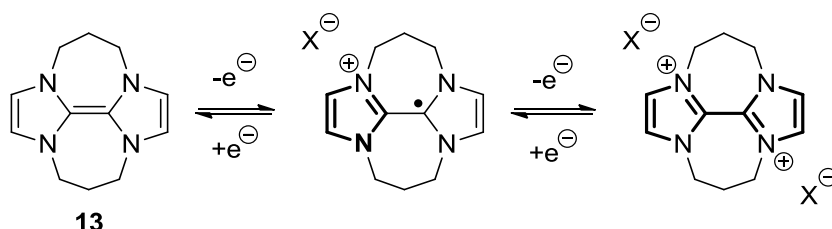
IV.1.1.1 Synthesis and stabilization

The synthesis to access the electron-rich compounds **11-16** is similar and consists in the deprotonation of their corresponding bis-iminium salt precursors as highlighted in Scheme 4, with the synthesis of the mono-bridged **12** as a representative example.⁴ The first step is an alkylation of two benzimidazolium moieties **17** to generate the intermediate **18**. Then, deprotonation of **18** by addition of a strong base leads to the dimerized compound **12** (Scheme 4).



Scheme IV.4. Synthesis of compound **12** via alkylation of **17**, followed by the deprotonation of the bis-iminium salt precursor **18**.

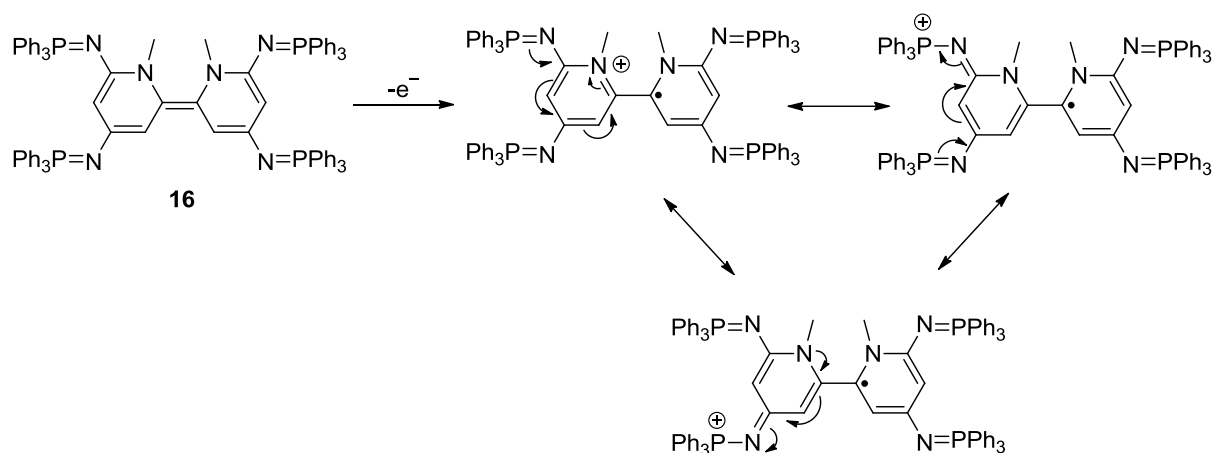
Compounds **12-16** were analyzed by cyclic voltammetry to get insight into their reducing properties. Compound **12** displayed enhanced reducing properties thanks to the presence of one bridge as compared to **11** (respectively: $E_{1/2} = -0.75$ eV for **12** and -0.61 eV for **11** vs SCE). Double bridged-olefin **13** synthesized by Taton and Chen¹⁴ from the corresponding bis-imidazol-2-ylidenes was also analyzed. As expected, such compound exhibits even greater reduction potential ($E_{1/2} = -1.20$ eV vs SCE) due to its greater gain in aromatization energy upon oxidation as compared to **12** (Scheme 5). The presence of a second bridge participates also in its enhanced reducing properties.



Scheme IV.5. Aromatic stabilization upon oxidation with compound **13** as a representative example of TAA (new aromatic rings shown in bold).

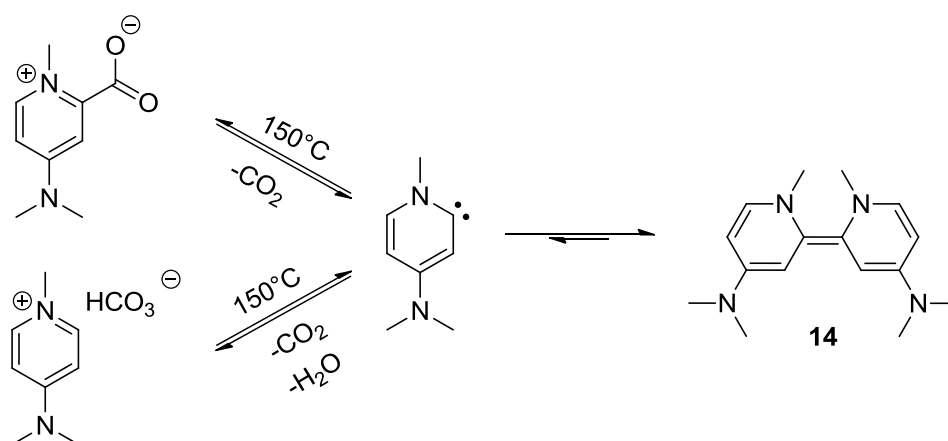
Interestingly, diaminoalkenes **15**, resulting from the dimerization of pyridylidene, were reported to display similar reduction potential despite the presence of only two nitrogen atoms directly connected to the C=C double bond ($E_{1/2} = -1.24$ eV vs SCE for **15**).^{15,16} This may be due to the pyridine moiety which has an extended π -conjugated system, thus allowing the radical formed to be more stabilized by delocalization than in compounds **13**. This reduction potential could be increased further, up to -1.71 V for **16** by introducing iminophosphorane moieties in *ortho* and *para* position of the nitrogen pyridine.¹³ This higher reduction potential

is related to the stabilization of the cationic oxidized state by conjugation with *ortho* and *para* substituents, which led the charge to be delocalized over the whole molecule (Scheme 6).



Scheme IV.6. Stabilization of the cationic oxidized state by the *ortho* and *para* substituents upon oxidation of compound **16**.

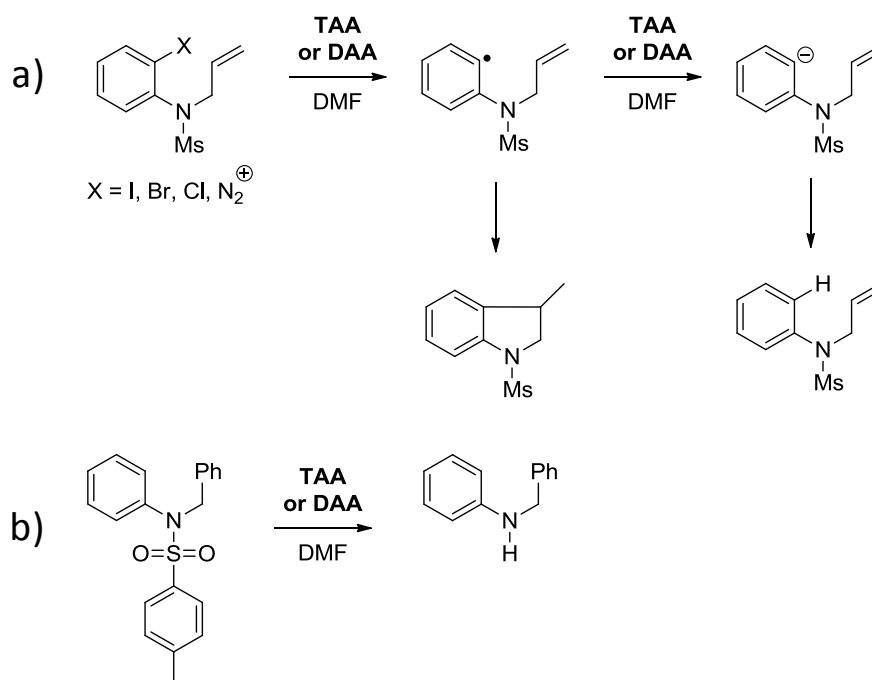
Last year, the group of Vanelle *et al.*⁶ reported the generation of an electron rich olefin **14** obtained through a base-free pathway. The formation of **14** proceeds through an air and moisture stable aminopyridinium carboxylate/carbonate precursor which can be thermally activated to generate *in-situ* a carbene that dimerizes into **14** ($E_{1/2}$ vs SCE = - 1.20 V) (Scheme 7).



Scheme IV.7. Compound **14** generated upon thermal activation of aminopyridinium carboxylate/carbonate precursor.

IV.1.1.2 Reactivity

The TAA and DAA compounds **11-16** presented earlier are able to undergo single or double-electron transfer reactions under mild conditions. They, thus, promote carbon-carbon bond formation by generating radicals or anionic species through the reduction of diazonium salts, alkyl/aryl halides (I, Br, Cl) or sulfones (Scheme 8).



Scheme IV.8. Representative examples for the reduction of diazonium salts, aryl halides (I, Br, Cl) and sulfones *via* single or double-electron transfer with **TAA/DAA 11-16**.

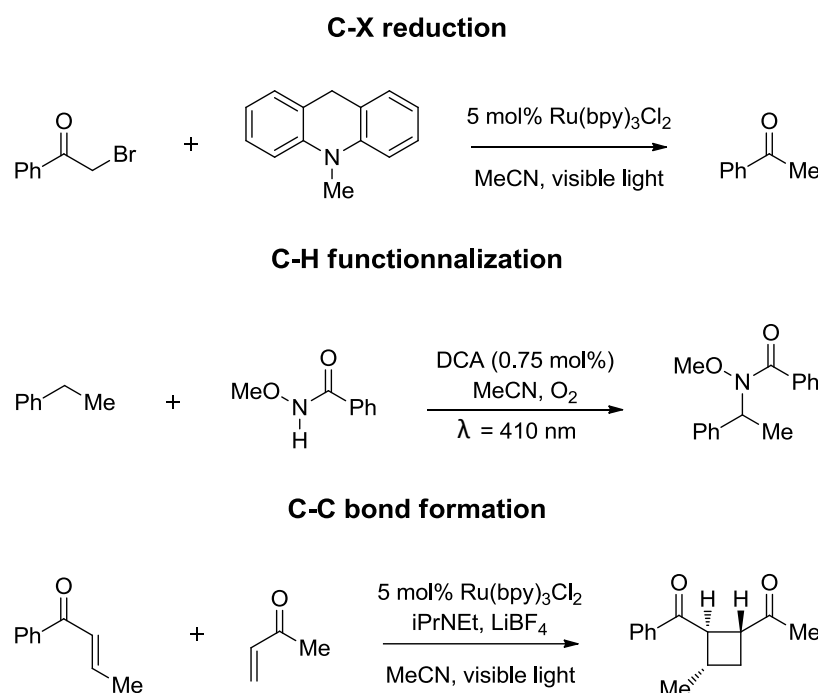
While the reducing power of DAAs synthesized in chapter 2 may not be strong enough to stoichiometrically react with organic substrates, irradiation of DAAs could enhance their reactivity. Therefore, their use in organic photoredox catalysis has been considered with a particular attention on their role in the photo-induced organocatalyzed atom transfer radical polymerization (OATRP).

IV.1.2 Photo-induced Organocatalyzed Atom Transfer Radical Polymerization (OATRP)

IV.1.2.1 Photoredox catalysis in molecular chemistry

Radical chemistry has gained increasing attention over the last few years and the renewed interest in photochemistry has notably led to the renaissance and development of photoredox

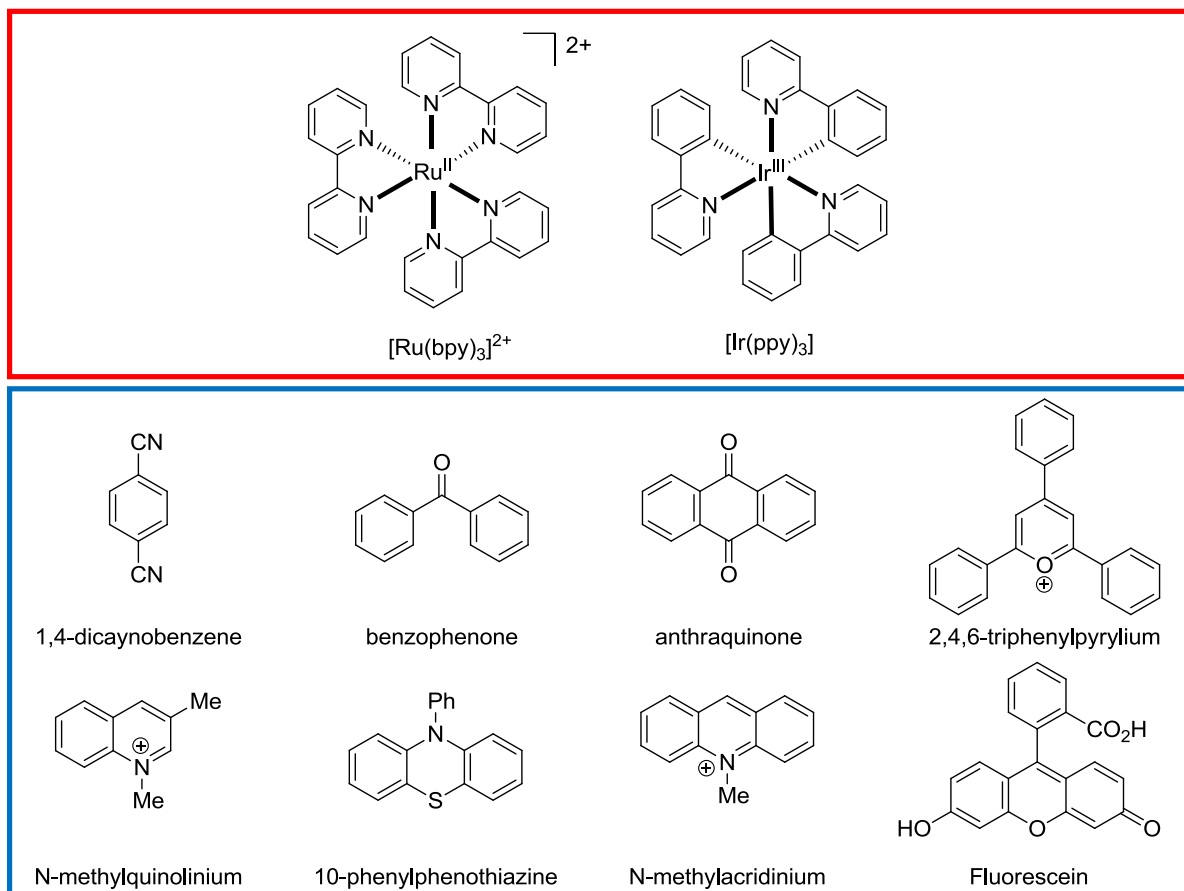
catalysis. This new field of research allows novel reactivity pattern to be accessed, thanks to the generation of open-shell intermediates upon excitation with light. Another advantage of using such visible light is its ability to selectively excite the photocatalyst preventing side reactions which may happened if irradiated with UV-light. The photoredox catalysis has been reported to allow for the reduction of C-X bonds (I, Br, Cl, N₂⁺, RSO₂), to perform C-H functionalization and to develop a wide range of C-C coupling reactions, thanks to its ability to generate various reactive intermediates via single-electron transfer (Scheme 9).¹⁷⁻²⁰



Scheme IV.9. Representative reactions using photoredox catalysis, including the C-X reduction, C-H functionalization and C-C coupling. DCA = dicyanoarene.¹⁷⁻²⁰

The photoredox catalysis was initially performed with metal complexes, such as Ru or Ir (Figure 2). Ever since, an important development of organic-based photoredox catalyst, whose main families include cyanoarenes, benzophenones, quinones, pyryliums, quinoliniums, thiazines, acridiniums and xanthenes (Figure 2), were reported to catalyze reactions such as those presented in Scheme 9.

Examples of metallic photoredox catalysts



Examples of organic photoredox catalysts

Figure IV.2. Most representative families of photoredox catalysts: metallic (red), organic (blue).

Ajouter un espace en photoredox et catalyts sur le titre en rouge

Depending on the nature of the metal complex or/and the organo-photoredox catalyst selected, the photocatalyzed reaction proceeds either through an oxidative, a reductive or both quenching cycles (Figure 3). In the oxidative quenching cycle, first the photoinduced electron transfer (PET) step happens when the catalyst excited by irradiation [cat*] is quenched by donating an electron to an oxidant [ox] present in the reaction. Then, the catalyst turnover step involves the reduction of the oxidized catalyst [cat^{•+}] by a reducing agent [red]. In the reductive quenching cycle, first the excited state [cat*] is quenched by accepting an electron from a reductant [red]. Then, the catalyst turnover involves the oxidation of [cat^{•-}] by an oxidant [ox].

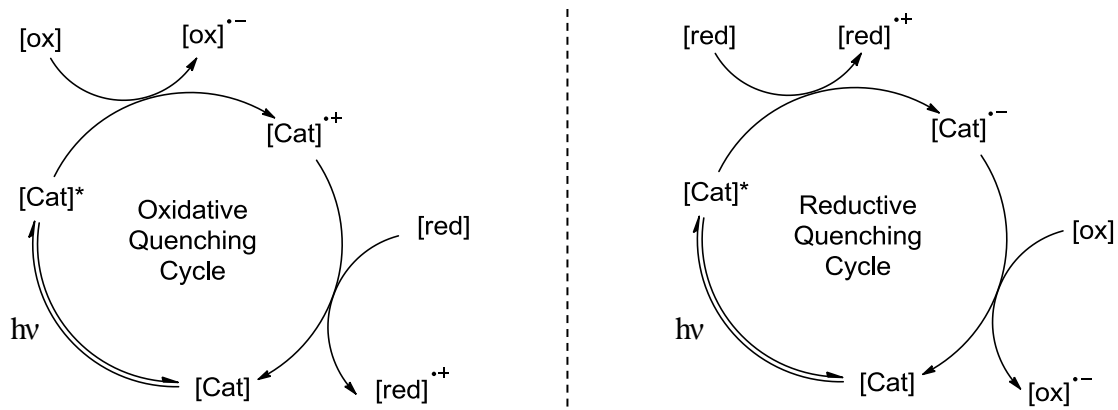


Figure IV.3. Oxidative and reductive quenching cycles of a photoredox catalyst

In order to know if such photoinduced electron transfer can happen with a selected set of catalyst and substrate ([ox] or [red]), the free energy of PET (ΔG_{PET}) must be < 0 and is determined following the general equation (1) where f term is the Faraday constant ($23.061 \text{ kcal.V}^{-1}.\text{mol}^{-1}$), E_{ox} and E_{red} are the ground state redox potentials obtained experimentally. $E_{0,0}$ is the excited state energy of the first singlet or triplet excited state (see IV.2.3) and w is the electrostatic work term and is here omitted as its correction is relatively small ($< 0.1 \text{ eV}$) compared to the other parameters and is relevant only in detailed photophysical studies.

$$\Delta G_{PET} = -f[E_{ox}(D^{\bullet+}/D) - E_{red}(A/A^{\bullet-})] - w - E_{0,0} \quad (1)$$

Moreover, the removal of such w term allows simpler calculation for the excited state redox potential of a precise photocatalyst. For the reduction of the excited catalyst, the general equation (2) is described as follow:

$$\Delta G_{PET} = -f[E_{red}^*(cat^*/cat^{\bullet-}) - E_{ox}(sub^{\bullet+}/sub)] \quad (2)$$

where E_{red}^* is the excited state reduction potential of the catalyst and is calculated by eq (3) where cat^* is either the singlet or triplet excited state and $E_{0,0}$ its corresponding value.

$$E_{red}^*(cat^*/cat^{\bullet-}) = E_{red}(cat/cat^{\bullet-}) + E_{0,0} \quad (3)$$

For the oxidation of the excited catalyst, the equation (4) is:

$$\Delta G_{PET} = -f[E_{red}(sub/sub^{\bullet-}) - E_{ox}^*(cat^{\bullet+}/cat^*)] \quad (4)$$

Where E_{ox}^* is the excited state oxidation potential of the catalyst and is calculated by eq (5).

$$E_{ox}^*(cat^{\bullet+}/cat^*) = E_{ox}(cat^{\bullet+}/cat) - E_{0,0} \quad (5)$$

For a thermodynamically favorable PET ($\Delta G_{PET} < 0$), the excited state photoredox catalyst acting as an oxidant must have a E_{red}^* positive, and if it acting as an excited state reductant E_{ox}^* must be negative. Moreover, the photoinduced oxidation of a substrate is to be feasible if E_{red}^* of the photoredox catalyst is more positive than E_{ox} of the substrate. Likewise, for a reduction of the substrate the E_{ox}^* of the photocatalyst must be more negative than the E_{red} of the substrate.

Recently, applications of the photoredox catalysis to polymer science have also been reported in the context of controlled radical polymerization, such as ATRP and RAFT. In this chapter, the attention is drawn toward the OATRP polymerization reaction, as it is the reaction employed with our dimers.

IV.1.2.2 Photoredox catalysis in polymer chemistry

The photo-induced organocatalyzed atom transfer radical polymerization (OATRP) is based on the same principle as the classical ATRP; with the metallic catalyst (Cu) being replaced by an organic species and light. The principle of atom transfer radical polymerization (ATRP), discovered in 1995,²¹⁻²⁴ relies on the existence of an equilibrium between a propagating radical and a dormant species (Figure 4). The dormant species is in the form of a macromolecular halogenated species (P_nX) which periodically reacts, with a rate constant of activation (k_{act}), with a transition metal complex in its lower oxidation state (Mt^m/L), to form the propagating radical species (P_n^{\bullet}) and the higher oxidation state metal complex (XMt^{m+1}/L). Then, XMt^{m+1}/L reacts with the propagating radical (P_n^{\bullet}) to regenerate the dormant species (P_nX) with a rate constant of deactivation (k_{deact}).

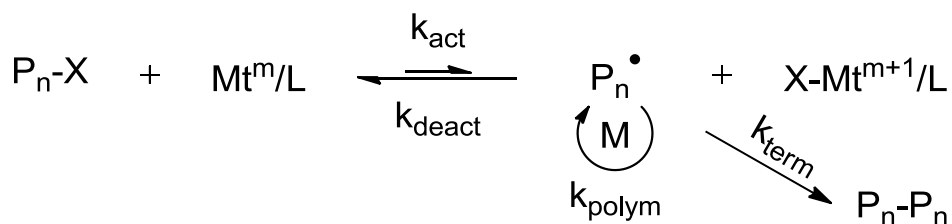


Figure IV.4. ATRP mechanism *via* active/dormant species equilibrium.²¹⁻²⁴

P = polymer, Mt = metal, L = ligand.

In the case of OATRP, the group of Hawker *et al.*²⁵ was the first to use an organic-based photoredox catalyst, the electron-rich 10-phenylphenothiazine, and to report the controlled polymerization of methacrylates ($\overline{M}_n = 12.000 \text{ g.mol}^{-1}$, $\overline{M}_w = 15.000 \text{ g.mol}^{-1}$, $\mathcal{D} = 1.25$).²⁶ The mechanism goes through an oxidative quenching cycle. Irradiation of the PTZ molecule at a wavelength of 380 nm form the excited PTZ* which is a strong reductant ($E_{ox}^* = -2.1 \text{ V vs SCE}$). Therefore, the alkyl bromide (Pn-Br) ($E_{\text{red}} = -0.8 \text{ V vs SCE}$) is reduced leading to the propagating radical species (Pn•) which react with the monomers present in the reaction mixture to form longer polymer chains. Also, a bromine anion and the oxidized radical cation (PTZ⁺) are formed. The latter being a strong oxidant ($E_{\text{ox}} = 0.68 \text{ V vs SCE}$) is able to deactivate the propagating radical (Pn•) and regenerate the ground-state PTZ and the dormant species (Pn-Br) (Figure 5).

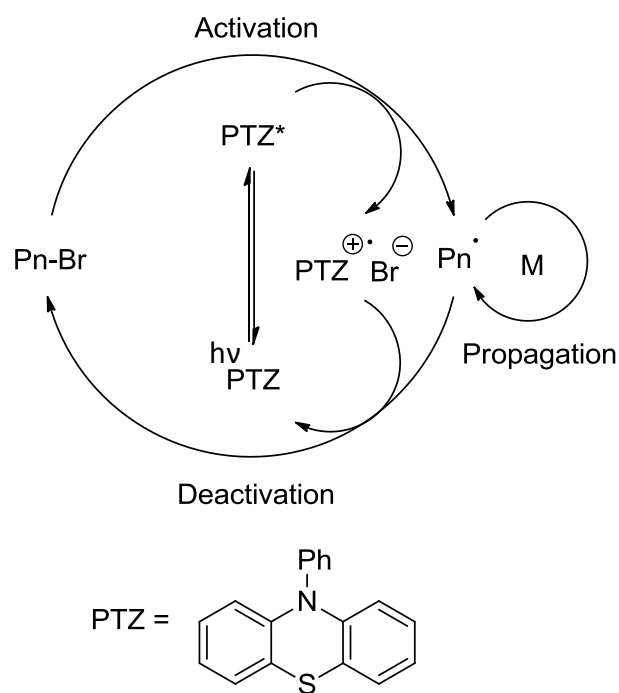
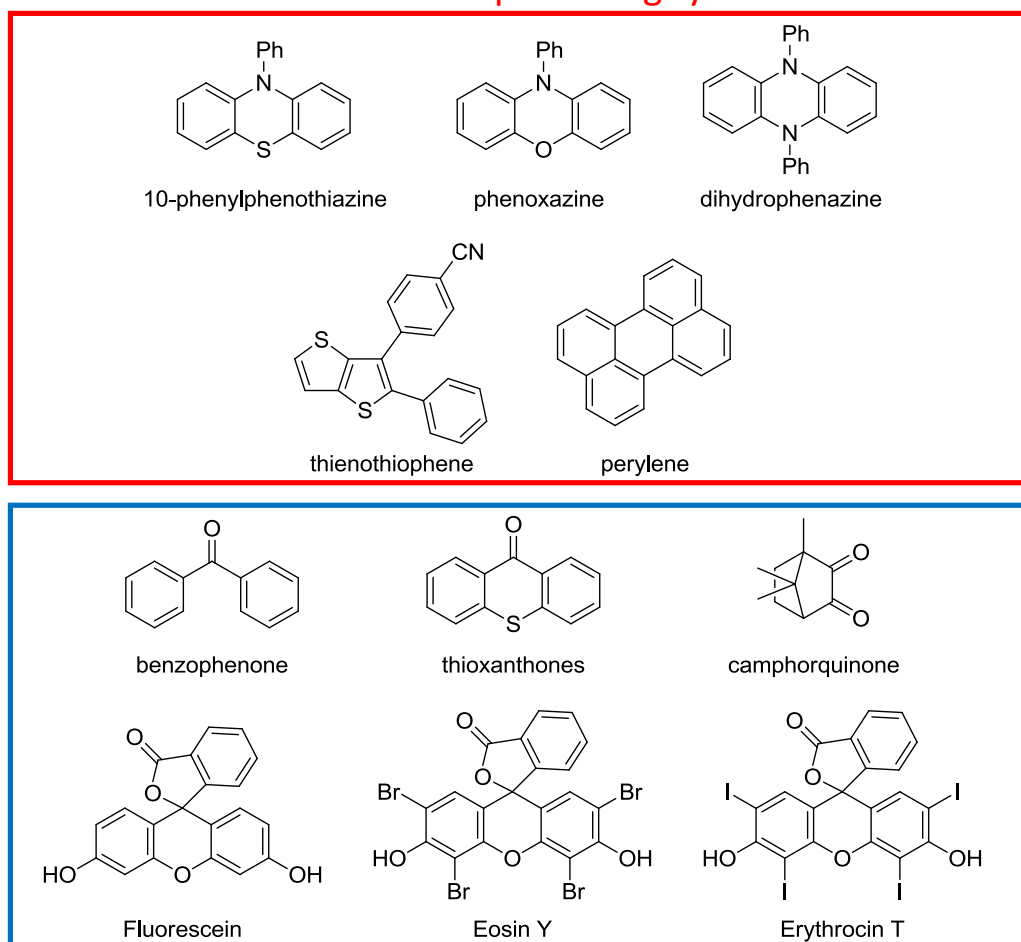


Figure IV.5. Oxidative quenching cycle in photo-induced metal free ATRP with PTZ (10-phenylphenothiazine).²⁶

Over the years more and more performant catalysts (Figure 6) were synthesized leading to PMMA with a range of controlled molecular weight ($\overline{M}_n = 5\text{-}120 \times 10^3 \text{ g.mol}^{-1}$) and low dispersity ($\mathcal{D} = 1.2\text{-}1.6$).²⁷⁻³¹ Photo-induced metal-free ATRP is not limited to electron-rich compounds, following an oxidative quenching mechanism. Indeed, recent studies have shown that a reductive quenching mechanism could occur with electron-acceptor dyes, in combination with amines, yielding monodisperse PMMA (Figure 6).³⁰

Oxidative quenching cycle

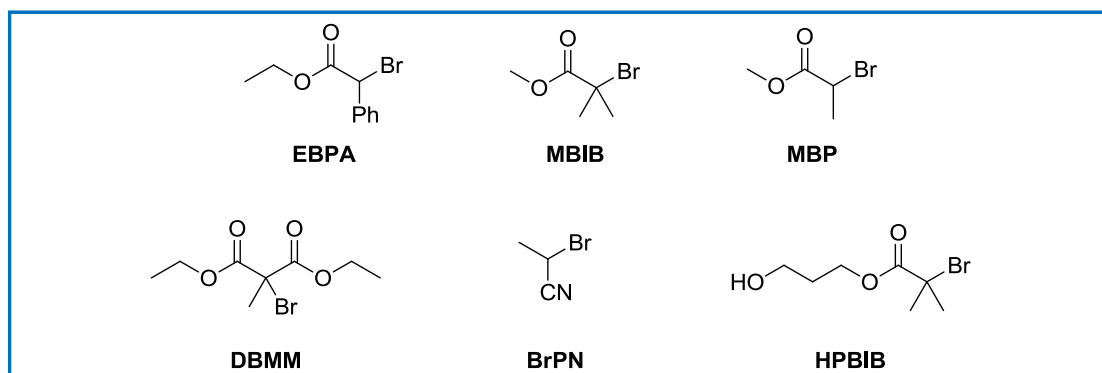


Reductive quenching cycle

Figure IV.6. Organophotocatalysts used in oxidative (red) or reductive (blue) quenching cycles in OATRP.^{32,33,30}

The scope of OATRP was extended using different initiators in order to get efficiencies close to 100%. Moreover, despite a focus on exclusively methacrylate-based monomers at the beginning, recent examples with other type of monomers, such as, acrylamides, acrylonitrile and styrene were reported (Figure 7).^{27,31}

Most representative initiators



Most representative monomers

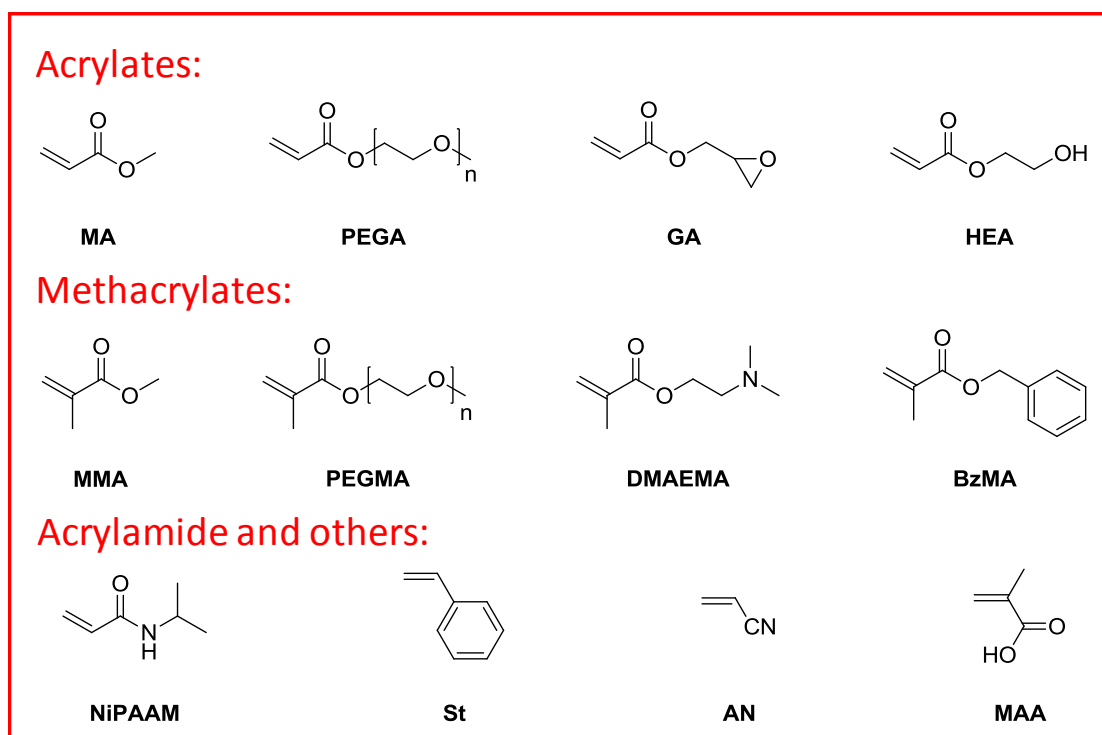


Figure IV.7. Scope of the main initiators and monomers employed in OATRP.^{27,31}

In the next part of this chapter, electrochemical and photo-physical characterizations of diaminoalkene **19** will be presented. Preliminary investigation of its stoichiometric and catalytic properties will then be described.

IV.2 Electrochemical and photo-physical characterization of diaminoalkenes with diisopropyl substituents **19**

IV.2.2 Potential of oxidation

The measurement of the potential of oxidation (E^0_{ox}) of the diaminoalkene **19** was performed by cyclic voltammetry (CV) in collaboration with Dr. L. Bouffier (NSYSA, Bordeaux). The potential of oxidation is the tendency for a molecule to give one electron to the electrode and thereby be oxidized. E^0_{ox} is measured in volt. The CV is a versatile electrochemical technique used to investigate electron transfer during the reduction and oxidation processes of molecular species and their reversibility. The CV method measures the Faradaic current as a function of the applied potential and gives information on the analyte. The current response is measured from an initial potential, which increases linearly to a limiting value. Then, a reverse potential is applied to go back to the starting potential value. In this way the species formed by oxidation can be reduced, and may thus reveal the reversibility of the electron transfer. It is worth noting that not all species can reversibly be oxidized, indeed some compounds led to irreversible systems when the formed radical is not stable enough and evolves par reacting chemically with its environment.

The CV setup is composed of a cell with three electrodes, in which the compound to analyze is dissolved in a solution composed of an electrolyte (called supporting electrolyte) and a solvent. The first electrode is the working electrode where a controlled potential is applied. The second electrode is the reference electrode which has a well-defined and stable equilibrium potential, and is used as a reference point against the potential of other electrodes. The last electrode is the counter electrode used to complete the electrical circuit. The current records the electrons flow between the working electrode and the counter electrode (Figure 8).

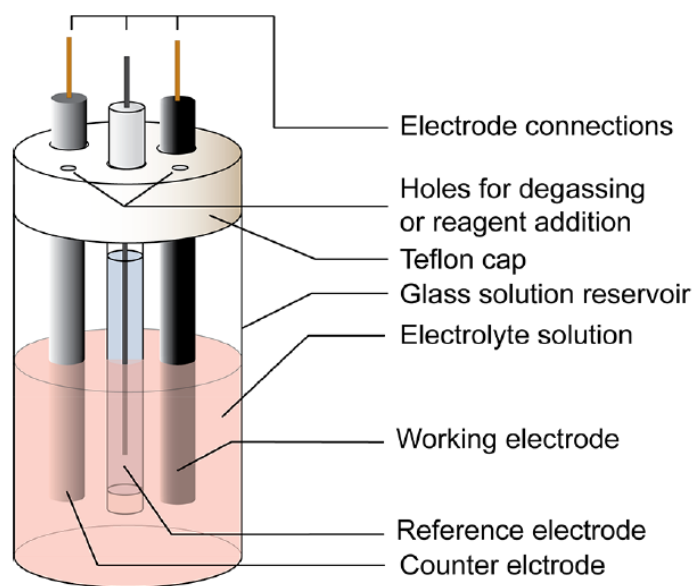
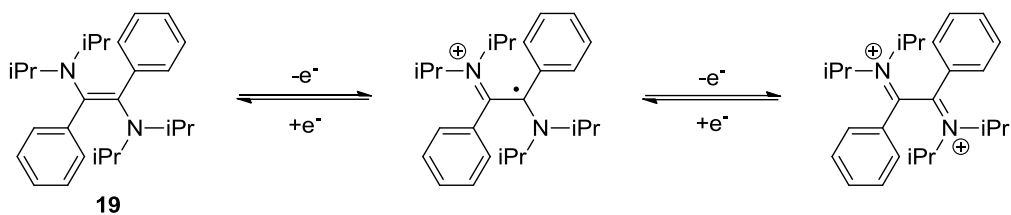


Figure IV.8. Setup for cyclic voltammetric experiment with the representation of an electrochemical cell (Reproduced from Elgrishi *et al.* 2017).

Using the conditions described in the experimental part, a voltammogram of dimer **19** was obtained (Figure 9). Two oxidation peaks could be observed at $E_{ox}^1 = 0.218$ V and $E_{ox}^2 = 0.559$ V, and the two corresponding reduction peaks at $E_{red}^1 = 0.114$ V and $E_{red}^2 = 0.456$ V certifying the reversibility of the oxidation. The number of electrons transferred in each oxidation can be calculated using the Nernst equation (eq 6) at a temperature of 298 K.

$$\Delta E = |E_{ox} - E_{red}| = 2.303 \frac{RT}{nF} = \frac{0.0592}{n} \quad (6)$$

According to this equation, 56.9 mV and 57.4 mV were calculated for ΔE^1 and ΔE^2 respectively. $\Delta E^1 = |0.218 - 0.114| = 0.104$ V and, $n = \frac{0.0592}{0.104} = 56.9$ mV; $\Delta E^2 = |0.559 - 0.456| = 0.103$ V thus, $n = \frac{0.0592}{0.103} = 57.4$ mV. Given that one electron corresponds to 60 mV; each oxidation involves the transfer of one electron. Therefore, the following oxidation pathway can be proposed with a first electron transfer generating a radical cation, represented here as an iminium radical. Then, a second transfer generates the bis-iminium (Scheme 10).



Scheme IV.10. Electrochemical oxidation/reduction of compound **19**.

The standard oxidation potential was also calculated following equation 7. The E_{ox} and E_{red} obtained experimentally were given by looking at their maximum and minimum peaks in the cyclic voltammogram.

$$E_{ox}^0 = \frac{E_{ox} + E_{red}}{2} \quad (7)$$

Finally, the value obtained with the cyclic voltammogram were converted vs SCE which is the international standard. Thus, oxidation potentials of -0.137 and 0.205 V vs SCE for $E_{ox}^{0,1}$ and $E_{ox}^{0,2}$ respectively were calculated.

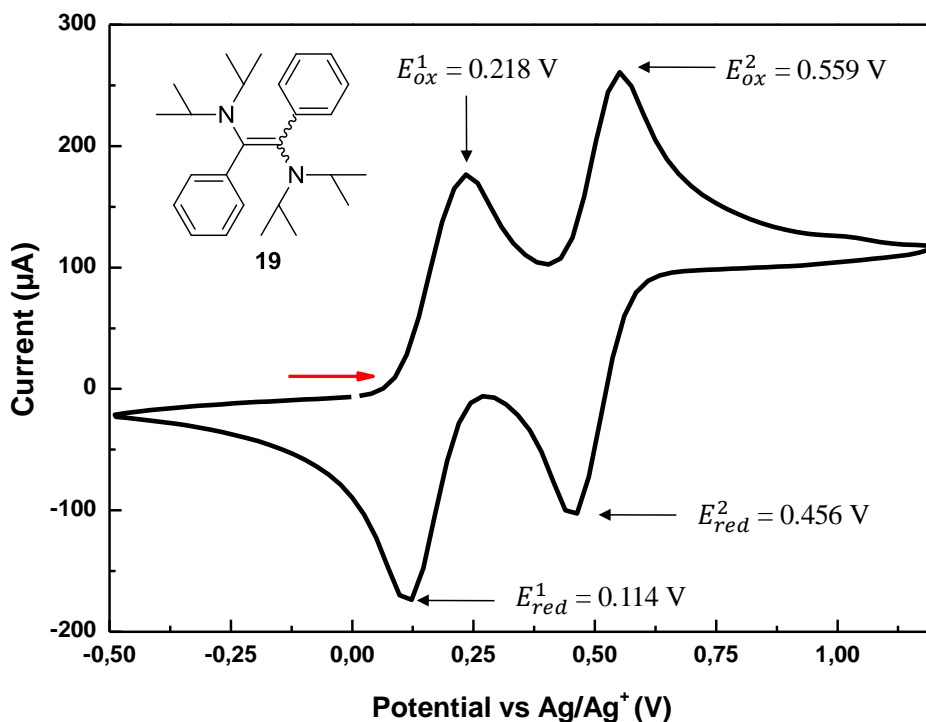
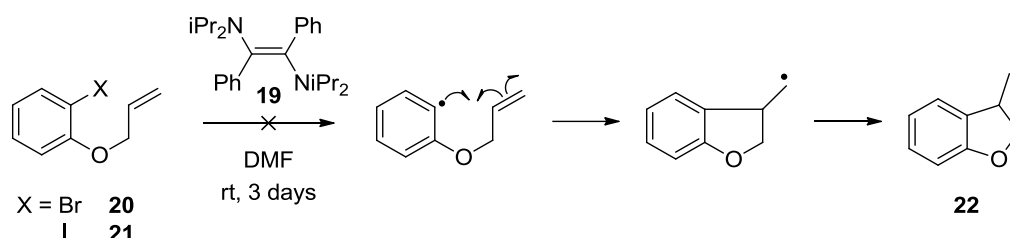


Figure IV.9. Cyclic voltammogram of dimer **19**.

(0.1 M TBAPF₆/ACN, WE: Pt, CE: Pt, Ref: Ag, scan rate: 100mV.s⁻¹)

As expected, in comparison with TAA **1**, DAA **19** displays a lower reduction potential ($E_{ox} = -0.137$ V). **20** and **21** were then used as standard substrate models for the reduction with our diamine and were synthesized following the work of Davies³⁴ and Maddaluno *et al.*³⁵ via deprotonation of 2-bromo/iodophenol with potassium carbonate in the presence of allyl bromide (Scheme 11).



Scheme IV.11. Synthesis of compound **22** via reduction of compound **20** and **21** by dimer **19** in dry DMF for 3 days.

The reduction reactions did not succeed as it could have been expected from their $E_{red} = -2.4$ and -2.2 V for **20** and **21** respectively, more negative than $E_{ox} = -0.137$ V of **19**, thus no conversion of **20** and **21** into **22** was observed.^{36,37} It is worth noticing that no degradation of the catalyst **19** was observed. Therefore, it would be of interest to change the conditions by heating the reaction or by using substrates easier to reduce such as diazonium salts ($E_{red} \sim 0.06$ V). Indeed, using an aryl diazonium salt would give in the case with **19** a Gibbs free energy of electron transfer of

$$\Delta G_{ET} = -23.061 (0.06 - (-0.137)) = -3.3 \text{ kcal. mol}^{-1}$$

which is < 0 , the reaction should thus be thermodynamically favorable.

Another solution to reduce such compounds would be to use **19** in its excited state as it absorbs near the visible and therefore might have a higher reducing potential upon irradiation. For this purpose, not only UV/Vis absorption analysis, but also the excited reduction potential of **19** are required. If **19** in its excited state revealed to be able to reduce such C-X bonds, its use as a photocatalyst in Organic Atom Transfer Radical Polymerization (OATRP) could be of interest.

IV.2.1 UV absorption

As reported in chapter 2, **19** was characterized by UV/Vis analysis leading to two λ_{max} at 229 nm and 388 nm in chloroform corresponding to the $\pi-\pi^*$ and $n-\pi^*$ transitions, respectively. It

is worth adding that **19** has a relatively high extinction coefficient ($\epsilon = 5388 \text{ L}\cdot\text{mol}^{-1}\cdot\text{cm}^{-1}$) (Figure 10).

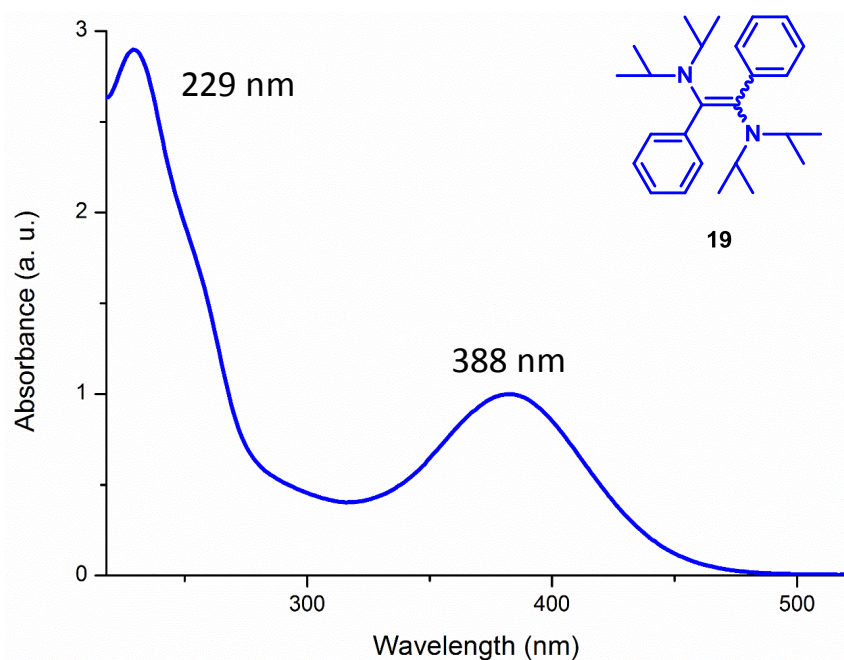


Figure IV.10. UV-Vis absorption of dimer **19** in CHCl_3 .

IV.2.3 Excited state oxidation potential

The excited state oxidation potential (E_{ox}^*) is traditionally calculated by the method of Rhem and Weller, using the excited state energy $E_{0,0}$ to correct the ground state redox potentials obtained by CV (Equation 8).

$$E_{ox}^*(PC^{\bullet+}/PC^*) = E_{ox}(PC^{\bullet+}/PC) - E_{0,0} \quad (8)$$

$E_{ox}(PC^{\square+}/PC)$ is given by cyclovoltammetry. $E_{0,0}$ is the energy difference between the lowest vibrational levels of both ground and excited states; which correspond to the crossing point between the normalized absorption and emission spectra of the compound. For DAA **19**, the crossing point is at 482 nm, which gives $E_{0,0} = \frac{hc}{\lambda} = \frac{1240}{482} = 2.572 \text{ V}$ (Figure 11).

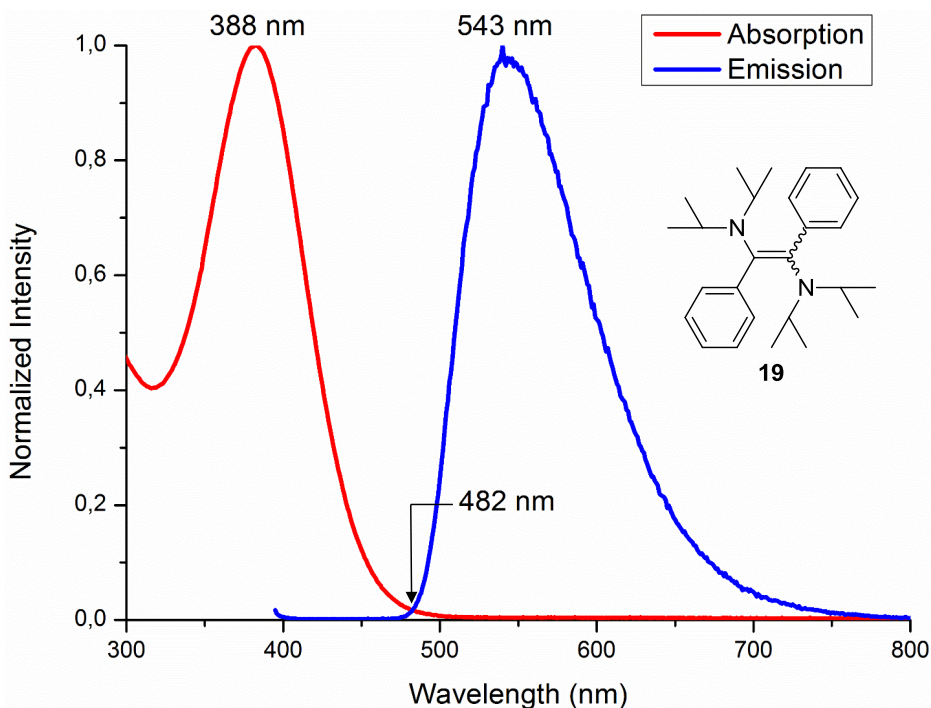


Figure IV.11. Normalized absorption and emission spectra of compound **19** in CHCl_3 .

The excited state oxidation potential E_{ox}^* of **19** obtained are -2.7 and -2.3 V vs SCE for the first and second potential respectively (Figure 12).

	1 st peak	2 nd peak
$E_{ox}(PC^{\bullet+}/PC)$	- 0.137 V	0.205 V
$E_{ox}^*(PC^{\bullet+}/PC^*)$	- 2.7 V	- 2.3 V

Figure IV.12. Redox potential of compound **19** in its ground state and excited state.

Those values fits with the minimum value required to reduce commonly employed alkyl bromide initiators ($E_{ox}^* < -0.8$ V)²⁹ as confirmed by calculating the respective (ΔG_{PET}) of the first and second potential which both revealed to be thermodynamically favorable ($\Delta G_{PET} < 0$):

$$\Delta G_{PET}^1 = -f[-0.8 - (-2.7)] = -23.061 \times 1.9 = -43.8 \text{ kcal.mol}^{-1}$$

$$\Delta G_{PET}^2 = -f[-0.8 - (-2.3)] = -23.061 \times 1.5 = -34.6 \text{ kcal.mol}^{-1}$$

Therefore, it may be anticipated that **19** will behave as an efficient organocatalyst in OATRP.

The characteristics described in this part showed that dimer **19** is a poor reducing agent in the ground state but a strong one in its excited state, thus it could be an efficient photocatalyst. In

the next part, the preliminary results obtained with **19** as organocatalyst for the polymerization of MMA *via* OATRP are presented.

IV.3 Photo-induced metal-free atom transfer radical polymerization

Based on the proposed mechanism for OATRP, the group of Miyake and co-workers determined the chemical and photo-physical properties for an efficient photocatalyst (PC). The photoexcitation of PC can be performed *via* various wavelengths; however if UV light is used, side reactions might appear and complicate the synthesis of well-defined polymers. Thus, the PC should preferably absorb in the visible range and preferably have its maximum of absorption (λ_{max}) close to the visible region along with a high molar extinction coefficient (ϵ). After excitation, PC should cross-over efficiently to the triplet excited state, which is indicated by a high rate of intersystem crossing (ISC) although some PCs are efficient in their singlet state. Its excited state lifetime has to be sufficiently long and has to be reducing enough to generate the initiating/propagating radical upon electron transfer ($E_{ox}^* = E_{ox}^*(\text{PC}^{*+}/\text{PC}^*) < -0.8 \text{ V vs SCE}$ for the reduction of the commonly employed alkyl bromides). Finally, the thermodynamic feasibility of activation and deactivation is evaluated by the ΔG_{PET} with the help of the excited state oxidation potential of PC^* (E_{ox}^*) and the standard oxidation potential of PC^{*+} ($E_{ox}^0 = E_{ox}^*(\text{PC}^{*+}/\text{PC}) > -0.8 \text{ V vs SCE}$). From the parameters determined in the previous part, the oxidation potentials and the visible light absorption described for **19** fit those requirements.

Thus, the organophotocatalyst efficiency of **19** was examined in the polymerization of methyl methacrylate (MMA) using conventional ethyl α -bromoisobutyrate (EBP) as the alkyl bromide initiator. All components used in the reaction have been dried and deoxygenated prior to use and polymers have been characterized by SEC (PS standards in THF) for the \overline{Mn} and D .

Initial polymerization conditions employed a N,N-dimethylacetamide (DMAc) solution of MMA, EBP and **19** (1000/10/1) irradiated with a blue LED for 8h. Poly(methyl methacrylate) (PMMA) was obtained with a conversion of 36 % ($\overline{Mn} = 42 \text{ kDa}$ and $D = 2.48$). Increasing the time of irradiation to 40h allowed the maximum conversion of 87% to be reached. Under those

conditions, PMMA of a number-average molecular weight (M_n) of 19 kDa was formed according to SEC analysis ($\mathcal{D} = 2.97$) (Figure 13). The experimentally measured number average molecular weight (M_n) is greater than the theoretical $M_{n,theo}$ (8.9 kDa) indicating a partial initiation. From $M_{n,exp}$ and $M_{n,theo}$, an initiator efficiency of 46% (I^*) was calculated following the equation: Initiator efficiency (I^*) = $\overline{M}_{n,theo} / \overline{M}_{n,SEC} \times 100\%$.³⁸

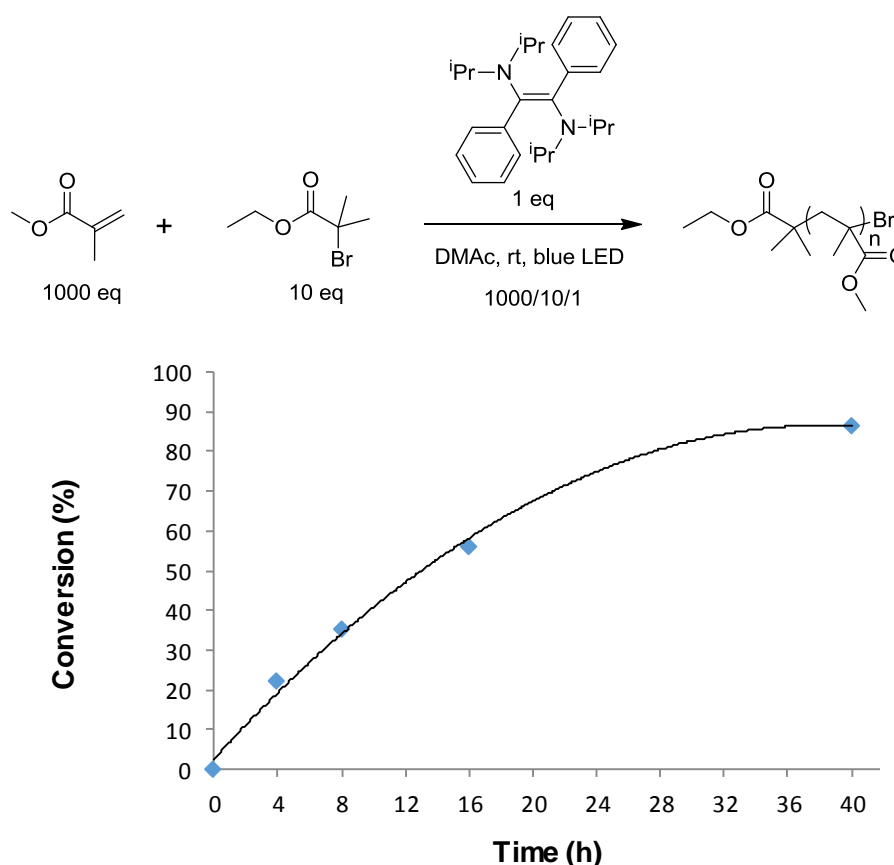


Figure IV.13. OATRP with dimer **19** and its conversion over time.

Given the poor initiation of EBP, α -bromophenylacetate (EBPA) was next selected as the presence of the phenyl facilitates its reduction (radical generated more stable).³⁹ However, similar results were obtained with a conversion after 32 h of 87% ($\mathcal{D} = 2.9$) and an initiator efficiency of $I^* = 40\%$. Increasing the amount of **19** (10 equivalents) improved the initiator efficiency, with $I^* = 60\%$ but also the dispersity (3.5; Table 1).

Table IV.1. Polymerization of methyl acrylate (MA, 1000 eq) with EBP or EBPA initiator (10 eq) and dimer **19** (1 or 10 eq) in DMAC. ($\overline{M}_{n,theo}$ and I^* have been calculated according to ref 36).³⁸

Conditions	Initiator	Time	Conv (%)	\overline{Mn}_{exp}	\overline{Mn}_{theo}	\mathcal{D}	I^*
1000/10/1	EBP	8H	36	42700	4600	2.5	10%
1000/10/1	EBP	32H	87	19300	8885	2.9	46%
1000/10/1	EBPA	32H	87	38500	3750	2.9	40%
1000/10/1 0	EBPA	32H	70	21900	8950	3.5	60%

Control experiments were performed, and different reactions were run in the absence of EBP in one hand, or in the absence of **19** on the other hand. In each case, after 24h no polymerization was observed, evidencing the initiating role of EBP and the catalytic role of **19** respectively.

To confirm the necessity of light for the polymerization reaction, the reaction was subjected to repeated sequential irradiation (1h) and dark periods (1h). At the end of each period, an aliquot was taken from the reaction mixture, quenched by addition of DDQ and analyzed by ^1H NMR spectroscopy to measure the conversion. While the conversion increased upon irradiation, no polymerization was observed in the absence of light, in agreement with control experiments proving the temporal control of the polymerization reaction (Figure 14).

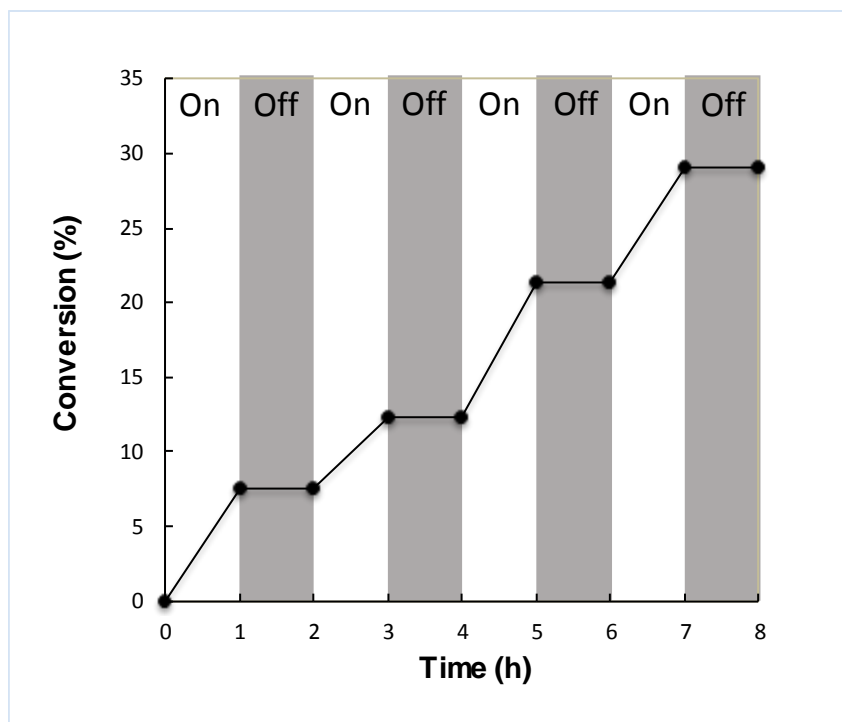


Figure IV.14. Plot of monomer (MMA) conversion vs time (h), demonstrating the control over polymerization propagation through irradiation and removal of light source.

It is worthy of note that, although monomer conversion follows a first-order kinetic during irradiation (Figure 15 a), the Mw of the polymer does not increase after the initial irradiation but decreases instead.

This suggests that under those conditions, initiation of novel polymer chains by reduction of Pn-Br ($E_{red}(\text{Pn-Br}/\text{Pn}^\bullet) = -0.8 \text{ V}$) by **19** in its excited state ($E_{ox}^* = (\text{19}^{\bullet+}/\text{19}^*) = -2.7 \text{ V}$) is favored ($\Delta G_{PET} < 0$) compared to the propagation of existing chains.

This may be due to the absence of the C-Br chain-end functions on the dormant growing polymer chains obtained because of the inability of the oxidized radical-cation **19-Br** complex ($E_{red}(\text{19}^{\oplus+}/\text{19}) > E_{ox}(\text{Pn-Br}^\bullet/\text{Pn-Br})$) to transfer its radical back to the chain-end.

It could also be due to the ability of **19**^{•+} ($E_{ox}^* = (\text{19}^{2+}/\text{19}^{\bullet+}) = -2.3 \text{ V}$) to transfer a second electron to Pn[•] ($E_{red}(\text{Pn}^\bullet/\text{Pn}^-) = -0.7 \text{ V}$) as confirmed with a $\Delta G_{PET} < 0$, leading to the inert dication **19**²⁺ (which precipitate in the media) and to an enolate function that may get protonated to a Pn-H polymer.

Finally, the absence of Br chain-end functions may also be due to the hydrolysis of **19**^{•+} during the reaction, thus preventing the reversibility of the electron transfer (Scheme 12).

As a result, only new chains could be initiated. Moreover, the concentration of MMA continually decreasing over time during the experiment, the Mw of the polymer produced in

each irradiation decreases, leading to shorter polymer chains and thus to a broader dispersity (Figure 15 b).

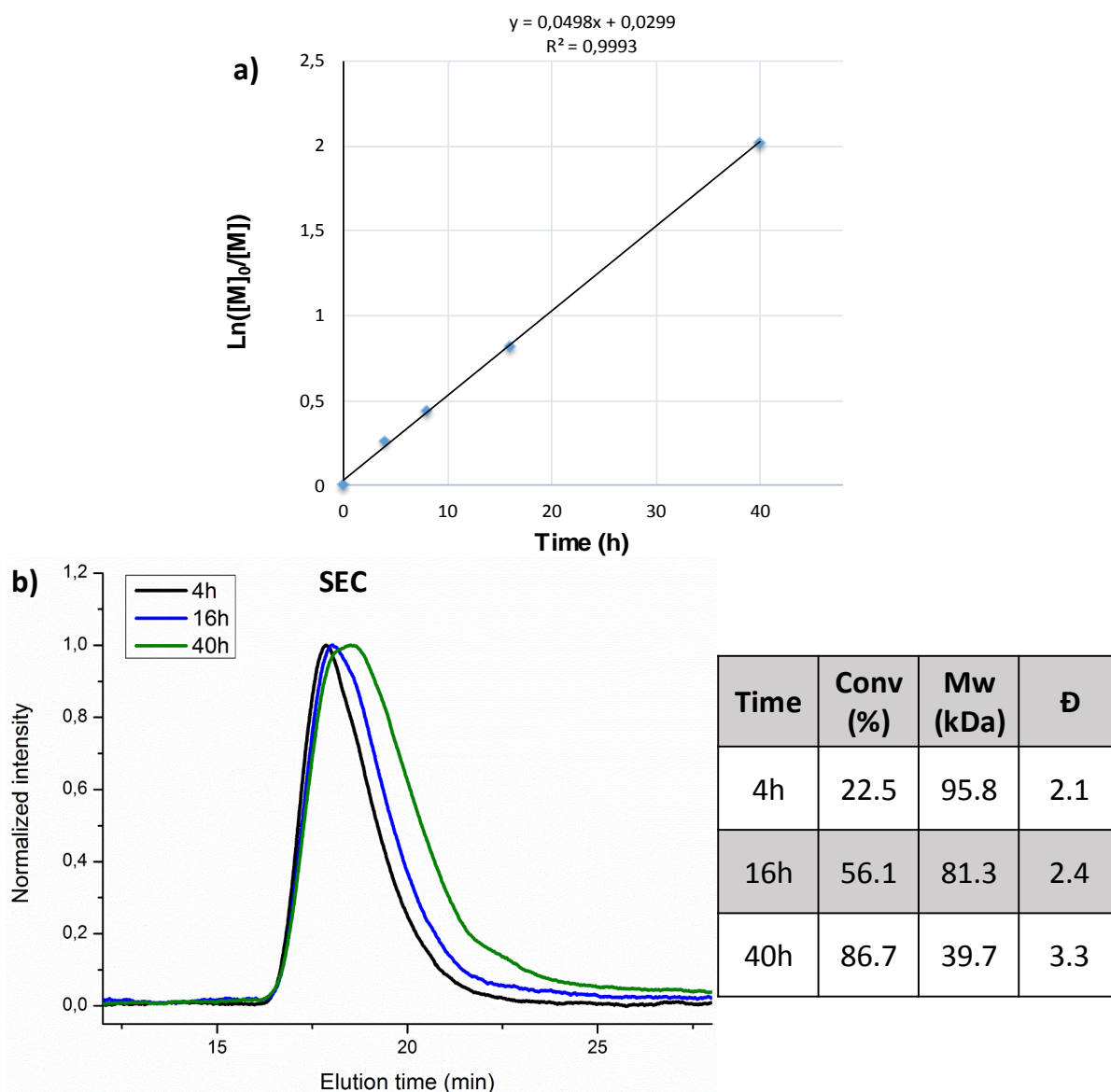
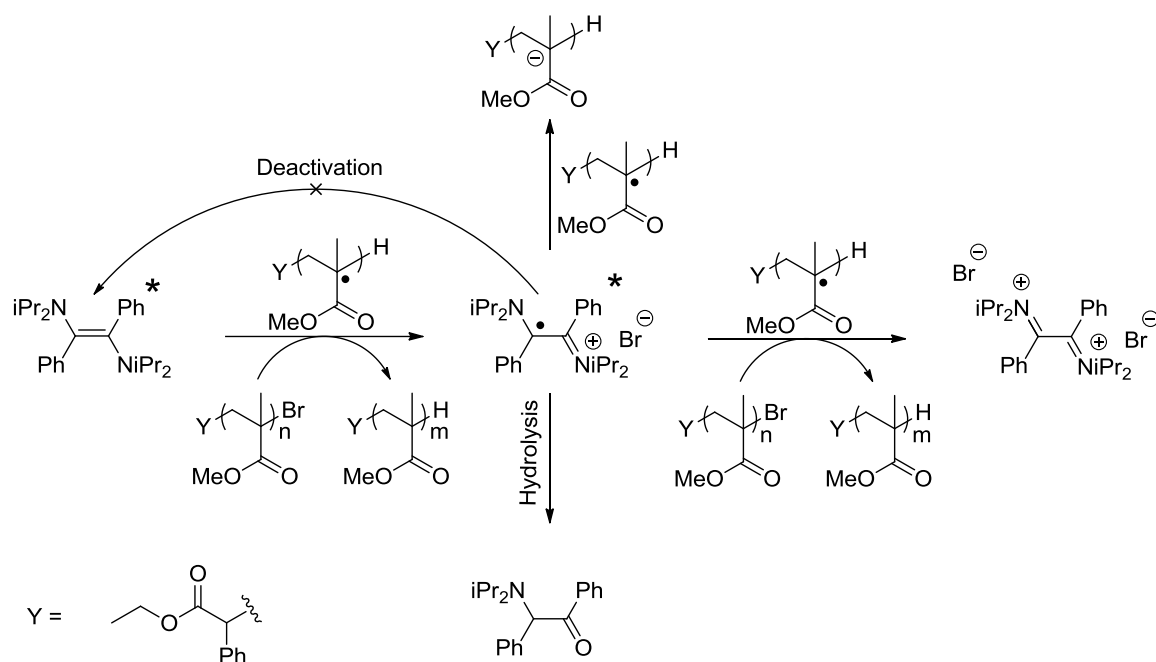


Figure IV.15. a) First-order kinetic plot of monomer conversion vs time of light irradiation. b) SEC (left) in THF with PS standards of polymers after 4/16/40h of irradiation. Table (right) of the molecular weight properties of the polymer at each time point.



Scheme IV.12. Reactions explaining possibly the high dispersity of the PMMA obtained at the end of the reaction by preventing the propagation of the polymer chains. (*i.e.* hydrolysis of **19**^{•+}, activation of a second Pn-Br leading to the transfer of the second electrons of **19**^{•+}, absence of deactivation step, reduction of Pn[•]).

Conclusion

In the first part of this chapter we presented the reducing properties of our diaminoalkene and its potential use as stoichiometric reducing agent. As expected from its structure and its standard oxidation potential values ($E_{ox}^{1,2}(PC^{\square+}/PC) = -0.137 \text{ V}$ and 0.205 V) dimer **19** did not compete, for the reduction of C-X bonds ($X = \text{Br}, \text{I}$), with TAA ($E_{ox}(PC^{\square+}/PC) = -0.61 \text{ V to } -1.71 \text{ V}$), bearing up to four nitrogen atoms on the double bond. Indeed, the reactions did not work ($\Delta G_{PET} > 0$); however, this inability to reduce C-X bond in its ground state could be a criteria for a use in OATRP.

The complete removal of metallic entities in ATRP has been possible only until recently. The use of specific organocatalyst enabled the synthesis of polymers with high controlled chain-end functionalities, molecular weight and dispersities. As an emerging research area, photo-induced metal-free ATRP gathers a wide range of economic and ecological concerns. Indeed by replacing the elevated temperature required to perform radical polymerization, photochemical processes allow a spatial and temporal control at ambient temperature giving access to complex macromolecular architectures. Several criteria have been described in order to have an efficient

photocatalyst. Among them, a PC should absorb in the visible light, have a low oxidation potential in its ground state and a high reducing potential in its excited state. Indeed, a strong reduction potential allows an efficient activation step with the reduction of alkyl bromide. The low oxidation potential is required for the deactivation step where the $PC^{+\bullet}Br^-$ complex will quench the activated radical species. All these criteria were found for dimer **19** which was tested on the photoinduced metal-free ATRP of MMA. The results revealed that **19** plays the role of catalyst as without its presence, no polymerization was observed. However, polymers obtained have a large dispersity and a higher mass than expected. This may be due to the inability of dimer **19** to reactivate already formed polymer chains when in their oxidized complex. Thus, a decrease of the molecular weight of polymer along with an increase of its dispersity over irradiation time has been observed. Therefore, in the future, a focus on the design of more efficient catalysts for the synthesis of well-defined polymers has to be done.

References

- 1 R. L. Pruett, J. T. Barr, K. E. Rapp, C. T. Bahner, J. D. Gibson and R. H. Lafferty, *J. Am. Chem. Soc.*, 1950, **72**, 3646–3650.
- 2 N. Wiberg, *Angew. Chem. Int. Ed. Engl.*, 1968, **7**, 766–779.
- 3 J. Broggi, T. Terme and P. Vanelle, *Angew. Chem. Int. Ed.*, 2014, **53**, 384–413.
- 4 E. Doni and J. A. Murphy, *Chem Commun*, 2014, **50**, 6073–6087.
- 5 J. A. Murphy, *J. Org. Chem.*, 2014, **79**, 3731–3746.
- 6 G. Tintori, P. Nabokoff, R. Buhaibeh, D. Bergé-Lefranc, S. Redon, J. Broggi and P. Vanelle, *Angew. Chem. Int. Ed.*, 2018, **57**, 3148–3153.
- 7 P. B. Hitchcock, M. F. Lappert, P. Terreros and K. P. Wainwright, *J. Chem. Soc. Chem. Commun.*, 1980, **24**, 1180.
- 8 M. F. Lappert, *J. Organomet. Chem.*, 1988, **358**, 185–213.
- 9 M. F. Lappert, *J. Organomet. Chem.*, 2005, **690**, 5467–5473.
- 10 R. McKie, J. A. Murphy, S. R. Park, M. D. Spicer and S. Zhou, *Angew. Chem. Int. Ed.*, 2007, **46**, 6525–6528.
- 11 J. Castells, F. López-Calahorra, F. Geijo, R. Pérez-Dolz and M. Bassedas, *J. Heterocycl. Chem.*, 1986, **23**, 715–720.
- 12 Y.-T. Chen, G. L. Barletta, K. Haghjoo, J. T. Cheng and F. Jordan, *J. Org. Chem.*, 1994, **59**, 7714–7722.
- 13 S. S. Hanson, E. Doni, K. T. Traboulee, G. Coulthard, J. A. Murphy and C. A. Dyker, *Angew. Chem. Int. Ed.*, 2015, **54**, 11236–11239.
- 14 T. A. Taton and P. Chen, *Angew. Chem. Int. Ed. Engl.*, 1996, **35**, 1011–1013.
- 15 J. A. Murphy, J. Garnier, S. R. Park, F. Schoenebeck, S. Zhou and A. T. Turner, *Org. Lett.*, 2008, **10**, 1227–1230.
- 16 J. Garnier, A. R. Kennedy, L. E. A. Berlouis, A. T. Turner and J. A. Murphy, *Beilstein J. Org. Chem.* 2010, **6**, 1-8.
- 17 J. M. R. Narayanam and C. R. J. Stephenson, *Chem Soc Rev*, 2011, **40**, 102–113.
- 18 C. K. Prier, D. A. Rankic and D. W. C. MacMillan, *Chem. Rev.*, 2013, **113**, 5322–5363.
- 19 N. A. Romero and D. A. Nicewicz, *Chem. Rev.*, 2016, **116**, 10075–10166.
- 20 Y. Du, R. M. Pearson, C.-H. Lim, S. M. Sartor, M. D. Ryan, H. Yang, N. H. Damrauer and G. M. Miyake, *Chem. - Eur. J.*, 2017, **23**, 10962–10968.
- 21 M. Kato, M. Kamigaito, M. Sawamoto and T. Higashimura, *Macromolecules*, 1995, **28**, 1721–1723.
- 22 J.-S. Wang and K. Matyjaszewski, *J. Am. Chem. Soc.*, 1995, **117**, 5614–5615.
- 23 K. Matyjaszewski and J. Xia, *Chem. Rev.*, 2001, **101**, 2921–2990.
- 24 K. Matyjaszewski, *Macromolecules*, 2012, **45**, 4015–4039.
- 25 B. P. Fors and C. J. Hawker, *Angew. Chem. Int. Ed.*, 2012, **51**, 8850–8853.
- 26 N. J. Treat, H. Sprafke, J. W. Kramer, P. G. Clark, B. E. Barton, J. Read de Alaniz, B. P. Fors and C. J. Hawker, *J. Am. Chem. Soc.*, 2014, **136**, 16096–16101.
- 27 S. Dadashi-Silab, S. Doran and Y. Yagci, *Chem. Rev.*, 2016, **116**, 10212–10275.
- 28 C. Kutahya, A. Allushi, R. Isci, J. Kreutzer, T. Ozturk, G. Yilmaz and Y. Yagci, *Macromolecules*, 2017, **50**, 6903–6910.
- 29 J. C. Theriot, B. G. McCarthy, C.-H. Lim and G. M. Miyake, *Macromol. Rapid Commun.*, 2017, **38**, 1-12.
- 30 Y. Yagci and G. Yilmaz, *Polym. Chem.*, 2018, **9**, 1757-1762.
- 31 E. H. Discekici, A. Anastasaki, J. Read de Alaniz and C. J. Hawker, *Macromolecules*, 2018, **51**, 7421–7434.
- 32 X. Liu, L. Zhang, Z. Cheng and X. Zhu, *Polym. Chem.*, 2016, **7**, 689–700.

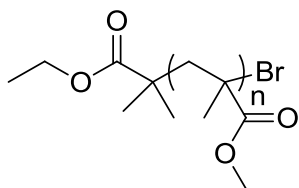
- 33 C. Kutahya, F. S. Aykac, G. Yilmaz and Y. Yagci, *Polym. Chem.*, 2016, **7**, 6094–6098.
- 34 X. Jin and R. P. Davies, *Catal. Sci. Technol.*, 2017, **7**, 2110–2117.
- 35 R. Lhermet, M. Durandetti and J. Maddaluno, *Beilstein J. Org. Chem.*, 2013, **9**, 710–716.
- 36 P. Allongue, M. Delamar, B. Desbat, O. Fagebaume, R. Hitmi, J. Pinson and J.-M. Savéant, *J. Am. Chem. Soc.*, 1997, **119**, 201–207.
- 37 L. Pause, M. Robert and J.-M. Savéant, *J. Am. Chem. Soc.*, 1999, **121**, 7158–7159.
- 38 $\overline{M}_{n\text{theo}} = [\text{monomer}]_0 / [\text{initiator}]_0 \times \overline{M}_{w\text{monomer}} \times \text{Conv \%} + M_{\text{initiator}}$
 Initiator efficiency (I^*) = $\overline{M}_{n\text{theo}} / \overline{M}_{n\text{SEC}} \times 100\%$
- 39 G. M. Miyake and J. C. Theriot, *Macromolecules*, 2014, **47**, 8255–8261.

Experimental part

Cyclovoltammetry experiments:

In this study, tetrabutylammonium hexafluorophosphate (TBAPF₆) was selected as the supporting electrolyte and a 0.1 M solution of TBAPF₆ was prepared in freshly distilled ACN dried over CaH₂. Following this step, 20 μM solution of dimer **6** was prepared in the TBAPF₆/ACN system. Additionally, to calculate the redox potentials versus ferrocene/ferrocenium (Fc/Fc⁺) redox couple, a 20 μM solution of ferrocene was also prepared. The electrochemical cell filled with the solution was deoxygenated by bubbling highly pure nitrogen gas for at least 15 minutes. The nitrogen atmosphere was kept over the solution during the all experiment. The working electrode and counter electrode selected were platinum; the silver wire was employed as the pseudo-reference electrode. The scan rate selected was 100 mV.s⁻¹ and the potential window was from -0.5 mV to 1.2 mV.

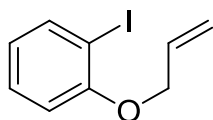
The oxidation potential of $E_{ox}^{0,1} = 0.166$ V vs Ag/Ag⁺. The silver electrode is a pseudo-reference, ferrocene (which oxidation potential is known) was thus analyzed in the same conditions in order to allow the conversion of the $E_{ox}^{0,1}$ given vs Ag/Ag⁺ to vs Fc/Fc⁺. Finally, a simple conversion from Fc/Fc⁺ reference to SCE reference gave potentials of $E_{ox}^{0,1} = -0.137$ V vs SCE and $E_{ox}^{0,2} = 0.205$ V vs SCE.



poly(MMA):

A solution of N,N-dimethylacetamide (DMAc) (2.5 mL), methyl methacrylate (1 mL, 9.35 mmol), dimer **19**, (0.0035 g, 9.35 μ mol) and EBPA (16.4 μ L, 93.5 μ mol) was irradiated with a blue LED for 32h. The resulting PMMA was obtained with a conversion of 87% in 56% yield with a weight-average molecular weight (M_n) of 19330 kDa and a large dispersity (\mathcal{D}) of 2.97.

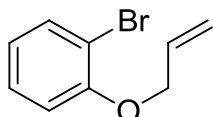
¹H NMR (CDCl₃, 300.2 MHz) δ ppm: 1.92 (m, 3H,), 1.89 (m, 2H,), 3.60 (s, 3H).



1-(Allyloxy)-2-iodobenzene:

To a solution of 2-iodophenol (1.1 g, 5 mmol) in anhydrous DMF (10 mL) under an argon atmosphere is added potassium carbonate (1.38 g, 10 mmol), followed by allyl bromide (0.65 mL, 7.5 mmol). After stirring 2 h at 60 °C, the mixture is hydrolyzed with water (10 mL) and extracted with Et₂O (2 \times 15 mL). Combined organic layers are washed with brine (10 mL), dried over anhydrous MgSO₄ and concentrated to provide the pure ether (1.39 g, 99%) as a pure orange oil.

¹H NMR (300 MHz, CDCl₃) δ ppm: 4.60 (dt, J = 4.7, 1.6 Hz, 2H), 5.32 (ddt, J = 10.6, 3.0, 1.6 Hz, 1H), 5.53 (ddt, J = 17.2, 3.0, 1.6 Hz, 1H), 6.06 (ddt, J = 17.2, 10.6, 4.7 Hz, 1H), 6.71 (td, J = 7.6, 1.3 Hz, 1H), 6.81 (dd, J = 8.2, 1.3 Hz, 1H), 7.28 (ddd, J = 8.2, 7.6, 1.6 Hz, 1H), 7.78 (dd, J = 7.6, 1.6 Hz, 1H);



1-(Allyloxy)-2-bromobenzene:

2-bromophenol (1.74 mL, 15 mmol) was added to a suspension of K₂CO₃ (6.20 g, 45 mmol) in DMF (50 mL) under N₂ followed by a slow addition of allyl bromide (1.56 mL, 18 mmol). The

mixture was allowed to stir at room temperature overnight before addition of 100 mL distilled water. The organic layer was extracted by ethyl acetate (3 x 50 mL) and the combined organic layer was washed with brine (3 x 50 mL), dried over MgSO₄ and the solvent removed under vacuum. A pure light yellow oil product was obtained (3.1g ,97% yield).

¹H NMR (300 MHz, CDCl₃) δ ppm : 7.57 (dd, *J* = 7.9, 1.7 Hz, 1H), 7.27 (ddd, *J* = 8.3, 7.4, 1.6Hz, 1H), 6.80 – 7.00 (2 H, m), 6.10 (ddt, *J* = 17.2, 10.4, 5.0 Hz, 1H), 5.52 (dq, *J* = 17.3, 1.7 Hz,1H), 5.34 (dq, *J* = 10.7, 1.5 Hz, 1H), 4.64 (dt, *J* = 5.0, 1.6 Hz, 1H).

Experimental part (general)

Materials

THF and Et₂O were dried over sodium/benzophenone and distilled prior to use. Dichloromethane, chloroform, DMF, DMAc and pentane were dried over CaH₂ and distilled prior to use. Acetonitrile solvent was dried using a MBraun Solvent Purification System (model MB-SPS 800) equipped with alumina drying columns. Benzaldehyde (Alfa Aesar, 98%), methyl acrylate (Sigma aldrich), *tert*-butyl isocyanide (ABCR), α -bromoisobutyrate (Sigma Aldrich), ethyl- α -bromophenylacetate (Alfa Aesar) and chlorotrimethylsilane (Sigma Aldrich) were dried over CaH₂, distilled and stored under argon. Piperidine (Alfa Aesar), morpholine (Sigma Aldrich), diethylamine (Alfa Aesar) were dry over KOH and distilled prior to use. *n*-Butyllithium solution 11M in hexanes, Lithium bis(trimethylsilyl)amide, Phosphazene (P₄-*t*Bu) 0,8M in hexane, carbon disulfide, potassium *tert*-butoxide, sodium methoxide and phenyllithium (1.9 M in dibutyl ether) were purchased from Sigma-Aldrich and used without further purification. Diisopropylformamide (Alfa Aesar) and piperidinoformamide (Sigma Aldrich) were stored under argon over activated molecular sieves 4 Å. Dibromobenzene (Sigma Aldrich), octasulfur and terephthalaldehyde (Sigma Aldrich) were dry under vacuum for one hour prior to use. Trifluoromethanesulfonic acid (TCI), Trifluoromethanesulfonic anhydride (ABCR), methyl trifluoromethanesulfonate (Alfa Aesar), trimethylsilyl trifluoromethanesulfonate (Sigma Aldrich), 2-thiophenecarboxaldehyde (Sigma Aldrich), and 1,8-Diazabicyclo[5.4.0]undec-7-ene (Sigma Aldrich) were distilled prior to use. 1,5,7-Triazabicyclo[4.4.0]dec-5-ene (Sigma Aldrich) was dried by azeotropic distillation of toluene. Finally, triethylsilane (Sigma Aldrich) was passed through neutral alumina and then distilled prior to use.

Characterization apparatus

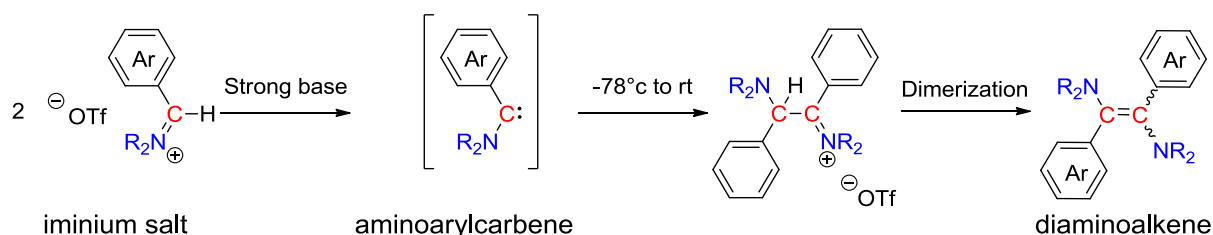
NMR spectra were recorded on a Bruker Avance 400 (1H, 13C, 19F, 400.2, 100.6 and 376.53 MHz respectively) in appropriate deuterated solvents. Molar masses were determined by size exclusion chromatography (SEC) in THF (1 mL/min) with trichlorobenzene as flow marker, using both refractometric (RI) and UV detectors. Analyses were performed using a three-column TSK gel TOSOH (G4000, G3000, G2000) calibrated with polystyrene standards. HRMS were recorded on various spectrometer: a Waters Q-TOF 2 spectrometer and a GCT premier waters mass spectrometer

in the chemical ionization (CI) mode. Melting point were determined by using a Stuart Scientific SMP3 apparatus. Ultraviolet visible spectra were collected on a Thermostated UV/Vis Spectrometer (Agilent Carry 4000). Fluorescence spectra were obtained via Spectrofluorimeter (Jasco FP-8500ST). XRay structures were done on a *Rotating Anode Rigaku FRX 3kW with microfocus (Hybrid Dectris Pilatus 200 K pixel detector)*. Electrochemical measurements were performed in solution. , TBAPF₆ was selected as the supporting electrolyte, and 0.1M of the TBAPF₆ solution was prepared in freshly distilled ACN over CaH₂. Following this step, both 20μM solutions of the investigated monomer was prepared in the TBAPF₆/ACN system. Additionally, to calculate the redox potentials versus ferrocene/ferrocenium (Fc/Fc+) redox couple, a 20μM solution of ferrocene was also prepared. The electrochemical cell filled with the appropriate solution was de-aerated by highly pure nitrogen gas bubbling for at least 15 min before each measurement, and the nitrogen atmosphere was kept over the solution during the process. In the electrochemical studies, the working and auxiliary electrodes were platin, and silver wire was used as the pseudo reference electrode. The voltammogram obtained with a scan rate of 100 mV.s⁻¹

General conclusion

Semi-conducting polymers are a great alternative to inorganic devices (silicon technology) allowing the development of flexible, light weighted and low cost devices. However, the presence of metallic residues in the final material has been proven to have a negative impact on their optoelectronic performances. To overcome such problematic, different routes free from metallic species have been reported. In this context, the development of a new transition metal-free methodology has been defined as the goal of this PhD. More precisely, this new approach relies on the use of tailored bis-aminoarylcarbenes as building blocks to construct PPV-type polymers *via* transition metal-free route thanks to their selective dimerization/polymerization reaction.

In this PhD was first studied the dimerization reaction of monofunctional aminoarylcarbene obtained *via* the deprotonation of its corresponding iminium salt precursor. The synthesis and characterization of the monoaminocarylcarbene salt precursor has been performed. Then, deprotonation with a strong base of the iminium salt precursor led to the transient aminoarylcarbene which instantly dimerized into a mixture of diaminoalkenes (80/20 E/Z). Surprisingly, in those conditions, only the products coming from the dimerization was observed (Scheme 1).



Scheme 1. Synthesis of diaminoalkenes *via* carbene dimerization.

The mechanism of the dimerization reaction was then investigated at an experimental and theoretical level. Experimentally, the successful isolation of the intermediate resulting from the addition of a free aminoarylcarbene onto its conjugated acid confirmed the proton-catalyzed pathway of the dimerization. However, not experiments have been able to rule out the direct

route with the dimerization of two free carbenes. Theoretically, DFT calculations explained the ratio obtained with a majority of *E*-isomer as it was found to be the thermodynamic isomer ($\Delta G = -35 \text{ kcal.mol}^{-1}$ and $-45 \text{ kcal.mol}^{-1}$ for *Z* and *E*-isomer respectively). As expected the proton-catalyzed pathway is favored with an activation barrier way shorter compared to the direct proton-free route. Finally, the selectivity of the dimerization reaction over side reactions such as the C-H insertion in α or β of alkyl group on the nitrogen atom has been explained based on their activation barrier. The activation barrier of C-H insertion ($E_a = 39,4$ and $45,- \text{ kcal.mol}^{-1}$ for insertion in α and β respectively) was found to be strongly higher compared to the dimerization *via* the addition of a carbene onto its conjugated acid ($E_a = 0.6 \text{ kcal.mol}^{-1}$) or *via* direct route ($E_a = 18.5 \text{ kcal.mol}^{-1}$). The scope of the dimerization reaction has been extended by using different alkyl groups on the amino atom (piperidine and diisopropyl group) and aryl groups (phenyl and fluorene group) leading to new diaminoalkene which were fully characterized (X-Ray, ^1H , ^{13}C NMR spectroscopy, absorption, emission and infrared spectroscopy) (Figure 1).

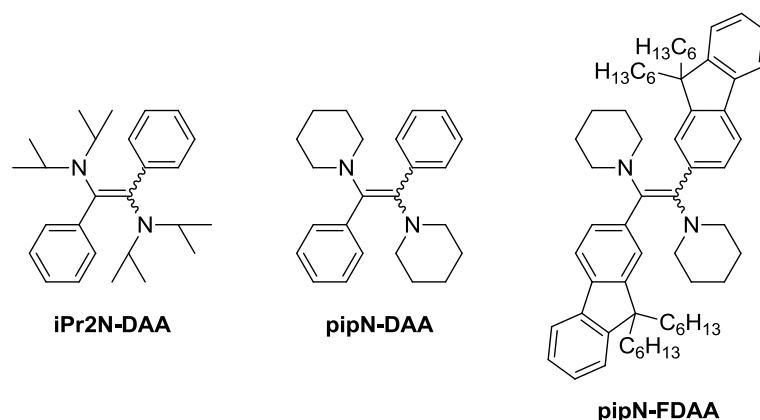
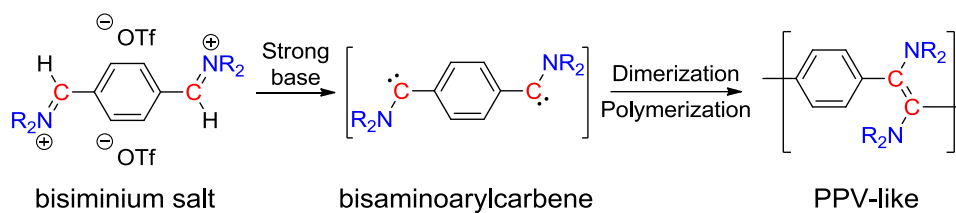


Figure 1. Scope of diaminoalkene synthesized *via* carbene dimerization.

The dimerization reaction was then investigated at a macromolecular level (Scheme 2). To this end, bi-functional iminium salt precursors were synthesized and characterized. Then, polymerization upon addition of strong bases, such as phosphazene (P₄-*t*Bu) or LiHMDS, on bis-iminium salt led to a mixture that turned deep red. After purification, polymers were characterized by SEC (PS standards) and led to a \overline{M}_n in a range of 3000-5900 g.mol⁻¹ ($D = 2.05$ - 2.08).



Scheme 2. Synthesis of amino-containing N-PPV polymers *via* repeated carbene dimerization/polymerization.

Moreover, by ^1H NMR spectroscopy, the E/Z ratio remained unchanged compared to the diaminoalkenes and aldehyde signals representing the chain-end functions of the polymers were observed. Spectrophotometric analysis confirmed the extension of the conjugation system compared to the diaminoalkenes as observed in UV/Vis experiment with a bathochromic shift of the maximum of absorption ($\lambda_{\text{max}} = 388$ nm in diaminoalkenes vs $\lambda_{\text{max}} = 462$ nm in N-PPV). Similar trend in the emission properties was observed with a red shift of the maximum of emission ($\lambda_{\text{max}} = 592$ and 666 for N-PPV in solution and in thin film, respectively, vs $\lambda_{\text{max}} = 540$ for the model compound) (Figure 2).

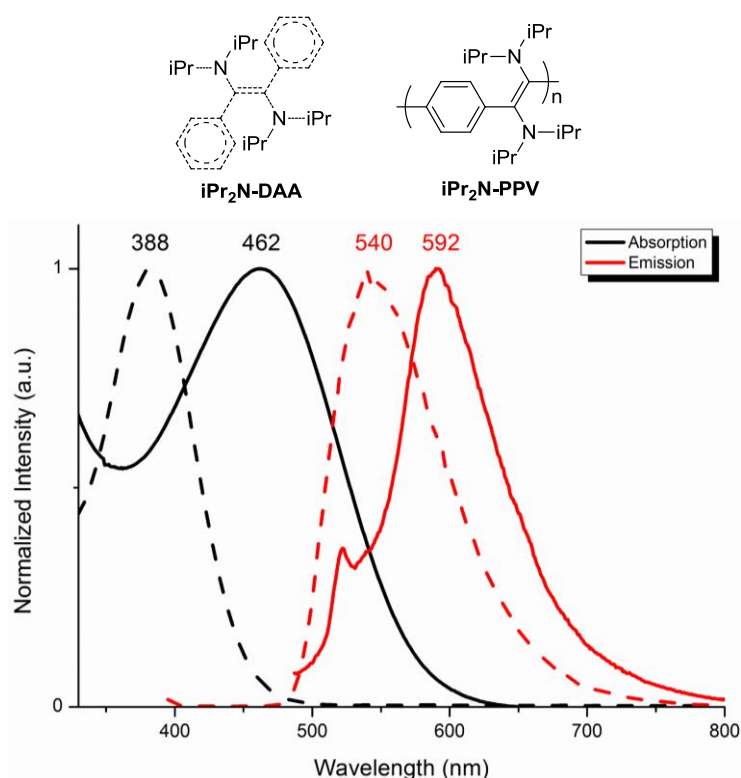
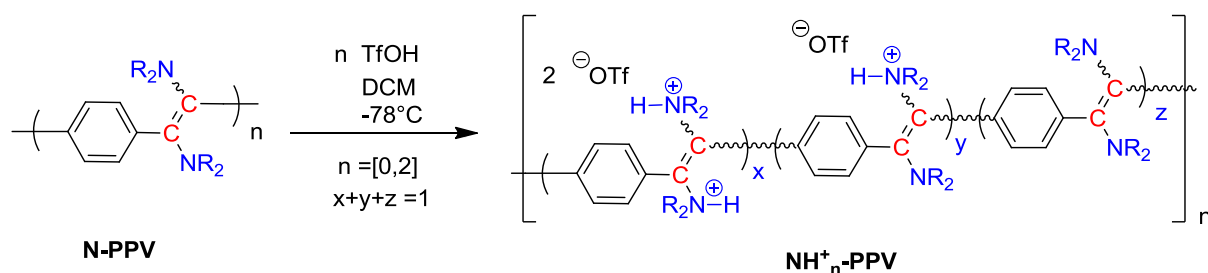


Figure 2. Absorption and emission spectra of N-PPV with diisopropyl substituents (plain line) and its corresponding diaminoalkenes (dashed line).

Furthermore, the emission on a large array of the visible spectra which even goes up, in the case of diisopropylamino polymer, to the infrared, coupled with a large stoke shift (160-290 nm) and

a small overlap between the λ_{max} emission and absorption makes these polymers good candidates in order to be integrated in optoelectronic devices.

In contrast to classical PPV, the physicochemical properties of these polymers could be modified thanks to the presence of the two nitrogen atoms next to the double bonds. Most notably, N-PPV could be protonated with TfOH to see the influence on their absorption/emission properties (Scheme 3).



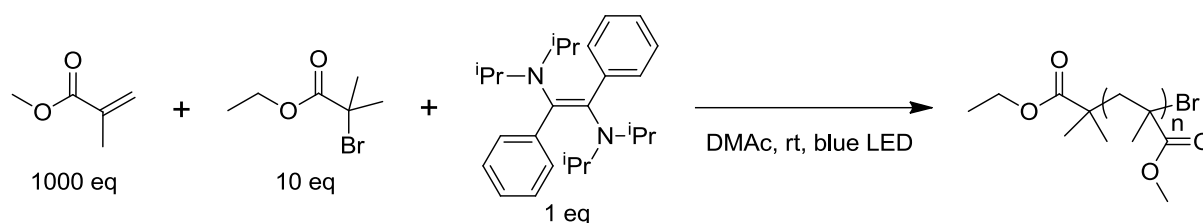
Scheme 3. Protonation of N-PPV polymers with TfOH.

In the case of **iPr₂N-PPV**, by UV/Vis analysis, protonation induced an hypsochromic shift of the maximum of absorption of the $n\text{-}\pi^*$ transition (from $\lambda_{\text{max}} = 462$ nm to 352 nm) and as expected no change for the $\pi\text{-}\pi^*$ transition ($\lambda_{\text{max}} = 252$ nm). Similar behavior was observed for the diaminoalkene **iPr₂N-DAA** (from $\lambda_{\text{max}} = 388$ nm to 325 nm).

Despite similarities, a different behavior upon protonation was observed for the polymer **pipN-PPV** with piperidine substituents. Indeed upon protonation, no blue shift but a loss of the conjugation was observed with the disappearance of the $n\text{-}\pi^*$ transition. This result, was also observed on the corresponding diaminoalkene **pipN-DAA**. This difference of behavior was explained based on the crystal structure of protonated **pipN-DAA**. Indeed, X-Ray analysis showed that protonation occurred on one nitrogen atom and on a C=C double bond carbon atom breaking the conjugation of the molecule and thus leading to the loss of the $n\text{-}\pi^*$ transition.

In the last chapter, because of structural similarity with the tetraaminoalkenes, diaminoalkenes synthesized in this project were investigated upon their reducing properties. As expected, with only two amino group next to the double bond, their reducing potential was found to be lower than tetraaminoalkenes ($E_{\text{ox}} = -0.171$ V vs SCE for diaminoalkenes vs $\Delta E = -1.71$ V vs SCE for the best tetraaminoalkenes). Thus, attempts to reduce C-X bonds (X = Br, I) failed.

However, the diaminoalkenes synthesized having an absorption near the visible, their irradiation should increase their reducing potential with a $E_{ox}^* = -2.572$ V vs SCE. These two potentials, when under irradiation or not, fit with the photocatalysts used in OATRP. Therefore, OATRP of MMA was attempted (Scheme 4).



Scheme 4. Synthesis of PMMA via polymerization of MMA with diaminoalkenes as organophotocatalyst and blue light.

Controlled experiment confirmed the catalytic role of the DAA, as without it, no reaction was observed. Moreover, the polymerization can be controlled by performing cycles of dark and irradiation periods. However, upon irradiations PMMA obtained did not increase in molar mass over time and got a broader dispersity. This result might be explained by the fact that after the successful C-BR reduction by DAA, the DAA-BR⁺ complex was not able to transfer back its radical back to the chain end. Thus, a focus on the design of more efficient catalyst for the synthesis of well-defined polymers has to be investigated.

Thanks to these encouraging results, the library of new N-PPV polymers could be extended by choosing diverse aryl and amino groups which could induce better physicochemical properties. Moreover, the process to make films of better quality has to be investigated in order to measure accurately the conductivity of the N-PPVs. In the case if good conductivity were obtained, they could be integrated *in fine* in optoelectronic devices. Moreover, the presence of amino groups in the polymer allows their post-modification and so the cationization of the polymers. Thus, by having different anions (through the use of various acid or by anion-exchange), the N-PPV polymers should have new electronic and ionic conductivity properties to be investigated.

Titre : Développement de polymères semi-conducteurs pour l'électronique organique par voie synthétique sans métaux.

Résumé : Dans cette thèse, la synthèse de polymères semi-conducteurs par une voie originale n'utilisant pas de métaux, afin de les intégrer dans des dispositifs électroniques organiques comme les OLED (Organic light emitting diode) a été développée. Le but est de développer et d'optimiser une nouvelle méthode de synthèse en s'appuyant sur des bis-aminoarylcarbènes acyclique en tant que blocs constructeurs afin d'obtenir de nouveaux polymères PPV-like. Dans un premier temps, la réaction de dimérisation est étudiée au niveau moléculaire avec la synthèse et caractérisations de diaminoalcènes obtenu à partir de carbènes acycliques monofonctionnels. Le mécanisme et la sélectivité de cette réaction de dimérisation ont également été examinés par voies expérimentales et théoriques. Dans un deuxième temps, la réaction de dimérisation a été étendue au niveau macromoléculaire avec la synthèse et caractérisations de nouveaux PPV-like polymères contenant des fonctions amino en α de la double liaison. Par la suite, l'influence de ces groupements amino sur les propriétés optoélectroniques de ces N-PPV une fois modifiés chimiquement a pu être étudié. Enfin, les caractéristiques particulières des diaminoalcènes synthétisés au cours cette thèse ont permis une étude préliminaire sur leurs applications potentielles en tant que catalyseur organiques dans la réaction de polymérisation radicalaire par transfert d'atomes.

Mots clés : Aminoarylcarbènes, Carbènes, Dimérisation, Electronique organique, OATRP, Polymères.

Title : Metal-free alternative, synthetic routes to efficient semi-conducting Polymers for Organic electronics.

Abstract: In this thesis, the study focuses on the synthesis of semi-conducting polymers by an original pathway free from metals, in order to integrate them into organic electronic devices such as OLEDs (Organic light emitting diodes). The aim is to develop and optimize a new methodology using acyclic bis-aminoarylcabenenes as building blocks to synthesize new PPV-like polymers. First, the dimerization reaction is studied at a molecular level with the synthesis and characterization of diaminoalkenes obtained from monofunctional acyclic aminoarylcabenenes. The mechanism and the selectivity of this dimerization reaction is also investigated experimentally and theoretically. In a second step, the dimerization reaction was extended at a macromolecular level with the synthesis and characterization of new PPV-like polymers containing amino functions in α of the double bond. Subsequently, the influence of these chemically modified amino groups on the optoelectronic properties of these N-PPVs has been studied. Finally, the specific characteristics of the diaminoalkenes synthesized during this thesis has allowed a preliminary study on their potential applications as organocatalysts in the atom transfer radical polymerization reaction.

Keywords: Aminoarylcabenenes, Carbenes, Dimerization, OATRP, Organic electronic, Polymers.